

COMBUSTION AND PRE-COMBUSTION  
CONTROL METHODS TO MINIMIZE EMISSIONS  
FROM MODULAR INCINERATORS

By

JOHN CHARLES WAGNER

A DISSERTATION PRESENTED TO THE GRADUATE SCHOOL  
OF THE UNIVERSITY OF FLORIDA IN PARTIAL FULFILLMENT  
OF THE REQUIREMENTS FOR THE DEGREE OF  
DOCTOR OF PHILOSOPHY

UNIVERSITY OF FLORIDA

1992



To my parents

## ACKNOWLEDGMENTS

The author wishes to thank Donald Clauson, Joseph Blake, Xie-Qi Ma, David Roskein, Britta Schmidt, and Jason Weaver for stack sampling and analysis; Henk van Ravenswaay for construction of the biomass feeder; Kaifa Awuma for HCl analysis; Jamie Forester for drawing the original incinerator circuitry; Mahadevan Sadanandan for kinetics code work; Michael Mahon for construction of the HCl continuous emission monitor; Scott Quarmby and Robert Driskell for their electrical engineering expertise; Donald Adams for setting up the continuous emissions monitor sampling system; Jonathan Carter, Chris Jeselson, Todd Yurchisin, Ronald Storer, William Calhoun, Thomas Cherry, Song Mu, Wilfred Schnell, Rodnie Barbosa, and others who helped in some way, even if it was just feeding garbage; Craig Saltiel for getting the kinetics code operational again; Charles Schmidt for VOST analysis; Bruce Green for refurbishing and maintaining the incinerator and helping install the control system; the Tennessee Valley Authority, Florida Governor's Energy Office, New River Waste Association, Florida Department of Environmental Regulation, Mick A. Naulin Foundation, Gatorade Fund, Supelco, Tacachale, and University of Florida for project funding; and especially Alex Green, whose advice, encouragement, and support made this all possible.

## TABLE OF CONTENTS

	<u>page</u>
ACKNOWLEDGMENTS .....	iii
LIST OF TABLES .....	vi
LIST OF FIGURES .....	viii
ABSTRACT .....	x
CHAPTERS	
1 INTRODUCTION .....	1
Combustion Fundamentals .....	3
State of the Art in Incineration .....	12
Some Combustion Strategies .....	15
The Need For a New Combustion Control System .....	19
Development of a New Combustion Control Strategy .....	20
2 INCINERATOR SYSTEM .....	24
Background .....	24
Incinerator Hardware .....	26
Incinerator Operation .....	30
Original Control System .....	31
3 INSTRUMENTATION .....	34
Sensors, Monitors, and Sampling Systems .....	34
Operations .....	40
4 REVIEW OF DATA FROM THREE YEARS OF TESTING .....	43
CCTL Trial Burn Data .....	44
Carbon Monoxide Data .....	47
Particulate Data .....	51
Volatile Organic Compound Data .....	53
Summary of Significant Relations .....	57
5 KINETIC MODELLING .....	58
Inputs to the Code .....	64
Waste Composition .....	65
Pyrolysis Steps .....	67
Results from the Kinetics Code .....	68
Conclusions from the Kinetics Code .....	75

6	EFFECT OF CHLORINATED INPUT ON CHLORINATED ORGANIC COMPOUND EMISSIONS .....	77
	PVC, HCl, and VOST Data from CCTL .....	79
	Review of Statistical Procedures .....	82
	Effect of Chlorine Input on HCl Emissions .....	87
	Review of HCl and VOST Data .....	89
	Conclusions from the Chlorinated Data Review .....	118
7	THE NEW COMBUSTION CONTROL SYSTEM .....	120
	The Combustion Control Strategy .....	120
	Implementation of the New Combustion Control Strategy .....	121
	Control System Components .....	123
	The Control System Program .....	131
8	EXPERIMENTS WITH OLD AND NEW CONTROL SYSTEMS .....	143
	Test Firings .....	143
	Experimental Firings .....	148
9	DISCUSSION, CONCLUSIONS, AND RECOMMENDATIONS .....	159
	Specific Results .....	160
	Recommendations for Future Work .....	167
	General Projections to Other Systems .....	171
	Final Summary .....	173

#### APPENDICES

A	DETAILED DESCRIPTION OF THE ORIGINAL CONTROL SYSTEM .....	174
B	DETAILS ON THE INSTRUMENTATION .....	184
C	DATA CALCULATIONS .....	186
D	VOST EMISSIONS .....	191
E	KINETICS CODE PROGRAM LISTING .....	193
F	KINETICS CODE INPUT FILE .....	198
G	TEMPERATURE-TIME PROFILE CALCULATIONS .....	201
H	BASE CASE KINETICS CODE OUTPUT .....	204
I	ADDITIONAL DETAILS ON THE CONTROL SYSTEM .....	209
J	ADDITIONAL DETAILS ON THE CONTROL COMPUTER PROGRAM .....	225
	REFERENCES .....	227
	BIOGRAPHICAL SKETCH .....	239

## LIST OF TABLES

3-1	Typical Protocol for Experimental Burns .....	42
4-1	Results of Measurements Taken During NHW-Only Experimental Burns from 08-31-89 to 08-10-91 .....	46
4-2	Results of Method 5 Particulate Measurements Taken During NHW-Only Experimental Burns from 09-27-88 to 08-03-89 .....	46
4-3	Linear Regression Results from CO Data Review .....	49
4-4	Linear Regression Results from Particulate Data Review .....	51
4-5	Linear Regression Results from VOST Data Review .....	55
5-1	Cottage Waste Characterization of 02-24-90 .....	66
5-2	Kinetic Code Results .....	72
6-1	CCTL PVC and HCl Test Data .....	80
6-2	Hydrogen Chloride, Temperature, Carbon Monoxide, and Volatile Organic Compound Data Used for Linear Regression and Nonlinear Analyses .....	81
6-3	Critical Values of t, F, and R <sup>2</sup> at the 5% Significance Level .....	85
6-4	Results of Linear Regression of VOST Data .....	90
6-5	Results of Quadratic and Higher Power Regressions of CCTL VOST data .....	96
6-6	Results of Logarithmic and Exponential Regressions of CCTL VOST data .....	98
6-7	Results of Fits to Linearized Versions of Nonlinear Functions .....	101
6-8	Parameters for Nonlinear Equation Fits .....	105
6-9	Results of Cross-Product Regression of CCTL VOST Data .....	113

6-10	Results of Regressions with Other Compounds .....	117
8-1	Protocol for Control System Experimental Burns .....	150
8-2	VOST Results for Latest Samples, Non-Blank Corrected and Blank Corrected .....	156

## LIST OF FIGURES

1-1	Effect of theoretical air on temperature for burning a typical 4500 BTU/lb waste .....	17
1-2	Primary chamber temperature for the 03-21-91 CCTL burn .....	21
1-3	Carbon monoxide levels during 11-23-91 burn .....	21
2-1	Incinerator system layout .....	27
2-2	Functional schematic of original CCTL incinerator control circuitry .....	32
3-1	Incinerator instrumentation layout .....	35
4-1	Quadratic fit of CCTL carbon monoxide data to primary combustion chamber temperature .....	50
4-2	Carbon monoxide data fitted with a quadratic function of PCC temperature and a linear function of oxygen concentration .....	50
4-3	Carbon monoxide data fitted with a quadratic function of PCC temperature and a linear function of carbon dioxide concentration .....	50
4-4	Particulate emissions compared to oxygen concentration .....	52
4-5	Particulate emissions data compared to natural gas input .....	52
4-6	Vost emissions compared to waste feed rate .....	56
4-7	Vost emissions compared to PCC temperature and waste feed rate and plotted against temperature .....	56
5-1	Kinetics code program flowchart .....	61
5-2	Temperature-time history for CCTL incinerator .....	63
5-3	Kinetic aromatic and chlorination sequences .....	69
5-4	Base case (Run 30) kinetics code output .....	71

6-1	HCl emissions compared to added chlorine input with both HCl and added Cl normalized to a 400-lb/hr waste feed rate .....	88
6-2	Comparison of DCB emissions to HCl emissions with and without outlying DCB data point .....	94
6-3	Replacement of the orthogonal function $H(t;\mu,p)$ with a Gaussian function $J(t;u,s)$ .....	109
7-1	On/off and alarm control system circuitry .....	125
7-2	Natural gas piping arrangements .....	127
7-3	Natural gas flow rate measurement orifice meter .....	129
7-4	Control program overall flowchart .....	133
7-5	Manual data entry screen .....	135
7-6	Control computer program data screen .....	135
7-7	Incinerator warm up logic .....	138
7-8	Temperature maintaining logic .....	139
7-9	Ram feeding logic .....	142
8-1	CEM data from 04-08-92 burn .....	154
8-2	Temperature and gas data from 04-08-92 burn .....	154
8-3	CEM data from 04-15-92 burn .....	157
8-4	Temperature and gas data from 04-15-92 burn .....	157
A-1	Original incinerator control system circuitry .....	175
A-2	Original biomass control subsystem .....	180
A-3	Original stoker control circuitry .....	181
I-1	Power supply board with transformer .....	214
I-2	Original modmotor circuitry .....	216
I-3	Modmotor modification and control circuitry .....	218
I-4	Override relays configuration .....	221
I-5	Stoker control circuitry with override relay .....	222

Abstract of Dissertation Presented to the Graduate School of  
the University of Florida in Partial Fulfillment of the  
Requirements for the Degree of Doctor of Philosophy

COMBUSTION AND PRE-COMBUSTION  
CONTROL METHODS TO MINIMIZE EMISSIONS  
FROM MODULAR INCINERATORS

By

JOHN CHARLES WAGNER

August 1992

Chairman: Dr. Alex E. S. Green  
Major Department: Mechanical Engineering

This dissertation summarizes the results of stack emission measurements made since 1988 using a two-stage 500 lb/hr modular incinerator located at the University of Florida-Tacachale-Clean Combustion Technology Laboratory (UF-T-CCTL). From the analysis of these results some statistically significant relationships have been developed between HCl emissions (a surrogate for PVC in the waste) and the emissions of a number of chlorinated organic compounds ( $C_6H_5Cl$ ,  $C_6H_4Cl_2$ ,  $CHCl_3$ ,  $CH_2Cl_2$ , and  $C_2Cl_4$ ). These compounds appear in the stack gases even under good combustion conditions. These type of relationships have not been previously reported in combustion literature and have important implications for the evolving discipline of Clean Combustion Technology. These results contradict widely quoted and widely accepted conclusions from other incinerator studies.

From the analysis of the stack emissions of the UF-T-CCTL incinerator a control strategy is developed that will minimize emissions of carbon monoxide and volatile organic compounds. A personal computer-based control system is developed to implement the combustion control strategy. The control system monitors carbon monoxide, carbon dioxide, oxygen, and hydrogen chloride emissions and incinerator and stack temperatures; maintains feed rate and output power levels; and fixes temperature levels in such a way as to operate the incinerator under desirable combustion conditions for emissions minimization.

The control system's strategy is based upon a review of previous combustion conditions and emissions data collected from the UF-T-CCTL incinerator, kinetic modelling of emissions, regulatory constraints, incinerator size and thermal characteristics, and desired feed rate and output power levels. The control system regulates the flow rates of natural gas into the two combustion chambers, primary chamber overfire and secondary chamber air flow, and waste charging frequency.

Experiments at an average 350-lb/hr waste feed rate with the control system installed and operating show a significant reduction in carbon monoxide emissions over those from before the installation of the control system. Also, the temperature versus time profile during incinerator operation has been considerably smoothed out.

## CHAPTER 1 INTRODUCTION

Modular-type incinerators have been used for many years for on-site medical and institutional waste disposal. These shop-built units usually have two combustion chambers. In the first chamber the waste is burned under substoichiometric conditions, i.e., with insufficient air for complete combustion. In the second chamber additional air and support fuel are introduced to burn out the combustion gases from the first chamber. This starved-air, two-stage method was developed to reduce the smoke generated from earlier one-stage units.

Increasing regulation and public awareness of incinerator emissions, particularly organic compounds, have brought incinerators under great scrutiny. The current method of operating modular incinerators in a starved-air mode is inadequate for controlling organic and acid emissions. The regulators' response has largely been to require post-combustion air pollution control devices. These devices can be many times the cost of the incinerator unit itself. A scrubber to control acid gas emissions could add \$200,000-\$800,000 to the the cost of an \$100,000 modular incinerator.

The objective of this research is to use the extensive experience of the Clean Combustion Technology Laboratory (CCTL) at the University of Florida in modular waste incineration to determine relations between emissions and operating conditions useful for control strategies to minimize emissions from modular incinerators. These strategies can be used as an alternate method of pollution control to requiring expensive post-combustion air pollution control devices by serving as a guide for upgrading, operating, and designing this general class of incinerators. Another objective of the research is to develop a combustion control system to implement some of these strategies and minimize emissions of carbon monoxide and volatile organic compounds from a two-stage modular incinerator.

The CCTL has operated a two-stage modular incinerator (see Chapters 2 and 3) at the Tacachale center in Gainesville, FL, for over 4 years. This institutional incinerator has been modified to burn hotter and run in an excess-air mode. Careful attention is given to what is burned in the CCTL unit. Metallic and chlorinated materials are mostly avoided. These low-cost combustion and pre-combustion strategies of burning hotter, operating in an excess-air mode, and avoiding toxic producing materials in the input waste stream should alleviate the need for expensive post-combustion control devices.

Data collected from three years of stack testing at the CCTL facility is reviewed here to determine desirable

operating conditions for minimal emissions for this type of modified incinerator (see Chapter 4). The combustion process in the incinerator is examined using simple chemical kinetic models (see Chapter 5). Emissions of chlorinated organic compounds are analyzed to determine if relationships exist between the level of these emissions and the level of chlorine in the input (see Chapter 6). Some widely quoted and accepted studies [1-2] have suggested that no such relationships exist. Studies by Green et al. [3-8] contradict this "conventional wisdom".

A simple combustion control system is developed to regulate the operation of the CCTL incinerator (see Chapter 7). The control strategy is based on the desirable operating conditions determined from the data review and kinetic modelling. Tests with the control system show lower incinerator emissions than without the control system (see Chapter 8).

Some combustion fundamentals and emissions control strategies are presented in this chapter.

### Combustion Fundamentals

Pyrolysis is the process of using high temperatures in an atmosphere of little to no oxygen to drive off, but not combust, lighter organic compounds from a more heavy or complex organic compound or mixture of such compounds.

Combustion is the chemical reaction of a fuel with air (or oxygen). The reaction is usually exothermic (releases

heat energy), which increases the temperature of the product gases substantially. Fuels normally contain carbon and hydrogen, which if combusted completely form carbon dioxide ( $\text{CO}_2$ ) and water ( $\text{H}_2\text{O}$ ).

Incineration is the combustion of waste. Waste and most other fuels also contain oxygen, chlorine, sulfur, nitrogen, metals, and ash (incombustible matter such as minerals and other metallic oxides). Chlorine and sulfur in the fuel usually generate hydrogen chloride ( $\text{HCl}$ ) and sulfur dioxide ( $\text{SO}_2$ ) as combustion products. Nitrogen in the fuel, and nitrogen in the air at high combustion temperatures, may generate nitrogen monoxide ( $\text{NO}$ ) and nitrogen dioxide ( $\text{NO}_2$ ). Mixtures of  $\text{NO}$  and  $\text{NO}_2$  are referred to as  $\text{NO}_x$ . Metals usually oxidize and remain with ash residue. Some of this residue may be drawn up with the combustion gases as particulates. Volatile (low boiling point) metals such as mercury, cadmium, and lead may vaporize and leave with the combustion gases as gases or on particulates. Organic compounds in the waste also can escape the combustion process and directly become stack gas emissions.

Products of incomplete combustion (PICs) form when there is insufficient oxygen (a substoichiometric amount) and/or insufficient mixing and time to fully burnout the carbon in the fuel. Very substoichiometric combustion can lead to sooting conditions. The principal PIC is carbon monoxide ( $\text{CO}$ ). The PICs may be gaseous, volatile, or semi-volatile. Gaseous compounds include  $\text{CO}$  and light alkanes. Volatile

organic compounds (VOCs) are those with boiling points below 100 °C and/or vapor pressures greater than  $10^{-1}$  mm Hg. Sampling methods for VOCs usually can measure those with boiling points up to 130 °C. The VOCs include light aromatics and chlorinated alkanes and alkenes. Semi-volatile organic compounds (SVOCs) are those with boiling points above 100 °C and/or vapor pressures between  $10^{-7}$  mm Hg and  $10^{-1}$  mm Hg. The SVOCs may condense into particulates or coagulate onto other particulates. When chlorine is present in the fuel, chlorinated PICs are also formed. Chlorinated alkanes are usually volatile, while most chlorinated aromatics are semi-volatile. The most toxic PICs are probably the polychlorinated dibenzo-p-dioxins (PCDDs) and polychlorinated dibenzofurans (PCDF). These are SVOCs with the most toxic being 2,3,7,8-tetrachlorodibenzo-p-dioxin (2,3,7,8-TCDD) [9].

#### Problems with Chlorine in Combustion

The destruction of organic compounds involves free radicals such as H, O, and OH. When the carbon and hydrogen atoms in the organics are oxidized, heat energy is liberated, increasing the temperature of the combustion gases. Higher temperatures lead to more free radicals and faster destruction of the organics. The conversion from CO to CO<sub>2</sub> is usually the step that limits the overall speed of the combustion. Chlorine acts as a flame inhibitor and retards combustion reactions by removing hydrogen atoms from the combustion gases [10-12]:

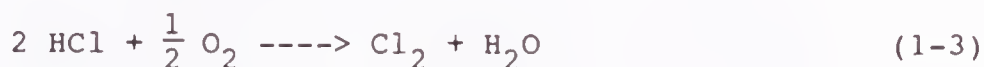


This has the effect of limiting the number of hydroxyl (OH) radicals and oxygen atoms, which are generated by the major chain branching reaction:



With less OH available the chemical reaction processes in combustion are slowed [10-11,13], which leads to lower temperatures and less organic destruction.

The Deacon reaction [14-16]



produces free chlorine from HCl, especially in the presence of  $\text{CuCl}_2$ , which is found on particulates. The free chlorine is then available to chlorinate organic compounds found in the stack gas and on the particulates. To reduce this effect, HCl and particle emissions should be minimized, and  $\text{O}_2$  levels should be decreased. Decreasing  $\text{O}_2$  levels has the side benefit of reducing the amount of air used.

### Residence Time Versus Temperature

Rules for incinerator operation, such as 1800 °F for 1 second in the last combustion chamber, are written for regulatory purposes. These rules seem somewhat arbitrary since, for good toxic destruction, there is much more flexibility due to the chemical and physical processes in combustion. Whereas a 1-second residence time may be needed

for four 9's (99.99%) destruction of an organic compound at 1800 °F, much less time is needed at 2000 °F.

Data for the time required for four 9's reduction in 2,3,7,8-TCDD at temperature in the range 1340-2240 °F [17] can be modelled as

$$t = \exp\left(\frac{1800 \text{ °F} - T}{77 \text{ °F}}\right) \text{ sec} \quad (1-4)$$

where  $t$  is time in seconds and  $T$  is temperature in °F. This equation can be solved for the temperature needed for a specific residence time:

$$T = 1800 \text{ °F} - 77 \text{ °F} \ln\left(\frac{t}{\text{sec}}\right) \quad (1-5)$$

At 1800 °F, 1 second is required for four 9's destruction. At 1900 °F, only 0.27 seconds are needed. For a half-second residence time the temperature need only be raised to 1853 °F.

A time versus temperature regulatory rule would allow older hospital incinerators with small afterburners to continue to operate, provided the last combustion chamber's minimum temperature meets this rule.

For a fixed mass flow rate through a chamber, assuming the gas mixture can be modelled as an ideal gas, the residence time in the chamber is proportional to the reciprocal of the absolute temperature:

$$t = \frac{V}{Q} = \frac{V P M}{\dot{m} R_u T_{\text{abs}}} = \frac{K}{T_{\text{abs}}} = \frac{K}{T + 460} \quad (1-6)$$

where  $Q$  is the volumetric flow rate,  $\Psi$  is the volume of the chamber,  $P$  is the absolute pressure in the chamber,  $M$  is the gas mixture's average molecular weight,  $\dot{m}$  is the mass flow rate through the chamber,  $R_u$  is the universal gas law constant,  $T_{abs}$  is the absolute temperature ( $T + 460$  for U.S.C.S. or  $T + 273$  for S.I.), and  $K$  is a constant defined by Equation 1-6 ( $P$  and  $M$  are taken as constants). Equations 1-5 and 1-6 can be combined and solved iteratively for the minimal operating temperature for four 9's destruction:

$$T_{min} = 1800 - 77 \ln \left( \frac{K}{T_{min} + 460} \right) \quad (1-7)$$

For example, choosing a starting value for  $T_{min}$  of 1800 in Equation 1-7, will converge to a solution for  $T_{min}$  in a couple of iterations.

### Emissions Control

Particulate emissions control can be achieved with dry scrubbers--baghouses, electrostatic precipitators, and cyclones. Bagothouses use fabric filters and capture particulate matter much like a vacuum cleaner. Electrostatic precipitators capture particulates by charging the particles as they pass by one series of plates and attracting them to another series of oppositely charged plates. Cyclones use centripetal forces from swirling the exhaust gases to remove the particles from the gas stream.

Acid gas and organic compound emissions control can be achieved with dry scrubbers--spray dryers--and wet scrubbers

--spray towers, packed towers, and venturi-type scrubbers. In dry scrubbers a powder such as lime is sprayed into the exhaust gases to neutralize the acid gases. In wet scrubbers, the spray is a solution of the neutralizing compound in water. Water spray is used to cool the combustion gases before they enter certain air pollution control devices.

Organic emissions control also can be achieved through controlling the combustion process. Combustion temperature, residence time, turbulence, and oxygen level are the parameters of interests here. Higher levels of each of these four parameters generally leads to more complete combustion and reduced emissions.

### Types of Incinerators

There are three types of incinerators used in municipal waste combustion: mass burn facilities, modular combustors, and refuse-derived fuel (RDF) fired units [18]. The most common incinerator for medical waste incineration is the modular combustor. These may be broken down into two classes: starved- (or controlled-) air types and excess-air types. Both types usually have a primary combustion chamber (PCC) and a secondary combustion chamber (SCC) or afterburner. In a starved-air unit, the waste is burned in the PCC with a substoichiometric amount of air generating many PICs and pyrolysis products. Combustion gases from the PCC pass into the SCC where more air is added to finish

burning out the PICs and pyrolysis products generated in the PCC. Typical PCC and SCC operating temperatures are 1400 °F and 1700 °F, respectively, in a starved-air unit. In an excess-air unit, the waste is burned in the PCC with more air than is needed for combustion. No additional air is added to the SCC in this case. In either type, natural gas or oil burners may be added to the PCC and SCC to aid in igniting and burning the waste and in bringing the temperatures in the chambers up to levels needed to sustain combustion.

Another type of incinerator, the rotary kiln, is used mainly in hazardous waste incineration. The PCC of an rotary kiln incinerator slowly rotates about its long axis to thoroughly burn out the waste and residue inside. Fluidized bed combustion for waste disposal is also becoming more popular [19].

#### Advantages of Starved-Air Incineration

Starved-air units have a few advantages over excess-air units. One advantage is that, with the lower temperature and turbulence, less particulates and metals are carried into the SCC and up the stack. Another advantage is that waste takes longer to burn, which distributes out over time the heat energy released from batch-fed waste. This allows for a steadier flow of steam from those units with heat recovery boilers.

### Problems with Starved-Air Incineration

Because starved-air units operate with insufficient air in the PCC for complete combustion, the SCC must burn out the large quantity of PICs being generated in the PCC. A tertiary combustion chamber may be required to sufficiently destroy the PICs. Starved-air units cannot handle high moisture content waste [20], such as in hospital red bags, since there is insufficient heat release to sustain combustion with substoichiometric burning. Starved-air units are usually designed for paper wastes (trash), and have small PCC and SCC burners for the low supplemental fuel requirements of paper wastes. Starved-air units are least able to adapt to changes in the waste constituents [20].

The destruction of organics at high temperature is a pyrolytic and oxidative process [13]. In a nonoxidative (starved-air) environment the pyrolysis process leads to a breakdown from large organic molecules to smaller and more unsaturated species. At some point these become highly carbonized structures and soot. In an oxidative (excess-air) environment carbon atoms become bonded to oxygen in CO and CO<sub>2</sub> and thus removed from the sooting process. Molecules that are not fully oxidized have a greater chance of being chlorinated in a starved-air environment [13].

### Advantages of Excess-Air Combustion in Primary Chamber

Burning overstoichiometric in PCC will greatly reduce the amount of PICs passing into the SCC. In this case, when

air is added to the SCC, the SCC acts like a tertiary combustion chamber in a starved-air unit.

The excess-air mode of operation more completely combusts the waste in the PCC, though it may increase particulate emissions. The SCC and hotter PCC of excess-air incinerator allows for longer high temperature residence time for toxic destruction than just the SCC of a starved-air incinerator.

#### Problems With Burning Too Hot

Burning above 1800 °F in the PCC can lead to ash slagging problems [20]. At 1880 °F in a reducing (oxygen-starved) atmosphere ash will start to deform. When the ash moves to a cooler or oxygen rich section of the furnace, it will harden into a slag (or clinker). This can have detrimental effects on refractory lined walls and can clog air ports and burners. However, in an oxidizing (excess-air) environment ash may not deform until the temperature reaches 2030 °F.

With high PCC temperatures some heavy metals can volatilize and be carried into the combustion gas stream. If the SCC temperature is too high, excessive NO<sub>x</sub> emissions can occur.

#### State of the Art in Incineration

Control systems for early modular incinerators were primarily concerned with safety and the operation of the incinerator [21-22], without regard to optimizing the

combustion process. Even into the mid-1980s, systems used on/off control of support-fuel burners to regulate the combustion temperature. These control systems slowly evolved from using electro-mechanical timers and relays to using programmable logic controllers [23-24]. Temperature-based control of the waste charging frequency [25] and the combustion air flow [26-28] followed. Eventually, computers were used to monitor and control the incinerator operations [29], especially when air pollution control devices are installed. These new control systems are still mainly concerned with regulating feed rate and operating temperatures. Air pollution control devices have been (and still are) added only when required by regulations.

The Basic Environmental Engineering, Inc. incinerator [30] uses a four stage unit with Basic's patented pulsed hearth™ primary stage, excess air in the second and third stages, reburn tunnels, and some recirculation from the outlet of the heat recovery boiler back to the fourth stage. Emissions of hydrocarbons and CO are typically less than 35 ppm, which is well below the 100 ppm CO level of typical state regulations.

State-of-the-art mass-burn [31-32] and large refuse-derived fuel (RDF) [33-34] incinerators incorporate travelling grate stokers, air preheaters, zone control of combustion air, dry gas scrubbers to neutralize acid gases, and fabric filters to capture particulates. Dry gas scrubbers and fabric filters have replaced electrostatic

precipitators as the desired post-combustion pollution control devices. Electric power generation is usually included. Continuous monitoring and regulation of combustion parameters is used to optimize combustion efficiency and control the formation of organic compounds. Homogenization of the waste by careful mixing is used to maintain a consistent quality of waste and steadier incinerator operation.

Incineration is the best way to deal with hazardous wastes [35]. Some hazardous waste incinerators use oxygen to supplement or replace the combustion air to achieve higher temperatures and avoid  $\text{NO}_x$  [36]. Medical waste is sometimes labelled bio-hazardous waste by regulatory agencies [37-38].

Incineration is the most widely used technology for the treatment of medical waste [39]. For medical waste incineration, the state of the art is a starved-air multi-stage modular unit. Most medical waste incinerators do not have air pollution control devices [39]. Most of those that do use wet scrubbers, which do not achieve a high degree of particulate control.

Several "State-of-the-Art-Reviews" have been written recently on medical waste incineration [40-43]. The recommendation of these reviews is to incorporate post-combustion pollution control devices as the principal means of minimizing toxic emissions.

Shands Hospital at the University of Florida, Gainesville, FL was going to replace its old starved-air

modular incinerator with a \$3.6 million, state-of-the-art, starved-air modular incinerator with post-combustion air pollution control devices, but is now reviewing other options for waste disposal.

### Some Combustion Strategies

The U.S. Environmental Protection Agency (EPA) lists "Good Combustion Practices" (GCPs) for minimal organic emissions from mass burn, RDF, and starved-air incinerators [18]. For a starved-air incinerator, the GCPs include an 1800-°F secondary chamber, 6-12 % oxygen in the flue gas, less than 50 ppm CO, and use of auxiliary fuel during warm up and prolonged high levels of CO. Recently, GCPs for modular excess-air incinerators have been added [44]. These new rules, which also apply to modular starved-air incinerators, include operating with less than 50 ppm CO (4-hour average) and not exceeding 110% of the average load (feed rate) used during the most recent PCDD/PCDF compliance test.

Regulations in Australasia (Australia, New Zealand, and nearby islands) require the afterburner to maintain a minimum of 1100 °C (2012 °F) for at least 1 second at 6-10% excess oxygen under turbulent conditions [45-47]. Danish regulations require the afterburner to be at least 850 °C (1562 °F) for a minimum of 2 seconds at 6% oxygen at a Reynolds number of 60,000 or more [48]. Bulley [45,47] also recommends avoiding the use of PVC and heavy metal pigments in medical plastics.

Green [3-5] advocates the 3 laws of Clean Combustion Technology--pre-combustion, combustion, and post-combustion measures to minimize emissions. The pre-combustion measures include avoiding or removing toxic materials and toxic producing materials from the input waste stream. The combustion measures include optimizing temperature and CO levels, using stokers, and coburning with natural gas. The post-combustion measures include hot gas clean up and use of scrubbers only as needed. Green's modelling [7-8] of the data from the Pittsfield-Vicon municipal waste incinerator emission test study [1] shows the benefit of lowering chlorinated inputs on incinerator emissions.

Wagner et al. [49] studied the emissions from the CCTL incinerator and found that for minimum CO and organic emissions when feeding institutional waste at a typical rate of 400 lb/hr in a modular incinerator the PCC temperature should be maintained in the range 1750 °F to 1800 °F, the SCC temperature should be maintained in the range 1825 °F to 1875 °F. This incinerator was a 500 lb/hr excess-air unit with additional air added to the SCC.

Hasselriis [50-52] also analyzed data from the Pittsfield-Vicon municipal waste incinerator emission test study [1]. Hasselriis found minimum CO and total PCDD and PCDF emissions for a furnace temperature range of 1600-1700 °F, and minimum CO at 8% oxygen. Minimum total PCDD and PCDF emissions were found at 9% oxygen and 15 ppm CO. The Pittsfield-Vicon incinerator [1] uses exhaust gas

recirculation to control the temperature of the gases entering the heat recovery boilers.

Hasselriis [53] shows the temperature and oxygen levels at which to operate a starved-air incinerator on a graph such as that in Figure 1-1. The PCC would be operated at 1500 °F and 70% theoretical air, while the SCC would be operated at 1800 °F and 160% theoretical air. Hasselriis's approach is to reduce the air to the PCC when the overall air to the incinerator is insufficient to keep CO and other emissions down. This approach makes the PCC even more starved, which reduces the rate that the waste is being pyrolyzed or gasified and sent to the SCC. With fewer waste gases entering the SCC, the SCC can more completely combust them.

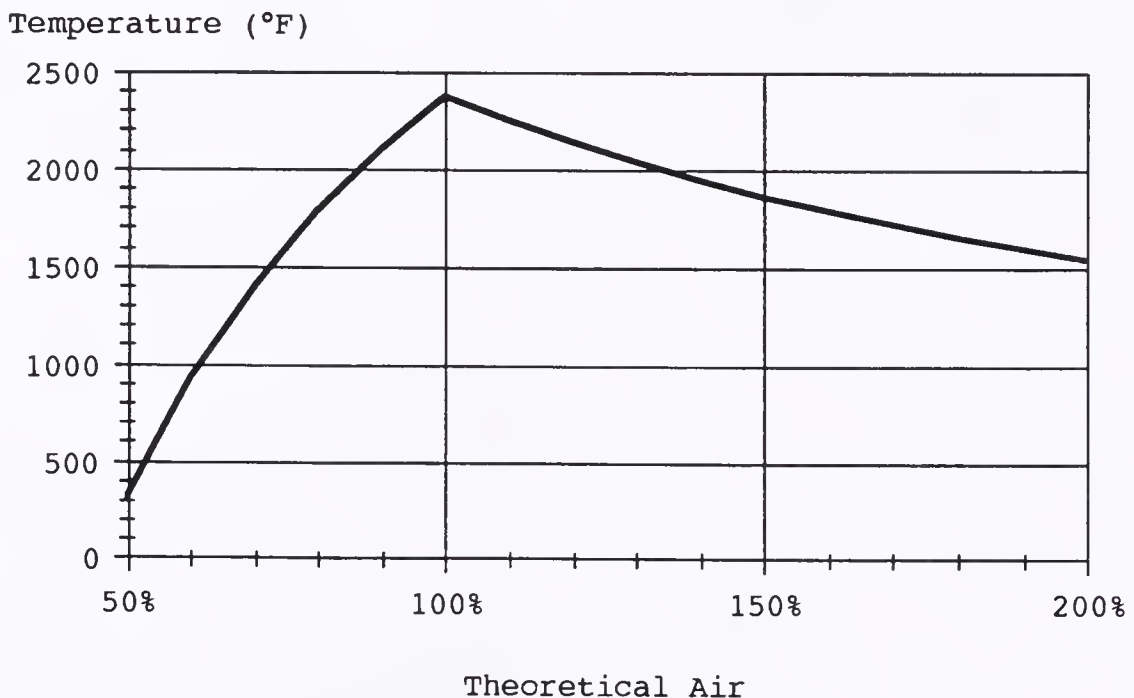


Figure 1-1. Effect of theoretical air on temperature for burning a typical 4500 BTU/lb waste (adapted from Hasselriis [53]).

Chung and Tsang [54] find that soot production from the combustion of polystyrene could be reduced by adding air to the pyrolysis zone of the flame, improving mixing, and using metal salts.

Nihart et al. [55] found that higher destruction efficiency generally correlated with low levels of CO, total hydrocarbons, and methane emissions. In a study on correlating incinerator operating parameters with performance, Stately et al. [56] found that principal organic hazardous constituents (POHCs) and products of incomplete combustion (PICs) generally increased with higher levels of CO, but the relationship depended on the compound studied. Weldon and Beacher [57] find that CO, combustion temperature, and residence time can be used as surrogates to monitor dioxin emissions from municipal waste combustors.

With sufficient mixing and oxygen it is generally believed [42] that 1800 °F is sufficiently high [58-59] to destroy 99.99% of most thermally stable compounds including chlorinated benzenes, phenols, dioxins, and furans. Carbon monoxide is a good index of combustion efficiency [58,60]. Most authorities agree that operation at less than 100 ppm CO minimizes organic emissions [61-62]. Lee [63] also advocates the 3-T (time, temperature, and turbulence (and oxygen)) approach to good combustion.

Acharya et al. [16] expects that minimal formation of dioxins will occur in hazardous waste incinerators with an oxidative, high-temperature, turbulent SCC with a 2-second

residence time if the combustion gases quench in air directly without being sent through a heat recovery boiler.

#### The Need For a New Combustion Control System

The 1990 Clean Air Act Amendments [64] mandate the eventual measurement of and limitations for the emissions of up to 189 pollutants in 250 source categories including incinerators. New Florida Department of Environmental Regulation and EPA regulations [37-38,65] for biohazardous and municipal incinerators have minimum temperature and residence time levels requirements; emission limits for particulates, CO, and HCl; and O<sub>2</sub> and temperature monitoring requirements. For biohazardous waste incinerators under 500-lb/hr capacity in Florida the new regulations require that the final chamber's temperature be maintained above 1800 °F with a residence time of at least 1 second, particulate emissions be less than 0.10 gr/dscf (grains per dry standard cubic foot) corrected to 7% O<sub>2</sub>, CO emissions be less than 100 ppm by volume dry basis corrected to 7% O<sub>2</sub>, and HCl emissions be less than 4 lb/hr.

Improving systems to automatically monitor and control combustion parameters is one of the research needs for municipal solid waste seen by the Solar Energy Research Institute [66].

The current control system of the CCTL incinerator is completely manually set. Blowers, feed systems, and stokers have to be turned on by hand when needed. The burner

controllers do not reset themselves after a failed ignition or a flame out. The control system does not maintain steady or even minimum temperature and oxygen levels. The system provides no alarms for burner outage, stoker breakdown, empty feed hooper, etc. The on/off control of the burners causes rapid, high-amplitude cycling of the primary combustion chamber (PCC) and secondary combustion chamber (SCC) temperatures. The system uses no feedback except, for PCC and SCC temperature, to regulate the combustion process.

Figure 1-2 illustrates some of these problems. The high-frequency, high-amplitude cycling of the PCC temperature and three burner outages (at 14:55, 15:45, and 16:05) are very evident. The PCC temperature reached only 1230 °F before garbage was fed in at 13:00, and did not reach 1800 °F until the fourth feed. Burns of July 21, 1990, and August 10, 1991, also had similar problems. The temperature controller and stoker also broke down during the August 10, 1991, burn. Figure 1-3 shows the carbon monoxide spikes that often occur following ram-feed charges into the incinerator. If a control system could reduce the amount of support fuel before waste is fed into the incinerator, these spikes could be minimized.

#### Development of a New Combustion Control Strategy

A versatile control system should be able to control emissions of CO, NO<sub>x</sub>, SO<sub>2</sub>, HCl, volatile and semi-volatile organic compounds (including dioxins), heavy metals, and

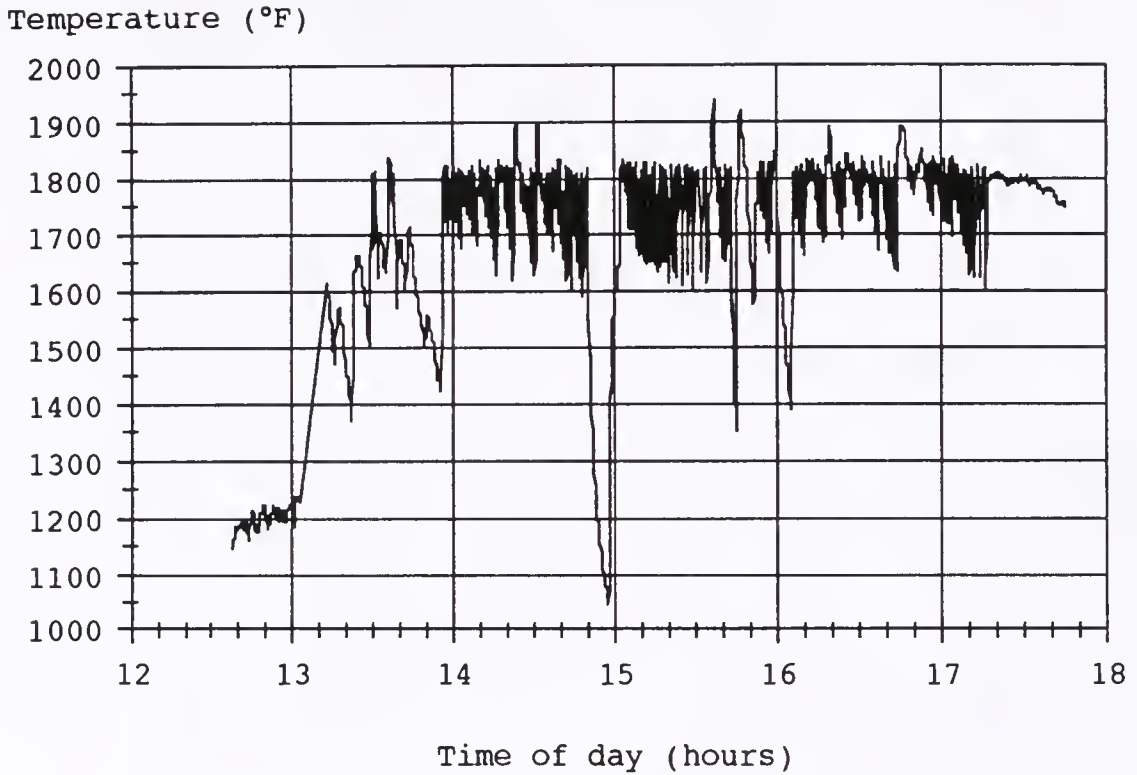


Figure 1-2. Primary chamber temperature for the 03-21-91 CCTL burn.

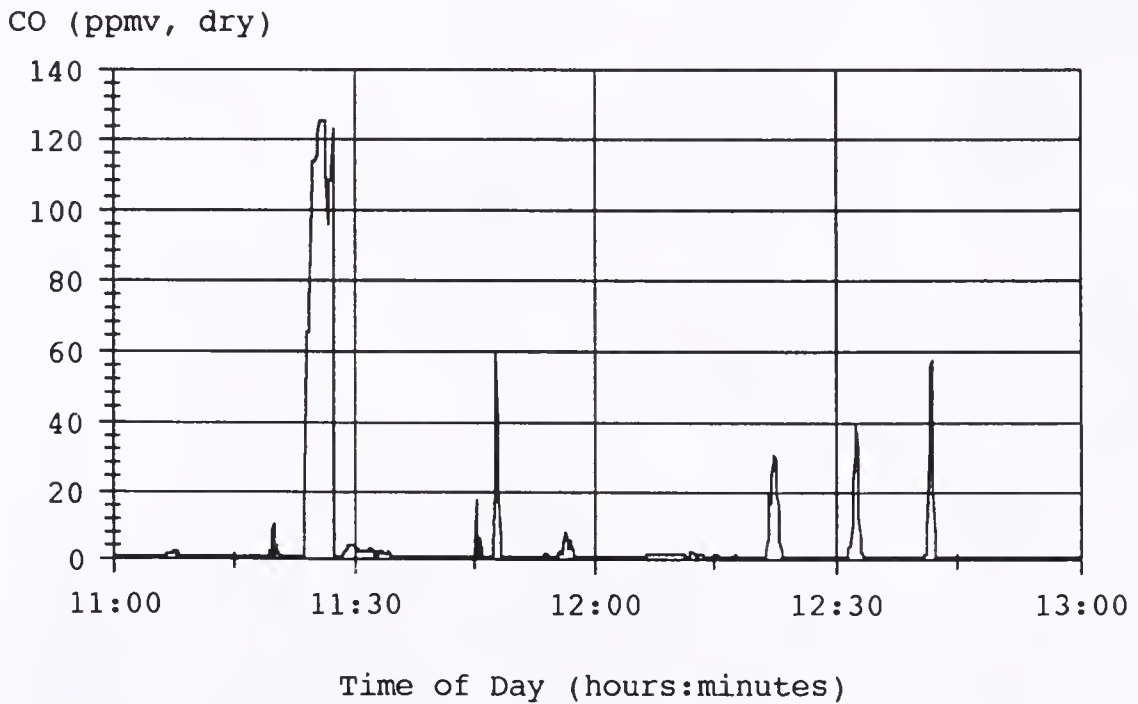


Figure 1-3. Carbon monoxide levels during 11-23-91 burn.

particulates. It also should maintain temperature,  $O_2$ , and minimum feed rate and output power levels. Not all emissions can be minimized by controlling the combustion conditions. The waste stream itself should be monitored to avoid halogenated materials, metals, toxic producing materials, non-combustibles, and excessive liquids. The stack gas may still need to be scrubbed for acid gases and filtered for particulates even under ideal combustion conditions.

One objective of this research is to develop a combustion control system that minimizes emissions of carbon monoxide and volatile organic compounds from a two-stage modular incinerator while maximizing the feed rate of garbage. Development of a new combustion control strategy should incorporate an understanding of the configuration and operation of the incinerator (Chapter 2), examining what instrumentation is available (Chapter 3), reviewing previous combustion conditions and emissions (Chapter 4), modelling of emissions (theoretical and/or empirical) and reaction mechanisms (Chapter 5), and reviewing regulatory constraints (Chapter 1), desired feed rate, and/or output power levels. Also other combustion control strategies should be reviewed (Chapter 1).

Certain surrogate pollutants that have simple relations to most other pollutants will be identified from the data review and modelling. Those pollutants that are representative of the effectiveness of the overall combustion process and are able to be monitored will serve as a basis for the

feedback control system. Carbon monoxide has been traditionally used as an indicator of combustion conditions. Analysis of the data review and modelling will show preferred operating and combustion conditions for various inputs. These conditions will include parameters such as PCC and SCC temperatures, oxygen, and feed rate.

Parts of a modular incinerator system that can be controlled include the flow rate of natural gas (or other supplemental/ignition fuel) into the two chambers, flow rate of air supplied to the burners and chambers, waste and/or other solid fuel charging frequency, stoking frequency, and ash removal rate.

## CHAPTER 2 INCINERATOR SYSTEM

### Background

The Interdisciplinary Center for Aeronomy and (other) Atmospheric Sciences (ICAAS) has been engaged in a program of Research and Development on co-combustion since 1980. Early work focused on the co-combustion of pulverized coal and natural gas at a level of 1 MMBTU/hr [67-71]. In 1985 a 535-hp, 20 MMBTU/hr boiler at the steam plant at Tacachale (then called Sunland Training Center (STC)) was made available for use by ICAAS. Tacachale is a state-funded center for training the developmentally and intellectually impaired. About 800 residents live at 48 cottages, which are organized into 8 facilities, at the center. The 1954-vintage boiler was originally oil-fired and was converted to use natural gas in 1965. Experiments with this boiler involved coburning natural gas with a slurry of pulverized coal in water or oil. Early experiments focused on high levels of coal-water slurry (25% to 60% by power input) to eliminate the boiler derating (decrease in output power) caused by the conversion to natural gas, and to replace oil by a cheap domestic fuel (coal) [72-78], while later experiments focused on low levels of coal-water and coal-oil slurries (5% to 20%) to enhance the radiation of the natural gas flame [79]. The radiation

enhancement experiments at this industrial level, and with a laboratory-scale setup led to a master's thesis [80] and two patents [81-82].

In 1987 a 500 lb/hr Environmental Control Products (ECP) incinerator was donated to ICAAS. The Clean Combustion Technology Laboratory (CCTL) was set up in front of the STC steam plant with the installation and refurbishing of the incinerator. The incinerator was made operational in December 1987 and since January 1988 has been used as an experimental facility for trial burns. It has not been used as a routine operating facility to burn cottage waste from the center.

Until April 1990 the weekly waste from 6 to 16 selected cottages was collected in dumpsters located at each cottage. The dumpsters were hauled to the CCTL site once or twice a week for experimental burns. The dumpsters were emptied with pitchforks onto a conveyor belt leading to the incinerator's hopper.

In May 1990 the dumpsters were removed from the cottages in a beautification effort. The waste from all of the cottages is now collected daily and delivered to a compactor. The compactor compresses and stores the waste. The compactor is emptied twice a day, and the waste is hauled to the Archer landfill. Since May 1990 one day's waste collected from all 48 cottages has been used in experimental burns once every two to eight weeks.

Early experiments have involved coburning cottage waste with locally available biomass [3,83-90], while later experiments have involved spiking the incinerator with polyvinyl chloride (PVC) to measure the effect of hydrogen chloride (HCl) emissions on volatile organic compounds (VOCs) emissions [4-6,91]. Other experiments have involved coburning with coal, paper, or tire chips.

A laboratory-scale combustor has also been set up simulate combustion and emission characteristics of waste disposal and energy recovery systems [92-93].

One of the goals of ICAAS is to avoid chlorinated materials in the waste stream so as to minimize emissions of chlorinated organic compounds. Sociotechnical motivational efforts, such as scoring each cottage or facility based on its waste quality, are used to try to maintain a consistent, low-toxic-producing, free-of-excess-liquids-and-noncombustibles waste stream. Before the dumpsters were removed, a Silver Dumpster award was presented to the cottage with the best scoring garbage. The regular rusty green dumpster for that cottage was replaced the week following a burn with an aluminum painted dumpster with the UF-STC-CCTL logo on it.

#### Incinerator Hardware

The incinerator system [94] (see Figure 2-1) consists of a lower or primary combustion chamber (PCC), an upper or secondary combustion chamber (SCC), a dual ram feeding

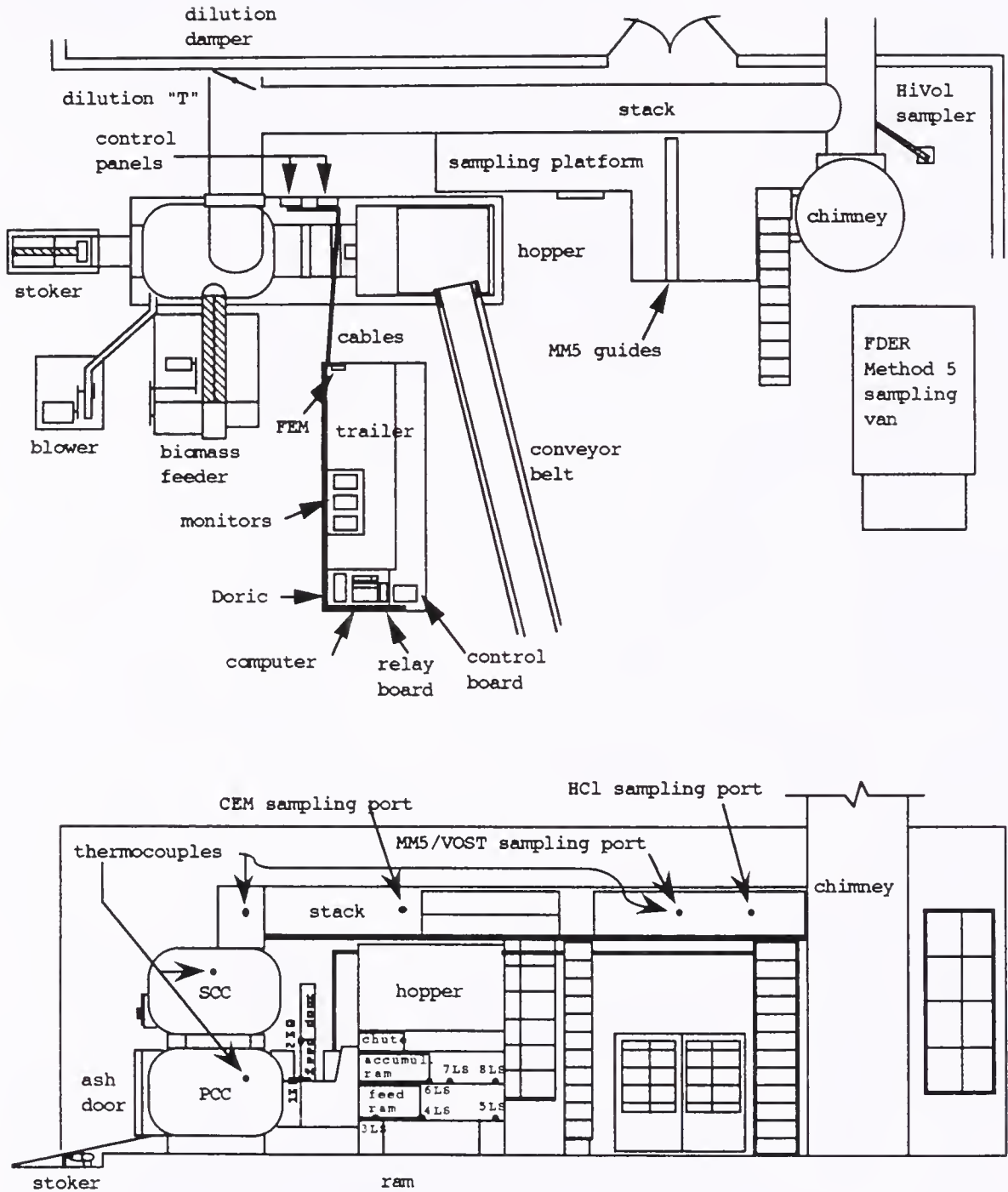


Figure 2-1. Incinerator system layout.

system, a waste hopper, and a biomass feeding system. A conveyor belt brings waste bags into the hopper. A water-cooled stoker with rake fingers pushes unburned garbage back toward the PCC burner and drags ash toward the ash door at the end of the PCC. An external blower (big blower) provides underfire air that comes through eight ports in the bottom of the PCC. The biomass feeding system has a blower (bio blower) for educating the biomass chips into the top of PCC, a main hopper with 12-inch auger, and two side hoppers with 6-inch augers that feed into the main hopper. The bio blower also provides overfire air. Each combustion chamber has a natural gas burner. A main blower provides air to the two burners. An auxiliary blower provides air to the secondary chamber. A butterfly valve (damper) at a "T" in the horizontal portion of the stack allows ambient air to cool and dilute the stack gases. The cooling is necessary since the glass sampling probes used for emissions testing cannot withstand the high temperatures directly from the incinerator. Data from emissions testing is corrected to a standard 7% oxygen content or is normalized to the waste feed rate. Either procedure negates the effect of the dilution air. The gases in the horizontal stack are assumed to be well-mixed by the time (0.9 seconds) they reach the sampling ports. A sampling platform runs the length of the horizontal portion of the stack to facilitate emissions testing. The 100-foot tall chimney provides sufficient draft for the combustion gases and the dilution air.

The incinerator was originally installed at the Veterans Administration hospital in Gainesville, FL, in 1972. In 1986 it was replaced with a larger unit. In 1987 it was donated to ICAAS and set up in front of the Tacachale (then called Sunland Training Center) steam plant. The incinerator is rated at 500 lb/hr of Type 1 waste. Type 1 waste or rubbish is classified as having approximately 25% moisture, 10% ash, and a higher heating value of 6500 BTU/lb. Type 2 waste or refuse is classified as having approximately 50% moisture, 7% ash, and a higher heating value of 4300 BTU/lb. Tacachale's cottage waste typically falls in the Type 1 and Type 2 categories. The two burners are rated at 1.15 MMBTU/hr each, though the PCC burner has been operated consistently at up to 1.8 MMBTU/hr without problem. The PCC and SCC chambers are 6 ft and 5 ft in diameter and 7 ft and 8 ft in length, respectively. The inside walls of the chambers are covered with an approximately 6-inch thick layer of refractory, except at the top of the SCC where it thins out considerably. The 36"-diameter horizontal stack is lined with 2" of refractory.

The additions of the big blower, biomass feeder and blower, stoker, dilution damper, and sampling platform are all modifications made to the incinerator by the CCTL group. The extra blowers convert the incinerator from a starved-air (in the PCC) type to an excess-air type.

### Incinerator Operation

Operation of the incinerator system is as follows: the incinerator is turned on, which fires the PCC and SCC burners; the cooling water to the stoker is turned on; garbage bags are weighed, placed on the conveyor belt, and fed into the hopper while the incinerator is warming up; the auxiliary blower turns on when the SCC temperature reaches 1500 °F; the ram-feed timer is turned on at the end of the 45-minute warm up phase; the ram-feed timer is set at the desired feed interval, usually 7 minutes, and manually held in to trigger the first feed; the stoker control subsystem is turned on and its timer set to operate using the same interval as the ram feeder, but set to trigger 3 minutes after each ram feed; the overfire and underfire blowers are turned on after the second ram feed; the hopper is kept at approximately 2/3 full while garbage remains to be fed; the PCC burner turns on and off as the PCC temperature falls below and rises above 1800 °F; the ram feed timer is turned off after the last bags of garbage are fed in; the stoker is left at the same triggering interval; the incinerator, stoker, and external blowers are shut off at the end of the 2-hour burndown period. Two hours has proved to be a sufficient time to burn out the waste in the incinerator after feeding is done. The stoker cooling water is left on; the ash is removed a day or so later.

The biomass feeder can be operated (turned on and off) manually, or be turned on once and be set to turn off for a

specified length of time with each ram feed. The biomass feeder requires several minutes for the material being fed to first reach the top of the 12-inch auger. The port in the top of the PCC must be open when feeding biomass. The biomass hopper being used is kept about half full and is checked for bridging (biomass arching over the auger) periodically.

### Original Control System

The original control system for the CCTL incinerator consists of temperature-based on/off burner controllers, a temperature-based on/off switch for the auxiliary (SCC) blower, manual on/off switches for the underfire (big) and overfire (biomass or bio) blowers, a timer-based ram-feed charging cycle with PCC upper and SCC lower temperature limits, a timer- and ram-feed-based biomass feed cycle, and a timer and/or ram-feed-based stoker cycle. The ram feeder, biomass feeder, and stoker all have manual on/off switches as well. Most modular incinerators have the same type of electro-mechanical timers and switches found in the CCTL control system.

The original control system circuitry is contained in three panels mounted on the burner side of the incinerator system. A functional schematic of the control circuitry is shown in Figure 2-2. A schematic of the entire control circuitry is shown in Figure A-1 in Appendix A. A detailed

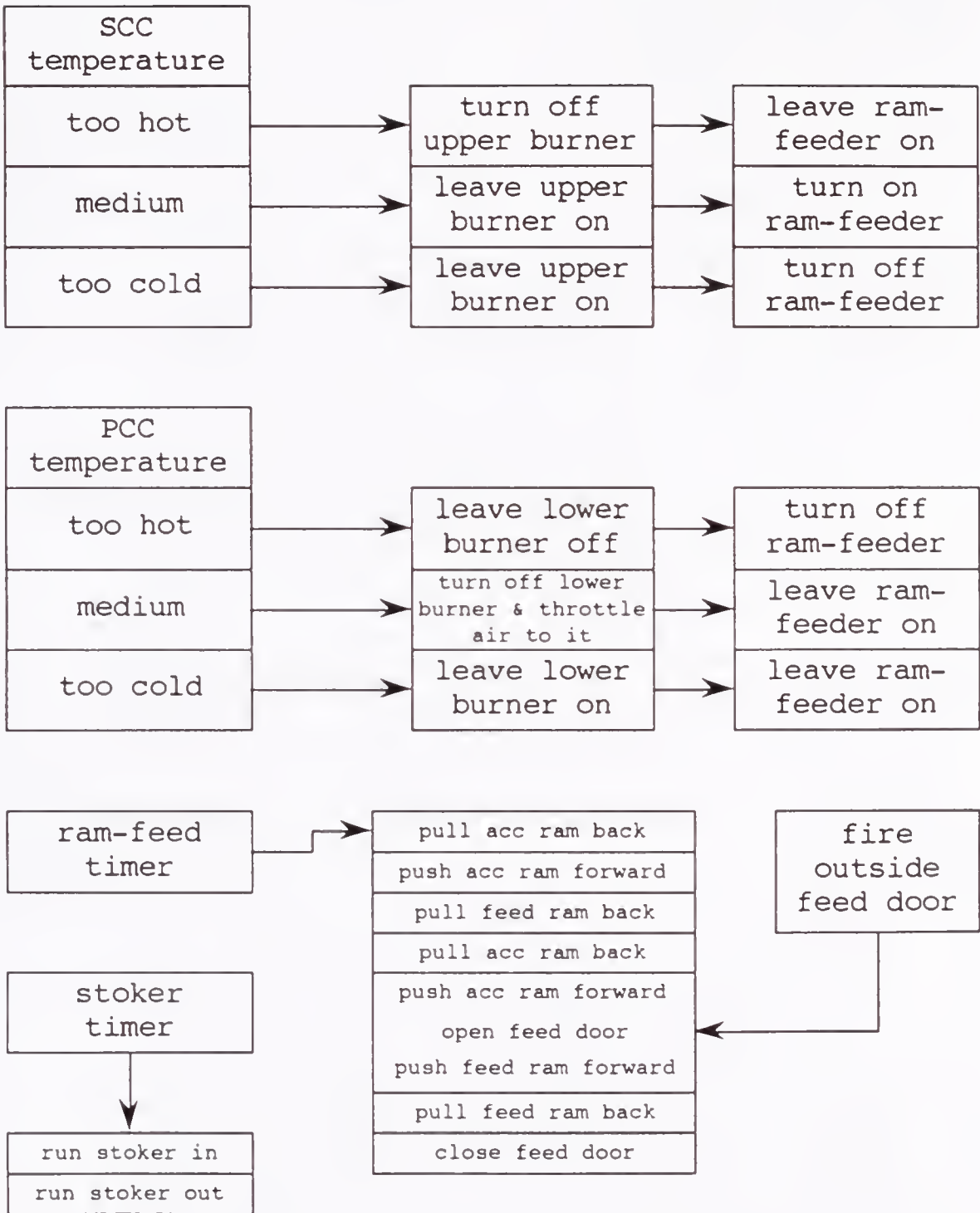


Figure 2-2. Functional schematic of original CCTL incinerator control circuitry.

description of the original control system in also in Appendix A.

The lower right panel contains Honeywell model R4795D and R4795A flame safety controllers for the upper and lower burners, respectively. These burner controllers are powered on and off via Compack API temperature limit switches in the upper right control panel. When powered on, a burner controller opens the valves for its burner. The burner controllers continually read flame rod currents to make sure the burners remain lit. If the flame rod current falls too low, the controller assumes the flame must have gone out and the controller goes into a lockout mode. The controller must then be reset manually by pressing a switch on its outer cover. During normal operation, the SCC temperature is between its two API temperature limits (1500 °F and 2500 °F) and the PCC temperature cycles between being below and between its two limits (1800 °F and 2500 °F).

The CCTL's ECP incinerator has a dual-ram feeding system [94]. Many modular incinerators have only a single ram for feeding the waste, and incorporate an air-lock between the waste and the ram. The dual ram of the CCTL's ECP system negates the need for an external air-lock by using its upper ram as the air-lock.

## CHAPTER 3 INSTRUMENTATION

### Sensors, Monitors, and Sampling Systems

The data acquisition system (see Figure 3-1) consists of a Zenith Z-158 personal computer; a QuaTech expansion board with a 16-channel digital input/output (I/O), 16-channel 8-bit analog to digital (A/D), and 8-channel 8-bit digital to analog (D/A) modules installed in the computer; and a Doric data logger with remote front end module (FEM). The data logger is connected to the computer through a standard RS-232 serial cable. A circuit board containing 6 relays, which convert on/off 110-volt AC signals to 5-volt DC signals, is connected to the digital I/O module. The FEM is installed in one of the incinerator control panels and is connected with a shielded cable to the data logger. The computer, data logger, and relay board are installed in an instrument trailer in front of the incinerator.

The continuous monitoring system consists of temperature, control setting, air flow rate, and stack gas composition monitors. One type-K thermocouple is located in each of the following places: the primary combustion chamber (PCC), the secondary combustion chamber (SCC), the stack before the dilution "T", and the stack at the middle sampling port 260" downstream of the "T". These thermocouples have

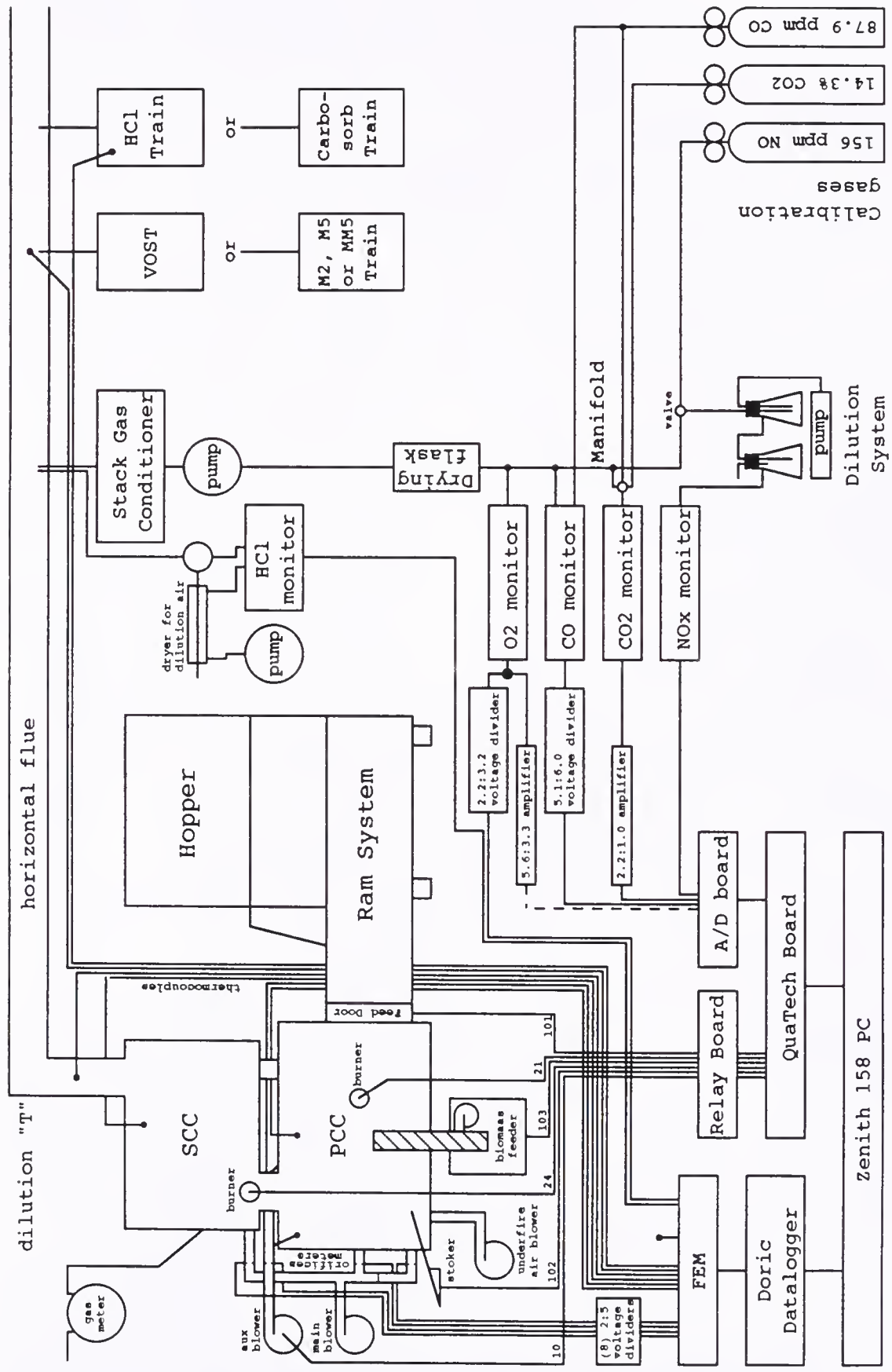


Figure 3-1. Incinerator instrumentation layout.

1/8"-thick leads, which makes them fairly rugged for the environment they are in. The thermocouples are connected to the FEM with type-K thermocouple wire. A thermocouple was installed in the continuous emissions monitoring (CEM) port 100" downstream of the "T" before the CEM system was installed. Another thermocouple has been occasionally installed in the PCC just above the ash door where the combustion gases exit the PCC. The thermocouples in the PCC and SCC are also read by the API temperature limit switches.

The incinerator control panel signal lines for the PCC burner, the SCC burner, the auxiliary blower, the ram feed door, the stoker, and the biomass feeder are connected to the relay board by a 7-wire cable.

Orifice meters are installed in the air lines that run from the main and auxiliary blowers to the two natural gas burners, to the secondary chamber, and to the closed under-fire air port. Honeywell Micro Switch pressure sensors are mounted on the taps around the orifice plates. These 0-1 psi sensors measure total and differential pressure and are wired through 2:5 voltage dividers to the FEM. The pressure sensors have been calibrated by a water U-tube manometer. These orifice plates are located too close (less than 8 diameters downstream and 2 diameters upstream) to bends and disturbances for accurate readings, though.

The CEM sampling line (see Figure 3-1) consists of a 1/2"-inch diameter stainless steel probe, a 11-cm glass fiber filter, a water-cooled condenser, a water collection bowl, a

diaphragm pump, 60 feet of 3/8"-outer diameter polyethylene tubing, a 500-ml drying flask filled with silica gel, and a 5-port sampling manifold. The filter, condenser, bowl, and pump sit up on the sampling platform while the manifold and drying flask are installed inside the instrumentation trailer. The filter is held in a glass filter holder and is backed by a stainless steel frit. The filter holder sits in a box near the stack. The pump sends about 10 standard ft<sup>3</sup>/hr of stack gas sample into the trailer. A vent line is installed before the drying flask so that the pump can draw more stack gas than the instruments require. This allows then instruments to respond faster to changes in the stack gas composition.

Four continuous emissions monitors are installed inside the instrumentation trailer. A Beckman 864 CO<sub>2</sub> monitor, a Beckman 866 CO monitor with zero/span accessories, a Servomex 777 Combustion Analyzer that monitors O<sub>2</sub>, and a Beckman 952A NO<sub>x</sub> analyzer are all connected to the manifold. The CO<sub>2</sub> and CO monitors are nondispersive infrared (NDIR) analyzers. The Servomex uses a paramagnetic cell for measuring O<sub>2</sub> content. The NO<sub>x</sub> analyzer uses the chemiluminescent reaction between NO and O<sub>3</sub> to measure both NO and NO<sub>2</sub>. The NO<sub>2</sub> in the gas sample is reduced to NO in a catalytic converter inside the meter. The meter reads both NO and NO<sub>2</sub> (NO<sub>x</sub>) when the NO<sub>2</sub> is reduced and reads just NO when the NO<sub>2</sub> is not reduced. The meter can read just NO<sub>2</sub> by rapid switching back and forth

between reading  $\text{NO}_x$  and reading NO and subtracting the two signals.

The 14.3%  $\text{CO}_2$ , 87.9 ppm CO, and 156 ppm  $\text{NO}_x$  span gas tanks are installed inside the trailer. The  $\text{O}_2$  analyzer uses ambient air drawn from outside the trailer as a 20.9%  $\text{O}_2$  calibration gas. The  $\text{O}_2$  analyzer has an accuracy of  $\pm 0.1\%$   $\text{O}_2$ . The  $\text{CO}_2$  monitor's accuracy is 0.1%  $\text{CO}_2$ . The accuracy of the CO monitor's is 1 ppm CO. A 7:1 dilution system is installed before the  $\text{NO}_x$  analyzer. The dilution is necessary since the highest range of the  $\text{NO}_x$  meter is only 0-25 ppm and the span tank has 156 ppm  $\text{NO}_x$ . The accuracy of the  $\text{NO}_x$  meter at its highest range is  $\pm 1$  ppm  $\text{NO}_x$ . More details on the use, calibration, and wiring hook-ups of the continuous emissions monitor are in Appendix B.

A new HCl continuous monitoring system was set up in July 1991 (see Figure 3-1). It consists of a glass sampling probe, a glass dilution chamber, a McNeil HC-3 HCl sensor cell, a membrane tube for drying the dilution air, two rotameters, a 24-volt power supply, a load resistor, and a diaphragm pump. The glass probe has a bend at the end. When it is inserted into the stack, the bent end points downstream. The stack gas is therefore drawn into the probe in a direction opposite stack gas flow so that particulate entrainment is minimized.

The analog outputs of the  $\text{CO}_2$ , CO, and  $\text{NO}_x$  monitors are connected to the 0- to 5-volt analog input of the QuaTech A/D

module. The analog outputs of the O<sub>2</sub>, HCl monitors are connected to the FEM.

Particulate concentration in the stack is measured with a standard EPA Method 5 [95] sampling train. This concentration is an integrated average (as opposed to continuous) measurement over an 1-hr sampling time. Hydrogen chloride in the stack is measured by EPA Method 26 [96]. Sampling times of 30 to 60 minutes produce an integrated average concentration. Semi-volatile organic compounds (boiling points greater than 100 °C or vapor pressures between 10<sup>-7</sup> mm Hg and 10<sup>-1</sup> mm Hg) and volatile organic compounds (b.p. less than 130°C or vapor pressures greater than 10<sup>-1</sup> mm Hg) in the stack gas are measured by EPA Modified Method 5 [97] and VOST [98-101] sampling trains, respectively. Modified Method 5 measurements are 1- to 4-hour integrated averages while VOST measurements are 20-minute averages. These four sampling systems use a pump and meter to draw a sample of stack gas through a filter, adsorbent trap, and/or impinger solution to collect the desired pollutant(s). An extended VOST method, which includes sampling for some of the lighter semi-volatile compounds, is being developed by the CCTL group [102-103]. The ash is weighed after each burn and samples of the ash are occasionally analyzed for composition, metal content [104], alkalinity (pH) [105], and leachability. Leachability is determined by using the EPA Extraction Procedure (EP)

Toxicity [106-107] or Toxic Characteristic Leaching Procedure (TCLP) [108] tests.

The data acquisition program records all temperature, control setting, air flow rate, and stack gas readings once every 11 seconds onto a pair of floppy diskettes. The CO<sub>2</sub> and CO readings recorded are actually the average of 10 successive readings, which helps to suppress noise, while the other readings recorded are just single readings. The program automatically can record up to 1800 readings during up to 5.75 hours on each pair of floppy diskettes. Gas meter readings, weather, settings of the underfire and biomass blowers, weights of garbage bags fed, quality of garbage, types of solid fuel(s), biomass continuous feed rate, and sampling times are manually recorded on data sheets.

#### Operations

The CO<sub>2</sub>, CO, NO<sub>x</sub>, and HCl monitors are turned on first and allowed to warm up for at least one hour while the sampling line is set up. At least 15 minutes before garbage is to be fed the data logger, computer, and amplifier are turned on and the data acquisition program is started. The O<sub>2</sub> analyzer is turned on and allowed to warm up. The sampling pumps are started, the CO<sub>2</sub>, CO, and NO<sub>x</sub> monitors are then calibrated (zeroed and spanned), and the O<sub>2</sub> analyzer is calibrated. After all garbage is fed, the calibrations of the CO<sub>2</sub>, CO, NO<sub>x</sub>, and O<sub>2</sub> monitors are checked, and the monitors are shut off. The data acquisition program is

stopped, and the amplifier, computer, and data logger are shut off. The floppy diskettes, containing the continuously monitored data, and any other data recorded by hand (garbage bag weights, HCl sampling time, natural gas meter readings, etc.) are taken back to the office for later analysis.

A typical example of the protocol used for a typical experimental burn at CCTL is shown in Table 3-1. All monitoring, sampling, and analysis procedures closely adhered to quality assurance/quality control (QA/QC) procedures [109] developed for CCTL's Florida Department of Environmental Regulation contract, "Measurement and Minimization of Toxic Incineration Products".

Table 3-1. Typical Protocol for Experimental Burns.

PROTOCOL FOR RUN A22, SATURDAY, SEPTEMBER 7, 1991

-----

Goals: 1. VOST sampling while burning straight good garbage.  
 2. HCl sampling while burning straight good garbage.  
 3. M2 volumetric flow rate measurement.  
 4. HCl (continuous) emissions monitoring.  
 5. NOx (continuous) emissions monitoring.

-----

Get VOST/Carbosorb stuff from Tacachale.	Thu.
Purge VOST and/or Carbosorb traps.	Fri.
Inform Tacachale of burn on Saturday.	Fri.
Bring VOST/Carbosorb stuff out to Tacachale.	Fri./Sat.
Open gate for garbage delivery.	08:15
Start CEM monitors.	09:00
Set up HCl sampling train with grey meter box at far right port.	09:00
Set up VOST/Carbosorb sampling train with blue meter box at M5 port.	
Hook up HCl meter box thermocouple to digital temperature reader.	
Set up stack CEM train.	09:20
Set up HCl CEM train.	
Set up cooling water system.	
Warm up incinerator on natural gas.	
Start computer.	
Calibrate CEM meters.	
Start feeding garbage.	1
Turn on the big and biomass blowers.	
Set ram feed timer to 5.75 minutes so that it feeds every 7.0 minutes.	
Set stoker timer to 5 minutes so that it stokes every 7 minutes.	
Run 1st HCl (A22A) for 45 minutes.	11:00
Run 1st VOST (A22A) for 20 minutes.	11:10
Run 2nd VOST (A22C) for 20 minutes.	12:05
Run 2nd HCl (A22B) for 45 minutes.	
Run 3rd VOST (A22B) for 20 minutes.	12:20
Set up MM5 probe with blue meter box at M5 port.	13:00
Connect probe thermocouple to digital temperature reader.	
Run M2 (A22D) stack gas volumetric flow rate measurement.	
Feed rest of garbage.	13:20
Do burndown and cleanup, with stoker timer set to 5 minutes.	

CHAPTER 4  
REVIEW OF EMISSIONS DATA FROM THE CCTL INCINERATOR

The goal of this review is to seek relationships between the operating conditions and the emissions, with emphasis on determining the effects of fuel rates, temperatures, and oxygen levels on carbon monoxide emissions and volatile organic compound emissions. The relationships found should be useful for control purposes. Rather than generating new emissions data, this review will examine the three years of accumulated emissions data from the CCTL incinerator

Simple relations exist between input rates of garbage, gas, and air and output temperature, output rates of stack gas, and concentrations of  $O_2$ ,  $CO_2$ ,  $H_2O$ ,  $HCl$ . These relations, such as increasing gas input rate raises temperature levels until the oxygen is exhausted, will serve as a basis for more complex models needed for various pollutant emissions. These models can then be analyzed to determine the best operating conditions for lowest emissions of certain pollutants at various input conditions.

High carbon monoxide emission levels have been used to indicate poor combustion conditions in an incinerator [9]. Though CO levels may not correlate well with chlorohydrocarbon (CHC) and principal organic hazardous constituents (POHCs) destruction efficiencies [9], avoidance

of high levels of CO can be a conservative bound on high levels of organic emissions. Benzene (C<sub>6</sub>H<sub>6</sub>), another product of incomplete combustion (PIC), can serve as a surrogate for other PIC and polynuclear aromatic hydrocarbon (PAH) emissions [9].

Particulate emissions is another measure of an incinerator's combustion performance. Semi-volatile organic compounds in the stack often condense on the particulate matter. Free chlorine in the stack gas can chlorinate organic compounds found on particulates and in the stack gas. Metal catalysts, especially cuprous chloride (CuCl<sub>2</sub>), present on particulates can help produce free chlorine from HCl via the Deacon reaction [14-15]:



#### CCTL Trial Burn Data

ICAAS has conducted trial burns at the CCTL incinerator for more than three years. During this time, incinerator operating conditions, temperature and oxygen levels, solid fuel feed rates, and natural gas rates have been monitored for most burns. Input power levels are calculated by multiplying the feed rate of a fuel by its higher heating value (HHV). The higher heating value represents the maximum energy available from the combustion of a fuel. Thermal efficiencies are always based on a fuel's higher heating value. The as-fired HHVs for gas, waste, and biomass are typically 1050 BTU/cuft, 4500 BTU/lb, and 7000 BTU/lb,

respectively. The HHVs for gas and biomass are averages of measured values. The HHV for waste is estimated from the waste's paper, plastic, food stuff, and water content.

Continuous emissions data for CO<sub>2</sub> and CO have been collected for one and one-half years. Particulate emissions were measured using EPA Method 5 [95] over a one year period. Some semi-volatile organic compounds have been detected in the stack gas using EPA Method 0010 [97] but have not been quantitatively measured. Volatile organic compounds (VOCs) in the stack gas have been measured during the last year using VOST [98-101]. Total bottom ash from most burns has been weighed. For several burns the ash has been broken down into categories or into two or three sizes. Fine bottom ash has been periodically analyzed for metal content, alkalinity, and leachability.

Over 1,000,000 temperature, 100,000 oxygen (O<sub>2</sub>), and 20,000 carbon dioxide (CO<sub>2</sub>) and carbon monoxide (CO) data points have been recorded at the CCTL using its continuous emissions monitors. These data were measured on a dry volume basis and have been reduced to single integrated values for each sampling run. Data calculations to determine integrated temperatures and emissions levels are given in Appendix C. The data collected cover a wide range of fuels, fuel loading, and operating conditions. Thirty-nine sampling runs occurred when just non-hazardous institutional waste was burned with natural gas assist. Thirty-three of these runs (see Table 4-1) include data for continuous emissions monitoring of O<sub>2</sub>,

Table 4-1. Results of Measurements Taken During NHW-Only Experimental Burns from 08-31-89 to 08-10-91.

run nbr	date	Sampling	Run Time min	stoker blower	big biomass blower	Natural Gas MHR/HR % of input	Waste MHR/HR % of input	Total Input MHR/HR % of input	Total Output MHR/HR % of input	PCC Temp of	SCC Temp of	Hot stack Temp of	Sample Port Temp of	Stack O <sub>2</sub> %	Stack CO <sub>2</sub> %	Stack CO ppmv	Stack CO ppmv #102	VOST renk- lb/g
K29A	08-31-89	HCl	46	Yes	Yes	2.31 65%	1.22 35%	3.53 69%	2.43 69%	1737	1921	1670	---	17.81	2.40	---	---	---
K30A	09-14-89	[HCl]	36	no/yes	Yes	2.37 62%	1.42 38%	3.79 70%	2.60 74%	1853	2020	1748	692	17.33	3.01	59.00*	230.0*	---
K31A	10-26-89	HCl	60	Yes	Yes	2.41 70%	1.03 30%	3.44 63%	2.84 83%	1804	2015	1751	1748	---	2.52	21.80	---	---
K33	11-05-89	none	60	Yes	Yes	2.27 68%	1.05 32%	3.32 66%	2.66 86%	1833	2029	1772	722	17.93	2.87	12.5	---	---
K35D	12-09-90	none	38	Yes	no	---	---	---	---	1563	1841	1561	549	17.44	1.90	3.53	10.2	---
K36A	01-20-90	none	20	Yes	Yes	1.90 55%	1.54 45%	3.44 62%	2.81 82%	1844	2034	1757	743	16.57	2.95	12.06*	38.8*	---
K36B	01-27-90	none	21	Yes	Yes	1.95 56%	1.56 44%	3.51 61%	2.65 61%	1842	2034	1780	785	17.16	2.96	10.47	39.1	---
K37	01-27-90	none	70	Yes	Yes	1.80 57%	1.45 43%	3.25 59%	2.95 89%	1872	2103	1826	784	17.35	2.44	35.70*	140.0*	---
K39A	02-09-90	HCl	58	Yes	Yes	2.41 64%	1.26 34%	3.67 68%	2.68 73%	1877	2103	1679	697	17.92	2.44	2.99*	131.9*	---
K40A	02-24-90	HCl	30	Yes	Yes	1.98 54%	1.70 46%	3.68 60%	2.26 55%	1829	1951	1703	700	17.84	2.66	4.48	183.0*	---
K41A	03-13-90	HCl	40	no	Yes	2.17 61%	1.42 39%	3.59 60%	2.48 67%	1853	2037	1784	732	17.64	2.66	111.00	433.0*	---
K42	04-26-90	none	20	no	Yes	2.55 64%	1.81 48%	4.36 72%	2.59 55%	1907	1857	1562	642	17.82	2.61	4.01	20.5	---
A03A	06-18-90	HCl, VOST	30	once	Yes	2.65 59%	1.81 48%	4.46 77%	2.48 53%	1922	1817	1631	695	17.64	2.49	5.91	20.9	---
A06C	08-04-90	HCl, 2 VOSTs	60	yes/no	Yes	2.44 60%	1.61 40%	4.05 70%	2.65 63%	1841	1916	1545	632	18.20	2.33	2.38	27.2	---
A07C	08-10-90	HCl, 2 VOSTs	60	Yes	Yes	2.14 50%	1.30 31%	3.44 58%	2.71 64%	1866	1977	1709	701	17.93	3.08	23.53	119.6	2*
A08A	08-24-90	HCl, VOST	30	once	Yes	2.66 69%	1.50 37%	4.16 73%	2.26 50%	1874	1840	1581	643	16.17	2.38	3.19	21.4	5.3*
A09	09-08-90	HMS, HCl	60	no	Yes	2.33 63%	1.59 39%	3.92 66%	2.74 68%	1828	1835	1581	596	17.32	2.31	3.78	19.2	4
A10	09-22-90	[HCl]	60	Yes	Yes	2.22 61%	1.58 39%	3.80 66%	2.67 69%	1853	1946	1866	706	17.50	2.67	4.06	16.6*	---
A11A	10-16-90	[HCl]	60	Yes	Yes	2.25 53%	2.03 47%	4.28 70%	2.56 60%	1782	1870	1869	577	17.86	2.59	---	---	---
A11B	10-16-90	HCl, VOST	60	Yes	Yes	1.59 50%	1.61 50%	3.20 58%	2.56 53%	1723	1907	1863	217	17.84	2.59	5.85*	25.7*	---
A13A	11-10-90	HCl, VOST	60	Yes	Yes	1.96 54%	1.69 43%	3.65 63%	2.85 84%	1760	1888	1633	683	17.71	3.03	1.91	8.3	3
A14A	12-01-90	HCl, VOST	60	no/	Yes	2.10 55%	1.94 45%	4.04 70%	2.59 68%	1773	1866	1611	684	17.63	2.84	6.42	38.1	3
A15A	12-15-90	HCl, VOST	45	Yes	Yes	2.54 63%	1.40 33%	3.94 66%	2.43 62%	1856	1778	1618	614	17.62	3.11	16.77	71.1	9
A16A	01-26-91	HCl, VOST	45	Yes	Yes	1.90 53%	1.54 38%	3.44 58%	2.64 71%	1773	1894	1636	670	17.60	---	---	---	---
A16B	01-26-91	HCl, VOST	50	Yes	Yes	1.87 53%	1.69 40%	3.56 60%	2.64 70%	1780	1922	1627	698	17.71	---	---	---	---
A17E	03-21-91	HCl, 2 VOSTs	45	no	Yes	2.05 48%	2.27 54%	4.32 76%	2.51 58%	1730	1834	1575	663	17.71	---	---	---	---
A18A	04-24-91	HCl, VOST	45	Yes	no	1.98 48%	2.02 58%	4.00 73%	2.21 52%	1813	1860	1618	689	17.67	2.53	7.8	11.7	8
A19A	07-13-91	HCl, 2 VOSTs	45	Yes	Yes	1.98 58%	1.60 44%	3.58 66%	2.57 70%	1878	1920	1686	723	17.85	2.44	2.94	13.4	---
A20E	07-22-91	HCl	45	Yes	Yes	1.68 62%	1.32 40%	3.00 58%	2.57 78%	1768	1926	1667	687	18.07	2.22	1.99	6.3	---
A21A	08-10-91	HCl	45	no/yes	Yes	1.58 50%	1.60 50%	3.18 58%	2.28 72%	1799*	1697*	1447*	700*	18.31*	2.35	2.77	14.9*	---
A21B	08-10-91	none	25	Yes	Yes	1.51 49%	1.61 51%	3.12 58%	2.82 91%	1791*	2021*	1771*	750*	16.31*	2.67	0.28	1.5*	---

\*: Appropriate #: Probably higher due to CO spikes #: Much higher due to CO monitor being pegged \*: one one VOST sample analysed \*: average of two VOST samples

Table 4-2. Results of Method 5 Particulate Measurements Taken During NHW-Only Experimental Burns from 09-27-88 to 08-03-89.

Date	Natural Gas MHR/HR % of input	Total Input MHR/HR % of input	Total Output MHR/HR % of input	PCC Temp of	SCC Temp of	Hot stack Temp of	Cooled stack Oxygen Content % dry	Cooled stack Temp of	Col- lected Volume M <sup>3</sup>	Cool- ing Moist. Content %	Average stack Flow Rate M <sup>3</sup> /sec	Run Time min	Per cent leac- kinetic	Parti- culate Emission lb/hr	Particulate Loading lb/GR/door # 7A O2
09-27-88	1.29 48%	2.68	1.95 73%	1835	1923	1682	16.30*	501	35.53	6.85	21.70	224	100.7	0.62	0.104*
11-08-88	1.52 61%	2.47	1.80 73%	1806	1812	1563	16.17	532	32.25	7.71	23.04	226	60.0	0.63	0.098
12-13-88	1.72 63%	2.77*	2.11*	1768	1804	1604	16.08	536	32.76	7.70	22.05	227	102.9	0.43	0.16*
01-26-89	1.45 48%	1.98 71%	1.83	1831	1819	1619	16.24	534	36.24	2.15	21.41	227	60.0	0.52	0.068
05-05-89	1.35 44%	1.52	2.00 57%	1867	1877	1690	17.76	451	26.93	6.46	21.50	211	60.0	0.51	0.093
08-03-89	1.98 62%	3.22	2.54 79%	1916	1995	1816	17.62	733	27.40	6.58	24.12	201	60.0	0.78	0.113

CO<sub>2</sub>, and CO on a dry basis. Most runs also have HCl and/or VOC sampling data. The other 6 runs (see Table 4-2) of the 39 include data on particulate and O<sub>2</sub> emissions. The CCTL data is analyzed here for relations between incinerator operating parameters and emissions of CO, particulates, and VOC. The VOC data includes benzene and some CHC and aromatic hydrocarbon emissions data. The VOC emissions will be studied here as a group, rather than as individual compounds. Individual chlorinated VOCs will be studied in Chapter 6.

#### Carbon Monoxide Data

Of the 33 sampling/CEM runs, 27 had full data for temperatures, O<sub>2</sub>, and CO. Both the big (underfire) and bio (overfire) blowers were on for 24 of these runs. The CO emissions for these 24 runs were compared to various operating parameters using linear regression analysis. A dimensionless statistical quantity, the coefficient of determination ( $R^2$ ), will be used here as a measure of the "goodness of fit" of a relation between a dependent variable (an output such as CO and other emissions data) and "independent" variables (inputs such as temperature or other operating parameters). Higher values of  $R^2$  indicate better fits, with 1.0 indicating a perfect fit. A more in depth explanation will be given in the Review of Statistical Procedures section in Chapter 6. A computer spreadsheet program was used to generate the linear regression results.

For linear, 2-parameter (1 independent variable and a constant) fits (see Table 4-3), the best  $R^2$ s were for CO versus  $CO_2$  with an  $R^2$  of 0.134; versus PCC temperature ( $T_{pcc}$ ), 0.140; versus SCC temperature ( $T_{scc}$ ), 0.148; and versus hot stack temperature ( $T_{hstk}$ ), 0.138. All other  $R^2$ s were less than 0.07, including CO versus  $O_2$ , though for the most part CO remains low (less than 24 ppmv dry basic or 100 ppmv dry basis corrected to 7%  $O_2$ ) as long as the dry  $O_2$  level is above 17.5%. The high level of oxygen here is due to dilution air being dumped into the CCTL stack. Without the dilution the oxygen level is about 12.4%. An  $R^2$  of 0.118 or more here indicates that, statistically, there is only a 10% probability the data had this relation by random chance (see Review of Statistical Procedures section in Chapter 6).

For quadratic (1 independent variable, its square, and a constant) fits, the  $R^2$ s for CO versus  $T_{pcc}$ ,  $T_{scc}$ , and  $T_{hstk}$  were 0.248, 0.198, and 0.196, with temperatures for minimum CO of 1730 °F (see Figure 4-1), 1805 °F, and 1560 °F, respectively. For an  $R^2$  of 0.248 the equivalent correlation coefficient,  $r$ , is 0.498. These quadratic fits have much improved  $R^2$ s over the linear fits. Bilinear (2 independent variables and a constant) fits for CO versus  $T_{pcc}$  and  $CO_2$  and versus  $T_{pcc}$  and  $O_2$  yielded  $R^2$ s of 0.228 and 0.148, respectively. Adding a  $T_{pcc}^2$  term to these last two fits increased the  $R^2$ s to 0.260 and 0.257, with PCC temperatures for minimum CO emission in the range of 1700 °F to 1760 °F, depending on  $CO_2$  or  $O_2$  concentration (see Figures 4-2 and 4-3).

Table 4-3. Linear Regression Results from CO Data Review.

Functional Relation -----	R <sup>2</sup> -----
CO = 32.34373 - 0.04878 (waste rate)	0.018162
CO = -14.47260 + 14.14515 (gas power)	0.033698
CO = 5.610229 + 2.643393 (input power)	0.001868
CO = 322.9732 - 17.3666 O <sub>2</sub>	0.065774
CO @ 7% O <sub>2</sub> = 1154.305 - 61.5348 O <sub>2</sub>	0.047535
CO = -91.0804 + 39.79183 CO <sub>2</sub>	0.133938
CO = -256.450 + 0.151814 Tpcc	0.140156
CO = -181.205 + 0.102442 Tsc	0.147616
CO = -156.989 + 0.103479 Thstk	0.138074
CO = -315.245 + 0.134705 Tpcc + 33.28944 CO <sub>2</sub>	0.227784
CO = -97.6802 + 0.134535 Tpcc - 7.273719 O <sub>2</sub>	0.148354
CO = 6742.107 - 7.755420 Tpcc + 0.002230 Tpcc <sup>2</sup>	0.248415
CO = 1851.408 - 2.044650 Tsc + 0.000565 Tsc <sup>2</sup>	0.198294
CO = 1542.362 - 1.97369 Thstk + 0.000632 Thstk <sup>2</sup>	0.196317
CO = 4725 - 5.524 Tpcc + 0.001598 Tpcc <sup>2</sup> + 18.50 CO <sub>2</sub>	0.260482
CO = 7930 - 8.472 Tpcc + 0.002433 Tpcc <sup>2</sup> + 2.418 O <sub>2</sub>	0.257185
(gas power) = 2.382266 - 0.16545 (waste power)	0.028966
Tpcc = 1801.244 - 0.03626 (waste rate)	0.001851
Tpcc = 1775.353 + 3.604221 (input power)	0.000597
Thstk = 1903.200 - 64.8644 (input power)	0.094770
Thstk = -162.634 + 0.952666 Tsc	0.984346

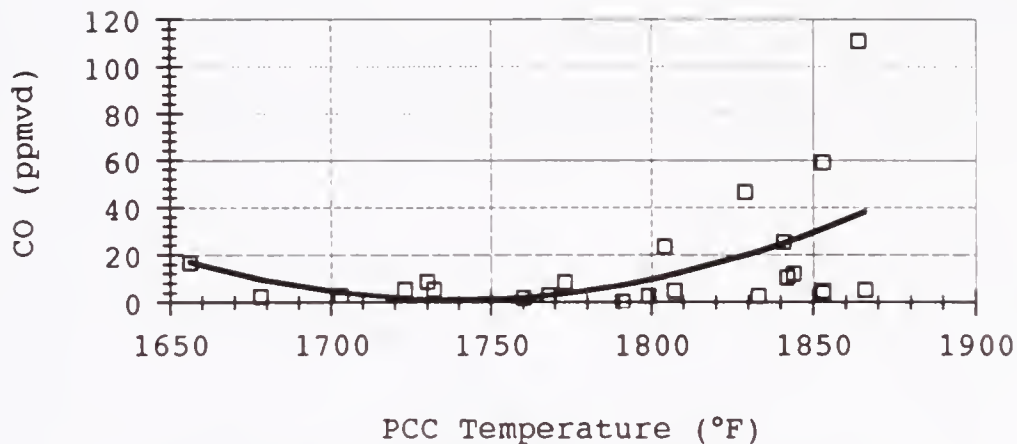


Figure 4-1. Quadratic fit of CCTL carbon monoxide data to primary combustion chamber temperature.

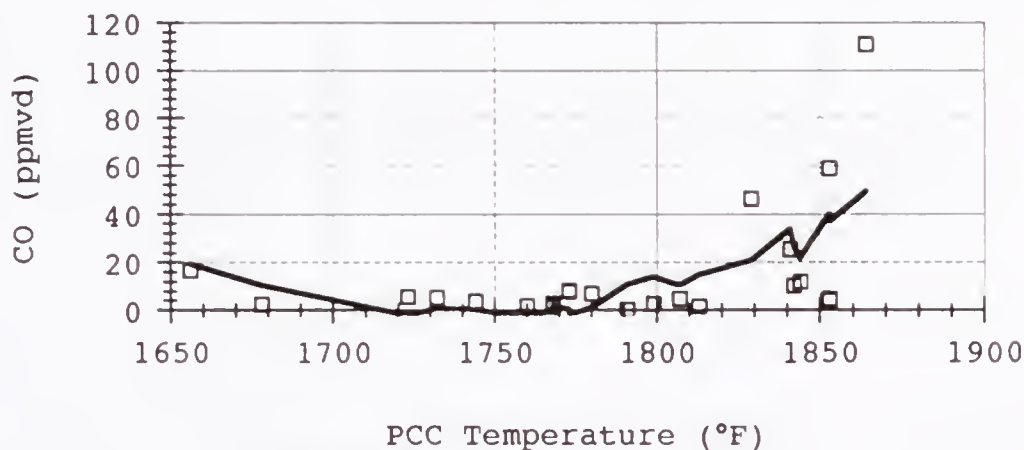


Figure 4-2. Carbon monoxide data fitted with a quadratic function of PCC temperature and a linear function of oxygen concentration.

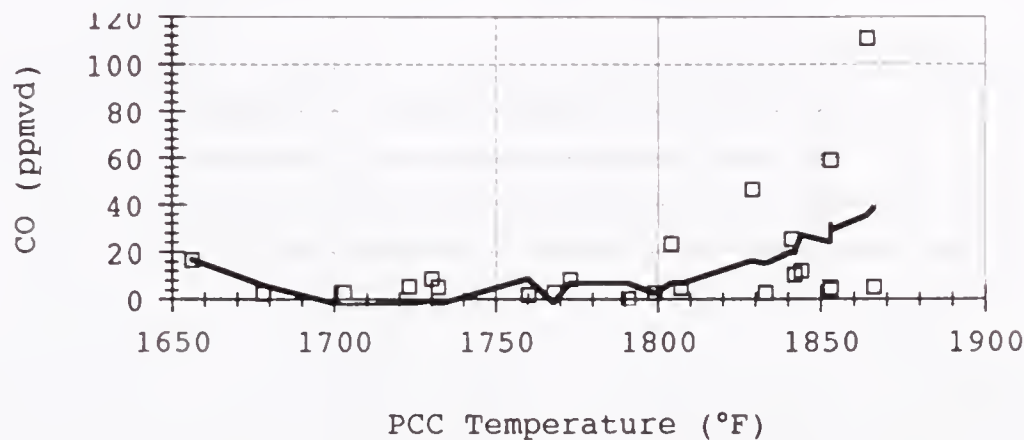


Figure 4-3. Carbon monoxide data fitted with a quadratic function of PCC temperature and a linear function of carbon dioxide concentration.

Particulate Data

Particulate emission results were compared to various operating parameters using linear regression analysis. The best 2-parameter fits (see Table 4-4) were for particulate emission (part) versus stack oxygen content with an  $R^2$  of 0.656 and versus natural gas input power, with an  $R^2$  of 0.765. Higher order fits were not attempted due to the low number of data points. These analyses show that to minimize particulate emissions, the oxygen in the stack should be as low as possible (see Figure 4-4), while the natural gas input should be as high as possible (see Figure 4-5). The result with low oxygen is expected since lower excess air leads to less carry over of particles from the PCC. The result with natural gas is also expected since the combustion of natural gas produces virtual no particulate emissions. However, high natural gas flow rates correspond to low waste feed rates, so there must be some trade-off between waste feed rate and particulate emissions.

Table 4-4. Linear Regression Results from Particulate Data Review.

<u>Functional Relation</u>	<u><math>R^2</math></u>
part = 0.166319 - 0.02840 (input power)	0.426045
part = 0.174602 - 0.05804 (gas power)	0.764566
part = 0.088428 - 0.00354 (waste power)	0.005993
part = 0.362099 - 0.00015 $T_{pcc}$	0.173282
part = 0.192295 - 0.00005 $T_{scc}$	0.065743
part = 0.243911 - 0.00009 $T_{hstk}$	0.237539
part = -0.864920 + 0.052694 $O_2$	0.655576

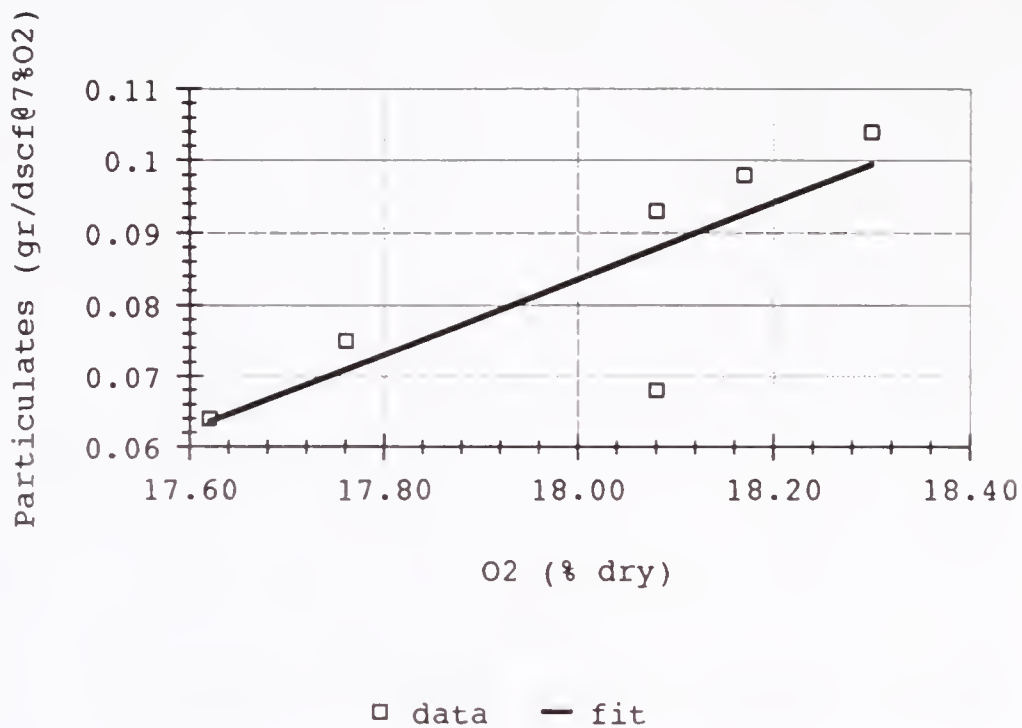


Figure 4-4. Particulate emissions compared to oxygen concentration.

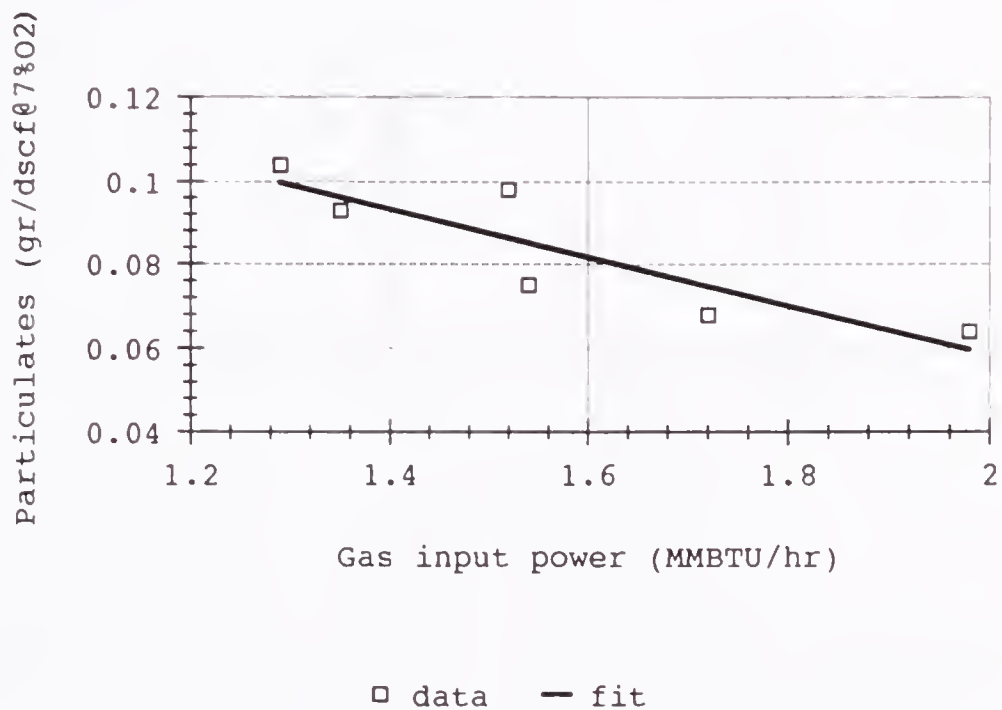


Figure 4-5. Particulate emissions data compared to natural gas input.

### Volatile Organic Compound Data

Eleven of the 33 runs in Table 4-1 occurred during VOST sampling. One of these runs occurred during two VOST samplings. A detailed list of the emissions of 43 volatile organic compounds sampled using VOST for these 12 samples is shown in Appendix D. To facilitate analysis of this data, the results from the twelve samples were ranked from 1 to 12, with the run with rank 1 having the highest number of compounds for which its emissions were the lowest or second lowest and the least number of compounds for which its emissions were the highest or second highest. The ranking scheme used emission values from four different ways of formatting the data: non-blank corrected  $\text{ng}/\text{m}^3$ , blank corrected  $\text{ng}/\text{m}^3$ , non-blank corrected  $\mu\text{g}/\text{kg}$ , and blank corrected  $\mu\text{g}/\text{kg}$  (see Appendix D). Blank correction involves subtracting from the emission value for a compound the amount of that compound that appeared on the field blanks taken along with the samples. The amount appearing on the field blanks is considered a baseline contaminant level. Usually the baseline contaminant level is much less than the emission value.

The final rankings appear in the last column of Table 4-1. For the run with two samplings, the average of the two rankings was used. The rankings were used in linear regression analysis against various combustion conditions. The  $R^2$ s for all analyses are shown in Table 4-5. The best 2-parameter fits were for VOST ranking (vr) versus waste feed

rate (WR) and versus PCC temperature (Tpcc), with  $R^2$ s of 0.255 and 0.140, respectively. VOC emissions fell with increasing PCC temperature and rose with increasing feed rate. For 3-parameter fits, best results were for VOST ranking versus WR and  $WR^2$  (see Figure 4-6) at an  $R^2$  of 0.329, and for VOST ranking versus WR and Tpcc (see Figure 4-7) at an  $R^2$  of 0.646. The curve for the WR- $WR^2$  case yields lowest VOC emissions at a waste feed rate of 315 lb/hr. The signs of the coefficients for the WR-Tpcc case,

$$vr = 59.39418 + 0.35314 \text{ WR} - 0.03774 \text{ Tpcc}, \quad (4-2)$$

are as expected; the positive sign on the WR term indicates that increasing the waste feed rate should increase emissions while the negative sign on the Tpcc term indicates that increasing the temperature should decrease emissions.

Equation 2 can be solved for PCC temperature for a VOST ranking in the lower half ( $vr \leq 6.5$ ):

$$\text{Tpcc} \geq 1402 \text{ }^\circ\text{F} + 0.936 \frac{\text{ }^\circ\text{F}}{\text{lb/hr}} \text{ WR}, \quad (4-3)$$

where PCC temperature is in  $^\circ\text{F}$  and waste feed rate is in lb/hr. For example, with a 400-lb/hr waste feed rate, the PCC temperature should be above 1776  $^\circ\text{F}$ .

The highest ranking VOST data point in Figure 4-7 is far away from the rest of the data points. With this point removed the regression of VOST ranking on WR and Tpcc results in  $R^2=0.773$  and Equation 4-3 becomes

Table 4-5. Linear Regression Results from VOST Data Review.

Functional Relation -----	R <sup>2</sup> -----
vr = 12.69634 - 2.80065 (gas power)	0.093899
vr = -2.53150 + 0.023015 (waste rate)	0.254762
vr = -1.41614 + 2.020129 (input power)	0.032896
vr = 43.32779 - 0.02075 T <sub>pcc</sub>	0.140380
vr = 15.75597 - 0.00485 T <sub>scc</sub>	0.013179
vr = 14.67748 - 0.00496 T <sub>hstk</sub>	0.011315
vr = 81.83877 - 4.22762 O <sub>2</sub>	0.085424
vr = 6.771868 - 0.26058 CO <sub>2</sub>	0.000581
vr = 7.194926 - 0.07187 CO	0.025160
vr = 7.329590 - 0.01956 CO @ 7% O <sub>2</sub>	0.039128
vr = 5.045536 + 0.299665 CO (w/o highest CO)	0.195718
vr = 4.972905 + 0.070243 CO <sub>7%</sub> (w/o high CO)	0.189035
vr=20.92161 - 0.10194 (waste rate) + 0.000161 wr <sup>2</sup>	0.328927
vr=33.10936 - 15.1771 (input power) + 2.131065 ip <sup>2</sup>	0.035105
vr = 129.6102 - 9.57080 O <sub>2</sub> + 0.149382 O <sub>2</sub> <sup>2</sup>	0.085428
vr = -2.52417 + 6.497911 CO <sub>2</sub> - 1.21779 CO <sub>2</sub> <sup>2</sup>	0.000975
vr=59.39418 + 0.035314 (waste rate) - 0.03774 T <sub>pcc</sub>	0.646163
vr (w/o high)=59.40090 + 0.030509 wr - 0.03691 T <sub>pcc</sub>	0.772550
T <sub>pcc</sub> ≥ 1401.54 + 0.93572 (waste rate)	
T <sub>pcc</sub> ≥ 1433.24 + 0.82658 (waste rate) (w/o highest vr)	

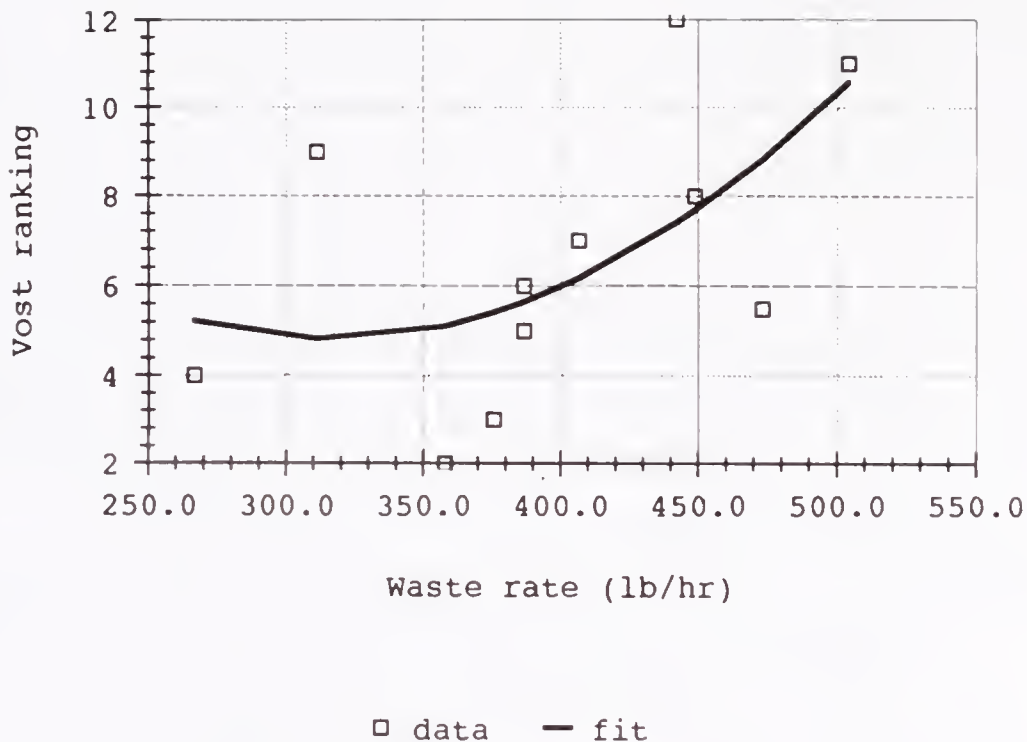


Figure 4-6. Vost emissions compared to waste feed rate.

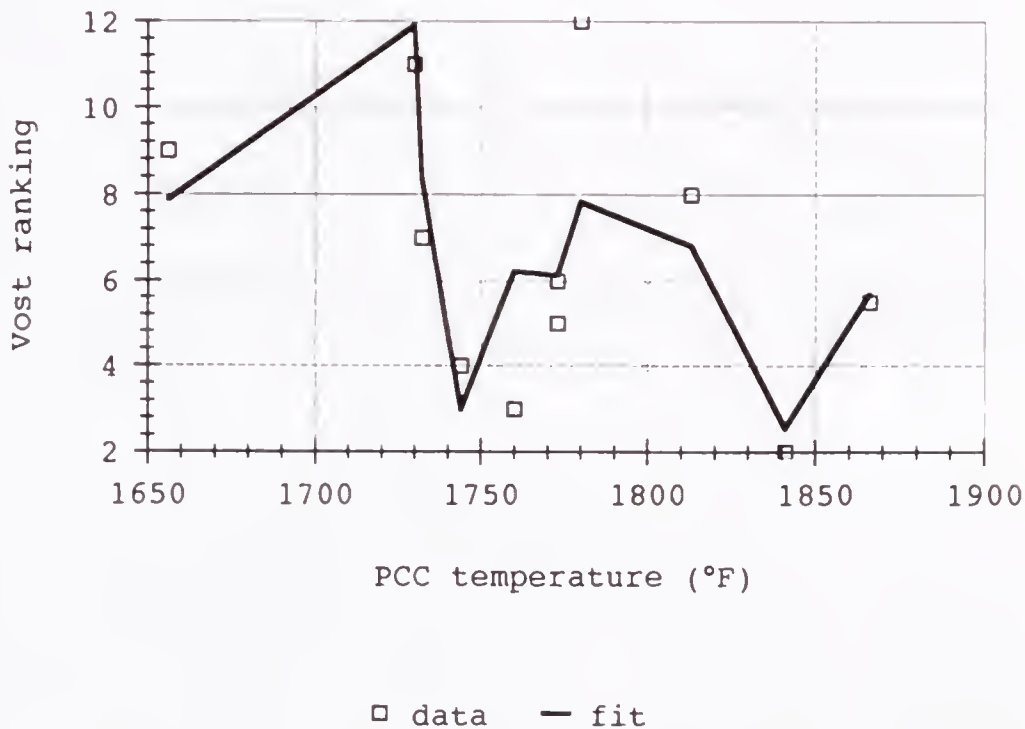


Figure 4-7. Vost emissions compared to PCC temperature and waste feed rate and plotted against temperature.

$$T_{pcc} \geq 1433 \text{ }^{\circ}\text{F} + 0.827 \frac{\text{ }^{\circ}\text{F}}{\text{lb/hr}} \text{ WR}, \quad (4-3)$$

For this equation, a 400-lb/hr waste feed rate yields a minimum PCC temperature of 1764 °F.

#### Summary of Significant Relations

The review of CO emissions data from CCTL shows that to operate the incinerator with low emissions, the diluted oxygen level should be under 17.5% (12.4% undiluted) , the PCC temperature should be about 1730 °F, and the SCC temperature should be about 1805 °F. Particulate data show using low levels of oxygen for low particle emissions. The VOST data show for low VOC emissions to use a 315-lb/hr feed rate, or use a PCC temperature of 1776 °F with a 400-lb/hr feed rate.

CHAPTER 5  
KINETIC MODELLING

Kinetic modelling of the combustion process can show fundamental bases for relationships between inputs to the incinerator, operating conditions, and emissions, whereas an energy analysis code, such as that of Kodres [110-113], will only calculate the temperature and major combustion products for given inputs of waste, air, and support fuel.

The concentration of CO and other minor species can be estimated from a thermodynamic equilibrium analysis. For CO the appropriate equilibrium reaction is



[114] with an equilibrium constant of

$$K_p = p_{\text{CO}} p_{\text{O}_2}^{1/2} p_{\text{CO}_2}^{-1} \quad (5-2)$$

The partial pressures of O<sub>2</sub> and CO<sub>2</sub> at the CCTL incinerator in the stack before the dilution "T" (see Figure 2-1 in Chapter 2) are estimated at 0.097 and 0.068, respectively. These estimates are based on O<sub>2</sub> and CO<sub>2</sub> measurements after the dilution "T" and a dilution factor of 1.5:1 based of mass flow determinations. For an average temperature of 1800 °F (1256 K),  $K_p = 10^{-7.278}$ . Solving Equation 5-2 with these values for  $p_{\text{CO}}$  yields  $p_{\text{CO}} = 1.15 \times 10^{-8}$  or 0.0115 ppm. Actual

values of CO at the same location average about 20 ppm. Therefore, equilibrium analysis is not realistic enough to describe the emissions from an incinerator.

Kinetic modelling also can show how minimizing toxic formation and maximizing toxic destruction are related. These relationships can be used to create or fine-tune empirical models (like those derived from reviewing test data) useful for controlling incinerator emissions.

A typical gaseous chemical reaction is of the form



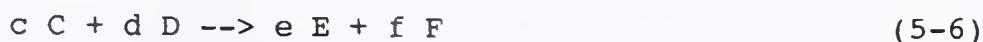
The kinetic reaction rate,  $k$ , is of the Arrhenius form,

$$k = A T^n \exp(-E_a/(R_u T)), \quad (5-4)$$

where  $A$  and  $n$  are constants for the reaction,  $T$  is the absolute temperature,  $E_a$  is the activation energy of the reaction,  $R_u$  is the universal gas law constant. The constant  $n$  is zero for most reactions. The ratio  $E_a/R_u$  is often listed in tables of chemical reaction rate parameters instead of just  $E_a$ . The change of concentration of the species in the above reaction is given by

$$\begin{aligned} -d[EG]/dt &= -d[J]/dt = d[E]/dt = d[GJ]/dt = k[EG][J] \\ &= [EG][J] A T^n \exp(-E_a/(R_u T)) \end{aligned} \quad (5-5)$$

For a more complex example,



equation 5-5 would become,

$$\begin{aligned} -\frac{1}{c} \frac{[C]}{dt} &= -\frac{1}{d} \frac{d[D]}{dt} = \frac{1}{e} \frac{[E]}{dt} = \frac{1}{f} \frac{d[F]}{dt} = k[A][B] \\ &= [A][B] A T^n \exp(-E_a/(R_u T)) \end{aligned} \quad (5-7)$$

The units of the constant A depend on the number of reactant species. For a system of reactions, the solution for the time-dependent concentrations of the species involved requires the solution of a coupled set of nonlinear differential equations.

A chemical pyrolysis/kinetics code for modelling coal-water-gas combustion [115-116] was modified for studying emissions from a modular incinerator. The code now uses the LSODE routine [117] to numerically solve the coupled kinetic differential equations. The LSODE routine is a Gear-type solver for stiff equations, such as those used in chemical kinetics. The reactions and their rate parameters are now in a data file that is read by the code. Inputs of species to the combustion system are now in lb/hr. The species' amounts are now calculated, displayed, and printed in kmol/hr. The concentration of the third body M is calculated as the total concentration of all species at each time step. The third body is used for energy transfer in reactions where a molecule is split into two or where two molecules recombine. The code is outlined in Figure 5-1 and listed in Appendix E. The code is currently run on the DEC VAX cluster at CIRCA at the University of Florida. It has also been run on SUN SPARC workstations. A typical run takes 2-3 minutes on the VAX as

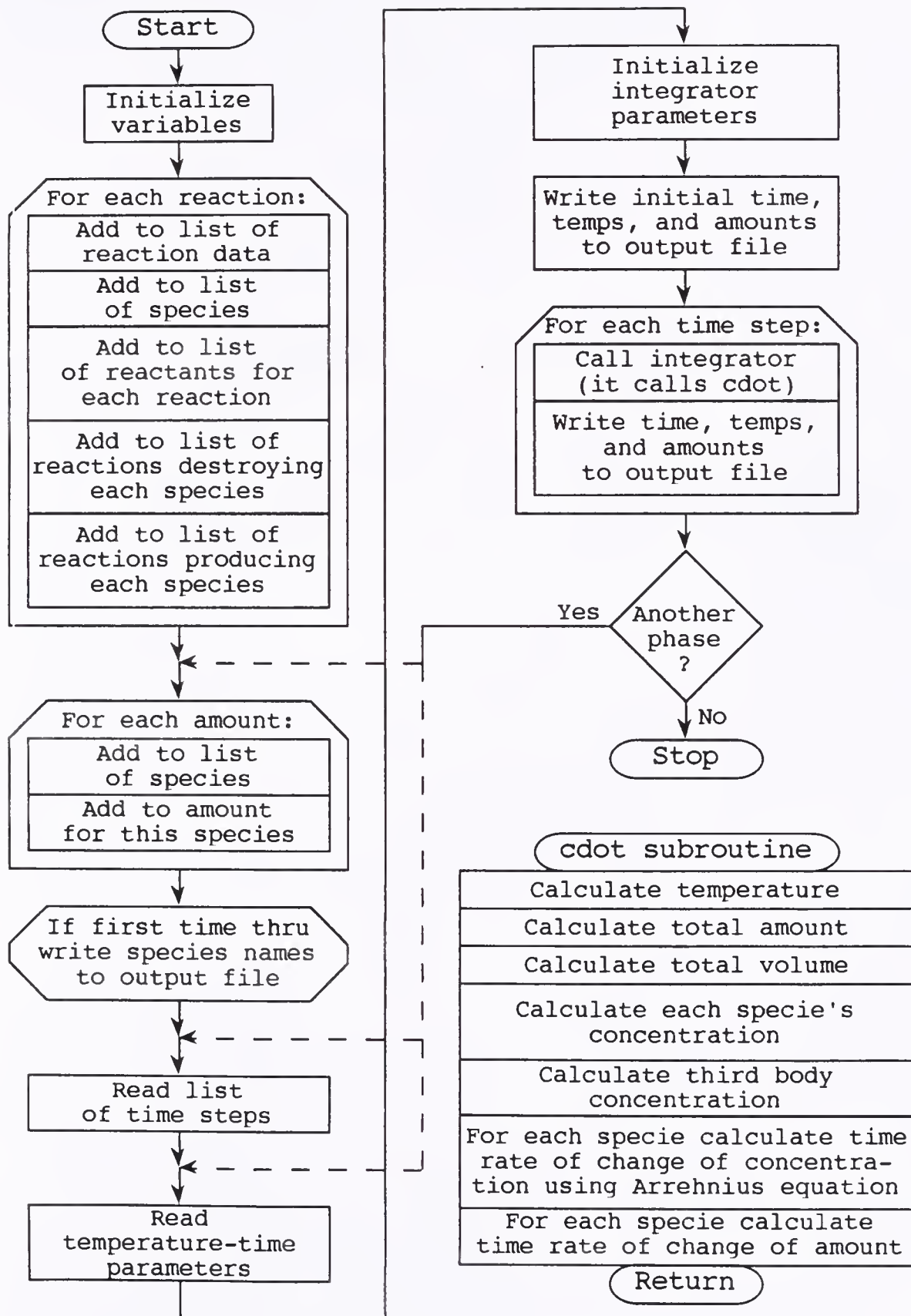


Figure 5-1. Kinetics code program flowchart.

opposed to an estimated 6-7 hours on an 4.77-MHz 8088-powered IBM PC.

Most of the reaction rates in the code input file (see Appendix F) were compiled from various sources [118-120]. Where reaction rates were not known estimates were generated from thermal destruction [121-124] and from similar reaction mechanisms. To get to gas-phase reactions the code uses a simplistic yet reasonable pyrolysis process. Semi-global reaction rates for the formation of chlorinated and non-chlorinated benzene, phenol, furan, and dioxin were developed in modelling data from the Pittsfield-Vicon incinerator study [1,7,125]. This modelling is still going on by the CCTL.

The kinetics code was written by CCTL to give quick results when studying combustion and pyrolysis processes. A commercial code could have been used, but using a code that one has written oneself has many advantages: the code can be modified at will to adapt to the problem at hand; the code can be made to run on existing hardware; the input to and output from the code can be made into any convenient form; and writing one's own code forces one to learn the fundamentals of the process. There are currently no reasonably-sized (mainframe computer-sized) kinetic models for chlorohydrocarbon combustion [126].

Rather than keeping track of heat of reactions, heat transfer, and combustion gas temperature, the code requires a temperature-time profile be imposed. This avoids modelling the heat transfer characteristics of the combustion system

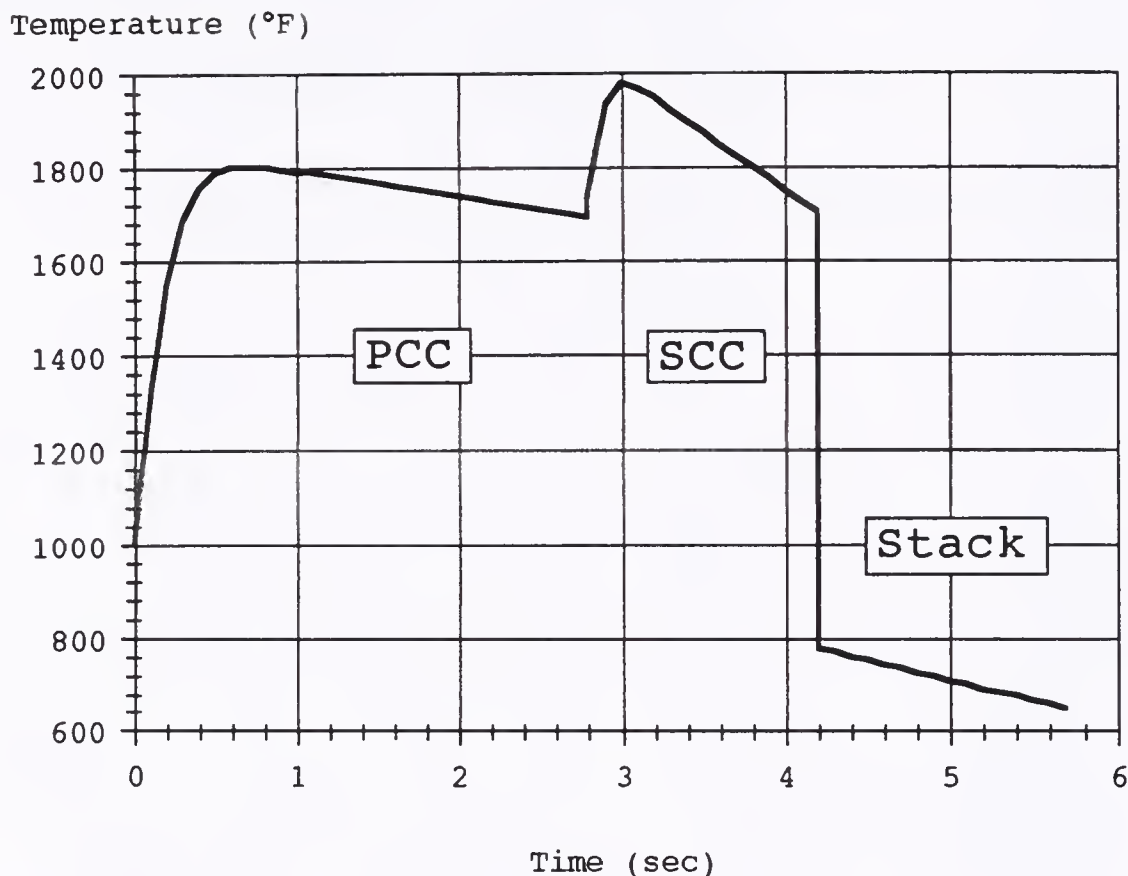


Figure 5-2. Temperature-time history for CCTL incinerator.

and greatly simplifies the computer code. A typical temperature-time profile for the CCTL incinerator is shown in Figure 5-2. This profile is based on measurements of flow rate and temperature at various places along the path of the combustion gases through the CCTL incinerator (see Appendix G). The code starts after the heating of a slug of pre-mixed input materials to 1000 °F. The code then follows the slug of gases as it travels through the incinerator along the temperature-time profile. The rapid rise in temperatures in the PCC and SCC as shown in Figure 5-2 is due to the heat released from the natural gas burners and waste combustion in

the PCC. The end of the profile at 5.7 seconds is at the end of the horizontal stack. The sampling ports for M5, VOST, and HCl are at 5.1 seconds. The sudden drop off after the SCC is due to the dilution "T" (see Figure 2-1 in Chapter 2) where ambient air is drawn in, diluting and cooling the stack gas. Since this code uses no fluid dynamics, the gaseous species are assumed to be instantly mixed and cooled when more air is added at the dilution "T" and instantly mixed when natural gas and air is added at input to the SCC. The code stops generating output when the slug reaches the 5.1-second sampling ports.

#### Inputs to the Code

The code requires an input file divided into four sections (see Appendix F). The first section lists, for each reaction, the chemical formula, the Arrhenius reaction rate constants ( $A$ ,  $n$ ,  $E_a/R_u$ ) ( $\text{kmol}/\text{m}^3\text{-K}$  based), and, if known, the enthalpy of reaction ( $\text{kcal}/\text{kmol}$ ), though it is not used by the code. By keeping the reaction and their rates in a data file instead of the main program, the program is made generic and does not have to be recompiled for a different set of reactions. The second section lists the input rates (in  $\text{lb}/\text{hr}$ ) of chemical species into the incinerator. The third section lists the time steps for which the code will produce output. The fourth section lists the temperature-time profile parameters. For simulating processes such as the CCTL incinerator with consecutive, different temperature-time

profiles and multiple input locations, the second, third, and fourth sections may be repeated with the new inputs as needed. The output file of the code lists the time, temperature, and effluent rate (in kmol/hr) of the various species at each time step. For the CCTL, the final time step ends where the combustion gases reach the sampling ports 260 inches downstream of the "T" at 5.1 seconds.

#### Waste Composition

The waste in the code is composed of five parts: water, polystyrene, PVC, ash, and a garbage "molecule". The pyrolysis/kinetics code was previously developed for a macromolecular model for the structure of coal with unit molecule such as  $C_{35}H_{26}O_3A$  [115-116], which is compatible with the mass fractions of carbon, hydrogen, oxygen, and ash (with an "atomic weight" of 50) for coal. The institutional waste at Tacachale contains about 25% by weight water, and 7% by weight ash, with the bulk mainly made up of plastics, paper, and some food stuffs (see Table 5-1). The coal pyrolysis model is used here since garbage, like coal, can be modelled to be made of large molecules due to its paper, plastic, and food stuff components.

To be compatible with typical measurements of  $O_2$ ,  $CO_2$ ,  $H_2O$ , and HCl in the stack at CCTL, 400 lb of waste was modelled to consist of 100 lb of water, 20 lb of polystyrene, 2 lb of PVC, and 278 lb of garbage "molecules". In the code, the PVC accounts for all of the chlorine in the waste. The

Table 5-1. Cottage Waste Characterization of 02-24-90  
(6 bags, all values in pounds).

Cottage	Paper and Cardboard	Plastic	Styrofoam	Ferrous Metal	Non-Fer. Metal	Rubber	Food	Cloth	Glass	Total
Peach	2.00	2.00	0.14	0.11	0.08	0.05	0.25	0.00	0.00	4.63
Tulip	3.10	2.10	0.00	0.00	0.00	0.00	0.00	0.00	0.00	5.20
Poplar	2.75	2.10	0.05	0.04	0.00	0.04	3.40	0.00	0.00	8.38
Pansy	4.00	1.75	2.00	0.00	0.05	0.11	1.25	1.00	0.00	10.16
Marigold	3.25	4.00	0.05	0.06	0.00	0.02	0.77	0.00	0.00	8.15
Lily	4.20	3.25	0.20	0.58	0.01	0.15	0.76	0.00	0.66	9.81
Totals	19.30	15.20	2.44	0.79	0.14	0.37	6.43	1.00	0.66	46.33
% by wt.	41.7%	32.8%	5.3%	1.7%	0.3%	0.8%	13.9%	2.1%	1.4%	

278 lb of garbage molecules includes 28 lb of ash. The unit molecular formula of the garbage is taken as  $C_{21}H_{42}O_{21}A$ , with a molecular weight of 701, where the ash "atom" A has an atomic weight of 71. This molecular weight is comparable to those used for coal molecules in the old pyrolysis/kinetics code, and used a set of C, H, and O empirical coefficients that were closest to whole numbers.

### Pyrolysis Steps

The breakdown of the garbage molecule occurs here in three pyrolysis steps, modelled after the coal pyrolysis process used in the pyrolysis/kinetics code:



The coal pyrolysis model is used here since the pyrolysis of garbage, like coal, can be modelled as the breakdown of large molecules. In the first step, all oxygen is driven off as loosely bound  $CO_2$  and  $H_2O$ , leaving a tar. In the second step, the remaining hydrogen is driven off as  $CH_2$ , leaving a char. In the third step, the char breaks down into  $C_2$  and ash. The  $CH_2$  and  $C_2$  enter into the combustion process as they are evolved. In the kinetics code the ash is ignored since it is never considered a gaseous component. The same reaction or decay rate is used for each of these steps:

$$k = 1000 \left( \frac{T}{3000 K} \right)^7 \text{ sec}^{-1} \quad (5-11)$$

This reaction rate was developed from modelling coal mass loss versus temperature and time data from Massachusetts Institute of Technology (MIT) [115-116,127]. Carbon monoxide levels increase by about 10% if the 1000 constant in Equation 5-11 is doubled to speed up the pyrolysis process.

The polystyrene first breaks down into its monomer styrene, which then breaks down into benzene and acetylene (see Figure 5-3). The PVC breaks down directly into HCl and acetylene. These breakdowns were modelled from thermal destruction of polymers [121-124]. The aromatic sequence is based on work by Green et al. [4,7,125].

#### Results from the Kinetics Code

Typical inputs of natural gas to the CCTL are 30 and 37 lb/hr of  $\text{CH}_4$  to the PCC and SCC, respectively. Typical waste input is 400 lb/hr (100 lb/hr of water, 20 lb/hr of polystyrene, 2 lb/hr of PVC, 250 lb/hr of ash-free garbage "molecules", and 28 lb/hr of ash). The ash is not actually included in the input file. Typical air inputs are 2679, 2679, and 9911 lb/hr to the PCC, SCC, and dilution "T", respectively. The air consists of 76.08% by weight  $\text{N}_2$ , 22.98%  $\text{O}_2$ , and 0.94%  $\text{H}_2\text{O}$ . The water content (1.5% by volume) in the air is due to the high humidity typically found in Florida. These inputs, with peak PCC and SCC temperatures of 1800 °F and 1975 °F, are considered the base case (Run 30) here. The output for this base case is listed in Appendix H

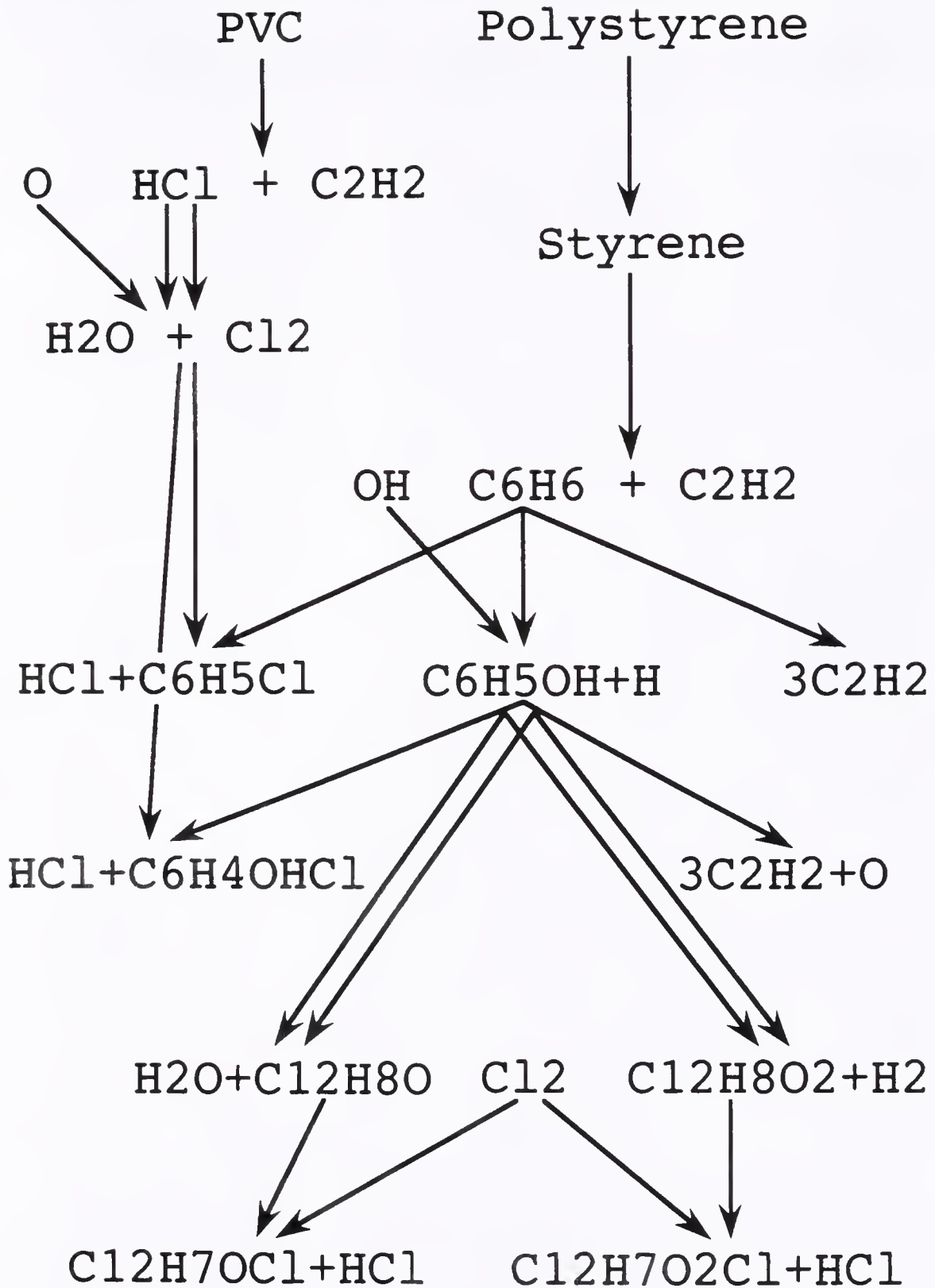


Figure 5-3. Kinetic aromatic and chlorination sequences.

and graphed in order decreasing emission rate in Figure 5-4. For all cases examined, excluding  $N_2$ ,  $O_2$ , and  $H_2O$ , the species' amount change little after the dilution "T" at 4.2 seconds. The sudden drop in temperature appears to halt most reactions.

The first kinetic code runs (Runs 1-19) used various waste pyrolysis rates to get the garbage, tar, and char burnouts in the appropriate range and do not yield results comparable to the later ones examined here.

Initial kinetic model studying (Runs 20-29) examined the effects on carbon monoxide and benzene due to varying the temperatures in the PCC and SCC, while keeping waste, air, and gas rates constant. For minimal carbon monoxide emission, the optimal peak PCC and SCC temperatures are 1875 °F and 2050 °F, respectively (see Table 5-2). This would correspond to measured temperatures of about 1850 °F for the PCC at 1 second in the temperature-time profile (see Figure 5-2) and about 1925 °F for the SCC at 3.5 seconds. These times are where the thermocouples are located in the temperature-time profile. For minimal benzene emission, optimal peak PCC and SCC temperature are 1900 °F and 2025 °F, respectively (see Table 5-2). This would correspond to measured temperatures of about 1875 °F for the PCC and about 1900 °F for the SCC. The residence time for each chamber was kept constant for these cases since the residence time decreases only 1% for each 25 °F rise in temperature (due to

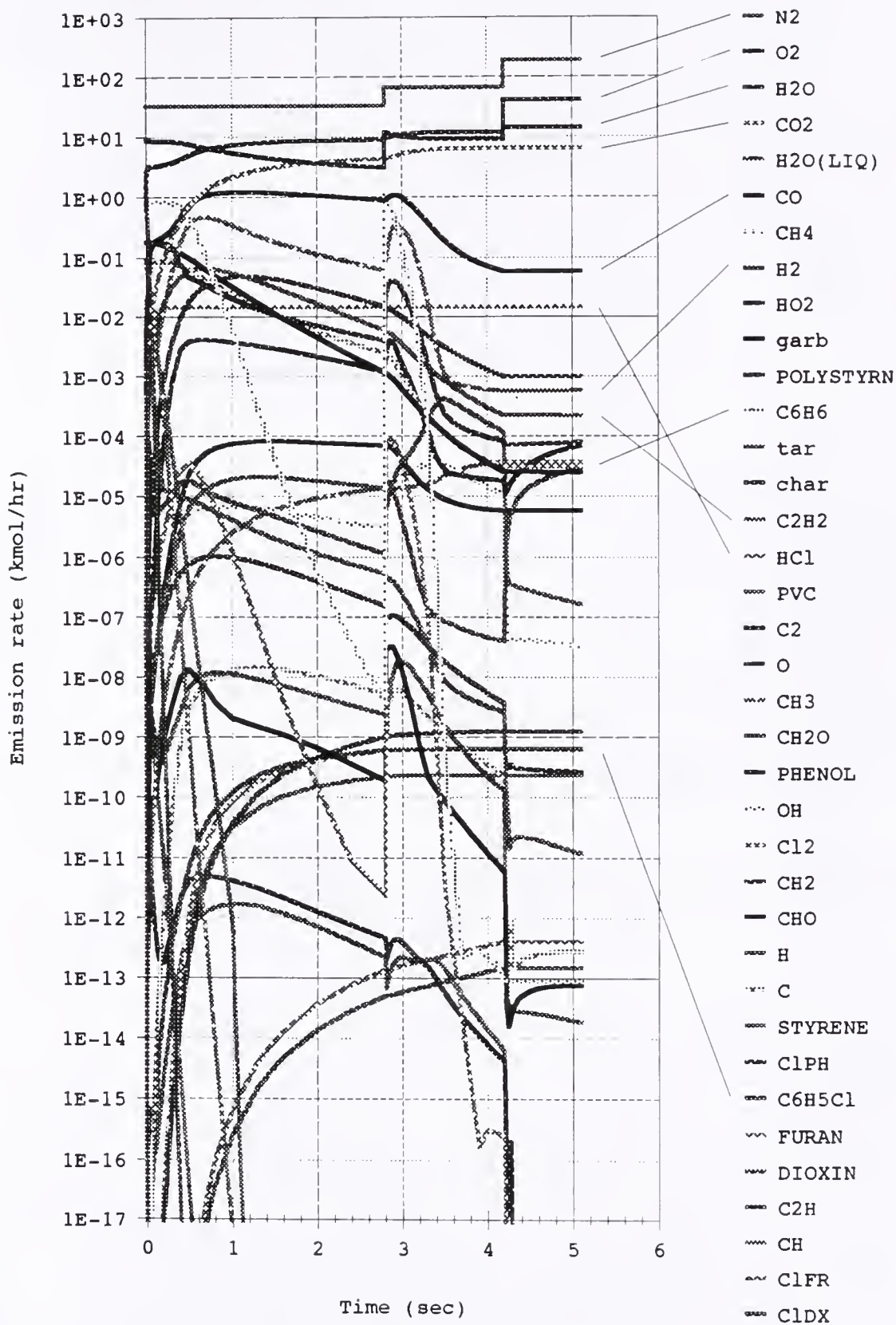


Figure 5-4. Base case (Run 30) kinetics code output.

Table 5-2. Kinetics Code Results.

Run	%	PCC air	SCC air	SCC waste	PCC gas	SCC gas	Tpcc max	Tscc max	O2 -kmol/hr--	CO2 hr--	HCl ---mol/hr---	CO hr---	C6H6 hr	C6H5Cl nmol/hr	O2 % dry	CO2 % dry	CO ppmvd	C6H6 µg/kg	C6H5Cl ng/kg
20	100	100	100	400	30.0	37.0	1875	2024	41.3	6.39	14.5	17.2	0.72	0.381	17.52	2.71	73	308	164
21	100	100	400	30.0	37.0	1899	2024	41.3	6.38	14.5	22.2	0.27	0.314	17.52	2.71	94	115	135	
22	100	100	400	30.0	37.0	1851	2024	41.3	6.39	14.5	15.6	1.68	0.458	17.52	2.71	66	722	197	
23	100	100	400	30.0	37.0	1801	2024	41.3	6.38	14.5	18.4	6.95	0.627	17.52	2.71	78	2988	270	
24	100	100	400	30.0	37.0	1825	2024	41.3	6.39	14.5	16.3	3.75	0.547	17.52	2.71	69	1612	235	
25	100	100	400	30.0	37.0	1850	2000	41.3	6.37	14.5	31.3	3.71	0.462	17.52	2.70	133	1595	199	
26	100	100	400	30.0	37.0	1900	2000	41.3	6.35	14.6	51.3	0.55	0.312	17.52	2.69	218	235	134	
27	100	100	400	30.0	37.0	1850	2048	41.3	6.40	14.5	7.9	0.74	0.460	17.52	2.72	33	318	198	
28	100	100	400	30.0	37.0	1825	2048	41.3	6.39	14.5	8.6	1.49	0.546	17.52	2.71	37	641	235	
29	100	100	400	30.0	37.0	1875	2048	41.3	6.40	14.5	7.3	0.29	0.384	17.52	2.72	31	126	165	
30	100	100	400	30.0	37.0	1800	1975	41.3	6.34	14.6	58.2	30.50	0.636	17.52	2.69	247	13112	273	
31	120	80	400	30.0	37.0	1800	1975	41.3	6.34	14.6	63.3	30.50	0.546	17.52	2.69	269	13112	235	
32	110	90	400	30.0	37.0	1800	1975	41.3	6.34	14.6	60.6	30.50	0.589	17.52	2.69	257	13112	253	
33	90	110	400	30.0	37.0	1800	1975	41.3	6.34	14.6	56.3	30.50	0.685	17.52	2.69	239	13112	294	
34	80	120	400	30.0	37.0	1800	1975	41.3	6.34	14.6	55.3	30.50	0.737	17.52	2.69	235	13112	317	
35	100	100	350	42.5	37.0	1800	1975	41.2	6.13	13.1	57.6	26.70	0.326	17.50	2.60	245	13118	160	
36	100	100	300	54.9	37.0	1800	1975	41.0	5.92	10.9	57.7	23.00	0.139	17.45	2.52	246	13184	80	
37	100	100	450	17.6	37.0	1800	1975	41.4	6.55	16.0	59.0	34.30	1.190	17.54	2.78	250	13107	455	
38	100	100	250	67.4	37.0	1800	1975	40.9	5.71	8.8	60.5	19.10	0.053	17.43	2.43	258	13138	36	
39	100	100	450	20.7	37.0	1800	1975	41.2	6.64	16.0	62.3	34.30	1.080	17.46	2.81	264	13107	413	
40	100	100	350	39.4	37.0	1800	1975	41.3	6.05	13.1	54.5	26.70	0.356	17.54	2.57	232	13118	175	
41	100	100	300	48.7	37.0	1800	1975	41.4	5.75	10.9	51.0	22.90	0.165	17.60	2.44	217	13126	95	
42	100	100	250	58.0	37.0	1800	1975	41.4	5.46	8.8	48.5	19.10	0.067	17.62	2.32	206	13138	46	
43	90	90	360	27.0	33.3	1800	1975	40.4	5.70	13.1	52.4	27.40	0.572	17.71	2.50	230	13088	273	
44	100	100	450	30.0	37.0	2004	2087	40.7	6.96	16.0	13.8	6.2E-05	0.189	17.27	2.95	59	2.4E-02	72	
45	100	100	400	42.5	37.0	2004	2087	40.5	6.75	14.5	14.3	5.5E-05	0.104	17.21	2.87	61	2.4E-02	45	
46	95	100	400	30.0	37.0	1877	2012	40.3	6.38	14.5	27.9	0.97	0.350	17.24	2.73	119	416	150	
47	95	95	400	30.0	37.0	1877	2065	39.4	6.40	14.5	8.6	0.14	0.350	17.07	2.77	37	60	150	
48	95	105	400	30.0	37.0	1877	1975	40.8	6.33	14.6	70.5	2.84	0.351	17.35	2.69	300	1221	151	
49	100	95	400	30.0	37.0	1800	2012	40.8	6.37	14.5	26.6	10.40	0.632	17.42	2.72	114	4471	272	
50	100	105	400	30.0	37.0	1800	1933	41.8	6.25	14.5	138.0	82.10	0.640	17.55	2.62	579	35295	275	
51	105	105	400	30.0	37.0	1730	1893	42.3	6.05	14.6	311.0	698.00	0.820	17.65	2.52	1298	300071	353	
52	105	100	400	30.0	37.0	1730	1933	41.8	6.21	14.6	165.0	332.00	0.810	17.55	2.61	693	142727	348	
53	105	95	400	30.0	37.0	1730	1975	41.3	6.35	14.6	79.3	123.00	0.797	17.52	2.69	336	52878	343	
54	100	95	400	30.0	37.0	1800	2019	40.8	6.38	14.5	22.6	8.35	0.631	17.42	2.72	96	3590	271	
55	100	95	400	30.0	37.0	1800	2060	40.4	6.39	14.5	8.8	1.48	0.627	17.43	2.76	38	636	270	
56	95	100	400	30.0	37.0	1877	2020	40.8	6.38	14.5	20.2	0.73	0.385	17.42	2.72	86	313	166	
57	90	100	400	30.0	37.0	1963	2066	40.4	6.40	14.5	10.4	2.9E-03	0.208	17.43	2.76	45	9.4E-01	89	
58	85	100	400	30.0	37.0	2055	2115	39.9	6.40	14.5	6.0	1.9E-07	0.122	17.40	2.79	26	8.2E-05	52	
59	80	100	400	30.0	37.0	2158	2167	39.5	6.41	14.4	1.1	3.3E-14	0.079	17.33	2.81	5	1.4E-11	34	
60	75	100	400	30.0	37.0	2272	2221	39.1	6.41	14.2	0.112	2.6E-26	0.056	17.34	2.84	0.50	1.1E-23	24	
61	70	100	400	30.0	37.0	2398	2279	38.6	6.41	14.2	0.004	2.6E-29	0.042	17.31	2.87	0.02	1.1E-26	18	

gas's higher velocity), and the accuracy of the residence time calculation is at best 5%.

Non-chlorinated benzene emissions were calculated by the code at levels of 100-3000  $\mu\text{g}/\text{kg}$  (output benzene over input waste), which compares well with typical emission measurements at CCTL (see Appendix D). For chlorinated benzenes, represented by monochlorobenzene in the code, the code's prediction of 100-300  $\text{ng}/\text{kg}$  is about an order of magnitude low, though the reaction rates in the code were designed [4,7,125] so that the code matched the results of the Pittsfield-Vicon data [1].

Varying the ratio of PCC air to total air from 60% to 40% (Runs 30-34) had little effect on the  $\text{CO}$ ,  $\text{C}_6\text{H}_6$ , or  $\text{C}_6\text{H}_5\text{Cl}$  concentrations. For cases where the waste, gas, and air rates were varied together so as not to change the temperature-time profile (Runs 30, 35-42), there was little effect on carbon monoxide, with possibly a minimum occurring with a 350  $\text{lb}/\text{hr}$  waste feed rate. Benzene emissions were negligibly affected. Chlorobenzene emissions were lower for lower feed rates.

When the waste, gas, and air rates are lowered to 90% of their base case values, with no change in the temperature-time history (Run 43),  $\text{CO}$  decreased from 247  $\text{ppm}$  to 230  $\text{ppm}$ , while  $\text{C}_6\text{H}_6$  decreased negligibly and  $\text{C}_6\text{H}_5\text{Cl}$  remained the same. When the waste rate is increased to 450  $\text{lb}/\text{hr}$ , with the rest of the inputs at their base case value and with peak PCC and SCC temperatures raised to 2004  $^\circ\text{F}$  and 2087  $^\circ\text{F}$  to account for

the extra power input from the waste (Run 44), CO decreased to 59 ppm. With these higher temperatures, if the waste rate is dropped back to 400 lb/hr and the gas rate to the PCC is raised to compensate (Run 45), CO increases almost negligibly to 61 ppm. Benzene emissions for the last two runs were all but eliminated, while  $C_6H_5Cl$  emissions were substantially reduced.

Decreasing the air flow rate into the PCC by 5% and increasing the air flow rate into the SCC by 5% from the base case, while raising the peak PCC temperature to 1877 °F to compensate (Run 48), increases CO emission from 247 ppm to 300 ppm (see Table 5-2). Increasing the air flow rate into the PCC by 5% and decreasing the air flow rate into the SCC by 5% from the base case, while lowering the peak PCC temperature to 1730 °F to compensate (Run 53), also increases CO emission, to 336 ppm. So, for the same total air flow rate, the base case is near optimal for CO emission. Decreasing either air rate solely by 5% (Runs 46 and 49) cuts CO emission in half, while increasing either air rate solely (Runs 50 and 52) by 5% doubles CO emission. However, the lowest PCC air rate cases had the lowest benzene emission, mostly likely due to the increased PCC temperature. Benzene emission trends followed those of CO. Chlorobenzene emissions were lower for lower PCC air rates, but were hardly affected by the SCC air rate.

Lowering the PCC air rate substantially while raising the PCC and SCC temperatures to compensate (Runs 30, 56-61)

decreases the CO and  $C_6H_6$  output, with most of the decrease due to increases in the PCC and SCC temperatures. Benzene and  $C_6H_5Cl$  emissions trends followed those of CO here as well.

#### Conclusions from the Kinetics Code

Carbon monoxide emissions predicted by the code are very high compared to actual measurements. The input amounts and reactions to the code need to be improved to reduce the CO emissions. The temperature-time profile could be fattened to allow more time at higher temperatures, which should reduce the CO emissions. The air brought in at the dilution "T" could be gradually mixed. This also would keep the temperature of the combustion gas higher until the two streams are fully mixed.

The fast quench of reactions after the dilution "T" may minimize formation of certain organics compounds that would otherwise form due to slow cooling.

The initial kinetics code modelling (Runs 20-29) shows minimal CO emissions with the PCC and SCC at 1850 °F and 1925 °F, respectively, while minimal benzene emissions with the PCC and SCC at 1875 °F and 1900 °F, respectively. Later kinetics code runs show lower CO with decreased air rates, mainly through increased temperatures. The PCC air rate can only be lowered so far before the incinerator becomes starved-air.

Results from runs 20-29 are questionable since the temperature was varied without changing the inputs levels of waste, air, or natural gas. Results from runs 31-34 are also questionable since air flow rates were varied without changing the temperature-time profile.

The significant conclusions relevant for minimization of emissions are to burn hotter, avoid chlorine in the input (the code has shown increased chlorinated organic emissions with increased PVC input in other studies [4,7,125]), and burn longer (have a greater residence time).

CHAPTER 6  
EFFECT OF CHLORINATED INPUT ON CHLORINATED ORGANIC  
COMPOUND EMISSIONS

Conventional wisdom on the subject of the effect of chlorinated input, particularly in the form of PVC, on the levels of chlorinated organic emissions from incineration can be summarized by the following statements:

There is no evidence that the amount of PVC in the waste affects the levels of PCDDs/PCDFs at the boiler outlet, tertiary chamber, or the stack. [1:10-4] There is no statistically significant relationships between the levels of PCDDs/PCDFs and  $\text{NO}_x$ ,  $\text{SO}_2$ , THC [total hydrocarbons], or HCl. [1:10-5].

There are multiple sources of chlorine in MSW [Municipal Solid Waste]. Hence attempting to reduce PCDD/PCDF emissions based on a strategy of lowering the chlorine content of MSW by separating chlorinated plastics is unjustified.... No relationship exists between PCDD/PCDF emissions and the amount of PVC in the waste (or the concentration of HCl in the flue gas).... Incinerator operating temperature significantly affects the levels of PCDDs/PCDFs produced, and the levels of PCDDs/PCDFs and carbon monoxide are related. [2]

These statements refer to the results of the Pittsfield-Vicon incinerator study [1]. This study attempted to determine the relation between operating temperature and PVC input on PCDD and PCDF emissions. However, only 4 pairs of runs studied PVC input, while the data analysis for PCDD/PCDF versus PVC/HCl relations used all 19 runs, which had many variations in temperature, CO, and input PCDD/PCDF levels that could

have obscured such relations. Also, only linear regression analysis was used to examine the data.

The above statements contradict a logical conclusion that reducing chlorinated input reduces chlorinated organic emissions. Obviously, if there is no chlorine in the input waste stream, there can be no chlorinated organic emissions. In MSW 50% of the chlorine comes from PVC in the waste. However, in Medical Waste Incineration (MWI) PVC accounts for most of the chlorine in the waste. Green et al. [3-8] has reanalyzed the Vicon data and found relationships between chlorinated hydrocarbon (ClHC) emissions and HCl levels. Emissions data from the CCTL incinerator has been compared to the results of emissions testing on several California medical waste incinerators [3-5,7]. Emissions of HCl and ClHCs from the CCTL incinerator were both about one-tenth the level as from the California incinerators, which indicates probable relations between chlorine levels and ClHC emissions levels.

Correlation of emissions with operating parameters is a crude field since stack sampling is a one decimal point science at best and stack emission data usually are very noisy. Many sampling runs are needed at identical and different operating conditions to form a sufficient set of data for statistical analysis. To evaluate the validity of the conventional wisdom, and to bring order to this crude field, data on chlorinated emissions from the CCTL incinerator will be analyzed to determine any relations

between chlorine input and HCl output, and between HCl output and chlorinated organic compound emissions. An attempt is made to systematically analyze the CCTL data using linear, multivariate, and nonlinear approaches.

#### PVC, HCl, and VOST Data from CCTL

Since the chlorine level in the waste is not known for each burn, it is useful to have a surrogate to indicate the level of chlorine in the waste and to compare chlorinated organic emissions with. The best surrogate is the major product of chlorine combustion, HCl. The CCTL has made over 30 measurements of HCl emissions with different levels of chlorine in the input [3] (see Table 6-1). The PVC pipe added during the earlier experiments was assumed to contain 40% PVC and 60% filler material. PVC itself contains 56.8% by weight chlorine.

Data from CCTL sampling runs where both HCl and VOST (volatile organic sampling train) measurements were made will be analyzed to determine if any relationships exist between chlorinated volatile organic compound (VOC) emissions and chlorine input. The VOST measurement procedure examines 43 compounds (see Appendix D). Twenty-seven of these compounds are chlorinated. However, only a few compounds show up in sufficient amounts and often enough to be considered indicators of overall volatile organic emissions. Benzene, toluene, (mono)chlorobenzene, the dichlorobenzenes, and chloroform fit this criteria. Other compounds such as

ethylbenzene, and the xylenes may also fit this criteria. Eighteen VOST runs occurred while sampling for HCl and burning just NHW or NHW and PVC. Six runs had PVC resin added into the incinerator while NHW was burning. Data for feed rates, temperatures, CO, HCl, and many VOC emissions for

Table 6-1. CCTL PVC and HCl Test Data.

Date/run	NHW input lb/hr	PVC input lb/hr	added Cl input lb/hr	HCl output lb/hr	400-lb/hr feed rate equivalent added Cl	
					input lb/hr	output lb/hr
12-13-88	-	292.0	0.00	1.40	0.00	1.92
12-20-88	A	210.5	0.00	0.91	0.00	1.73
12-20-88	B	207.0	12.50 p	2.84	5.26	5.49 10.16
01-12-89	-	312.4	6.50 p	1.48	4.18	1.89 5.35
02-09-90	A	279.6	0.00	0.26	0.00	0.37
02-09-90	B	300.8	4.65 p	1.06	1.20	1.40 1.60
02-24-90	A	377.5	0.00	0.24	0.00	0.25
02-24-90	B	378.1	3.02 p	0.69	1.51	0.73 1.60
03-13-90	A	313.0	0.00	0.28	0.00	0.36
03-13-90	B	312.8	10.00 p	2.27	2.19	2.91 2.80
04-12-90	A	316.5	0.00	0.39	0.00	0.49
04-12-90	B	312.0	18.00 p	4.09	2.36	5.24 3.03
06-16-90	A	407.9	0.00	0.59	0.00	0.58
06-16-90	B	407.7	9.00 r	5.11	4.15	5.02 4.07
06-30-90	A	378.6	9.00 r	5.11	4.12	5.40 4.35
06-30-90	B	379.1	18.00 r	10.22	8.20	10.79 8.65
10-16-90	B	356.6	0.00	0.76	0.00	0.85
12-01-90	A	386.5	0.00	1.12	0.00	1.16
12-01-90	B	393.6	9.17 r	5.21	3.74	5.29 3.80
12-15-90	A	310.7	0.00	1.80	0.00	2.32
01-26-91	A	387.4	0.00	0.66	0.00	0.68
01-26-91	B	442.4	0.00	0.61	0.00	0.55
03-21-91	E	503.8	0.00	1.40	0.00	1.11
03-21-91	F	184.8	5.25 r	2.98	2.75	6.45 5.95
04-24-91	A	448.3	0.00	1.59	0.00	1.42
04-24-91	B	416.3	3.00 r	1.70	3.05	1.64 2.93
07-13-91	A	354.7	0.00	0.83	0.00	0.94
07-13-91	B	231.1	0.00	0.60	0.00	1.04
07-27-91	B	292.3	0.00	0.84	0.00	1.15
08-10-91	A	356.7	0.00	0.99	0.00	1.11
09-07-91	A	337.1	0.00	1.03	0.00	1.22
09-07-91	B	351.2	0.00	1.03	0.00	1.17

p=PVC pipe (22.7% Cl), r=PVC resin (56.8% Cl)

Table 6-2. Hydrogen Chloride, Temperature, Carbon Monoxide, and Volatile Organic Compound Data Used for Linear Regression and Nonlinear Analyses.

HCl g/kg	Tpcc °F	Tscc °F	tp		ts		CO mg/kg	CO /1000	mR	CO/1000	2 Toluene Benzene		CB	DCB	MC	CF	CT	TCA	TCE	PerC	
			mR	mR	µg/kg	µg/kg					C6H6	C6H5Cl									CH2Cl2
1.378	1779	1900	2.239	2.360	2.211	471.10	1033.0	28.48	72.23	757.30	13.14	N/A	N/A	N/A	0.000						
1.440	1741	1811	2.201	2.271	1.862	44.33	251.2	36.14	2.31	N/A	34.95	10.83	42.16	1.162	0.000						
1.679	1754	1859	2.214	2.319	2.704	92.67	79.2	46.17	29.03	N/A	5.99	15.75	6.02	0.000	0.000						
1.696	1772	1900	2.232	2.360	2.814	59.68	210.1	55.77	77.75	8.01	0.00	N/A	N/A	N/A	0.000						
2.095	1882	2018	2.342	2.478	2.224	54.98	118.1	79.78	56.03	4.91	33.85	30.50	16.97	2.350	4.954						
2.095	1841	1935	2.301	2.395	0.615	37.06	43.4	39.38	22.56	0.00	2.88	2.10	0.00	9.239	3.497						
2.783	1678	1803	2.138	2.263	2.205	90.97	9.5	N/A	31.20	N/A	N/A	45.84	0.00	N/A	N/A						
2.906	1792	1874	2.252	2.334	3.111	59.10	108.5	70.89	34.82	0.00	7.66	15.98	3.36	0.000	0.000						
3.000	1762	1904	2.222	2.364	0.939	0.00	0.0	0.00	23.24	1.16	4.82	0.50	0.00	0.000	0.000						
3.537	1809	2029	2.269	2.489	0.691	43.04	47.5	48.01	63.12	22.67	0.00	12.72	46.33	14.940	2.262						
5.778	1705	1796	2.165	2.256	6.154	43.38	117.0	88.51	107.00	N/A	0.00	N/A	8.58	N/A	5.509						
5.833	1841	1891	2.301	2.351	9.958	487.30	59.8	24.74	18.16	29.36	19.12	22.31	2.95	0.000	0.000						
7.331	1806	2033	2.266	2.493	0.446	41.12	99.6	43.27	58.63	21.10	0.00	10.43	78.29	34.770	2.424						
9.062	1799	1955	2.259	2.415	5.385	60.21	1286.0	151.10	102.00	4.87	12.58	30.74	2.68	0.000	0.000						
9.967	1767	1898	2.227	2.358	3.143	57.19	220.5	32.47	28.30	N/A	74.17	24.84	24.73	3.043	0.000						
10.630	1765	1877	2.225	2.337	2.050	138.90	598.8	285.40	360.10	102.20	48.14	25.62	22.39	9.936	9.048						
14.480	1751	1821	2.211	2.281	3.160	17.48	77.3	N/A	83.29	N/A	N/A	0.00	299.90	N/A	N/A						

these 18 runs is shown in Table 6-2. The CO, HCl, and VOC emissions were normalized to the waste (including any added PVC) feed rate. Carbon monoxide emission is listed in (mg/hr CO)/(kg/hr input waste), or mg/kg for short; HCl is listed in g/kg; and the VOCs are listed in  $\mu\text{g}/\text{kg}$ . These unit result in data ranges of 1 to 1000 so that very small numbers are avoided.

The analysis of this data will use standard statistical procedures for linear and multivariate regression. Also some nonlinear analysis of the data will be performed based on earlier analysis of Vicon data by Green et al. [3-8].

#### Review of Statistical Procedures

In statistical analysis data is usually modelled using a simple linear equation:

$$\hat{Y} = \alpha + \beta X, \quad (6-1)$$

where  $\hat{Y}$  is the fit to the dependent variable  $Y$ ,  $\alpha$  is the intercept,  $\beta$  is the slope, and  $X$  is the independent variable.

The intercept and slope are determined by a least squares method. The least squares method determines  $\alpha$  and  $\beta$  that minimize the sum of squared errors (SSE). The SSE is the sum of the squares of the differences for each data point between the model's prediction for the dependent variable and the actual value of dependent variable:

$$\text{SSE} = \sum_{i=1}^n (\hat{Y}_i - Y_i)^2. \quad (6-2)$$

The slope and intercept are calculated by

$$\beta = \frac{SSXY}{SSXX}, \quad \alpha = \bar{Y} - \beta \bar{X}, \quad (6-3a,b)$$

where  $\bar{V}$  is the average value of  $V$  for  $V=X$  or  $V=Y$  and

$$SSVW = \sum_{i=1}^n (\bar{V} - V_i)(\bar{W} - W_i), \quad (6-4)$$

with  $V=X$  and  $W=Y$  for  $SSXY$  and with  $V=X$  and  $W=X$  for  $SSXX$ . A measure of how well the model fits the data is the correlation coefficient,  $r$  [128]:

$$r = \beta \sqrt{\frac{SSXX}{SSYY}}. \quad (6-5)$$

The  $SSYY$  (defined by Equation 6-4 with  $V=Y$  and  $W=Y$ ) is the sum of the squares of the differences between the average value of the dependent variable and the actual value of dependent variable for each data point. When the model fits the data (dependent variable) well,  $r$  is near 1 for positive  $\beta$  and near -1 for negative  $\beta$ . If the model does not fit data well,  $r$  is near zero.

For multivariate regression a typical model is

$$\hat{Y} = \beta_0 + \beta_1 X_1 + \beta_2 X_2 + \dots + \beta_m X_m, \quad (6-6)$$

where  $\hat{Y}$  is the fit to the dependent variable  $Y$ ,  $\beta_0$  is the intercept,  $\beta_j$  are the coefficients or parameters, and  $X_j$  are independent variables or are made up of functions of the independent variables, e.g.,  $X_2^2$ ,  $X_1 * X_3$ ,  $\ln(X_2)$ , etc. The  $\beta_j$ s are also determined by the same least square method used in linear regression. Equation 6-6 also can be written as

$$\hat{Y} = \beta_0 X_0 + \beta_1 X_1 + \dots + \beta_m X_m, \quad (6-7)$$

where  $X_0$  is a dummy variable always equal to 1. The inclusion of  $X_0$  is necessary when using matrix methods to solve for the least-square coefficients. The  $\beta_0$  is therefore also a coefficient, albeit the coefficient of an independent variable whose value is always 1.

The most frequently used statistical quantity for determining how well a multivariate regression model fits a set of data is the coefficient of determination,  $R^2$  [128-130]:

$$R^2 = 1 - \frac{SSE}{SST}, \quad (6-8)$$

where  $SST=SSYY$ . For linear regression ( $m=1$ ),  $R^2=r^2$ . An  $R^2$  value of 0.500 is equivalent to an  $r$  value of 0.707, so  $R^2$  is a more conservative measure of fitness. The correlation for a model is statistically significant at the 5% level [130] if:

$$F = \frac{(n - m - 1) R^2}{m (1 - R^2)} > F(m, n-m-1, 5\%) \quad (6-9)$$

or

$$R^2 > \frac{F(m, n-m-1, 5\%)}{m F(m, n-m-1, 5\%) + (n-m-1)}, \quad (6-10)$$

where  $m$  is the numbers of coefficients in the model excluding the intercept,  $n$  is the number of data points, and  $F$  is a statistical quantity, the  $F$ -value or the inverted beta ( $F$ ) distribution, and  $F(m, n-m-1, P\%)$  is the critical  $F$ -value for a  $P\%$  significance level [129-130]. A  $P\%$  significance level

indicates that there is only a  $P\%$  likelihood that the data ended up along the lines of the model by random chance.

Critical F-values and their associated minimum  $R^2$  are listed in Table 6-3. When the  $R^2$  exceeds the minimum  $R^2$  for a  $5\%$  significance level, the correlation is well-fit.

The  $R^2$  can be negative if the intercept (constant) term is not included. Negative  $R^2$ s indicate that the fit is worse than fitting data to the mean of the dependent variable.

Most statistical books never consider models where there is no intercept term. Some statistical equalities are no longer valid when the intercept is excluded. The intercept is often not counted among the coefficients of (or degrees of freedom of) a multivariate regression model, as is the case for  $m$  in Equations 6-9 and 6-10. The definition of  $R^2$  is based on SST, which equals SSE when the model only contains the intercept parameter. The  $R^2$  is therefore zero when the model contains only the intercept parameter.

Table 6-3. Critical Values of  $t$ ,  $F$ , and  $R^2$  at the  $5\%$  Significance Level [128].

DOF	$t(5\%/2)$	$F(5\%)$					$R^2(5\%)$				
		$m=1$	$m=2$	$m=3$	$m=4$	$m=5$	$m=1$	$m=2$	$m=3$	$m=4$	$m=5$
8	2.306	5.32	4.46	4.07	3.84	3.69	0.399	0.527	0.604	0.658	0.698
9	2.262	5.12	4.26	3.86	3.63	3.48	0.363	0.486	0.563	0.617	0.659
10	2.228	4.96	4.10	3.71	3.48	3.33	0.332	0.451	0.527	0.582	0.625
11	2.201	4.84	3.98	3.59	3.36	3.20	0.306	0.420	0.495	0.550	0.593
12	2.179	4.75	3.89	3.49	3.26	3.11	0.284	0.393	0.466	0.521	0.564
13	2.160	4.67	3.81	3.41	3.18	3.03	0.264	0.370	0.440	0.495	0.538
14	2.145	4.60	3.74	3.34	3.11	2.96	0.247	0.348	0.417	0.470	0.514
15	2.131	4.54	3.68	3.29	3.06	2.90	0.232	0.329	0.397	0.449	0.492
16	2.120	4.49	3.63	3.24	3.01	2.85	0.219	0.312	0.378	0.429	0.471
17	2.110	4.45	3.59	3.20	2.96	2.81	0.207	0.297	0.361	0.411	0.452

A coefficient is statistically significant [128] at the 5% level if the range defined by the coefficient  $\pm$  (its t-value times its standard error) does not include zero, i.e., there is a 95% or greater probability that the coefficient is not zero. The t-value is from the Student's t test for 2.5% (half of the 5%, indicating a two tailed ( $\pm$ ) test) and the number of degrees of freedom (DOFs) (number of data points minus number of coefficients (including the intercept)). The t-values for 5% significance level are listed in Table 6-3. The t-values average around 2.2 for 8 to 17 DOFs.

If the t-ratio for a coefficient (the absolute value of the coefficient divided by its standard error) is greater than its t-value, then the range defined by the coefficient  $\pm$  (its t-value times its standard error) does not include zero, and the coefficient is statistically significant at the 5% level. The standard error of a coefficient is a measure of how well the dependent variable is fit by all of the independent variables compared to how well the independent variable whose coefficient is being tested is fit by the other independent variables. In other words, the standard error partially answers the question, "does this independent variable add any new information to the fit?". Statistically significant coefficients are labelled well-defined.

Two strategies are useful in multivariate regression analysis. One strategy is to start with a linear model and add independent variables, one at a time, hoping to increase  $R^2$ . The other strategy is to start with many independent

variables and throw out, one at a time, those whose coefficients are least defined, until only well-defined coefficients remain. Both strategies are used here in the analysis of the CCTL ClHC data.

A computer program in BASIC was written to facilitate linear regression analysis of the CCTL data. The program reads a file containing the data shown in Table 6-2, with each column headed by the compound's or temperature's name. The user specifies a dependent variable and the independent variables to which to fit the dependent variable. These variables can be made up of any function of the compounds and/or temperatures. The program determined the number of valid data points (N), the number of degrees of freedom (DOF), the coefficients by least-square calculation, the coefficient of determination ( $R^2$ ), the standard error of the dependent variable ( $S_y = \sqrt{SSE/DOF}$ ), the standard error of the coefficients, and the t-ratios of the coefficients. The user can also specify that data points for a compound's highest or zero values not be used. The program is interactive, and all output is written to a file for later editing and printout. The program can also plot the data and the fit to the computer screen.

#### Effect of Chlorine Input on HCl Emissions

Figure 6-1 shows a graph of HCl output plotted against added Cl input (from Table 6-1) where both the HCl output and added Cl input are in lb/hr and are normalized to a 400-lb/hr

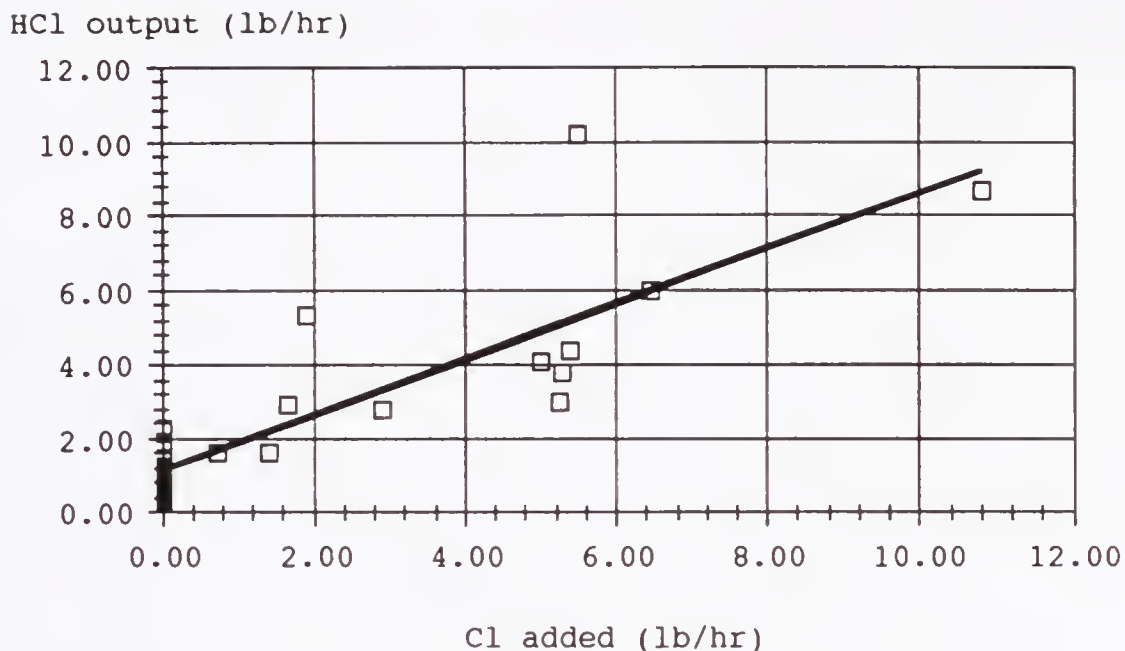


Figure 6-1. HCl emissions compared to added chlorine input with both HCl and added Cl normalized to a 400-lb/hr waste feed rate.

waste feed rate. The normalization is necessary to present the data in a 2-dimensional plot. The linear regression fit shown on the graph is

$$\text{HCl} = 1.114 \text{ lb/hr} + 0.7478 \text{ Cl}, \quad (6-11)$$

with a coefficient of determination,  $R^2$ , of 0.735 (or a correlation coefficient,  $r$ , of 0.857). The 1.114 lb/hr constant indicates a 0.2785% chlorine content in the waste. The 0.7478 factor implies that not all of the chlorine ends up as HCl, or at least not immediately. Chlorine does tend to be a flame inhibitor [10-12], which would explain a slow burn out. When the unnormalized data is subject to a regression analysis with HCl output as the dependent variable

and NHW feed rate and added Cl input as independent variables, the resulting fit is

$$\text{HCl} = 0.002647 \text{ NHW} + 0.6878 \text{ Cl}, \quad (6-12)$$

with  $R^2=0.791$  (or  $r=0.889$ ). This fit is reasonably close to the fit using the normalized data. These are strong correlations for sampling data, which is usually noisy. These correlations indicated that HCl is a good surrogate for chlorine level in the waste when comparing chlorine input to ClHC output.

#### Review of HCl and VOST Data

##### Linear Regression of VOST Data

Using linear regression analysis, certain VOC emissions (see Table 6-2) were compared to PCC and SCC temperatures (Tpcc and Tsc), CO and HCl emissions, and other VOC emissions. The emissions of the three dichlorobenzenes isomers were added together to reduce noise and represent total dichlorobenzene (DCB) ( $\text{C}_6\text{H}_4\text{Cl}_2$ ) emissions. The most abundant chlorinated VOCs are usually the chlorinated benzenes. Table 6-4 shows the more significant and provocative results of the linear regression analysis of the CCTL VOST data.

When comparing DCB emissions with only one other variable (Tpcc, Tsc, CO, HCl, benzene (benz) ( $\text{C}_6\text{H}_6$ ), or a constant), DCB correlated best with HCl (see Table 6-4). Benzene and HCl were the only variables with which DCB correlated better than with the constant.

Table 6-4. Results of Linear Regression of VOST Data.

N = 18	DOF = 17	R <sup>2</sup> = 0.00000	Sy = 93.42252
DCB = 80.7164			
t-ratios: 3.665611			
N = 18	DOF = 17	R <sup>2</sup> = 0.43094	Sy = 70.47431
DCB = 12.78747 HCL			
t-ratios: 6.040355			
N = 18	DOF = 17	R <sup>2</sup> = -0.00467	Sy = 93.64058
DCB = .0452231 TPCC			
t-ratios: 3.646247			
N = 18	DOF = 17	R <sup>2</sup> = -0.00305	Sy = 93.56474
DCB = 4.236982E-02 TSCC			
t-ratios: 3.652979			
N = 18	DOF = 17	R <sup>2</sup> = -0.29441	Sy = 106.2888
DCB = .173191 CO			
t-ratios: 2.552246			
N = 18	DOF = 17	R <sup>2</sup> = 0.06174	Sy = 90.49268
DCB = .1809384 BENZ			
t-ratios: 3.92931			
N = 18	DOF = 16	R <sup>2</sup> = 0.43842	Sy = 72.16439
DCB = 11.93067 + 11.64256 HCL			
t-ratios: .4615735            3.534248			
N = 18	DOF = 16	R <sup>2</sup> = 0.22943	Sy = 84.53244
DCB = 47.02865 + .1187602 BENZ			
t-ratios: 1.865959            2.182596			
N = 18	DOF = 16	R <sup>2</sup> = 0.51214	Sy = 67.26074
DCB = 10.06716 HCL + 7.241128E-02 BENZ			
t-ratios: 3.843409            1.631948			
N = 18	DOF = 15	R <sup>2</sup> = 0.51229	Sy = 69.45615
DCB = 1.731203 + 9.932466 HCL + 7.157446E-02 BENZ			
t-ratios: 6.714881E-02            2.94955            1.50734			
N = 18	DOF = 12	R <sup>2</sup> = 0.54260	Sy = 75.20243
DCB = 162.3137 + 10.36122 HCL + .0733088 TPCC +-.1431177 TSCC			
+-.8.012414E-02 CO + 7.840911E-02 BENZ			
t-ratios: .2378798    2.78692    .1074836    .2986687    .8245681    1.496185			
N = 16	DOF = 15	R <sup>2</sup> = 0.86688	Sy = 35.96808
DCB = 1.172582 CB			
t-ratios: 13.57282			
N = 16	DOF = 14	R <sup>2</sup> = 0.87694	Sy = 35.79583
DCB = 2.374752 HCL + 1.02933 CB			
t-ratios: 1.069912            6.468899			
N = 16	DOF = 14	R <sup>2</sup> = 0.86780	Sy = 37.10136
DCB = 1.203028 CB +-.8.747807E-03 BENZ			
t-ratios: 9.110809            .3124599			
N = 16	DOF = 14	R <sup>2</sup> = 0.87419	Sy = 36.19415
DCB = -11.95812 + 1.256567 CB			
t-ratios: .9017802            9.862969			
N = 16	DOF = 15	R <sup>2</sup> = 0.37296	Sy = 58.0848
CB = 11.73746 HCL			
t-ratios: 6.031283			
N = 16	DOF = 15	R <sup>2</sup> = 0.02181	Sy = 72.54803
CB = .1564587 BENZ			
t-ratios: 4.234791			

Table 6-4--continued

N = 16	DOF = 14	R <sup>2</sup> = 0.47377	Sy = 55.0789
CB = 8.850081 HCL + 6.353128E-02 BENZ			
t-ratios: 3.467547		1.637655	
N = 16	DOF = 14	R <sup>2</sup> = 0.42450	Sy = 57.59947
CB = 24.22029 + 9.315372 HCL			
t-ratios: 1.119753		3.213522	
N = 16	DOF = 14	R <sup>2</sup> = 0.26619	Sy = 65.04101
CB = 45.64516 + 9.704254E-02 BENZ			
t-ratios: 2.159265		2.253571	
N = 16	DOF = 13	R <sup>2</sup> = 0.49644	Sy = 55.913
CB = 16.62184 + 7.5515 HCL + 5.553001E-02 BENZ			
t-ratios: .765124		2.438079	1.362822
N = 17	DOF = 16	R <sup>2</sup> = -0.00000	Sy = 64.09
DCBNH = 64.28157			
t-ratios: 4.13543			
N = 17	DOF = 16	R <sup>2</sup> = 0.56711	Sy = 42.16752
DCBNH = 10.39355 HCL			
t-ratios: 7.776075			
N = 17	DOF = 16	R <sup>2</sup> = -0.00367	Sy = 64.20749
DCBNH = 3.604275E-02 TPCC			
t-ratios: 4.120771			
N = 17	DOF = 16	R <sup>2</sup> = 0.00194	Sy = 64.02768
DCBNH = 3.381346E-02 TSCC			
t-ratios: 4.143218			
N = 17	DOF = 16	R <sup>2</sup> = -0.29114	Sy = 72.82439
DCBNH = .1455898 CO			
t-ratios: 3.104457			
N = 17	DOF = 16	R <sup>2</sup> = -0.05507	Sy = 65.83092
DCBNH = .1379067 BENZ			
t-ratios: 3.920989			
N = 15	DOF = 14	R <sup>2</sup> = 0.71696	Sy = 36.04159
DCBNH = 1.093592 CB			
t-ratios: 9.196751			
N = 15	DOF = 13	R <sup>2</sup> = 0.79317	Sy = 31.97295
DCBNH = 5.243255 HCL + .6699222 CB			
t-ratios: 2.188558		3.038759	
N = 16	DOF = 15	R <sup>2</sup> = -0.00000	Sy = 21.62017
CF = 18.47035			
t-ratios: 3.417245			
N = 16	DOF = 15	R <sup>2</sup> = 0.18904	Sy = 19.46967
CF = 2.759574 HCL			
t-ratios: 4.230403			
N = 16	DOF = 15	R <sup>2</sup> = -0.00149	Sy = 21.63627
CF = 1.032326E-02 TPCC			
t-ratios: 3.411432			
N = 16	DOF = 15	R <sup>2</sup> = -0.01073	Sy = 21.73589
CF = 9.592172E-03 TSCC			
t-ratios: 3.375538			
N = 16	DOF = 15	R <sup>2</sup> = -0.24627	Sy = 24.13603
CF = 4.024925E-02 CO			
t-ratios: 2.530979			

Table 6-4--continued

N = 16	DOF = 15	R <sup>2</sup> = -0.25635	Sy = 24.23343
CF = 3.081376E-02 BENZ			
t-ratios: 2.496823			
N = 16	DOF = 15	R <sup>2</sup> = -0.08386	Sy = 22.50843
CF = .1374679 DCB			
t-ratios: 3.100568			
N = 16	DOF = 15	R <sup>2</sup> = 0.00967	Sy = 21.51539
CF = .1785547 CB			
t-ratios: 3.455145			
N = 16	DOF = 14	R <sup>2</sup> = 0.23870	Sy = 19.52628
CF = 7.00692 + 2.058866 HCL			
t-ratios: .9555842      2.095115			
N = 18	DOF = 17	R <sup>2</sup> = -0.06432	Sy = 144.0312
TOL = .2243945 BENZ			
t-ratios: 3.061644			
N = 18	DOF = 17	R <sup>2</sup> = 0.00000	Sy = 230.1399
CO = 293.732			
t-ratios: 5.414964			
N = 18	DOF = 17	R <sup>2</sup> = 0.00079	Sy = 230.0489
CO = .1650963 TPCC			
t-ratios: 5.418351			
N = 18	DOF = 17	R <sup>2</sup> = -0.03263	Sy = 233.8647
CO = .1530162 TSCC			
t-ratios: 5.278073			
N = 18	DOF = 17	R <sup>2</sup> = -0.48323	Sy = 280.2827
CO = 31.76112 HCL			
t-ratios: 3.772317			
N = 18	DOF = 17	R <sup>2</sup> = -0.88773	Sy = 316.1997
CO = .4417769 BENZ			
t-ratios: 2.745622			
N = 18	DOF = 17	R <sup>2</sup> = 0.59837	Sy = 46.08064
TSCC = 1.06815 TPCC			
t-ratios: 175.0104			
N = 18	DOF = 16	R <sup>2</sup> = 0.60280	Sy = 47.23651
TSCC = -178.2177 + 1.168262 TPCC			
t-ratios: .4224669      4.928285			
N = 18	DOF = 17	R <sup>2</sup> = -0.10853	Sy = 396.7123
BENZ = .695395 CO			
t-ratios: 2.745622			
N = 17	DOF = 16	R <sup>2</sup> = 0.22603	Sy = 334.1598
BENZ = 3.553316 DCBNH			
t-ratios: 3.920989			
N = 18	DOF = 17	R <sup>2</sup> = 0.04792	Sy = 367.6522
BENZ = 37.56748 HCL			
t-ratios: 3.401603			

Adding a constant as a second independent variable to HCL did not improved DCB's correlation with it. Adding a constant as a second independent variable to benzene improved

DCB's correlation with it, raising  $R^2$  to statistical significance at the 5% level (above 0.219 from Table 6-3 for 16 DOF and 1 coefficient excluding the constant). Adding a benzene as a second independent variable to HCl brought the  $R^2$  to over one-half (or  $r$  to over 0.7). Adding a third, fourth, fifth, or sixth compounds as independent variables did little to improve the correlation. In all cases with HCl as an independent variable, the coefficient of the HCl term was well-defined (statistically significant at the 5% level). Also, the coefficient for HCl was positive in all of these cases, which indicates that increasing HCl emissions leads to larger chlorinated organic emissions.

Chlorobenzene (CB) ( $C_6H_5Cl$ ) emission data existed for 16 of the 18 runs. The other two had contamination problems which resulted in indeterminable values for the emissions of CB. Dichlorobenzene correlated very well with just CB (see Table 6-4). Adding a constant, HCl, and/or benzene improved this correlation only slightly. CB itself did not correlate as well as DCB did with HCl and/or benzene, with or without a constant term, though the correlations were still well-fit (statistically significant at the 5% level).

Figure 6-2 shows the relation between DCB and HCl emissions. It is apparent from this graph that the highest DCB emission case is an outlier in that it lies far away from the rest of the data set. DCB emissions without this outlying point (DCBNH) were also compared to T<sub>pcc</sub>, T<sub>scc</sub>, CO, HCl, benzene, CB, or a constant. DCBNH correlated much

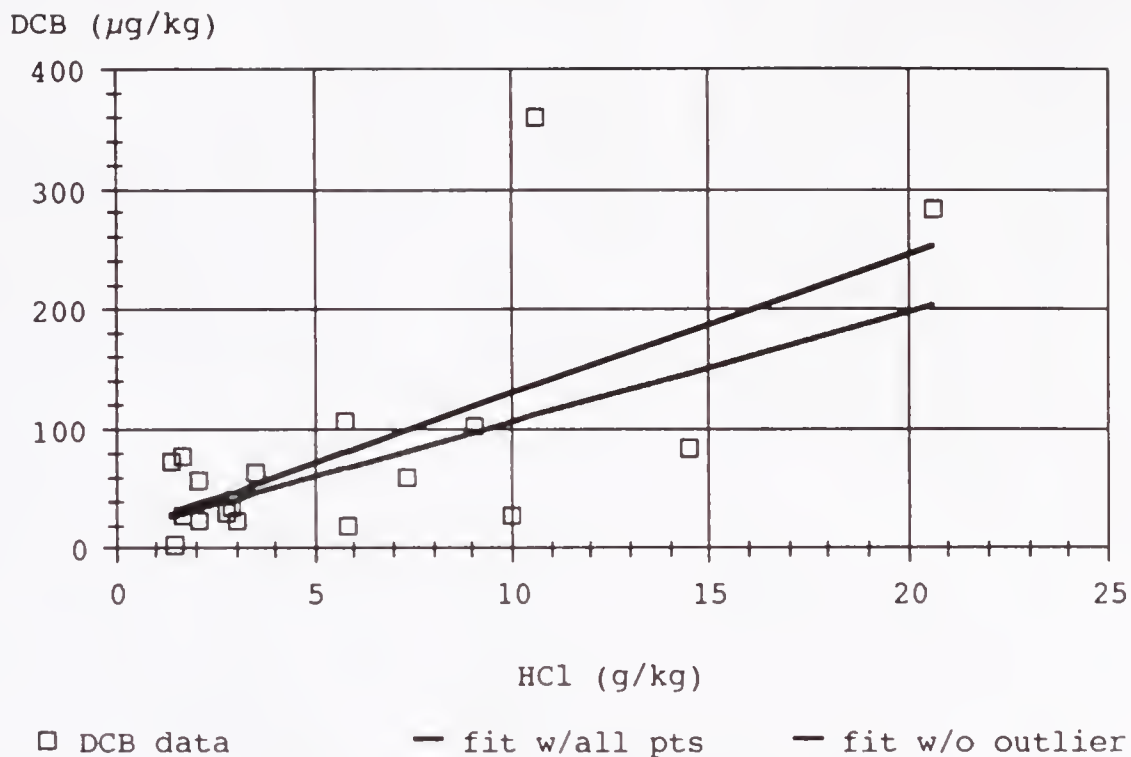


Figure 6-2. Comparison of DCB emissions to HCl emissions with and without outlying DCB data point.

better with HCL than DCB did (see Table 6-4), but not as well with CB and not at all with benzene. When DCBNH was compared to HCl and CB together, the  $R^2$  rose to 0.793 and both coefficients were well-defined.

Chloroform (CF) ( $\text{CHCl}_3$ ) did not correlate well with any other one variable. The coefficient for HCl in CF-HCl comparison was still positive, though. Adding a constant made the correlation well-fit, though neither the constant nor the HCl coefficient was well-defined. Benzene does not correlate with CO or HCl, but does somewhat with DCBNH. Toluene (Tol) ( $\text{C}_6\text{H}_5\text{CH}_3$ ) did not correlate well with benzene. Carbon monoxide did not correlate with any one of the other variables. The two temperatures correlated well with each

other, though, with  $R^2=0.598$ , not as well as expected. The relatively small range of temperatures (as compared to the ranges of HCl and CO) may explain why no other variables correlate with T<sub>pcc</sub> and T<sub>scc</sub>. Essentially, combustion conditions were always maintained in a favorable range.

#### Quadratic and Higher Power Regressions of VOST Data

When DCB emission is compared to the square of any other one variable (see Table 6-5), the best correlations are with  $CB^2$  and  $HCl^2$ . All fits with other independent variables were worse than with the unit power of the same independent variable. The correlations improve with additional squared terms, reaching  $R^2=0.936$ , with  $HCl^2$ ,  $CB^2$ , and constant terms. All three coefficients here are well-defined, and the  $HCl^2$  coefficient is positive. Replacing the  $HCl^2$  term with an  $HCl*CB$  term slightly raises the  $R^2$  to 0.940.

Since CB is a chlorinated emission similar to DCB, good correlations between them may not have much importance for combustion control. Correlations between DCB or CB with HCl and nonchlorinated compounds would have a greater impact for reducing chlorinated emissions. Correlation of DCB with benzene,  $benzene^2$ , and  $HCl*benzene$  produces  $R^2=0.699$  (see Table 6-5), with all three coefficients well-defined and the  $HCl*benzene$  coefficient positive. Replacing the  $HCl*benzene$  term with a  $benzene/HCl$  term slightly raises the  $R^2$  to 0.729. Again all three coefficients are well-defined. The  $benzene/HCl$  coefficient is negative, which still indicates

Table 6-5. Results of Quadratic and Higher Power Regressions of CCTL VOST data.

N = 18	DOF = 17	R <sup>2</sup> = 0.24015	Sy = 81.43581
DCB = .76519 HCL <sup>2</sup>			
t-ratios: 4.80169			
N = 16	DOF = 15	R <sup>2</sup> = 0.76221	Sy = 48.07209
DCB = 5.109778E-03 CB <sup>2</sup>			
t-ratios: 9.824875			
N = 18	DOF = 16	R <sup>2</sup> = 0.42562	Sy = 72.98197
DCB = 45.49169 + .5721405 HCL <sup>2</sup>			
t-ratios: 2.272987      3.443274			
N = 16	DOF = 14	R <sup>2</sup> = 0.87483	Sy = 36.10252
DCB = 36.26396 + 4.374033E-03 CB <sup>2</sup>			
t-ratios: 3.548965      9.891598			
N = 16	DOF = 14	R <sup>2</sup> = 0.87029	Sy = 36.7502
DCB = .342879 HCL <sup>2</sup> + 4.040254E-03 CB <sup>2</sup>			
t-ratios: 3.415551      7.983147			
N = 16	DOF = 13	R <sup>2</sup> = 0.93590	Sy = 26.80954
DCB = 28.7535 + .2677527 HCL <sup>2</sup> + 3.691222E-03 CB <sup>2</sup>			
t-ratios: 3.647856      3.519627      9.678116			
N = 16	DOF = 13	R <sup>2</sup> = 0.93962	Sy = 26.0207
DCB = 29.98737 + .041425 HCL*CB + 2.454528E-03 CB <sup>2</sup>			
t-ratios: 3.969738      3.735022      4.058922			
N = 18	DOF = 16	R <sup>2</sup> = 0.10213	Sy = 91.24786
DCB = 66.58484 + 6.586645E-05 BENZ <sup>2</sup>			
t-ratios: 2.783338      1.349058			
N = 18	DOF = 15	R <sup>2</sup> = 0.72945	Sy = 51.73121
DCB = .7286648 BENZ + -4.578459E-04 BENZ <sup>2</sup> + -.2951189 BENZ/HCL			
t-ratios: 7.655041      5.422572      3.216665			
N = 16	DOF = 11	R <sup>2</sup> = 0.86691	Sy = 31.24958
CB = -4.374617E-04 BENZ <sup>2</sup> + 15.9371 HCL + -2.551265 HCL <sup>2</sup>			
+ 7.637888E-02 HCL*BENZ + .4691296 BENZ/HCL			
t-ratios: 5.103206      5.866625      6.025134      5.747261      4.700213			
N = 16	DOF = 12	R <sup>2</sup> = 0.59960	Sy = 51.89364
CB = -7.22339E-05 BENZ <sup>2</sup> + 15.57616 HCL + -1.078351 HCL <sup>2</sup>			
+ 2.375371E-02 HCL*BENZ			
t-ratios: 1.201609      3.454164      2.280274      1.997967			
N = 17	DOF = 15	R <sup>2</sup> = 0.72512	Sy = 34.70344
DCBNH = 34.97016 + .5006529 HCL <sup>2</sup>			
t-ratios: 3.63494      6.290484			
N = 17	DOF = 15	R <sup>2</sup> = 0.77604	Sy = 31.32476
DCBNH = 42.20004 + 2.584194E-02 HCL <sup>3</sup>			
t-ratios: 5.151674      7.209502			
N = 17	DOF = 15	R <sup>2</sup> = 0.79113	Sy = 30.25106
DCBNH = 45.55987 + 1.281298E-03 HCL <sup>4</sup>			
t-ratios: 5.88175      7.537618			
N = 17	DOF = 15	R <sup>2</sup> = 0.79354	Sy = 30.07613
DCBNH = 47.38391 + 6.248966E-05 HCL <sup>5</sup>			
t-ratios: 6.213101      7.59299			
N = 17	DOF = 15	R <sup>2</sup> = 0.79148	Sy = 30.22575
DCBNH = 48.47109 + 3.027304E-06 HCL <sup>6</sup>			
t-ratios: 6.357373      7.545597			

Table 6-5--continued

N = 18	DOF = 16	R <sup>2</sup> = 0.37761	Sy = 75.97088
DCB = 57.07049 + 2.706515E-02 HCL <sup>3</sup>			
t-ratios: 2.934453		3.115666	
N = 18	DOF = 16	R <sup>2</sup> = 0.34146	Sy = 78.14612
DCB = 62.36766 + 1.264731E-03 HCL <sup>4</sup>			
t-ratios: 3.200026		2.880301	
N = 18	DOF = 16	R <sup>2</sup> = 0.32004	Sy = 79.40675
DCB = 65.04958 + 5.958991E-05 HCL <sup>5</sup>			
t-ratios: 3.324337		2.744235	
N = 18	DOF = 16	R <sup>2</sup> = 0.30804	Sy = 80.10433
DCB = 66.50948 + 2.834325E-06 HCL <sup>6</sup>			
t-ratios: 3.390429		2.668854	

that increasing HCl emissions leads to larger chlorinated organic emissions. Correlation of CB with HCl, HCl<sup>2</sup>, benzene<sup>2</sup>, HCl\*benzene, and benzene/HCl produces R<sup>2</sup>=0.867, with all five coefficients well-defined. Removing the benzene/HCl term drops the R<sup>2</sup> to 0.600.

Without the outlying DCB data point, DCBNH correlates increasing well with a constant and increasing powers of HCl, reaching R<sup>2</sup>=0.794 when DCBNH is correlated to a constant and HCL<sup>5</sup>. The coefficient of the HCL<sup>5</sup> term is again positive, and both coefficients are well defined. With the outlying DCB data point included, DCB does not show the same trend.

#### Logarithmic and Exponential Regressions of VOST Data

Among correlations between ln(DCB) with HCl and ln(HCl), the best correlation is for ln(DCB) compared to a constant and HCl (see Table 6-6), with an HCl coefficient of 0.12 and an R<sup>2</sup> of 0.337. When this is rearranged so that DCB is compared to exp(0.12\*HCl), the R<sup>2</sup> is 0.386. Adjusting the constant inside the exponential to 0.09 increased R<sup>2</sup> to 0.427, which is similar to when DCB was compared to just HCl.

Table 6-6. Results of Logarithmic and Exponential Regressions of CCTL VOST data.

N = 18	DOF = 16	R <sup>2</sup> = 0.32928	Sy = .9454387
LN(DCB) = 2.796971 + .7569348 LN(HCL)			
t-ratios: 6.27269		2.802672	
N = 18	DOF = 15	R <sup>2</sup> = 0.34474	Sy = .9651268
LN(DCB) = 2.9802 + .3217996 LN(HCL) + 7.430962E-02 HCL			
t-ratios: 5.422455		.4116615	.5948726
N = 18	DOF = 16	R <sup>2</sup> = 0.33734	Sy = .9397441
LN(DCB) = 3.156092 + .1224286 HCL			
t-ratios: 9.376461		2.853939	
N = 18	DOF = 17	R <sup>2</sup> = 0.38605	Sy = 73.20099
DCB = 25.99868 EXP(.1224286*HCL)			
t-ratios: 5.707494			
N = 18	DOF = 17	R <sup>2</sup> = 0.42659	Sy = 70.74328
DCB = 37.4337 EXP(.1*HCL)			
t-ratios: 6.006659			
N = 18	DOF = 17	R <sup>2</sup> = 0.30547	Sy = 77.85713
DCB = 65.02806 EXP(.05*HCL)			
t-ratios: 5.179112			
N = 18	DOF = 17	R <sup>2</sup> = 0.40431	Sy = 72.10447
DCB = 51.77347 EXP(.075*HCL)			
t-ratios: 5.839072			
N = 18	DOF = 17	R <sup>2</sup> = 0.42726	Sy = 70.7017
DCB = 43.10288 EXP(.09*HCL)			
t-ratios: 6.011855			
N = 17	DOF = 15	R <sup>2</sup> = 0.30503	Sy = .8889994
LN(DCBNH) = 3.160113 + .1067814 HCL			
t-ratios: 9.924029		2.565848	
N = 17	DOF = 16	R <sup>2</sup> = 0.74469	Sy = 32.38346
DCBNH = 28.38596 EXP(.10678*HCL)			
t-ratios: 10.66086			
N = 17	DOF = 15	R <sup>2</sup> = 0.74515	Sy = 33.41552
DCBNH = 2.036366 + 27.86313 EXP(.10678*HCL)			
t-ratios: .1640824		6.622523	
N = 17	DOF = 15	R <sup>2</sup> = 0.79732	Sy = 29.79921
DCBNH = 45.95645 + .4832573 EXP(.3*HCL)			
t-ratios: 6.03825		7.681802	
N = 17	DOF = 15	R <sup>2</sup> = 0.61419	Sy = 41.11397
DCBNH = 8.443166E-02 BENZ + .4658655 EXP(.3*HCL)			
t-ratios: 3.468954		5.101031	
N = 17	DOF = 14	R <sup>2</sup> = 0.84635	Sy = 26.85691
DCBNH = 37.03874 + .4426029 EXP(.3*HCL) + 3.945057E-02 BENZ			
t-ratios: 4.5992		7.392473	2.113452
N = 17	DOF = 14	R <sup>2</sup> = 0.84790	Sy = 26.72123
DCBNH = 40.36302 + .4593917 EXP(.3*HCL) + 3.153373E-05 BENZ <sup>2</sup>			
t-ratios: 5.528729		7.991403	2.157473

Since DCBNH fit increasing well with higher powers of HCl, an equation of the form

$$\text{DCBNH} = A \exp(B \text{ HCl}) \quad (6-11)$$

was sought to fit the DCBNH-HCl data. The exponent function incorporates all powers of its argument, exponential functions are more likely to have a physical meaning than the  $x^5$  function. Equation 6-11 was converted to

$$\ln(\text{DCBNH}) = \ln(A) + B \text{ HCl} \quad (6-12)$$

so that the linear regression program could determine the parameters A and B. The result (see Table 6-6) was  $\ln(A)=3.1601$  or  $A=23.573$  and  $B=0.10678$ . When B is plugged back into Equation 6-11 and linear regression analysis is used to solve for A, the resulting  $R^2$  is 0.745 and A is 28.386. This  $R^2$  is somewhat less than the  $R^2$  of 0.794 from fit of DCBNH against a constant and  $\text{HCl}^5$ . Adding a constant term to Equation 6-11 doesn't increase  $R^2$ . By adjusting B in this equation to 0.3 the  $R^2$  can be brought up to 0.797. Replacing the constant term with a benzene term reduces  $R^2$  to 0.614. Adding the constant term back in raises  $R^2$  to 0.846. Replacing the benzene term with its square raises  $R^2$  slightly to 0.848. All three coefficients here are well-defined.

#### Linear Regression Fits to Nonlinear Equations

In a phenomenological study of the data from the Pittsfield-Vicon incinerator [1] Green et al. [3-5] modelled

total chlorinated dioxin, furan, benzene, and phenol emissions with an equation of the form

$$Y = a X \exp(n X) + b X \exp(m X) F(t; \mu, p) Z^q \quad (6-13)$$

where

$$F(t; \mu, p) = (t/2)^\mu \exp(p/2 - p/t), \quad (6-14)$$

Y is total emission of the group of compounds of interest in ( $\mu\text{g}$  output compound)/(kg input waste), X is HCl emission in g/kg, t is absolute temperature in R (Rankine) divided by 1000, and Z is CO emission in mg/kg divided by 100. The first term in Equation 6-13 represents baseline emissions with ideal combustion conditions (no CO). The second term represents the effect of the temperature and CO on emissions. The temperature, HCl, CO, and chlorinated emissions were measured at the duct after the Vicon's secondary combustion chambers. To fit this equation to the CCTL data using linear regression the first term was ignored and the rest of the equation was converted to the form

$$[\ln(\frac{Y}{X}) - \mu \ln(\frac{t}{2})] = \text{const} + m[X] + p[-\frac{1}{t}] + q[\ln(Z)] \quad (6-15)$$

where

$$\text{const} = \ln(b) + \frac{p}{2}, \quad (6-16)$$

and  $\mu=1$ , which was a typical value used in the previous studies [3-5]. Here the CCTL PCC and SCC temperatures are available instead of the stack (duct) temperature. Fits were made using the same temperature on both sides of

Table 6-7. Results of Fits to Linearized Versions of Nonlinear Functions.

term	1	HCl	-1/t	ln(Z)	R <sup>2</sup>
parameter	const	m	p	q	
Y(DCB, tp)	3.8583	-0.0250	3.0055	-0.0387	0.0253
Y(DCB, tp)	2.5212	-0.0251		-0.0449	0.0244
Y(DCB, ts)	9.5254	-0.0286	16.8888	0.1123	0.0640
Y(DCB, ts)	2.4595	-0.0257		-0.0294	0.0238
Y(DCB, tp)	4.0702	-0.0263	3.5311		0.0243
Y(DCB, tp)	2.4951	-0.0268			0.0230
Y(DCB, ts)	8.1244	-0.0249	13.4244		0.0575
Y(DCB, ts)	2.4424	-0.0268			0.0232
Y(CB, tp)	-2.7787	-0.0712	-13.0726	-0.0245	0.2544
Y(CB, tp)	3.0003	-0.0693		0.0064	0.2334
Y(CB, ts)	-2.8095	-0.0662	-13.8065	-0.0983	0.2712
Y(CB, ts)	2.9402	-0.0703		0.0221	0.2354
Y(CB, tp)	-2.5518	-0.0718	-12.5250		0.2537
Y(CB, tp)	3.0045	-0.0691			0.2334
Y(CB, ts)	-1.3022	-0.0694	-10.0838		0.2633
Y(CB, ts)	2.9546	-0.0696			0.2348
term	1	HCl	-1/t	Z	R <sup>2</sup>
parameter	const	m	p	r	
Y(DCB, tp)	4.6034	-0.0195	4.2797	-0.0813	0.0626
Y(DCB, tp)	2.6926	-0.0201		-0.0806	0.0606
Y(DCB, ts)	6.9640	-0.0205	10.3450	-0.0584	0.0756
Y(DCB, ts)	2.6288	-0.0205		-0.0761	0.0571
Y(CB, tp)	-2.6699	-0.0654	-13.3092	-0.0863	0.3313
Y(CB, tp)	3.2304	-0.0626		-0.0848	0.3084
Y(CB, ts)	-4.7246	-0.0601	-18.9387	-0.1186	0.3866
Y(CB, ts)	3.1681	-0.0635		-0.0802	0.3013

Equation 6-15. The results of fitting this equation to DCB and CB emission data from CCTL are listed in Table 6-7. The R<sup>2</sup>s listed in Table 6-7 are for the fit to Equation 6-15, not to Equation 6-13. All 18 DCB data points were used. One of the CB values was zero, which caused the left side of Equation 6-15 to be negative infinity, so only 15 CB data

points were used. In general the fits were better using  $t_s$   $((T_{sc}+460)/1000)$  for  $t$  than using  $t_p$   $((T_{sc}+460)/1000)$  for  $t$ . Fits without the  $[-1/t]$  term and using  $t=t_p$  were not much worse than fits with that term. When using  $t=t_s$ , the fits did degrade when the  $[-1/t]$  term was excluded. Fits without the  $\ln(Z)$  term were not much worse than with that term.

Fits were also made with

$$\left[ \ln\left(\frac{Y}{X}\right) - \mu \ln\left(\frac{t}{2}\right) \right] = \text{const} + m[X] + p\left[-\frac{1}{t}\right] + r[Z], \quad (6-17)$$

where the  $\ln(Z)$  term in Equation 6-15 was replaced by  $Z$ . Equation 6-17 can be converted to an equation similar to Equation 6-13:

$$Y = aX \exp(nX) + bX \exp(mX) F(t; \mu, p) \exp(rZ). \quad (6-18)$$

Fits to Equation 6-17 were quite improved over those to Equation 6-15 (see Table 6-7), especially for the CB- $t_s$  case.

To determine  $R^2$ s for  $Y$  instead of the left-hand sides for Equations 6-15 and 6-17, the equations were rearranged as

$$Y = g X (t/2)^\mu \exp(m X - p/t) Z^q \quad (6-19)$$

and

$$Y = g X (t/2)^\mu \exp(m X - p/t + r Z), \quad (6-20)$$

respectively. Using  $\mu=1$  and the parameters  $m$ ,  $p$ ,  $q$ , and  $r$  as determined by Equations 6-15 and 6-17, linear regression analysis was used to solve for  $g$  and calculate  $R^2$  (see

Table 6-7). For the cases involving DCB, all but the DCB-tp-Equation 6-20 case had smaller  $R^2$ s than with

$$Y = h X, \quad (6-21)$$

which had  $h=12.79$  and  $R^2=0.431$ . For CB, using the 15 nonzero points, all four cases larger  $R^2$ s for Equation 6-20 than for Equation 6-21 ( $R^2=0.373$ ). The CB-ts-Equation 6-20 case had the largest  $R^2$  of the four. With the zero CB point added (i.e. using all 16 CB data points), only the CB-ts-Equation 6-20 case had a larger  $R^2$  than with Equation 6-21. The two largest  $R^2$ s for DCB and CB suggest that there may be some nonlinear temperature and/or CO influence on chlorinated organic emissions.

#### Nonlinear Least-Squares Fits

Since the parameters determined from regression analysis on the linearized equations (Equations 6-15 and 6-17) may be the parameters that minimize  $R^2$  for the nonlinearized equations (Equations 6-13 and 6-18), a nonlinear least squares program, NLFIT, was used to redetermine those parameters for the DCB data.

The NLFIT program is written in FORTRAN and runs on a personal computer. The NLFIT program requires the user to write a subroutine that includes the function to which the data is being fit and the partial derivatives of that function with respect to the parameters (not the independent variables) in the function. The program uses these

derivatives to calculate the partial derivative of sum of squared errors (SSE or chi) with respect to the parameters. The program iterates on the values of the parameters by calculating what changes to the parameters will minimize SSE. The program requires the user enter initial estimates of the parameters before it starts iterating. The user can specify that certain parameters be fixed, i.e., the program will use the values of those parameters as given and not change or search on them. The program runs until it cannot lower SSE by more than  $10^{-7} * \text{SSE}$ . The program then prints out the current values of the parameters, their estimated errors, SSE, and  $R^2$ . The program creates a file with columns of independent variables, the dependent variable, the fit to dependent variable based on the final parameters, and the error between the fit and the dependent variable. The usual method of using the NLFIT program is to, for the first run, estimate initial values for all parameters fix certain parameters and let the program vary the others, and for the next and subsequent runs, to fix or release (let vary) one or more additional parameters while starting with the parameter values produced by the previous run.

Equation 6-17 was rewritten as (Model 1)

$$Y = aX \exp(nX) + gX \exp(mX) \left(\frac{t}{2}\right)^\mu \exp\left(-\frac{p}{t}\right) z^q \quad (6-22)$$

for the NLFIT program. The parameters a and n were fixed at zero so that the first term was ignored and  $\mu$  was again fixed at 1. The resulting parameters produced by the NLFIT program

are listed in Table 6-8. For  $t=tp$ ,  $R^2$  was 0.446, which is only slightly better than the  $R^2$  (0.431) for the fit of DCB

Table 6-8. Parameters for Nonlinear Equation Fits.

model 1:

$$Y = aX \exp(nX) + gX \exp(mX) \left(\frac{t}{2}\right)^\mu \exp\left(-\frac{p}{t}\right) z^q \quad (6-22)$$

Y=DCB,  $t=tp$ :

a	n	b	m	$\mu$	p	q	$R^2$
0	0	0.0310	6.24e-4	<u>1</u>	-13.6	-0.162	0.446

Y=DCB,  $t=ts$ :

0	0	1.10	6.40e-4	<u>1</u>	-5.79	-0.173	0.443
-46.3	0	14.7	2.06e-4	<u>1</u>	-3.00	-0.045	0.445
0	0	5.78e08	9.38e-5	-16.5	34.7	-0.189	0.447
0	0	1.12e04	0	-7.01	12.8	-0.173	0.445
0	0	14.8	0	0	0	-0.135	0.442
0	0	14.5	1.32e-3	0	0	-0.139	0.442
0	0	3.33	5.82e-4	0	-3.57	0.175	0.444
0	0	6.30e02	4.19e-4	-4.67	6.95	-0.182	0.445

model 2:

$$Y = a X \exp(n X) + b X \exp(m X) H(t;\mu,p) z^q \quad (6-23)$$

$$H(t;\mu,p) = (t/v)^\mu \exp(p/v - p/t) \quad (6-24)$$

Y=DCB,  $t=ts$ ,  $v=2.360$ :

a	n	b	m	$\mu$	p	q	$R^2$
0	0	12.9	0	<u>1</u>	0.535	0	0.432
0	0	15.2	0	<u>1</u>	-5.95	-0.173	0.443
0	0	15.1	0.000611	<u>1</u>	-5.92	-0.175	0.443
0	0	31.0	-0.00366	-974	2283	-0.629	0.553
0	0	31.0	-0.00366	-974	2283	-0.629	0.553
0	0	30.4	0	-988	2315	-0.664	0.553
0	0	14.3	0	-447	1056	0	0.461
0	0	17.4	-0.0129	-526	1242	0	0.467

Y=DCB,  $t=tp$ ,  $v=2.239$ :

0	0	12.7	0	<u>1</u>	-9.73	0	0.433
0	0	14.9	0	<u>1</u>	-13.8	-0.161	0.446
0	0	14.8	0.000639	<u>1</u>	-13.9	-0.163	0.446
0	0	17.2	-0.00816	-767	1696	-0.154	0.451
0	0	15.5	0	-515	1135	-0.176	0.450
0	0	13.0	0	-470	1042	0	0.436
0	0	14.9	0	-5.25	0	-0.161	0.447

Note: all zero values and underlined values were fixed.

Table 6-8--continued

$$\text{model 3: } Y = a X \exp(n X) + b X \exp(m X) J(t;u,s) Z^q \quad (6-26)$$

$$J(t;u,s) = \exp(-((t-u)/s)^2/2) \quad (6-25)$$

Y=DCB, t=ts:

a	n	b	m	u	s	q	R <sup>2</sup>
0	0	30.6	0	2.35	0.0777	-0.653	0.550
0	0	14.3	0	2.37	0.115	0	0.459
0	0	17.3	-0.0126	2.36	0.106	0	0.465
0	0	31.2	-0.00383	2.35	0.0781	-0.617	0.550

Y=DCBNH, t=ts:

a	n	b	m	u	s	q	R <sup>2</sup>
0	0	12.2	0	2.41	0.152	-0.0208	0.594
0	0	12.0	0	2.42	0.159	0	0.593
0	0	11.5	0.0379	2.76	0.350	0	0.640

Y=DCB, t=tp:

a	n	b	m	u	s	q	R <sup>2</sup>
0	0	42.8	0	0.574	1.066	0	0.433

$$\text{model 5: } Y = aX \exp(nX) + bX \exp(mX) H(t;\mu,p) \exp(rZ) \quad (6-27)$$

Y=DCB, t=ts, v=2.360:

a	n	b	m	$\mu$	p	r	R <sup>2</sup>
0	0	17.5	0	$\frac{1}{2.36}$	$\frac{2.36}{2.36}$	-0.0955	0.460
0	0	17.2	0.00157	$\frac{1}{2.36}$	$\frac{2.36}{2.36}$	-0.0977	0.460
0	0	20.0	0.0760	-9781	22702	-0.6788	0.701
0	0	31.2	0	-7739	17991	-0.3467	0.658
0	0	9.4	0	-10953	25443	0	0.586
0	0	17.4	-0.0129	-526	1242	0	0.467

$$\text{model 6: } Y = aX \exp(nX) + bX \exp(mX) J(t;u,s) \exp(rZ) \quad (6-28)$$

Y=DCB, t=ts:

a	n	b	m	u	s	r	R <sup>2</sup>
0	0	17.3	-0.0127	2.36	0.1057	0	0.465
0	0	75.4	0.0756	2.32	0.0236	-0.677	0.701
0	0	73.7	0	2.33	0.0264	-0.345	0.659
0	0	36.7	0	2.32	0.0222	0	0.587
0	0	15.1	0.137	2.32	0.0157	0	0.694
0	0	14.3	0	2.37	0.1145	0	0.459

model 3 revisited, Y=DCB, t=ts:

a	n	b	m	u	s	q	R <sup>2</sup>
0	0	15.1	0.137	2.32	0.0157	0	0.694
0	0	49.0	0.0778	2.32	0.0214	-1.280	0.701
0	0	64.0	0	2.32	0.0256	-0.771	0.651
0	0	36.7	0	2.32	0.0222	0	0.587
0	0	14.3	0	2.37	0.1145	0	0.459

versus just HCl. For  $t=ts$ ,  $R^2$  was 0.443. Starting with the values of  $g$ ,  $m$ ,  $\mu$ ,  $p$ , and  $q$  just produced by the NLFIT program and letting the NLFIT program vary parameter  $a$ , with  $t=ts$ , resulted in  $R^2=0.445$ . This indicates that adding an HCl term does not improve the fit, or that the second term fits the data as well or better than an HCl. Fixing  $a$  to zero again and releasing  $\mu$  resulted in  $R^2=0.445$ . Almost all parameters generated by NLFIT so far were indicated by the program to be not well-defined, i.e., their estimated errors exceeded the absolute value of the corresponding parameters.

In the previous analysis of the Vicon data [3-8], the value 2 was chosen as a divisor in Equation 6-14 since it was near the average value of  $t$ . In the CCTL data, the average for  $tp$  is 2.239 and for  $ts$  is 2.360. To use these values, Equations 6-13 and 6-14 were rewritten as (Model 2)

$$Y = a X \exp(n X) + b X \exp(m X) H(t; \mu, p) Z^q \quad (6-23)$$

and

$$H(t; \mu, p) = (t/v)^\mu \exp(p/v - p/t), \quad (6-24)$$

where  $v$  is the average of  $tp$  or  $ts$ , depending on which is being used for the fit. The  $F$  and  $H$  functions in Equations 6-14 and 6-24 are somewhat orthonormal and have values near 1, which makes the  $b$  parameter less sensitive to changes in  $\mu$  and  $p$ . The  $(t/2)^\mu \exp(-p/t)$  subterm in Equation 6-22 causes the  $g$  parameter to be very sensitive to  $\mu$  and  $p$  since it absorbs the  $\exp(p/2)$  term.

With  $a=0$ ,  $n=0$ ,  $m=0$ ,  $\mu=1$ , and  $q=0$ , all fixed, and  $t=ts$  the NLFIT iterated on parameters  $b$  and  $p$  and produced  $R^2=0.432$ . Letting  $q$  vary raised  $R^2$  slightly to 0.443. Letting  $m$  vary as well did not increase  $R^2$ . When  $\mu$  was also allowed to vary,  $R^2$  rose to 0.553. With noisy data values of  $R^2$  over 0.5 are noteworthy. This large increase indicates a definite relationship between DCB emissions and SCC temperature. Since  $m$  was indicated as being not well-defined, it was set to zero, and the NLFIT program was reran. The  $R^2$  remained at 0.553. The four varying parameters ( $b$ ,  $\mu$ ,  $p$ , and  $q$ ) were all well-defined. Fixing  $q=0$  resulted in  $R^2=0.461$ , which indicates DCB emission is dependent on the CO level as well. Allowing  $m$  to again vary raised  $R^2$  slightly to 0.467, again indicating it is not a significant parameter.

With  $t=tp$  and the parameters  $a$ ,  $m$ ,  $\mu$ ,  $p$ , and  $q$  all being varied by the NLFIT program, the resulting  $R^2$  was 0.451. Only the parameter  $b$  was well-defined. Fixing  $m$  at zero reduced  $R^2$  only to 0.450. Fixing  $q$  to zero as well reduced  $R^2$  to 0.436.

The parameters  $\mu$  and  $p$  had very large absolute values as compared to  $t$  and  $v$  in Model 2. To determine if another function could also represent  $H$ , but without the large parameter values in the pre-exponential factor and exponent,  $H$  was plotted (see Figure 6-3) against  $t$  for the parameter values determined for Model 2 for the  $a=n=m=0$  case. The resulting curves appeared Gaussian (shaped like a normal bell curve), which suggest a function like

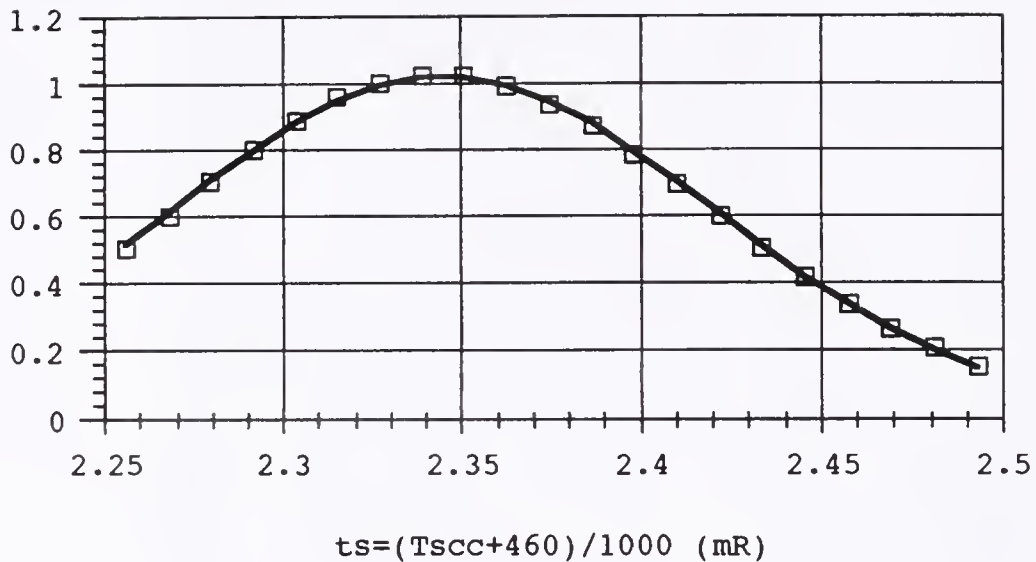


Figure 6-3. Replacement of the orthogonal function  $H(t; \mu, p)$  with a Gaussian function  $J(t; u, s)$  ( $\mu = -988.03$ ,  $p = 2314.8$ ,  $u = 2.3447$ ,  $s = 0.07569$ ).

$$J(t; u, s) = \exp(-((t-u)/s)^2/2) \quad (6-25)$$

could replace H. Equation 6-15 was rewritten as (Model 3)

$$Y = a X \exp(n X) + b X \exp(m X) J(t; u, s) z^q, \quad (6-26)$$

The parameters  $u$  and  $s$  were estimated from the plots for initial values for the NLFIT program. The 1.02 multiplier on  $J(t; u, s)$  is absorbed into the  $b$  parameter. Again  $a$  and  $n$  were fixed at zero. Allowing the NLFIT program to vary  $b$ ,  $m$ ,  $u$ ,  $s$ , and  $q$ , the program produced  $R^2 = 0.550$  with  $t = ts$ . The parameter  $m$  was not well-defined here as well. When  $m$  was fixed to zero,  $R^2$  remained at 0.550. Fixing  $q$  at zero

reduced  $R^2$  to 0.459. These results were very similar to those from Model 2. For  $t=tp$  the program had difficulty iterating on the parameters for Model 3, so this model was not pursued further.

Since Equation 6-17 performed better in the linearized fits than Equation 6-15, Equation 6-18 was rewritten as (Model 5)

$$Y = aX \exp(nX) + bX \exp(mX) H(t;\mu,p) \exp(rZ) \quad (6-27)$$

for the NLFIT program. With  $t=ts$  and  $a=n=m=\mu=p=0$  the NLFIT program iterated on  $b$  and  $r$ , resulting in  $R^2=0.460$ . The  $R^2$  did not increase when  $m$  was allowed to vary. Releasing  $\mu$  and  $p$  resulted in a very large increase in  $R^2$  to 0.701, one of the largest\* values seen for fits with all 18 data points. The fit appeared to zero in on the largest DCB data point. A poor fit to the largest DCB data point was usually the cause of low  $R^2$  values for both linear and nonlinear fits. Fixing  $m$  to zero reduced  $R^2$  to 0.658. Fixing  $r$  to zero as well reduced  $R^2$  to 0.586. Allowing  $m$  to vary, but keeping  $r$  fixed at zero reduced  $R^2$  to 0.467, which matches the  $a=n=q=0$  result from Model 2. This is expected since when  $q=0$  in Model 2 and  $r=0$  in Model 5, the models are identical. Normally, letting an additional parameter vary would raise  $R^2$  instead of lowering it (in this case from 0.586 to 0.467), but the NLFIT program would not iterate on the values of the parameters left over from the  $m=r=0$  case, and new starting values for  $\mu$  and  $p$  were needed to get the program to run. In any

nonunimodal model there may be many local minimums to SSE, and which minimum is reached depends on the starting values of the parameters and the minimization (optimization) scheme used.

As in Model 2, the parameters  $\mu$  and  $p$  in Model 5 had very large absolute values as compared to  $t$  and  $v$ . Using the same Gaussian function as in Model 3, Equation 6-27 was rewritten as (Model 6)

$$Y = aX \exp(nX) + bX \exp(mX) J(t;u,s) \exp(rZ). \quad (6-28)$$

With  $t=t_s$ ,  $a=n=r=0$ , and with  $u$  and  $s$  estimated from plotting  $H(t;\mu;p)$  against  $t$ , the NLFIT program iterated on  $b$ ,  $m$ ,  $u$ , and  $s$ , producing  $R^2=0.465$ , which exactly matches the result from Model 3 when  $q=0$ . This is expected since Models 3 and 6 are identical when  $q=0$  and  $r=0$ . Releasing  $q$  produced  $R^2=0.701$ , but with reasonable values of  $u$  and  $s$  when compared to the large values of  $\mu$  and  $p$  for the  $a=n=0$  case of Model 5. Fixing  $m$  to zero reduced  $R^2$  to 0.659. The last two cases match  $R^2$ s with those from Model 5. Fixing  $r$  to zero at this point reduced  $R^2$  to 0.587, which is much larger than the previous 0.465 result with the same parameters being searched on by the NLFIT program. Again the starting values of the parameters decided which minimum of SSE was reached. Letting  $m$  vary again increased  $R^2$  to 0.694, the highest result so far with 4 varying parameters. Fixing  $m$  at zero again reduced  $R^2$  to 0.459, which matches an earlier result with Model 3.

Since Model 3 and Model 6 are identical when  $q=0$  and  $r=0$ , Model 3 was run starting with the same parameters that produced  $R^2=0.693$  in Model 6. The resulting  $R^2$  and parameters were nearly identical, as expected. Allowing  $q$  to vary increased  $R^2$  to 0.701, the same value reached when the five corresponding parameters were allowed to vary in Model 6. Fixing  $m$  at zero reduced  $R^2$  to 0.651, just less than the 0.659 produced from Model 6. Fixing  $q$  to zero reduced  $R^2$  to 0.587, which matches the result from Model 6 for  $m=r=0$ . However, restarting with the parameter values that produced  $R^2=0.693$  in Model 6, but with  $m$  fixed at zero, produced at  $R^2$  of 0.459, which matches the last result from Model 6 but is much less than the 0.693 produced for the same varying parameters in the last run.

#### Cross-Product and Kinetic-Type Fits

The chlorobenzene data also shows an outlying data point, which corresponds to DCB's outlying data point. Chlorobenzene without its outlying data point (CBNH) correlates nearly as well against a constant and HCl ( $R^2=0.520$ ) as DCBNH does ( $R^2=0.586$ ). When CBNH is correlated against a constant, HCl, and benzene,  $R^2$  raises to 0.625 (see Table 6-9). When HCl<sup>2</sup>, benzene<sup>2</sup> and HCl\*benzene terms are added for a full quadratic fit,  $R^2$  raises to 0.836. The coefficient for the HCl\*benzene term is most defined (had the highest t-ratio), and that for the HCL term is least defined.

Table 6-9. Results of Cross-Product Regression of CCTL VOST Data.

N = 15      DOF = 13      R<sup>2</sup> = 0.52028      Sy = 35.40277  
 CBNH = 25.86152 + 6.934025 HCL  
 t-ratios: 1.944647      3.75487

N = 17      DOF = 15      R<sup>2</sup> = 0.58583      Sy = 42.5986  
 DCBNH = 12.56213 + 9.185404 HCL  
 t-ratios: .8232941      4.60617

N = 15      DOF = 12      R<sup>2</sup> = 0.62495      Sy = 32.58126  
 CBNH = 19.83266 + 5.62701 HCL + 4.365779E-02 BENZ  
 t-ratios: 1.56476      3.052403      1.830047

N = 15      DOF = 9      R<sup>2</sup> = 0.83619      Sy = 24.86342  
 CBNH = 37.8468 + -.2265194 HCL + -.4566562 HCL<sup>2</sup> + .0223694 HCL\*BENZ  
 + -1.533097E-04 BENZ<sup>2</sup> + .1154009 BENZ  
 t-ratios: 1.68688      0.04576145      1.149435      2.942266      1.260709      .8945258

N = 15      DOF = 13      R<sup>2</sup> = 0.77618      Sy = 24.18176  
 CBNH = 40.96126 + 9.305592E-03 HCL\*BENZ  
 t-ratios: 5.856131      6.714425

N = 16      DOF = 14      R<sup>2</sup> = 0.52667      Sy = 52.23701  
 CB = 46.92768 + 1.152342E-02 HCL\*BENZ  
 t-ratios: 3.12764      3.946856

N = 17      DOF = 15      R<sup>2</sup> = 0.68548      Sy = 37.12176  
 DCBNH = 39.27749 + 1.205203E-02 HCL\*BENZ  
 t-ratios: 3.92413      5.717672

N = 18      DOF = 16      R<sup>2</sup> = 0.50137      Sy = 67.9991  
 DCB = 45.85885 + 1.507093E-02 HCL\*BENZ  
 t-ratios: 2.515294      4.011015

N = 17      DOF = 15      R<sup>2</sup> = 0.81574      Sy = 28.41355  
 DCBNH = 43.63743 + 7.322855E-04 HCL<sup>2</sup>\*BENZ  
 t-ratios: 5.943372      8.148909

N = 18      DOF = 16      R<sup>2</sup> = 0.47129      Sy = 70.02033  
 DCB = 55.49216 + 8.302565E-04 HCL<sup>2</sup>\*BENZ  
 t-ratios: 3.116792      3.776563

N = 15      DOF = 13      R<sup>2</sup> = 0.82621      Sy = 29.30751  
 DCBNH = 42.61009 + 7.325179E-04 HCL<sup>2</sup>\*BENZ      <15 CBNH data points only>  
 t-ratios: 5.263596      7.861577

N = 16      DOF = 14      R<sup>2</sup> = 0.46742      Sy = 74.46829  
 DCB = 56.30337 + 8.246443E-04 HCL<sup>2</sup>\*BENZ      <16 CB data points only>  
 t-ratios: 2.789283      3.505306

N = 15      DOF = 13      R<sup>2</sup> = 0.86956      Sy = 25.39067  
 DCBNH = 33.70483 + 6.368112E-02 HCL\*CB  
 t-ratios: 4.568109      9.309327

N = 16      DOF = 14      R<sup>2</sup> = 0.86310      Sy = 37.75556  
 DCB = 31.5768 + .0796827 HCL\*CB  
 t-ratios: 2.884789      9.394919

N = 15      DOF = 12      R<sup>2</sup> = 0.89225      Sy = 24.0194  
 DCBNH = 22.32535 + .1524385 HCL\*CBNH + -1.054418E-03 HCL<sup>2</sup>\*BENZ  
 t-ratios: 2.232892      2.711866      1.589553

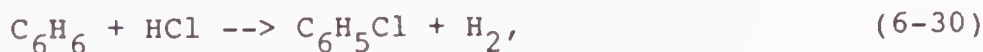
N = 16      DOF = 13      R<sup>2</sup> = 0.95174      Sy = 23.26247  
 DCB = 25.42964 + .1282401 HCL\*CB + -7.715356E-04 HCL<sup>2</sup>\*BENZ  
 t-ratios: 3.706678      11.42232      4.886605

Successively dropping the least defined term until only well-defined terms remain resulted in

$$\text{CBNH} = 40.96 + 0.009306 \text{ HCl} \cdot \text{benzene}, \quad (6-29)$$

with  $R^2=0.776$  ( $r=0.881$ ). With all 16 data points,  $R^2$  drops to 0.527.

When DCBNH is correlated against a constant and HCl\*benzene, the resulting  $R^2$  is 0.685. With all 18 data points of DCB this correlation falls to  $R^2=0.501$ . Equation 6-29 is suggestive of a kinetic model of chlorobenzene formation from benzene:



whose rate of reaction is dependent on the product of the HCl and benzene concentrations. Dichlorobenzene can be formed from benzene by reacting it with 2 HCl's:



The rate of this reaction is dependent on the product of benzene concentration and the square of HCl concentration. This suggests a model to fit the DCBNH data to HCl and benzene:

$$\text{DCBNH} = A + B \text{ HCl}^2 \cdot \text{benzene}. \quad (6-32)$$

A linear regression analysis of this model results in  $A=43.68$ ,  $B=0.0007323$ , and  $R^2=0.816$  ( $r=0.903$ ), the highest  $R^2$  for a two parameter model so far. The coefficients are very

well-defined. With all 18 data points,  $R^2$  drops to 0.471. If only the 15 data points corresponding to the CBNH data are used,  $R^2$  becomes 0.826. With all 16 points that correspond to the CB data  $R^2$  becomes 0.467. The similarity in  $R^2$ s between the 15-point and 17-point cases, and between the 16-point and 18-point cases, indicates that the two DCB data points not covered by CB data are typical of the other 16 data points.

Dichlorobenzene can also be formed from chlorobenzene by reacting it with HCl:



The rate of this reaction is dependent on the product of chlorobenzene concentration and HCl concentration. This suggests a model to fit the DCBNH data with CBNH and HCl:

$$\text{DCBNH} = A + B \text{HCl} \cdot \text{CBNH}. \quad (6-34)$$

A linear regression analysis of this model results in  $A=33.70$ ,  $B=0.06368$ , and  $R^2=0.870$  ( $r=0.932$ ). The coefficients are again very well-defined. With all 16 data points,  $R^2$  drops slightly to 0.863. Combining the methods of DCB formation in Equations 6-31 and 6-33 produces of model that can be represented by

$$\text{DCBNH} = A + B \text{HCl} \cdot \text{CBNH} + C \text{HCl}^2 \cdot \text{benzene}. \quad (6-35)$$

Linear regression of this model results in  $R^2=0.892$ , though coefficient C is not well-defined. With all 16 data points,

$R^2$  raises to 0.952, and all three coefficients are well-defined.

### Fits with Other Volatile Organic Compounds

Most other VOCs were not detected enough times during the 18 VOST runs for statistical analysis. Even the most commonly detected VOCs have several zero-valued (not detected) data points. Chlorobenzene and carbon tetrachloride (CT) have 1 zero point each; methylene chloride (MC) has 2; 1,1,1-trichloroethane (TCA) has 3; chloroform has 4; trichloroethylene (TCE) has 5; and perchloroethylene (PERC) has 10. Reasonable correlations may still be achieved with these data, especially if the zero points for one VOC correspond with those of another VOC, or with low HCl data points.

The 15 data points of carbon tetrachloride ( $\text{CCl}_4$ ) do not correlate with HCl and a constant ( $R^2=0.000$ ) (see Table 6-10). Using the same kinetic approach as before but with CT and CF,



CT was correlated with a constant and  $\text{HCl} \cdot \text{CF}$ . The result for the 13 data points with both CT and CF data was  $R^2=0.176$ . Adding an  $(\text{HCl} \cdot \text{CF})^2$  term raised  $R^2$  to 0.477. A fit of CT data against all quadratic terms of HCl and CF (a constant, HCl,  $\text{HCl}^2$ ,  $\text{HCl} \cdot \text{CF}$ ,  $\text{CF}^2$ , and CF) produced  $R^2=0.573$ . Again the strategy of throwing out the least well-defined terms one at a time (making sure to keep the same number of data points)

Table 6-10. Results of Regressions with Other Compounds.

N = 15    DOF = 13    R<sup>2</sup> = 0.00006    Sy = 13.14461  
 CT = 17.92497 + -1.718162E-02 HCL  
 t-ratios: 3.372693    .0273047

N = 13    DOF = 11    R<sup>2</sup> = 0.17592    Sy = 9.223951  
 CT = 14.38505 + 1.407985E-02 HCL\*CF  
 t-ratios: 4.662381    1.532379

N = 13    DOF = 10    R<sup>2</sup> = 0.47732    Sy = 7.704503  
 CT = 10.65122 + .112461 HCL\*CF + -1.306633E-04 (HCL\*CF)<sup>2</sup>  
 t-ratios: 3.538813    2.698114    2.401374

N = 13    DOF = 7    R<sup>2</sup> = 0.57287    Sy = 8.324526  
 CT = -1.002409 + 3.068977 HCL + -.1131313 HCL<sup>2</sup> + -.0174499 HCL\*CF  
 + .7533582 CF + -6.955545E-03 (CF)<sup>2</sup>  
 t-ratios: .1373565    1.787931    1.129546    .3081661    2.118065    .904165

N = 13    DOF = 9    R<sup>2</sup> = 0.56706    Sy = 7.391299  
 CT = 2.889738 HCL + -.1321422 HCL<sup>2</sup> + -8.665424E-03 CF<sup>2</sup> + .7397838 CF  
 t-ratios: 3.402676    3.079554    2.342544    2.888609

N = 12    DOF = 10    R<sup>2</sup> = 0.02907    Sy = 221.4022  
 MC = 121.6666 + -6.547953 HCL  
 t-ratios: 1.283286    .5471741

N = 11    DOF = 9    R<sup>2</sup> = 0.36506    Sy = 25.73189  
 MCNH = 1.619011 + 3.269773 HCL  
 t-ratios: .1362864    2.274755

N = 11    DOF = 9    R<sup>2</sup> = 0.53558    Sy = 12.43109  
 CF = 6.07818 + .4133894 MCNH  
 t-ratios: 1.293594    3.22163

N = 11    DOF = 9    R<sup>2</sup> = 0.63030    Sy = 11.09123  
 CF = 7.312712 + .0338138 HCL\*MCNH  
 t-ratios: 1.872917    3.917115

N = 16    DOF = 14    R<sup>2</sup> = 0.15117    Sy = 70.42095  
 TCA = .8841438 + 5.320214 HCL  
 t-ratios: 3.159901E-02    1.579032

N = 13    DOF = 11    R<sup>2</sup> = 0.03422    Sy = 10.09458  
 TCE = 4.356813 + .3333363 HCL  
 t-ratios: 1.007599    .6243408

N = 16    DOF = 14    R<sup>2</sup> = 0.00673    Sy = 2.819275  
 PERC = 1.487426 + 4.370739E-02 HCL  
 t-ratios: 1.404945    .3080469

N = 13    DOF = 7    R<sup>2</sup> = 0.76005    Sy = 1.773524  
 PERC = .2703843 + .3543648 HCL + -6.142516E-02 HCL<sup>2</sup> + .1143868 HCL\*TCE  
 + .2080915 TCE + -2.786053E-02 (TCE)<sup>2</sup>  
 t-ratios: .2126463    1.091385    3.121332    2.940455    1.002909    4.223488

N = 13    DOF = 9    R<sup>2</sup> = 0.70857    Sy = 1.723748  
 PERC = .524154 HCL + -7.424924E-02 (HCL)<sup>2</sup> + .1362114 HCL\*TCE  
 + -2.643186E-02 TCE<sup>2</sup>  
 t-ratios: 3.152755    4.875449    4.463712    4.206428

until only well-defined terms remain is used here. In this case the constant and HCl\*CF terms can be dropped, leaving four well-defined coefficients and  $R^2=0.567$ . The 12 methylene chloride (MC) ( $\text{CH}_2\text{Cl}_2$ ) data points do not correlate with HCl and a constant, but one value is an order of magnitude higher than the rest and is probably the result of contamination, since MC is frequently used in chemical analyses performed near where the VOST traps were analyzed. MC without that outlying point (MCNH) correlates somewhat with HCl and a constant ( $R^2=0.365$ ). Chloroform correlates well with a constant and MCNH ( $R^2=0.536$ ), and with a constant and HCl\*MCNH ( $R^2=0.630$ ), but only 11 data points are shared between CF and MCNH.

The 16 data points of 1,1,1-trichloroethane ( $\text{CCl}_3\text{CH}_3$ ) do not correlate well with HCl and a constant ( $R^2=0.151$ ). The 13 trichloroethylene (TCE) ( $\text{C}_2\text{HCl}_3$ ) data points also do not correlate well with HCl and a constant ( $R^2=0.034$ ). The 16 data points of perchloroethylene (PERC) ( $\text{C}_2\text{Cl}_4$ ) do not correlate with HCl and a constant ( $R^2=0.007$ ). A fit of PERC data against all quadratic terms of HCl and TCE produced  $R^2=0.760$ . The constant and TCE terms can be dropped, leaving four well-defined coefficients and  $R^2=0.709$ .

#### Conclusions from the Chlorinated Data Review

The main conclusions from this study of CCTL's VOST, HCl, CO and temperature study are: (1) there is a strong dependence of HCl emission level on the level of chlorine in

the waste; (2) there is a strong dependence of ClHC (notably DCB and CB) emissions on HCl emissions; (3) there is a strong dependence of DCB and CB on each on other and on products of HCl and nonchlorinated benzene; (4) and there is almost certain evidence of nonlinear relations existing between ClHC emissions and CO and temperature. The relationship between HCl output and chlorine input was positive and well-defined. In nearly all of the different regression analyses performed here, the relationship between a chlorinated organic emission and HCl emission was also positive and well-defined. These results contradict the conventional wisdom and lead to a conclusion that increased levels of chlorine in the input does lead to increased chlorinated organic emissions.

CHAPTER 7  
THE NEW COMBUSTION CONTROL SYSTEM

The Combustion Control Strategy

The combustion control strategy is based primarily on the data review, since the review used empirical data. The temperatures are adjusted about 50 °F hotter to allow a higher waste feed rate, to keep the SCC well above 1800 °F as some regulations require, since the kinetics code modelling suggests higher temperatures, and since the residence time in the secondary chamber is about 0.7 seconds, which indicates a SCC temperature of at least 1827 °F according to Equation 1-5. The control strategy is therefore to maintain a primary combustion chamber (PCC) temperature of  $1775 \pm 25$  °F, a secondary combustion chamber (SCC) temperature of  $1850 \pm 25$  °F, and a feed rate of 315 to 400 lb/hr. A kinetics code run with these conditions (Run 40 in Chapter 5) showed slightly lower CO emissions and greatly reduced chlorobenzene emissions than the base case (Run 30), which represented typical previous operating conditions.

To help avoid transient puffs of CO during feeding, the control system is to lower the flow rate of natural gas to the PCC when the ram feed system is triggered. When the feed door opens to let the charge into the incinerator, the PCC natural gas flow rate is cut again, and the SCC natural gas

flow rate is lowered if needed. These reductions should help keep the natural gas from competing with the waste for the available oxygen. When a high level of carbon monoxide (CO) is sensed, the PCC natural gas rate is to be reduced by 20%, or by 10% along with a reduction of the SCC natural gas flow rate. When a high level of hydrogen chloride is sensed, the next feed is to be delayed for one minute to help reduce the rate of chlorine entering the incinerator.

This method of reducing the support fuel when more waste fuel is added is nearly an opposite approach from that of Hasselriis [53]. His approach is to reduce the air to the PCC when the overall air to a starved-air incinerator is insufficient to keep CO and other emissions down, an approach that makes the PCC even more starved. Incinerators made by Joy Energy Systems reduce underfire air to the PCC before each ram feed [40]. This keeps the freshly-fed waste from rapidly releasing volatile matter, which would overwhelm the SCC and create a puff of smoke. The CCTL incinerator is run in the excess-air mode and reducing the natural gas to the PCC shifts the combustion to even more excess air.

#### Implementation of the New Combustion Control Strategy

Analyses of the data review and kinetic modelling have shown desirable operating and combustion parameters. These include parameters such as PCC and SCC temperatures, and waste feed rate. To maintain these parameters at the desired levels, the inputs to the incinerator--garbage and/or other

solid fuel, natural gas, air--must be adjusted by the control system in response to any changes in the parameters.

The combustion conditions, temperature, oxygen, and carbon monoxide are monitored with the existing equipment. The personal computer currently used for data acquisition is the brains for the new control system.

The control system accepts information entered manually into the computer by the incinerator operator(s). This information may include the quality and wetness of the garbage, heating value of the biomass, continuous feed rate of biomass using the auger, when garbage has run out, etc.

The input rates of garbage and biomass are regulated by having the control system signal when ram feeds occur and when biomass feeding starts and stops. These signals are sent through the computer's parallel port and energize relays that actually run the feeders. The stoker, auxiliary blower, and biomass blower are also controlled in the same manner.

Natural gas flow rate to the PCC is controlled by a proportioning valve (a modutrol motor, or modmotor for short, mounted on a butterfly valve with an interconnecting linkage). The modmotor is converted from a resistance input set level to a voltage input set level. The computer sends out a 0- to 5-volt analog signal through the QuaTech D/A module indicating 0% to 100% valve opening.

Natural gas flow rate to the SCC is controlled by a parallel valve arrangement. An extra line has been installed leading to the upper burner. This second, smaller line has

its own on/off valve. The control system opens or closes this valves as needed to step the SCC gas flow rate up or down. The larger line is always open, so a minimum gas rate is sustained, preventing the existing burner controller from sensing a flame out. The on/off valve is also controlled through the QuaTech D/A module.

Either of the above methods of gas control prevent burner outages from being caused by cycling the gas line on and off since at least some gas is always flowing and the burner controller is always on.

The new control system ties into the existing incinerator control system in such a way that, with the new system off, the incinerator operates as before. An external timer with a half-minute cycle has been added to the system. This timer receives a reset command from the computer every time it reads the monitors and/or sends out control signals. If the timer is not reset due to a failure in the system, an alarm sounds alerting the incinerator operator(s). The control system may then be disconnected until the computer or system is restarted.

### Control System Components

#### Straight On/Off Control

To control incinerator components such as the ram feeder, biomass feeder, alarm timer, stoker, auxiliary blower, biomass/overfire blower, and conveyor belt, and to provide a temperature override switch for the burner

controllers, a way is needed to turn on and off 110-VAC power lines using a small digital computer signal. Figure 7-1 shows a schematic of the circuit built to accomplish this control subsystem. While commercial circuit boards exist to perform this type of control, none would have the flexibility to be modified at will as parameters changed during the development of the control system. Also, building the circuitry oneself can keep the whole system simple and cheap and gives one a better understanding of the system's components.

#### Alarm Timer

The control computer program can fail for a variety of reasons--power failure (transient or lasting), breakdown, programming error, or random glitch--an alarm is needed to alert the incinerator operators that the program has stopped running. A timer with a 30-second interval has been set up for this alarm (see Figure 7-1). Under normal operations the control program will send out a pulse to reset the timer once every data gathering cycle, i.e., about every 15 seconds. If the control program or the computer itself stops running, this timer will not be reset and after 30 seconds the timer will energize the alarm relay. The alarm relay then powers visible (a light) and audible (a bell) warnings to alert the operator(s), and turns off the override relay(s), allowing the incinerator to run under more or less original conditions of temperature-controlled, approximately half-open gas

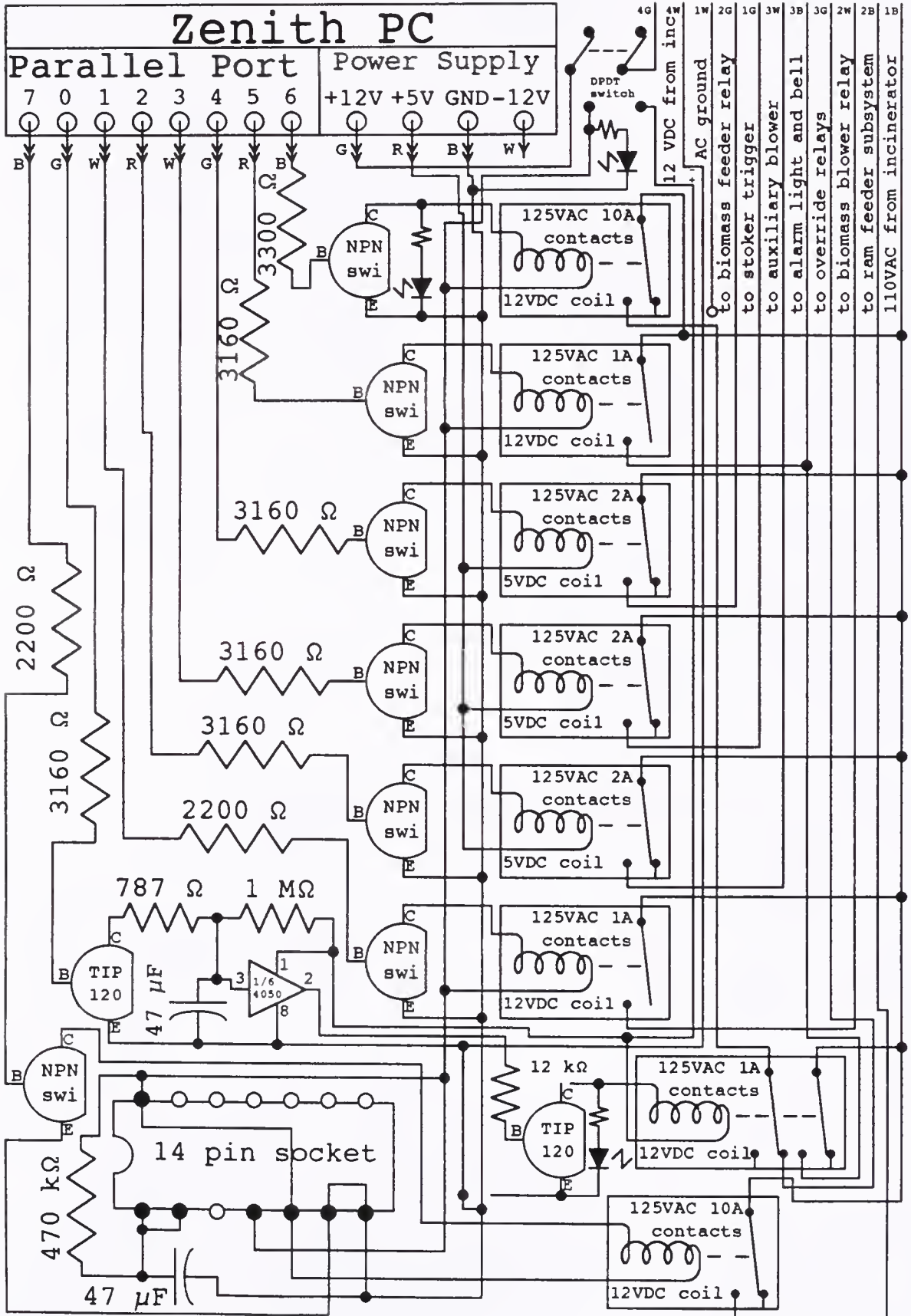


Figure 7-1. On/off and alarm control system circuitry.

valves. The operator(s) can then determine the problem and restart the computer system. The 12-volt power supply for this timer comes from a separate power supply located in the upper right incinerator control panel, instead of from the computer. The 12-volt line for the computer would be off if the computer shuts down.

The computer program also can turn on the alarm light and bell directly if a problem is sensed in the incinerator's operation, or if the program needs some manual input from or something done by the operators.

#### Proportional Control

To regulate the amount of natural gas being fed into the incinerator, the original manually-set stopcock-like gate valve located between the on/off safety valves and the lower burner was replaced by butterfly valves. This 1-1/2" butterfly valve (Midco MBF-150) has a mounting plate for a Modutrol motor (modmotor) and a linkage for connecting the valve to the modmotor. The modmotor has a 160° shaft rotation that translates through the linkage as a 90° valve rotation between fully closed and fully open.

A specially modified modmotor was installed on top of the butterfly valve. The modmotor was modified so that the computer's 0- to 5-volt analog signal would set the valve position proportionally from closed to open.

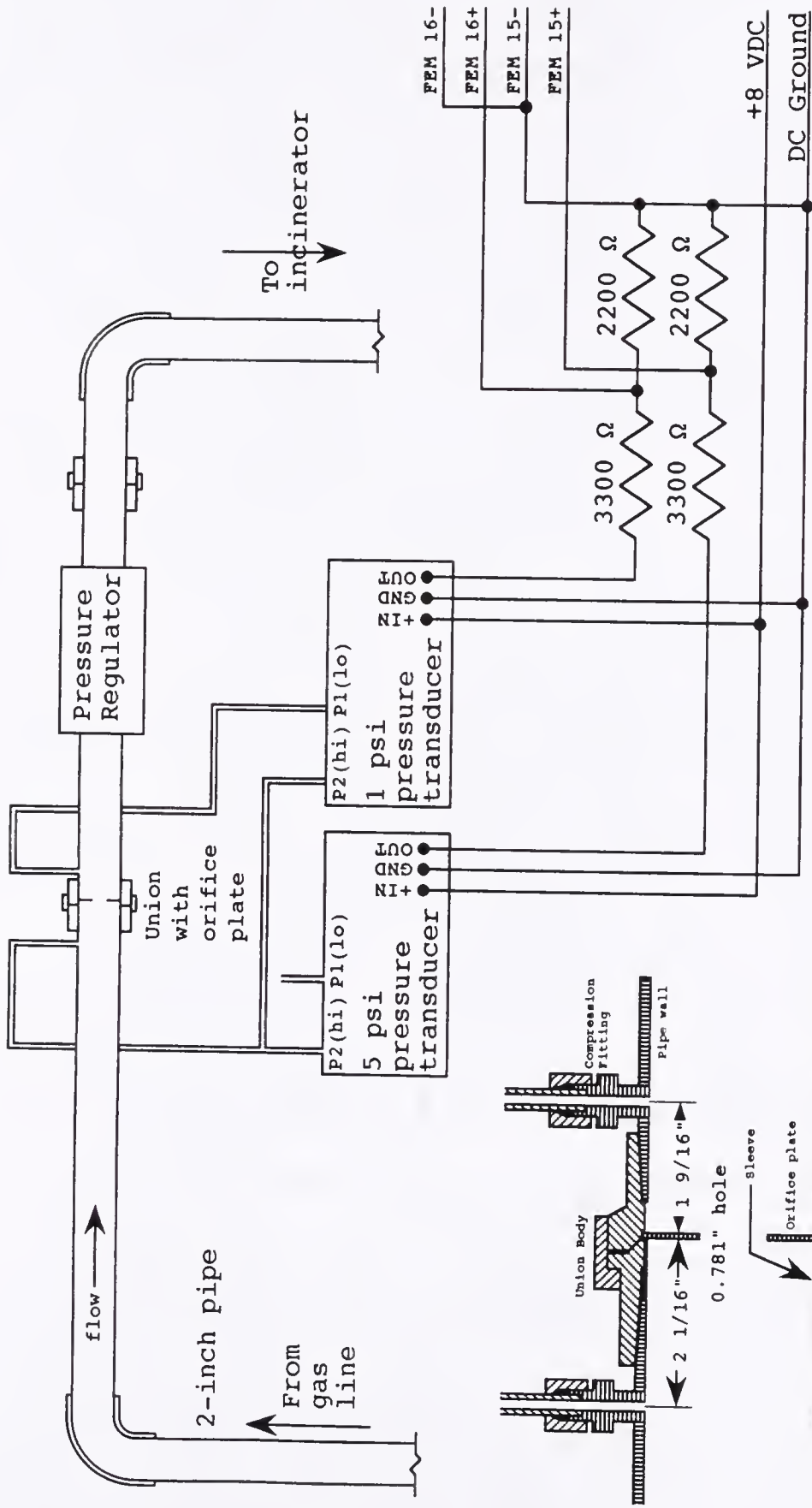
The original gate valve and new butterfly valve and modmotor are shown in the piping diagrams in Figure 7-2.



Initially, both the upper and the lower burner gas lines were to be controlled from the computer via modmotors. While the old gate valve was easily removed from the lower burner gas line by disconnecting the pipe from the lower burner and the union downstream of the gate valve, no union existed between the upper burner and the gate valve in the upper burner gas line, and the gate valve could not be removed from the upper burner gas line without damaging the delicately repaired upper burner. Instead, a parallel piping circuit was installed across the gate valve in the upper burner gas line. Figure 7-2 also shows this piping arrangement. When the solenoid valve is energized by the control system, extra gas is allowed to flow into the upper burner to more quickly warm up the incinerator. The parallel piping arrangement provides for two levels of gas flow during incinerator operation.

#### Gas Line Orifice Meter

Since the natural gas flow is now regulated by the control system, the gas flow rate should be measured on-line. Figure 7-3 shows the orifice metering system developed for this on-line measurement. An 1/16-inch thick orifice plate with a centered 0.781-inch hole is installed in a union in the 2-inch natural gas supply line. The union is located more than 8 pipe diameters downstream and more than 2 pipe diameters upstream of any disturbance, which minimizes any effects of bends on the flow stream. The size of the orifice was calculated to produce a 1-psi pressure drop for a



Orifice meter detail (1/2 scale)

Figure 7-3. Natural gas flow rate measurement orifice meter.

3900-ft<sup>3</sup>/hr natural gas flow rate. A 1-psi pressure transducer measures this drop, while a 5-psi pressure transducer measures the gauge pressure of the gas upstream of the orifice. The outputs of these transducers is sent through voltage dividers to the Doric's Front End Module (FEM). The FEM is now installed inside the instrument trailer for better protection.

The equation for the natural gas flow rate is derived from a Honeywell flow meter handbook [131] as

$$Q = 20009 \left(1 + 0.321 \frac{\Delta P}{P_1}\right) \left(1 + \frac{0.582}{\sqrt{Q}}\right) \sqrt{\frac{\Delta P \cdot P_1}{T_1}} \quad (7-1)$$

where  $Q$  is the natural gas flow rate in ft<sup>3</sup>/hr corrected to standard temperature and pressure of 68 °F and 14.696 psia,  $\Delta P$  is the pressure drop across the orifice in psi,  $P_1$  is the upstream absolute pressure in psia, and  $T_1$  is the upstream absolute temperature, which is taken as the ambient temperature. This equation must be solved iteratively for  $Q$ . The first iteration calculates  $Q$  without the  $(1 + 0.582/\sqrt{Q})$  term. The next iteration uses this value of  $Q$  in the term. Fortunately, only three iterations are needed to produce a flow rate "accurate" to four digits.

During installation the P2 (high pressure) port of the 5-psi pressure transducer broke off. The static upstream gauge pressure of the natural gas would have been measured by this transducer. This pressure has been measured at 4.8-5.2 psig at the orifice meter and at the gas company's meter. An upstream gauge pressure estimate of 5 psig or the gas

company's meter pressure reading will be used here until the transducer can be repaired or replaced.

#### Patching Into the Incinerator's Existing Control Circuitry

When the control system is operating a master override signal is sent from the on/off control board. This 110-VAC signal energizes the following four relays: the API override relay, the gas line override relay, the biomass override relay, and the stoker override relay. When energized the API override relay bypass the temperature set points on the burner controllers so that the burner controllers are always on. The gas line override relay allows the computer to set the lower burner gas level and turn on or off the upper burner extra gas line. With the control system off the lower burner gas valve is set to half-open. The biomass and stoker override relays bring these subsystems under computer control.

The incinerator is started with the control board off. The closed upper burner extra gas line valve and half-open lower burner gas valve produce the same gas flow as before, when the control system was not installed. The use of the override relay allows for future experimental burns that do not use the control system.

#### The Control Computer Program

The control computer program was written in interpretative (uncompiled) BASIC. This computer language was chosen over other languages for the following reasons:

easier program maintenance (no recompilation needed to amend or modify program), the original data acquisition was written in interpretative BASIC, access to computer hardware not found in other languages, high-level computer statements not found in other languages, interpretative BASIC came with the control computer, program speed is not an issue since the data acquisition hardware limits the rate at which system readings can be made, easier program debugging, the English like syntax of BASIC makes the program readable to people other than just the author, and interpretative BASIC is available for or even comes with nearly every type of personal computer. Even though interpretative BASIC is a very unstructured language, the control program was written as modularly as possible, with most repeated set of program steps written as separate subroutines. The program contains comments for most of the non-trivial program statements. The program contains more than 1080 lines of code and comments and is over 46000 characters long. The program is outlined in Figure 7-4.

The computer program has the following ten functions: start logging data, start controlling incinerator, start logging and controlling, stop logging and/or controlling, CEM calibration, shell to operating system, Doric terminal, manual data entry and control, view recently recorded data, and exit program. The manual data entry and control function has two purposes. The first purpose is to allow the user to enter observed data (such as atmospheric pressure, when the

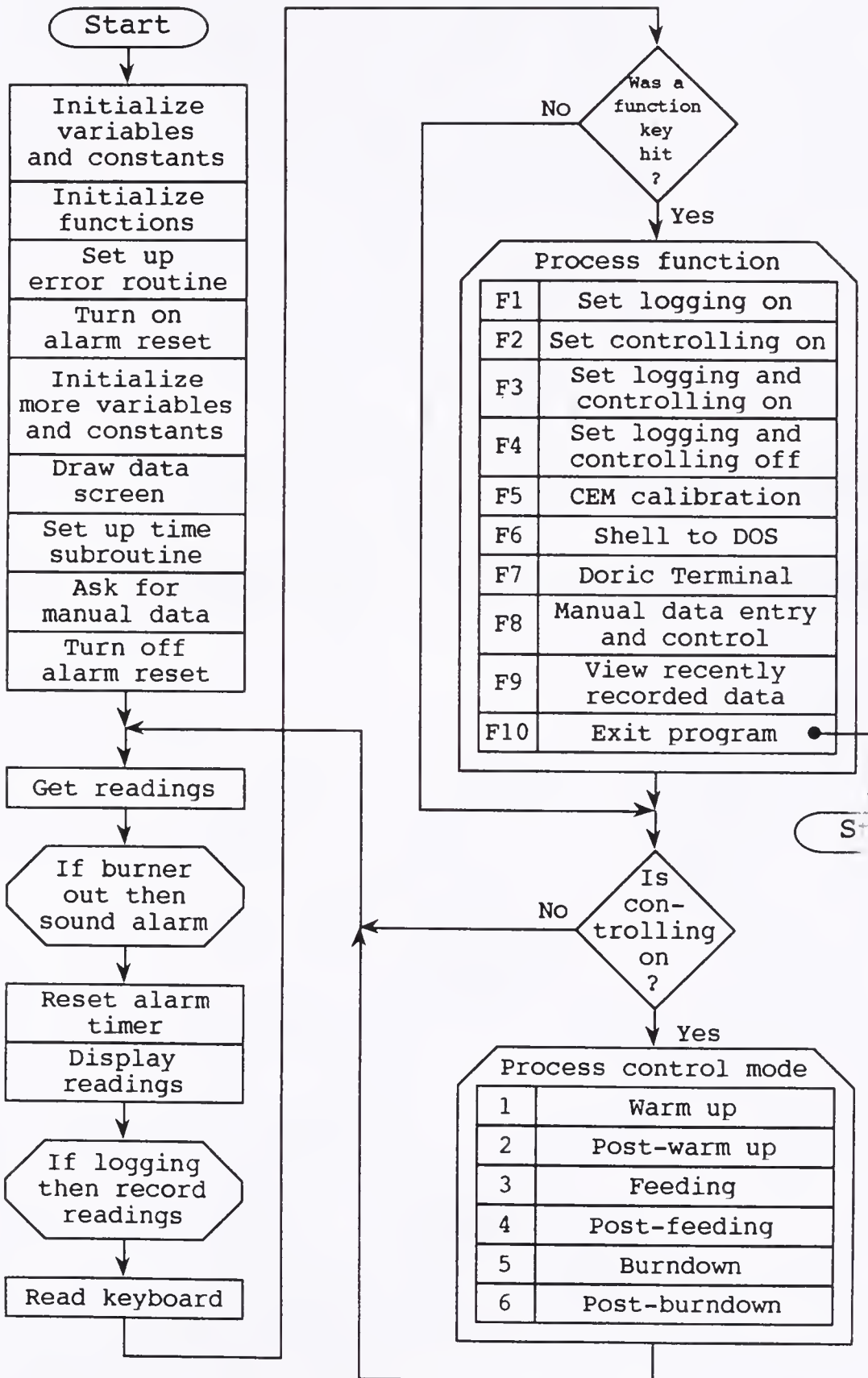


Figure 7-4. Control program overall flowchart.

garbage is used up, and whether or not the big underfire blower is on) which the computer program has no way of directly measuring. The second purpose is to allow the user to manipulate the control settings and even change the control mode of operation. The manual data entry and control function screen is shown in Figure 7-5. More manual data and control entries can be added later as needed.

The computer program's main operation is as follows: initialize constants, variables, and arrays; set up a program error catching routine; draw the data screen; set up a subroutine for updating the displayed time and relay readings every two seconds; ask for manually entered data; read, display, and, if logging, record all temperature, CEM, orifice meter, incinerator system status, and control system status readings; reset the alarm timer; check if the user pressed a function key; if user did press a function key then execute the appropriate function; if controlling then execute the current control mode function; and loop back to the read and display data step. The data display screen is shown in Figure 7-6.

If during the course of operation the computer program encounters a condition requiring human assistance (such as turning on the big (underfire) blower, resetting a burner controller, checking the stoker, manually entering data, or fixing a program run-time error) the computer will display an appropriate message on the screen, beep the computer's speaker, and turn on the alarm light and bell at the incinerator

Manual Data Entries:		Control Values:
A. Bio feed rate: ####	L. Logging: XXX	0. Alarm reset: XXX
B. Big blower: XXX	M. Controlling: XXX	1. Bio blower: XXX
C. Atm pressure: ##.##	N. Ctrl mode: XXXXXXXXX	2. Aux blower: XXX
D. Gas pressure: #.#	O. Feedng interval: #.#	3. Stoker trigger: XXX
E.	P.	4. Biomass feeder: XXX
F. Time inc on: ##:##	Q. Cntr prt smping: XXX	5. Alarm: XXX
G. Garb done at: ##:##	R. Right prt smping: XXX	6. Master override: XXX
H.	S.	7. Ram feed trigger: XXX
I. Warm up length: ###	T. Stoker: XXXXX	
J. Burndownlength: #.#	U.	8. UB valve: ### % open
K.	V.	9. LB valve: ### % open
New Value:		

Figure 7-5. Manual data entry screen.

ICAAS - Univ of Florida - Tacachale - Clean Combustion Technology Laboratory			
Date: MM-DD-YY	Time of last feedng: HH:MM:SS	Ambient temp: #### °F	
Time: HH:MM:SS	Current data pt numbr: #####	PCC temperature: #### °F	
Message:	and time: ##### or HH:MM:SS	Above door temp: #### °F	
XX		SCC temperature: #### °F	
		Hot stack temp: ### °F	
		Meter box temp: #### °F	
Master override: XXX	Control mode: LoGgInG	Sampling port temp: #### °F	
Aux blower: XXX	XXXXXXXXXXXXXXXXXXXXXXXXXXXX		
Bio blower: XXX		HCl concentration: ### ppm	
Ram feed trigger: XXX	Upper burner: XXX	O2 concentration: ##.## %	
Biomass feeder: XXX	Lower burner: XXX	CO2 concentration: ##.## %	
Stoker trigger: XXX	Auxiliary blower: XXX	CO concentration: ### ppm	
Alarm: XXX	Ram feed door: XXXXXX	NOx concentration: ### ppm	
Alarm reset: XXX	Stoker: XXX	UB air rate: ##.## lb/min	
	Biomass feeder: XXX	LB air rate: ##.## lb/min	
UB valve: ### % open	Centr prt smping: XXX	SC air rate: ##.## lb/min	
LB valve: ### % open	Right prt smping: XXX	Nat gas rate: ##### cuft/hr	
F1 Start data logging <input type="checkbox"/> F2 Start controlling <input type="checkbox"/> F3 Start logging and cntrllng F4 Stop logging and/or controlling <input type="checkbox"/> F5 CEM calibration <input type="checkbox"/> F6 Shell to DOS F7 Doric Terminal <input type="checkbox"/> F8 Manual data/control <input type="checkbox"/> F9 View data <input type="checkbox"/> F10 Exit program			

Figure 7-6. Control computer program data screen.

control panels to alert the incinerator operator(s) as to the assistance needed of the problem encountered. After attending to the situation, the operator(s) may need to tell the computer to continue the program, which then turns off the alarm light and bell. Program run-time errors may require modifying and restarting the program.

The alarm light and bell is also lit and sounded if the computer program fails to reset the alarm timer at least once every 30 seconds, which can happen if the computer loses power or the program crashes for some reason. The alarm timer is reset once every time data is read and displayed, which is about once every 15 seconds. The alarm timer is held reset during lengthy functions (such as shell to operating system, Doric terminal, manual data entry and control, and view recently recorded data) when data is not being read and displayed, but while the user is there at the computer.

When the program is switched into the control mode, the master override relay is energized. This relay sends a 110-VAC signal that turns on four override relays that allow the program direct control of turning on and off the aux (auxiliary) blower, the bio (biomass or overfire) blower, the biomass feeder, and the upper burner extra gas line valve; triggering the ram feeder and stoker; and setting the lower burner gas line butterfly valve position. If the alarm timer is not reset every 30 seconds, in addition to turning on the alarm light and bell, the timer also cuts off the master override 110-VAC signal. When the master override signal is off, the incinerator operates just like it did before the control system was installed. This condition is therefore a fall back position when the control program fails to operate.

The control part of the program is divided into the following six modes of operation: warm up, post-warm up,

feeding, post-feeding, burndown, and post-burndown. During the warm up phase (see Figure 7-7) the burners are set to their highest gas rates. When the SCC temperature reaches 1850 °F or levels off, the aux blower is turned on. The temperature is considered levelled off when four consecutive temperature readings vary no more than 3 °F from the average of the four readings. This method of determining levelness was based on "eyeballing" the data from the first control system test. If the SCC temperature reaches 1850 °F with the aux blower on, then the upper burner extra gas line valve is shut off.

The post-feeding, burndown, and post-burndown modes share most of the same computer code, which is referred to as the keeping mode. The mode is responsible for maintaining temperatures, taking care of stoking, determine when the next feed will be, taking care of high CO and high HCl readings, and when the post-warm up and burndown phases are finished. The temperature and feed rate levels maintained by this keeping code are based on the desirable combustion conditions determined earlier from reviewing the last three years of data and from kinetic modelling. These levels were a PCC temperature ( $T_{pcc}$ ) of 1775 °F, an SCC temperature ( $T_{scc}$ ) of 1850 °F, and a garbage feed rate of 315-400 lb/hr. The keeping code attempts to maintain temperatures within 25 °F of these levels. The temperature maintaining logic is as shown in Figure 7-8. To maintain the feed rate, the code calls for a ram feed once every 6.5 minutes. When the CO is

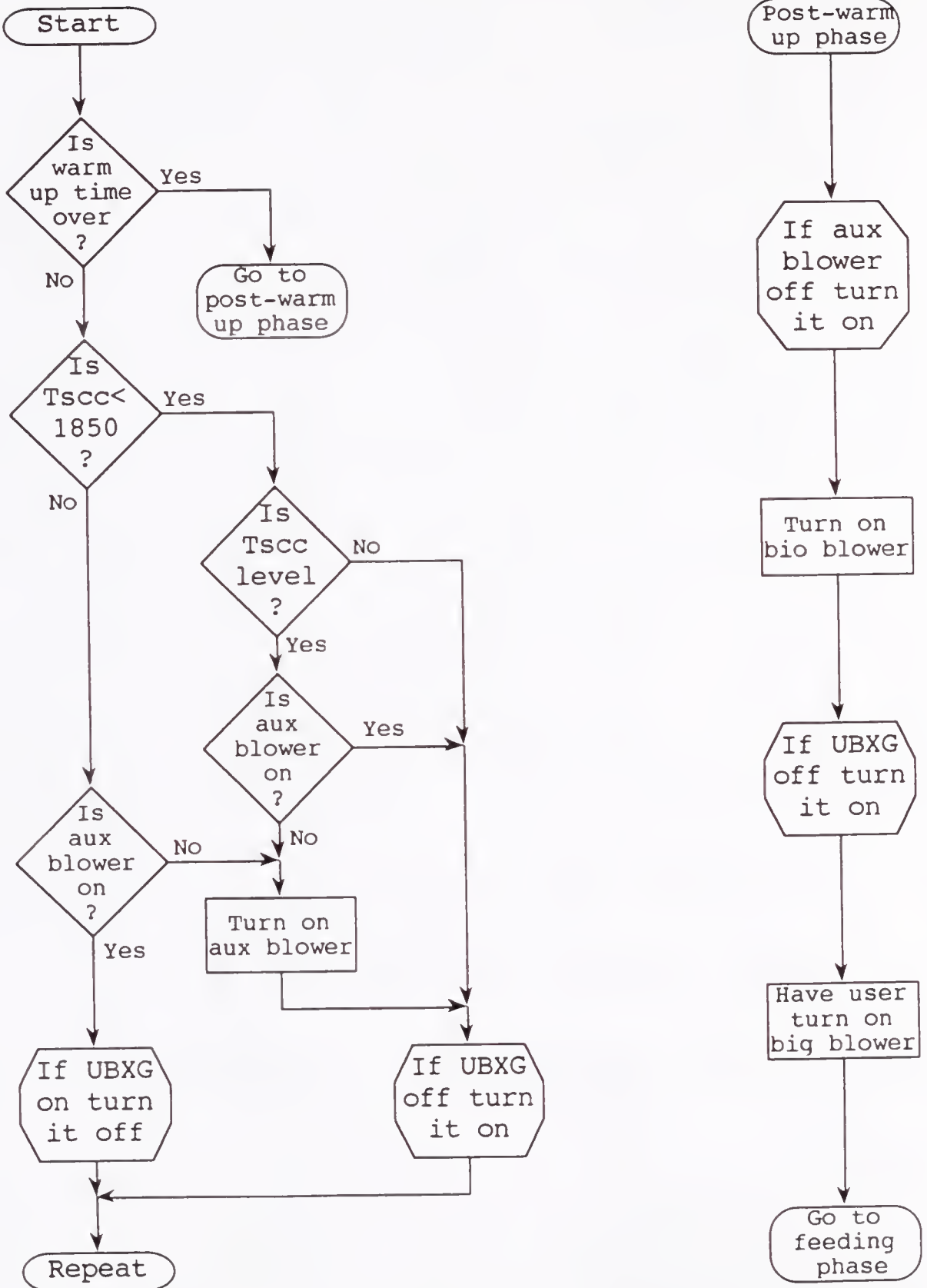


Figure 7-7. Incinerator warm up logic.

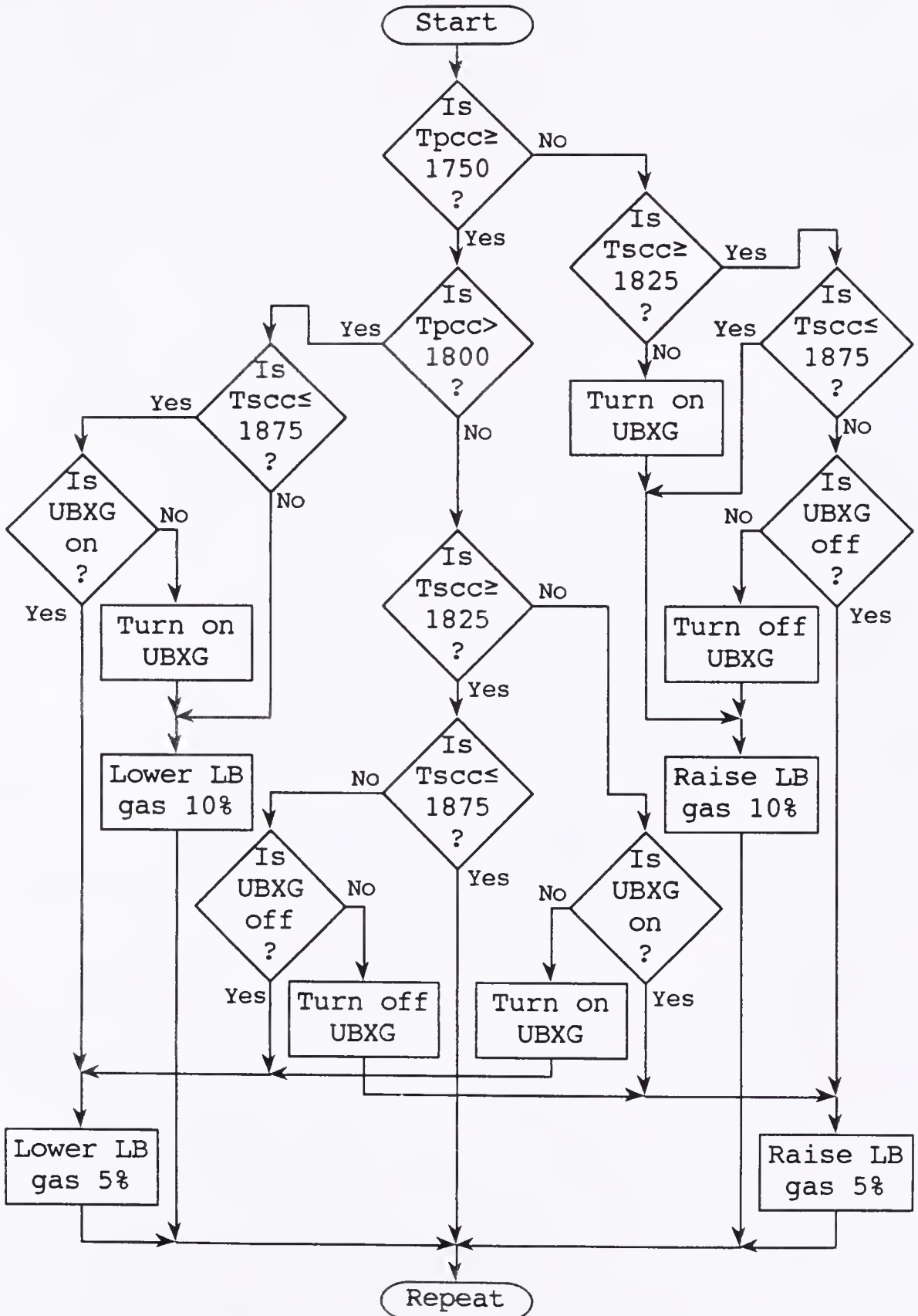


Figure 7-8. Temperature maintaining logic.

above 50 ppm, the lower burner gas is lowered by 20% if the upper burner extra gas line valve (UBXG) is closed or by 10% if the UBXG is open, in which case the UBXG is then closed. The lower amount of gas should decrease the competition for oxygen. When HCl is above 200 ppm, the next feed is delayed by one minute to help lower the overall HCl emissions.

During burndown the stoker is triggered every 7.5 minutes, while during post-feeding the stoker is triggered 2 minutes after each ram feed. Since the stoking cycle is 5.5 minutes long, stoking stops just after the next ram feed. The total time for warm up and post-warm up is 45 minutes, while the length of burndown is 2 hours. These times are adjustable through the manual data entry and control function.

The logic used to maintain the temperatures (see Figure 7-8) is more of a "brute force" method than a traditional application of control theory. Depending on what is in the incinerator at any one time the reaction to a change in gas rate may vary considerably. The logic is somewhat based on adaptive control [132] and fuzzy logic [133]. Adaptive control is used where a fixed model of the system cannot be defined. The control system reads data from the process and modifies the model on-line as needed. The system can take care of disturbances (such as a ram feed) this way. In fuzzy logic the control system needs only to know if a parameter, such as temperature, is too hot or slightly cool, not its precise value. The control system's output is, for example, large decrease or small increase in a control parameter. A

more conventional control system could be used, but the time lag in system operation and response makes it difficult to predict, say, how to change the natural gas flow rates with temperatures, especially when two parameters (PCC and SCC temperature) are not independent of each other.

The feeding phase (see Figure 7-9) is entered after the post-warm up phase and every 6.5 minutes thereafter (unless delayed by high HCl readings) until the garbage is used up. This time interval is equivalent to 360 lb/hr for average (39-lb) ram charges. This time interval is adjustable through the manual data entry and control function. The natural gas rate to the PCC is lowered by 25% just after the ram is triggered, unless the PCC temperature is too cold. The rate is again lowered by 25%, if the UBXG is closed or by 12.5% if the UBXG is open, in which case the UBXG is then closed. The lower amount of gas should decrease the competition for oxygen and prevent the generation of excess CO.

The post-burndown phase is entered at the end of burndown. It consist solely of the computer informing the operator(s) via displaying a message on the computer screen, beeping the computer's speaker and turning on the alarm light and bell that burndown is over. After the operator clears the message on the computer, the computer program continues with the burndown phase. At this point the operator should shut off the incinerator after the stoker finishes its current cycle and exit the computer program.

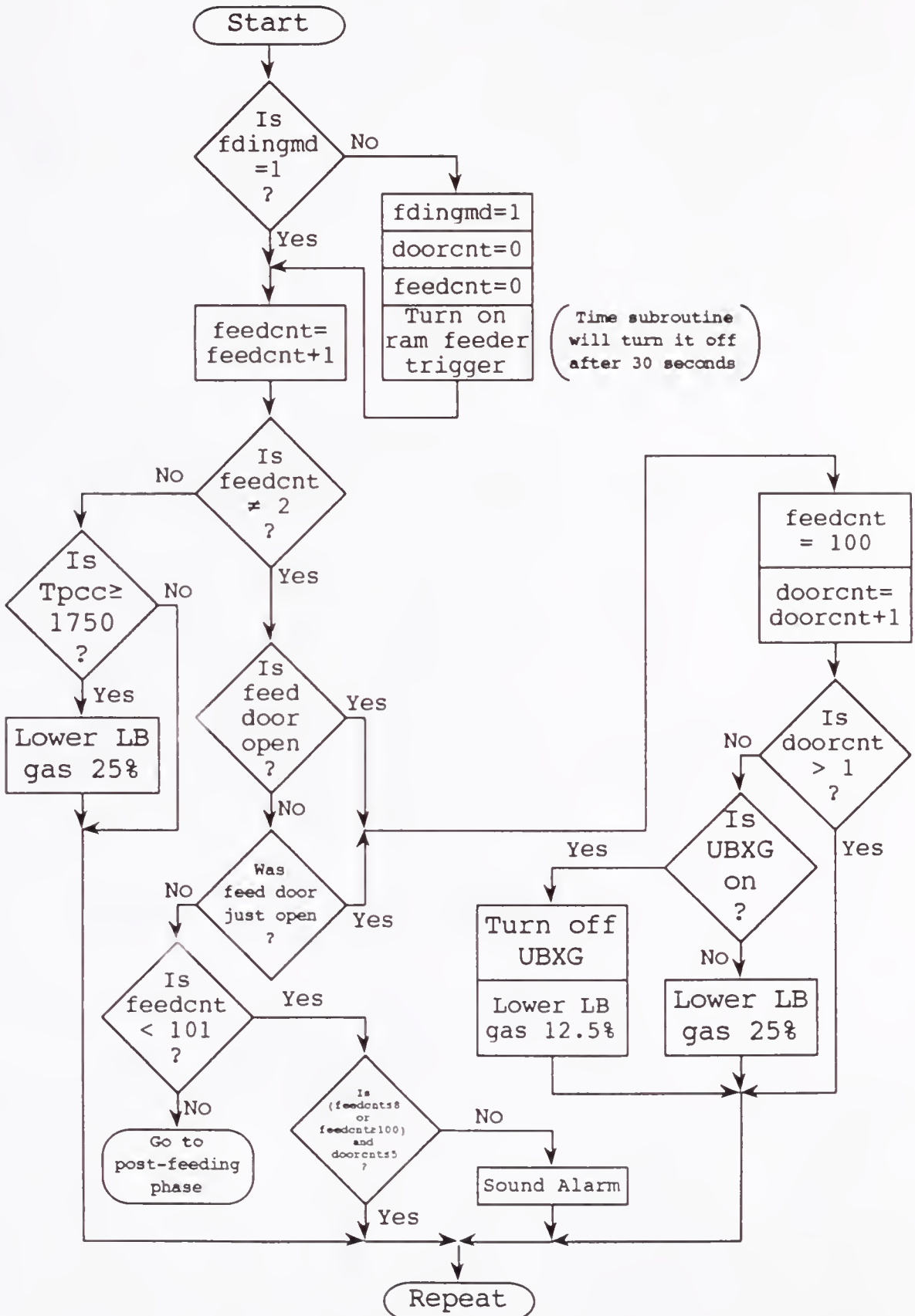


Figure 7-9. Ram feeding logic.

CHAPTER 8  
EXPERIMENTS WITH OLD AND NEW CONTROL SYSTEMS

After the control system was installed the incinerator test-fired twice. These tests were followed by two experimental firings which included garbage feeding, continuous emissions monitoring, and VOC emissions testing.

Test Firings

Test Firing of March 20, 1992

The incinerator was test fired on just natural gas on Friday, March 20, 1992. The goal of this firing was to test the operation of the control computer program and parts of the control system, particularly the lower burner butterfly valve, upper burner extra gas line valve (UBXG), and the natural gas orifice flow meter (NGOM). The digital and analog aspects of the control system had already been tested as the items were installed.

With the new control system off, the incinerator was fired up with the lower burner (LB) butterfly valve (LBBV) set at 25% open, the upper burner shut off, and the UBXG closed. The auxiliary (aux), biomass (overfire or bio), and underfire (big) blowers were all off. The NGOM measured 1142 standard cuft/hr using the atmospheric pressure of 29.91 in Hg (14.691 psia), gas pressure of 4.825 psig, and ambient temperature of 81 °F (540.67 R). The standard temperature

and pressure (STP) used here for the volumetric flow rate is 68 °F and 29.921 in Hg (14.696 psia). The PCC temperature (Tpcc) rose to 865 °F. The LBBV was then set to 50% opened. The flow rate increased to 1637 cuft/hr, while Tpcc rose to 1090 °F. The LBVP was further opened to 75%. The flow rate increased to 1712 cuft/hr, while Tpcc rose to 1130 °F. At this point the gas flow rate was measured at the gas company's meter, a positive displacement type. The flow rate corrected to STP was measured at 1707 cuft/hr. The orifice meter is measuring the flow rate fairly accurately. The LBBV was next opened fully (100%). The flow rate only increased to 1715 cuft/hr. At 75% the butterfly valve plate is inclined only 22.5° from horizontal and offers little resistance compared to other restrictions (elbows, other valves) in the gas line. The lower burner stayed lit the whole time, i.e., there were no flame outs. The Tpcc gradually rose to 1300 °F.

The LBBV was lowered to 50% or 1652 cuft/hr and the upper burner (UB) was turned on. Total gas flow was now 2614 cuft/hr as or 2638 cuft/hr as measured by the gas meter. The upper burner, therefore, supplies about 962 cuft/hr. The gas flow rate here is approximately what is was before the control system was installed. Turning on the UBXG brought the total flow to 2738 cuft/hr, or an additional 124 cuft/hr, a little less than desired for using the UBXG for high and low upper burner gas settings. The Tpcc fell to 1255 °F. The SCC temperature (Tsc) could not be measured at this

point since the leads to its thermocouple were loose. Also, the hot stack and new reinstalled above door thermocouples' leads were both discovered to be accidentally reversed.

Raising the LBBV to 100% with both UB and UBXG on increased the gas flow to 2776 cuft/hr, with the gas meter reading 2801 cuft/hr. Later these readings rose to 2798 and 2805 cuft/hr, respectively. The orifice meter's reading agreed in all four cases to within 1% of the gas meter's reading.

The TscC thermocouple's leads were then reconnected and the hot stack thermocouple's leads were unreversed. (The above door thermocouple's leads were unreversed the next day.) The temperature levelled off at 1850 °F, which is 200 °F hotter than it used to reach during warm up before the control system was installed, and sufficient to meet the temperature requirements for medical waste incineration in Florida. Turning on the aux blower lowered the temperature to 1775 °F, eventually. The Tpcc eventually rose to 1405 °F, which is also 200 °F hotter than it used to reach during warm up before the control system was installed. Turning on the bio blower caused Tpcc to fall slowly to 1275 °F and then even more slowly rise to 1310 °F, while TscC just slowly fell to 1750 °F. The upper burner also experienced no flame outs.

The control computer program, which until this point was acting only in its data logging mode, was now switched to its control mode. The warm up phase was entered, which initially turned the aux and bio blowers off, as expected. After some newly discovered bugs in the program were fixed, the program

sensed the temperatures were level and turned on the aux and bio blowers and requested the big blower be turned on (which was not used for this test) and then switched to its post-warm up mode. Since no incinerator start time was entered, the program calculated it was past the 45-minute warm up and post-warm up phases and attempted to enter its feeding phase, which led to the discovery of more bugs in the program. After being coerced to run through its feeding phase, it properly lowered the LB gas rate and triggered the ram feeder (no garbage was used in this test). The program was now coerced into its post-feeding mode which properly increased the LB gas rate. The incinerator was now shut off. The program was later fixed and tested in all modes of operation without using the incinerator.

#### Test Firing of March 31, 1992

The incinerator was again test fired on just natural gas on Tuesday, March 31, 1992. The goal of this test was to the operation of the debugged control computer program. The control program was started first, then the incinerator was switched on. The program was switched to control mode for the warm up phase. The program switched on the bio blower when T<sub>pcc</sub> leveled off at 1185 °F, switched on the aux blower when T<sub>scc</sub> leveled off at 1555 °F, and requested that the big blower be turned on when T<sub>pcc</sub> leveled off at 1045 °F. The program then switched to the post-warm up phase. Temperatures dropped when each blower was turned on and did not

recover. The blowers were turned off through the program's manual data entry and control (MDEAC) function (see Chapter 7), and the program was reset to the warm-up phase of control. The PCC and SCC temperatures reached 1280 °F and 1740 °F, respectively, before the blowers were turned back on by the program. The program was subsequently modified to delay turning on the bio and big blowers until the end of the warm up phase.

The program entered the feeding phase at the end of the 45-minute warm up phase. It turn on the ram feed trigger and lowered the LB gas rate by 50%. When the feed door opened, the program cut the LB gas rate by 25% and turned the UBXG off. These events worked as programmed. However, closing the LB gas valve by 50% does not cut the flow in half since the flow rate is not proportional to the valve angle. The program also failed to shut off the ram feed trigger, resulting in a double feed. The trigger had to be shut off through the program's MDEAC function.

The program properly entered the post-feeding phase and triggered the stoker, while raising the LB gas rate as needed. The UBXG was not turned back on for some reason and had to be turn on through the program's MDEAC function. The program triggered the next ram feed 7.5 minutes after the feed door was opened for the last ram feed, not 7.5 minutes after the last ram feed was triggered.

Through the program's MDEAC function, the program was informed that the garbage was used up (no garbage was

actually fed in this test). This should have put the program into the burndown phase, but did not. The program had to be manually placed in burndown mode through the MDEAC function as well. The stoker's shear pin broke causing the stoker motor to stay on through to the next time it was to be triggered. The program caught this condition and sounded the alarm, but did not display a message about the problem as it should have. The program was later informed that garbage was used up about 2 hours earlier, simulating the end of burndown. The program properly entered the post-burndown phase, but it also did not display a message to that effect.

The program was subsequently modified to keep track of when the last ram feed was triggered, as well as to fix the UBXG turn on problem, the ram feed triggering problem, the nonlinear flow rate to valve angle problem, the burndown phase change problem, and the stoker and post-burndown messages problem. The natural gas flow rate was modelled as an exponential-quadratic function of the valve angle. The inverse of this relation is used to calculate the valve angle needed:

$$w = -11.16 + \sqrt{103.4 - 1156 \ln\left(1 - \frac{u}{100}\right)} \quad (8-1)$$

where  $w$  is the valve angle in percent open and  $u$  is the flow rate in percent of maximum flow rate.

#### Experimental Firings

The new control system was designed so that it could be turned off or on at the flick of a switch. This was done to

facilitate comparing emissions from the incinerator with the new control system operating versus those from running the incinerator with its original control system. While many experiments have been performed in the past, the best comparisons are between experimental runs made during the same firing.

The first experimental firing was designed to test how well the incinerator could be brought up to optimal operating conditions from start up and how the incinerator's emissions compared with and without the new control system running. The incinerator was started and run with its new control system and control computer program in control with logging mode while emission measurements were made. Then the control computer program was to be switched to its just logging mode, which shuts off the new control system, and the same emission measurements were to be made. Hardware problems and a lack of personnel and garbage prevented sampling without the control system running.

The operating and emissions measurement protocol for the first experimental firing is shown in Table 8-1. This protocol is typical of all the experiments that have been made with the incinerator.

The second experiment was originally designed to test how well the incinerator's emissions could be controlled after the incinerator had been already running. The incinerator was to be started without the control system running and later run with the new control system operating.

Table 8-1. Protocol for Control System Experimental Burns.

PROTOCOL FOR RUN C01, Wednesday, APRIL 8, 1992

-----

- Goals:
1. Test of new incinerator control system.
  2. VOST sampling with and without control system running.
  3. Optional HCl sampling w/ and w/o control system running.
  4. Optional Carbosorb sampling w/ and w/o control sys. running.
  5. M2 volumetric flow rate measurement.
  6. HCl (continuous) emissions monitoring.
  7. NOx (continuous) emissions monitoring.
- 

Replace condenser in VOST train	Wed.
Purge VOST and/or Carbosorb traps.	Mon. & Tue.
Check operation of ECP incinerator, burners, and stoker.	Tue.
Inform Tacachale of burn on Wednesday.	Thu.
Bring CO2 meter, HCl CEM train, and other equip. out to Tacachale.	Tue.
Bring VOST/Carbosorb stuff out to Tacachale.	Tue./Wed.
Open gate for garbage delivery.	08:15
Start CEM monitors.	09:00
Set up HCl sampling train with grey meter box at far right port.	09:00
Set up VOST/Carbosorb sampling train with blue meter box at M5 port.	09:00
Hook up HCl meter box thermocouple to Tcstk thermocouple line or into digital temperature reader	
Set up stack CEM train.	09:20
Set up HCl CEM train.	
Set up cooling water system.	
Start computer and control program in logging mode.	09:30
Start up incinerator.	
Switch control program to control-warm up with logging mode.	
Warm up incinerator on natural gas.	
Calibrate CEM meters.	10:00
Computer will turn on aux and bio blowers.	
Computer will request big blower be turned on.	
Computer will start feeding garbage at 7.5 minute intervals.	10:15
Computer will start stoking at 7.5 minute intervals.	10:19
Run 1st HCl (C01E) for 45 minutes. and run 1st VOST (C01A) for 20 minutes.	11:00
Run 2nd VOST (C01B) for 20 minutes.	11:30
Switch computer program out of control mode, but still logging.	11:50
Run 2nd HCl (C01F) for 45 minutes. and run 3rd VOST (C01C) for 20 minutes.	12:10
Run 4th VOST (C01D) for 20 minutes.	12:40
Switch computer program back into control mode and still logging.	13:00
Set up MM5 probe with blue meter box at M5 port.	13:15
Connect probe thermocouple to digital temperature reader.	
Run M2 (C01G) stack gas volumetric flow rate measurement.	
Feed rest of garbage.	13:30
Inform computer when garbage has run out.	
Do cleanup.	
Computer will do burndown with stoking every 7.5 minutes.	

The same emission measurements were again to be made without and with the new control system were turned on. Since the same lack of garbage and personnel problems can recur, and since getting data with the new control system running has a higher priority, the second experimental firing was performed the way the first was originally planned.

#### Experimental Firing of April 8, 1992

The first full control system burn was on Wednesday, April 8, 1992. The waste feed rate averaged 333 lb/hr during sampling. The warm up phase of this burn was lengthened to accommodate CEM calibration. Temperatures reached 1430 °F in the PCC and 1840 °F in the SCC. The control program turn on the aux blower when the TscC leveled off for the first time. The control program did turn off or on the UBxG as the TscC cross the 1825 °F threshold, but it also did whenever the TscC leveled off. The program did not automatically enter the post-warm up phase. That phase had to be started through the program's MDEAC function. These problems were fixed before the next burn. The program did turn on the bio blower and request the big blower be turned on during the post-warm up phase.

During the first three feedings the control program dropped the LB gas rate by 50% when triggering the ram feeder and by 25%, with turning off the UBxG, when the feed door opened. This brought about very low temperatures--900 °F in the PCC and 1600 °F in the SCC. The control program did not

have the time to bring the LB gas rate back up to 100% between these feeds. At this point the program was modified (1) to drop the LB gas rate by 25% and then by 12.5% (instead of by 50% and then by 25%), (2) to shorten the built-in delay before continuing to the post-feeding phase, (3) to adjust the LB gas rate linearly instead of proportionally, i.e., to reduce the LB gas rate by say 25% of full capacity, not by 25% of its current value. Before the next burn the program was further modified (1) to eliminate the delay before the post-feeding phase, (2) to not drop the LB gas rate when triggering the ram feed if  $T_{pcc}$  is less than 1750 °F, (3) more quickly raise the LB gas rate when  $T_{scc}$  is less than 1875 °F, and (4) to limit the LB gas rate to 99.5% of its full capacity since this rate is achieved with only a 68% LB opening. The last modification will make the flow rate respond faster by not having the valve close 32% from full open without any significant reduction in gas flow rate.

The control program properly triggered the stoker after each ram feed and several times correctly alerted the operator with the alarm that the stoker has broken down. The stoker's lower limit switch had to be replaced. With the switch broken the stoker overran its lower stop point and broke its shear pin when its rake hit the inside back wall of the PCC. The stoker motor continued to spin. When it came time to trigger the stoker again, the program sounded the alarm when it sensed that the stoker motor was still running. However, the control program waited until the user pressed

the <Return> key before continuing its control operations. Before the next burn the program was modified to sound the alarm but not wait for user input. The control program also properly alerted the operators with the alarm the one time lower burner went out.

Figure 8-1 shows a plot of  $O_2$ ,  $CO_2$ , and CO levels during garbage feeding. Figure 8-2 shows a plot of total natural gas flow rate, SCC temperature, and PCC temperature during the same period. After the problematic first three feeds the CO remained at the lowest level yet recorded at CCTL, averaging 0.2 ppm. Even the spike at 12:17 was low. These CO levels are very far below the levels reported for the Basic incinerator (35 ppm) [30], the Swedish-American Hospital in Rockford, IL (9.5 ppm average) [134], the -Vicon incinerator (5.5 ppm average with 1800 °F at PCC exit), an average of four hospital waste incinerators tested by Illinois Pollution Control Board (88 ppm) [135] the and the levels recommended for good combustion practices (50 ppm) [18,44]

The SCC temperature averaged 1850-1900 °F. The dip in temperatures and gas rate at 12:40 was when the lower burner went out. The  $CO_2$  concentration stayed as level as  $T_{SCC}$ . The PCC temperature varied much more than desired and averaged around 1650 °F. The data shows that the natural gas flow rate does not increase quick enough to keep  $T_{PCC}$  from falling below 1700 °F. The control program modifications mentioned above should help reduce amplitude of this

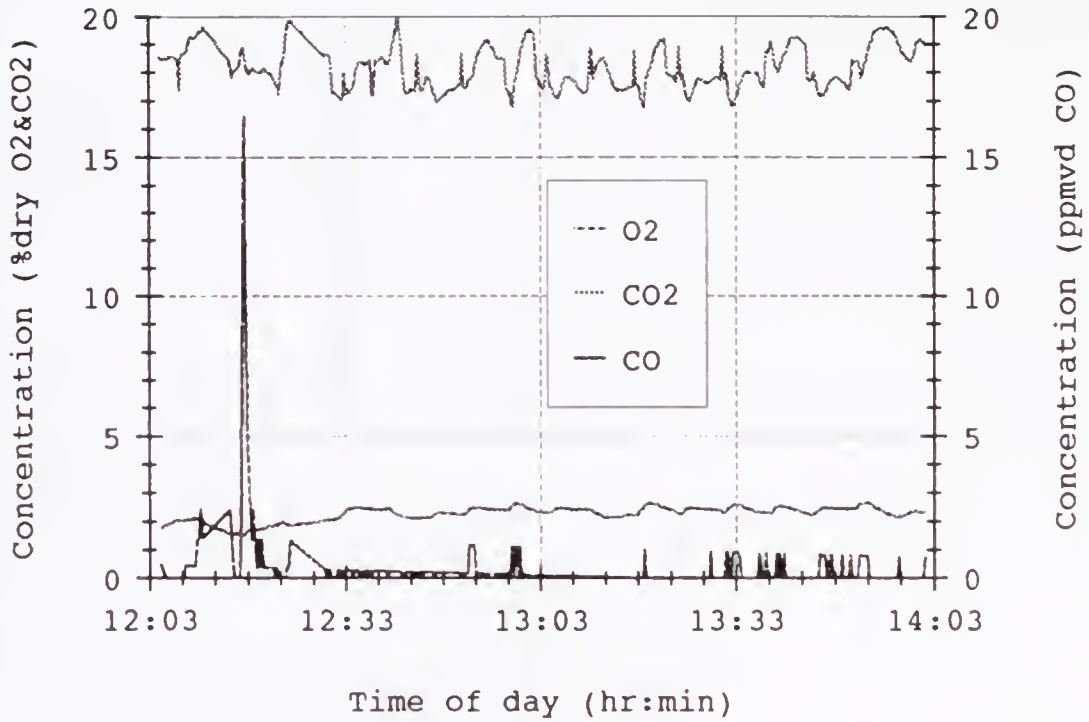


Figure 8-1. CEM data from 04-08-92 burn.

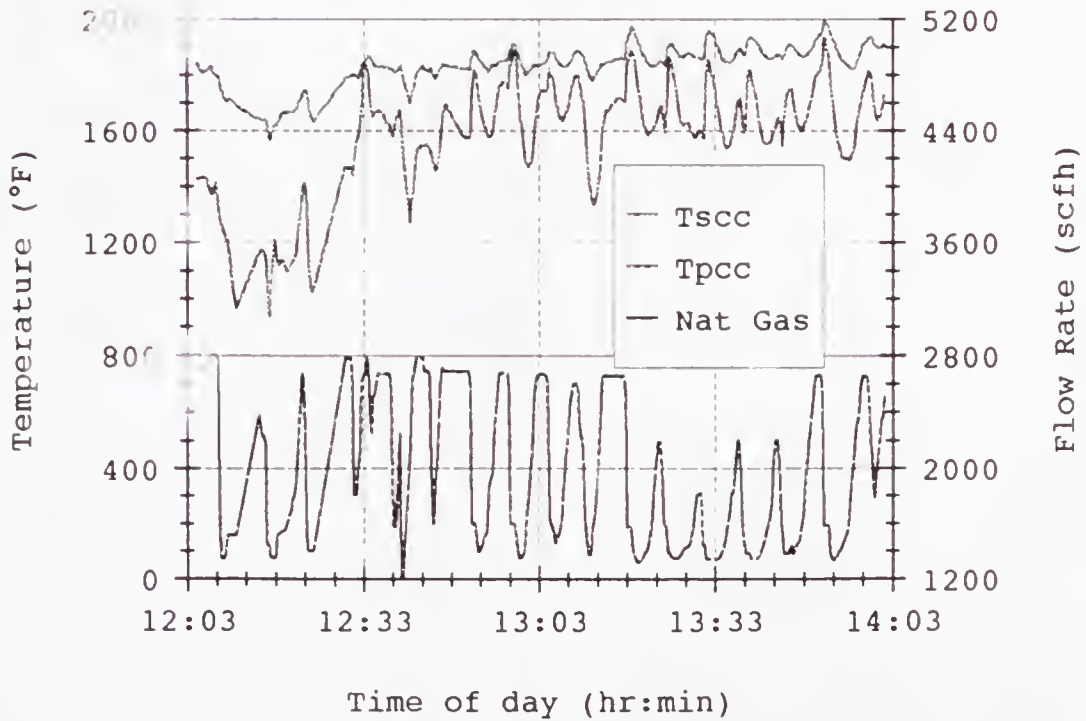


Figure 8-2. Temperature and gas data from 04-08-92 burn.

variation and keep T<sub>pcc</sub> from falling as far. The frequency of this variation is much less than before the control system was installed (see Figure 1-2). This should help keep emissions from the transient puffs down.

Volatile organic emissions, using the same ranking scheme used before, were the second lowest of 14 VOST runs analyzed so far. The lowest emissions were from a run not in the original set of 12 VOST runs studied earlier. Emissions from these runs previously had been found to much less than those from several California hospital incinerators [3-5,7]. Full results from both of these runs are shown in Table 8-2. VOST results for the latest run are tentative pending receipt of latest GC/MS response factors.

During the CEM calibration check after sampling, the program sensed a high level of CO (albeit from the span gas tank) and properly lowered the LB gas rate just as if there was a high level of CO in the stack gas. Implementation of the control program's CEM calibration function would eliminate this minor problem.

#### Experimental Firing of April 15, 1992

The second full control system burn was on Wednesday, April 15, 1992. The waste feed rate was approximately 369 lb/hr during controlled operation. The incinerator was operated and emissions tests were performed both with and without the control system running. Results (see Figures 8-3 and 8-4) show low CO (less than 1 ppm) during controlled

Table 8-2. VOST Results for Latest Samples, Non-Blank Corrected and Blank Corrected.

Date Sampled	9/7/91	4/8/92	9/7/91	4/8/92
Run Number	A22C	C01A CtrlSys	A22C	C01A CtrlSys
Volume collected (dsl)	18.17	19.04	18.17	19.04
Vol. flow rate (dscf/hr)	204831	200000	204831	200000
Total feed rate (lb/hr)	310.71	332.80	310.71	332.80
Date Analyzed	9/11/91	4/13/92	9/11/91	4/13/92
	Concentration (ng/m <sup>3</sup> )		Emission Rate (µg/kg)	
Benzene	924	3370	38.02	126.44
Toluene	243	608	9.99	22.81
Ethylbenzene	0	75	0.00	2.82
o-Xylene	0	16	0.00	0.60
m&p-Xylene	X	82	X	3.07
2-Ethyltoluene	369	X	15.17	X
1,3,5-Trimethylbenzene	0	X	0.00	X
Chlorobenzene	0	1381	0.00	51.81
1,2-Dichlorobenzene	244	227	10.04	8.52
1,3-Dichlorobenzene	321	424	13.21	15.89
Methylene chloride	317	0	13.03	0.00
Chloroform	117	81	4.83	3.04
Carbon tetrachloride	12	X	0.51	X
	Blank Corrected Concentration (ng/m <sup>3</sup> )		Blank Corrected Emission Rate(µg/kg)	
Benzene	-1513	1825	-62.28	68.47
Toluene	-556	544	-22.88	20.41
Ethylbenzene	-80	75	-3.29	2.82
o-Xylene	-75	16	-3.11	0.60
m&p-Xylene	X	82	X	3.07
2-Ethyltoluene	369	X	15.17	X
1,3,5-Trimethylbenzene	-26	X	-1.05	X
Chlorobenzene	-7	1381	-0.30	51.81
1,2-Dichlorobenzene	244	227	10.04	8.52
1,3-Dichlorobenzene	321	424	13.21	15.89
Methylene chloride	28	-31233	1.15	-1172
Chloroform	117	81	4.83	3.04
Carbon tetrachloride	12	X	0.51	X

operation, and slightly higher (2 ppm) during non-controlled operation after 13:38. The temperatures stayed higher after the first few ram feeds than during the April 8, 1992, firing. Some CO (4 ppm) was evident after the first three feeds. The natural gas rate was not cut down as much for the first few feeds to keep the temperatures higher. During controlled operation temperatures were hotter and tended to

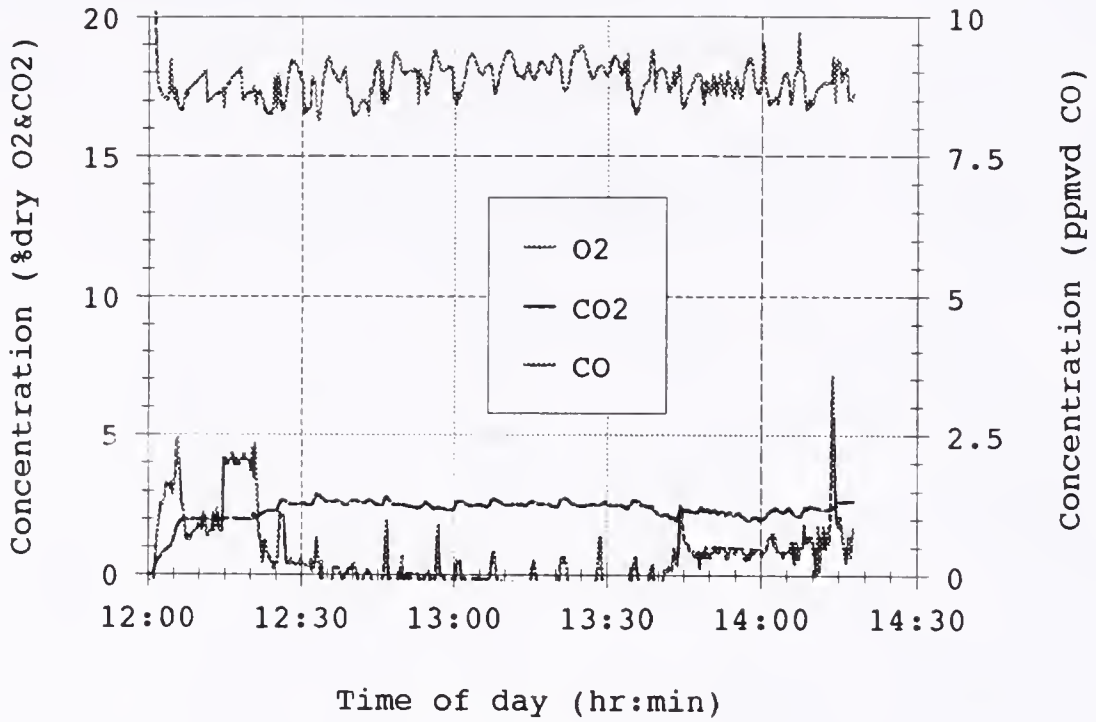


Figure 8-3. CEM data from 04-15-92 burn.

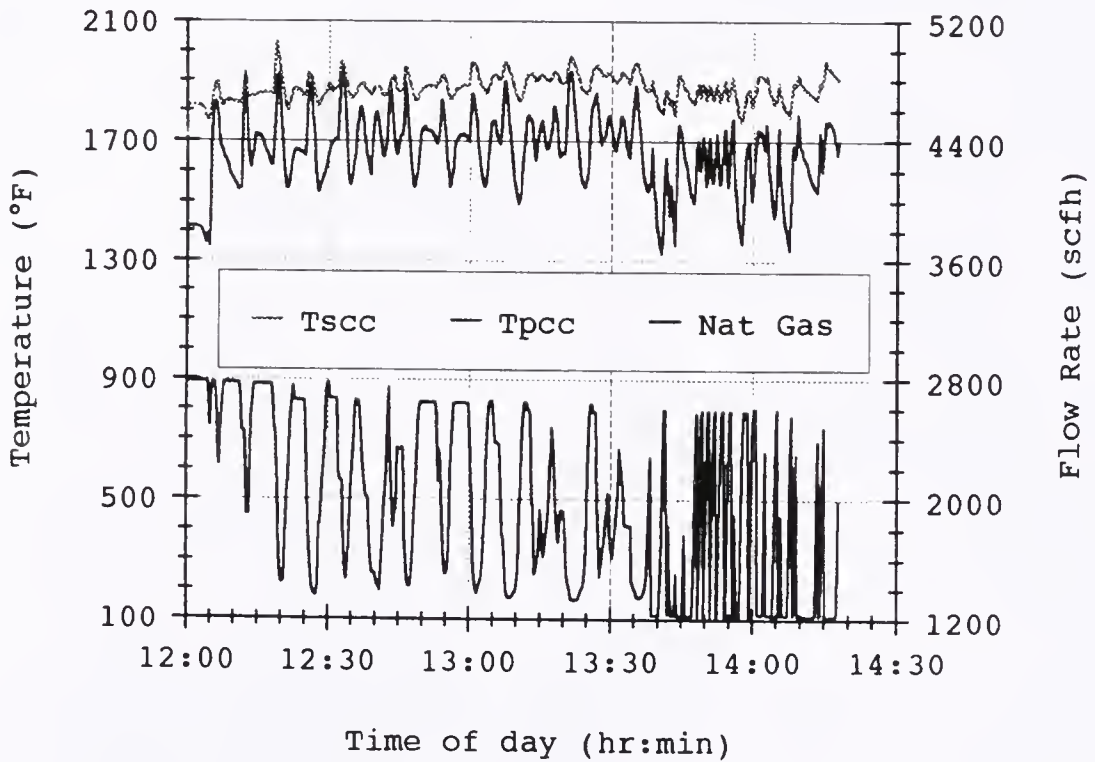


Figure 8-4. Temperature and gas data from 04-15-92 burn.

fluctuate more than in the April 8, 1992, test. Temperatures and natural gas flow rate fluctuated much more rapidly during non-controlled operation than during controlled operation. Lower burner outages were a problem during the non-controlled operation. VOST samples were taken, but were not analyzed due to budget constraints. The control program ran without need for on-site modifications, although a few minor bugs turned up.

#### Paper Burn of June 9, 1991

While not a planned test of the control system, the paper burn of June 9, 1991, did use the control system to operate the CCTL incinerator. During this burn the upper burner controller failed; its flame rod current amplifier had worked its way loose. Before the controller failure the control system kept CO emissions below 4 ppm. During this burn the damper at the dilution "T" was kept closed. For comparison with earlier results, the equivalent diluted CO concentration would have been less than 2 ppm.

After the controller failure the upper burner was kept off by its controller. The control system kept CO emissions less than 20 ppm with the upper burner off, except for a spike to 90 ppm after one of the ram feeds. The spike and higher level of CO probably would have been avoided if the upper burner could have been on.

The other components of the control system worked as expected. The burner controller was fixed the next day.

CHAPTER 9  
DISCUSSION, CONCLUSIONS, AND RECOMMENDATIONS

The goal of this research is to use the extensive experience of the CCTL in modular waste incineration to determine relations between emissions and operating conditions useful for control strategies to minimize emissions, particularly those of chlorinated organic compounds, from modular incinerators. These control strategies are to (1) avoid organically-bound chlorine in the input waste stream, (2) burn the waste hotter using an excess-air mode of operation in the PCC, and (3) avoid transient disruptions to the combustion process by lowering the rate of support fuel when waste is being fed into the incinerator. This investigation shows that these strategies can serve as a guide for upgrading and operating this general class of incinerators, which are commonly used in institutional and medical waste disposal.

The specific results from the analysis and modelling of the CCTL emissions data and from the implementation of the control system designed to implement control strategies (2) and (3) are presented here. Recommendations for future work, general projections to other systems, and a final summary follow.

## Specific Results

### Results from the Data Review

Analysis of carbon monoxide emissions from the CCTL incinerator compared to temperature, oxygen, and carbon dioxide levels suggest that the PCC of an excess-air modular incinerator be run at 1700-1760 °F, while the SCC be run at around 1805 °F. The particulate emission data suggests using low oxygen levels and high levels of natural gas, which is not conducive to maximizing waste feed rate since the natural gas and waste compete for the available air.

Volatile organic compounds emissions were lowest at a 315 lb/hr feed rate based on waste feed rate alone. When based on both PCC temperature and waste feed rate, volatile organic compounds emissions were found to be low for

$$\text{PCC temperature} \geq 1402^{\circ}\text{F} + 0.936 \frac{^{\circ}\text{F}}{\text{lb/hr}} (\text{feed rate}). \quad (9-1)$$

This relation would have to be scaled for incinerators of different sizes. Since the CCTL incinerator is rated at 500 lb/hr, the relation may be rewritten as

$$\text{PCC temperature} \geq 1402^{\circ}\text{F} + 468^{\circ}\text{F} \frac{\text{feed rate}}{\text{capacity}}. \quad (9-2)$$

Equation 9-2 could serve as a rule for setting PCC temperatures in excess-air modular incinerators. At full-capacity the PCC temperature should be 1870 °F, but at less than full-capacity, lower temperatures would mean less support fuel would be required to keep emissions low.

## Results from Kinetic Modelling

Carbon monoxide emissions predicted by the kinetics code were found to be very high compared to actual measurements. To correct this, the input amounts and reactions to the code need to be improved to reduce the CO emissions. The temperature-time profile could be broadened to allow more time at higher temperatures, which should reduce the CO emissions. The air brought in at the dilution "T" could be gradually mixed in by adding some fluid dynamics to the code. This also would keep the temperature of the combustion gas higher until the two streams are fully mixed.

The fast quench of reactions after the dilution "T" may minimize formation of certain organic compounds that would otherwise form due to slow cooling.

The initial kinetics code modelling shows minimal CO emissions with the PCC and SCC at 1850 °F and 1925 °F, respectively, while minimal benzene emissions occur with the PCC and SCC at 1875 °F and 1900 °F, respectively. Later kinetics code runs show lower CO with decreased air rates, mainly due to increased temperatures. The PCC air rate can only be lowered by about 25% before the PCC becomes starved-air.

The significant conclusions that can be obtained from the kinetics code relevant to minimization of emissions are to burn hotter, avoid chlorine in the input (the code has shown increased chlorinated organic emissions with increased

PVC input in other studies [4,7,125]), and burn longer (have a greater residence time).

#### Summary of Analysis of CCTL's VOST and HCl Data

The main conclusions from the study of CCTL's VOST, HCl, CO and temperature study are: (1) there is a strong dependence of HCl emission level on the level of chlorine in the waste; (2) there is a strong dependence of chlorinated hydrocarbon (ClHC) (notably chlorobenzene (CB) and dichlorobenzene (DCB)) emissions on HCl emissions; (3) there is a strong dependence of CB and DCB on each other and on products of HCl and nonchlorinated benzene; (4) and there is almost certain evidence of nonlinear relations existing between ClHC emissions and CO and temperature. The relationship between HCl output and chlorine input was positive and well-defined. In nearly all of the different relations studied, the relationship between a chlorinated organic emission and HCl emission was also positive and well-defined. This leads to a conclusion that increased levels of chlorine in the input does lead to increases in chlorinated organic emissions. This conclusion appears to be in contradiction with the conventional wisdom on this subject [1-2].

#### The Combustion Control System

The combustion control system uses a proportioning valve to regulate the amount of natural gas entering the PCC and uses an extra gas line to the SCC burner to increase gas flow

to the SCC as needed. The control system uses direct digital control of the ram-feed system, the stoker, the auxiliary (SCC air) blower, the biomass (overfire air) blower, and the biomass feeder. The system provides alarms for burner outages, stoker breakdown, and system failure. The system can be disabled to allow the incinerator to operate as before the control system was installed.

The combustion control strategy is based primarily on the data review since the review used empirical data. The temperatures suggested from the data review were adjusted about 50 °F higher (1) to allow a higher waste feed rate, (2) to keep the SCC well above 1800 °F as some regulations require, (3) since the kinetics code modelling suggests higher temperatures, and (4) since the residence time in the secondary chamber is about 0.7 seconds. The SCC temperature should be at least 1827 °F according to

$$T = 1800 \text{ °F} - 77 \text{ °F} \ln\left(\frac{t}{\text{sec}}\right), \quad (9-3)$$

an equation developed in Chapter 1 to relate temperature (T) for 99.99% toxic destruction to residence time (t).

The control strategy is to maintain a PCC temperature of  $1775 \pm 25 \text{ °F}$ , an SCC temperature of  $1850 \pm 25 \text{ °F}$ , and a feed rate of 315 to 400 lb/hr. To help avoid transient puffs of CO during feeding, the control system lowers the flow rate of natural gas to the PCC when the ram feed system is triggered. When the feed door opens to let the charge into the incinerator, the PCC natural gas flow rate is cut again, and

the SCC natural gas flow rate is lowered if needed. These reductions should help keep the natural gas from competing with the waste for the available oxygen. It should also keep the system operating more smoothly by keeping the temperature down and thereby letting the waste take longer to burn to more evenly distribute its energy release over the feed cycle interval.

When a high level of carbon monoxide (CO) is sensed, the PCC natural gas rate is reduced by 20%, or by 10% along with a reduction of the SCC natural gas flow rate. When a high level of hydrogen chloride is sensed, the next feed is to be delayed for one minute to help reduce the rate of chlorine entering the incinerator and exiting as HCl.

#### Experimental Results for the Control System

The goal of the combustion control system is to minimize CO and VOC emissions by maintaining the PCC temperature in the range 1750 °F to 1800 °F, the SCC temperature in the range 1825 °F to 1875 °F, and the feed rate in the range of 315 to 400 lb/hr.

During actual operation the incinerator tended to keep the SCC temperature much higher than 75 °F above the PCC temperature. As a result, at times the control system would be raising the PCC gas rate because the PCC temperature was too low, and the next minute it would be lowering the SCC gas rate because the SCC temperature was too high. If the SCC

gas rate were to be modulated like the PCC gas rate, this would no longer be a problem.

At times during the second experimental firing both the PCC and SCC temperatures were 250 °F above their desired values, even with the PCC gas rate at its lowest level (15%) and the SCC extra gas line off. These high temperatures were a result of paper burning. Theoretically, the PCC gas rate could have been lowered to 0% by closing the butterfly valve, while keeping the burner controller and pilot on. Here again being able to modulate the SCC gas rate could have lowered SCC temperatures. Also slowing down the feed rate of garbage would have helped keep the temperatures down.

The control system appears to have met its emissions reducing goals, with CO and VOC emissions well below those from uncontrolled operation, and has no trouble maintaining a specified feed rate. The temperatures do tend to fluctuate more than desired, but at a much lower frequency than during non-controlled operation. The reduced frequency should lower emissions caused by transient changes to the combustion conditions.

#### Control System Costs

The control system was put together at almost no cost. The butterfly valves cost \$70 each. Wire, electrical, and electronic components were an additional \$185. Graduate and undergraduate student labor was used to construct and install the control system. The modmotors and pipe fittings used

were found at the CCTL. The computer (\$700), data logger (\$3500), I/O board (\$200), D/A board (\$200), A/D board (\$200), O<sub>2</sub> monitor (\$1500), HCl monitor (\$550), other CEM monitors (state surplus, \$5000-\$12000 new), sampling lines, pressure sensors (\$80 each) thermocouples, stoker, extra blowers, and instrument trailer (state surplus) were all already on hand. A from-scratch, all-new control system would probably cost over \$40,000. However, emission control devices to clean up the stack gases from not burning well could cost more than \$100,000.

#### Improvements in Non-Controlled Incinerator Operation

The modifications made in installing the control system have also improved the operation of the incinerator when the system is not running under computer control. The flow rate of natural gas to the lower burner can be adjusted with the simple turn of a potentiometer. The flow rate of gas to the lower burner can now be set higher than it was previously set to, so warming up the incinerator can occur faster. Additional gas can be fed to the upper burner by turning another potentiometer. The higher gas flow rates allow the incinerator secondary combustion chamber's temperature to reach 1850 °F during warm up. The orifice meter installed in the natural gas line allows for on-line measurement of gas to the incinerator. The addition of a motor starter and on/off switch to the biomass blower allows independent operation of the biomass blower and the biomass feeder. The calibration

switch added to the biomass feeder control circuitry allows the biomass feeder to be calibrated without interference from the ram feeder.

### Recommendations for Future Work

#### Additional Species and Reactions for the Kinetics Code

The kinetics code currently looks only at the major species, nonchlorinated and chlorinated benzenes, and C<sub>1</sub> (single carbon atom in molecule) hydrocarbon reactions. To better model the combustion of garbage, particularly plastics, additional reaction mechanisms need to be considered. These should be global or semi-global reactions involving the conversion of polymer hydrocarbons to both simpler and more complex compounds in one or two steps, and then to chlorinated compounds in additional steps. Smaller chlorinated compounds could be combined into larger ones. These results could then be compared to CCTL VOST data which typically includes chlorinated C<sub>1</sub> to C<sub>3</sub> hydrocarbons and chlorinated and nonchlorinated single ring aromatics. Some work is underway on modelling the chlorination of benzene, phenol, dibenzofuran, and dibenzo-p-dioxin [7,125].

#### Additional Tests to Better Determine Data Relationships

The good data fits for comparing chlorobenzene to the product of HCl and benzene emissions, and for comparing dichlorobenzene to the product of HCl and chlorobenzene emissions, suggest a kinetic model of chlorinated organic emissions where nonchlorinated compounds are successively

chlorinated by chlorine from HCl in the combustion (stack) gases. The good data fits for comparing dichlorobenzene to the product of benzene and the square of HCl emissions suggest another kinetic model where benzene is formed from smaller nonchlorinated compounds (precursors) while dichlorobenzene is formed from smaller chlorinated compounds, and where HCl is responsible for chlorinating the precursors. Typical chemical reactions for this second model might be



In both models, more HCl in the stack gas leads to more chlorinated organic emissions for the same nonchlorinated organic compound emission level. The nonchlorinated organics in the stack can be reduced through good control of the combustion process. The HCl in the stack can be reduced greatly by monitoring what is burned [3-5]. Chlorinated waste should be avoided, or better yet, not even produced. Chlorinated plastics like PVC have many legitimate uses, (e.g., pipes and siding) but their use in disposable products should be limited to recyclables.

Compounds containing benzene rings, such as polystyrene, should be avoided when chlorine is present. The successive chlorination model proposed above uses benzene as a precursor to chlorinated benzenes. If the benzene molecules are not

sufficiently destroyed in the incineration process, they can be chlorinated by the HCl present.

While CCTL has acquired much VOST data in the 1 to 7 g HCl/kg waste range, more data is needed in the 10 to 20 g/kg range to better determine relations between chlorinated organic emissions and HCl emission. The noise in the data itself makes determining relations with just low HCl values difficult. The temperature range in the CCTL data is very small compared to the HCl and CO ranges, which span more than an order of magnitude. Many more CCTL data runs are needed with an expanded temperature range (1400- to 2000-°F PCC temperatures) to properly determine the effects of temperature on VOC emissions. For a good range of temperature and HCl levels, with three runs at each condition to reduce noise, at least 50 runs are needed.

#### Additional Control System Aspects

More experimental burns are needed to fine-tune the control system. The control system will be used during future experimental burns at the CCTL, but testing of the control system will not be the focus of these burns.

Other aspects to consider for the control system include the addition of digital input signals for the big blower, bio blower, and upper burner extra gas line valve; addition of digital control of the big blower, of the conveyor belt, and to turn incinerator on and off; proportional control of the upper burner gas rate, all air rates, and the dilution

damper. The computer could remotely restart the burner controllers after a flame-out. The upper burner gas rate could also be simply lowered permanently by closing somewhat the gate valve in the upper burner gas line.

The feed hopper should be maintained with a minimum level of waste to keep the charging mass consistent. An electrode two-thirds up from the bottom of the hopper could signal the conveyor belt to send more waste into the hopper.

The control system could include support for biomass feeding and continuous emission monitors calibration, faster feeding of waste when waste is first fed in to warm up the incinerator quicker, and programmable lowest PCC gas rate and stoker delay. Some of the delays in system could be better accounted for. The control system could try to reduce  $\text{NO}_x$  emissions by lowering temperatures as necessary. If the temperatures are too high, the waste feed rate could be lowered.

The manual data entered into the computer could be recorded to diskette, along with the times this data was entered. Problems encountered by the control system could be recorded to diskette, along with the times they occurred.

One of the strategies to minimize emissions of chlorinated organic compounds is to avoid chlorinated materials in the waste stream. When burning a high (greater than 1%) chlorine content waste, chlorine-free biomass fed through the biomass feeder could supplant some of the waste,

thus maintaining a desired output power level, while meeting HCl emission limits and keeping chlorinated organic compound emissions low. If the HCl emission rate is high while simultaneously feeding both waste and biomass, the control system could slow the waste feed rate down while speeding up the biomass feed rate. As the HCl emission rate lowers, the ratio of waste feed rate to biomass feed rate could then be raised.

The control system response time could be quickened. The samplings line from the stack to the CEMs can be made shorter. The control program can be compiled, which would at least double its speed. A faster data logger could be used, or the thermocouples and voltage signals could be wired directly to another A/D board in the computer. The control systems response to low or high temperatures could be made a function of the difference between the actual temperature and the desired temperature.

#### General Projections to Other Systems

While the control strategies have been designed for a specific type of modular incinerator, their principles can be applied to other systems. The CCTL incinerator and its control system can be used as a guide for designing future and retrofitting older institutional and medical waste incinerators.

The strategy of avoiding chlorine in the input waste is best implemented at an institution or hospital by purchasing

and using nonchlorinated plastic disposables. While the properties and costs of PVC disposables make them the most commonly used at hospitals, nonchlorinated substitutes are now emerging [136].

The strategy of burning the waste hotter using an excess-air mode of operation in the PCC can be adapted to existing institutional and medical waste incinerators by adding extra burner and blower capacity. Since this would likely reduce the residence time in the SCC, the extra burner capacity must be capable of producing temperatures meeting the requirements of Equations 9-2 and 9-3.

The strategy of avoiding transient disruptions to the combustion process by lowering the rate of support fuel when waste is being fed into the incinerator requires the addition of proportioning valves, a stoker, and a control system such as the one developed for the CCTL incinerator. Factors to consider for such a retrofit include incinerator capacity, fuel types, number of burners per chamber, burner capacity, ram feed charging size, ash removal rate, air flow rates, and whether or not a heat recover boiler is present. The stack gases, if cooled slowly by a boiler, should not be cooled to certain temperature ranges (350 °F to 600 °F) that can promote formation of dioxins.

A future incinerator design would include the extra burner and blower capacity, proportioning valves, stoker, a large enough SCC for at least one second of residence time, and smaller ram feed charges. The control system logic would

be hard-wired into the control hardware for faster response. Such an incinerator operated with the above pre-combustion and combustion control strategies should be capable of competing emissions-wise with starved-air incinerators with post-combustion pollution control devices.

#### Final Summary

This work contains the only substantial body of controlled data that clearly shows relationships between input levels of chlorine and output levels of chlorinated organic emissions and between operating conditions and emissions. These relations support the pre-combustion and combustion concepts of Clean Combustion Technology as applied to modular incineration. By controlling what is burned, and how it is burned, emissions can be substantially reduced without using expensive post-combustion air pollution control devices.

APPENDIX A  
DETAILED DESCRIPTION OF THE ORIGINAL CONTROL SYSTEM

The original control system circuitry is contained in three panels mounted on the burner side of the incinerator system. A functional schematic of the control circuitry is shown in Figure 2-2 in Chapter 2. A schematic of the entire control circuitry is shown in Figure A-1.

The left panel contains a power switch, two 3-phase relays for the main and auxiliary blowers, three dual 3-phase relays for the feed door, accumulator (upper) ram, and feed (lower) ram motors, and three current overload switches for the three motors. An overload switch trips if its motor draws too much current, which would occur if the door or a ram feeder jammed. Circuitry in the upper right control panel provides for the necessary reversing and cycling actions needed to free the jam. The main switchbox for the incinerator system contains three 60-amp fuses and is located above the left control panel.

The lower right panel contains Honeywell model R4795D and R4795A flame safety controllers for the upper and lower burners, respectively, and a Honeywell R4795A flame safety controller to detect flames in the ram feed system. These burner controllers are powered on and off via Compack API temperature limit switches in the upper right control panel.

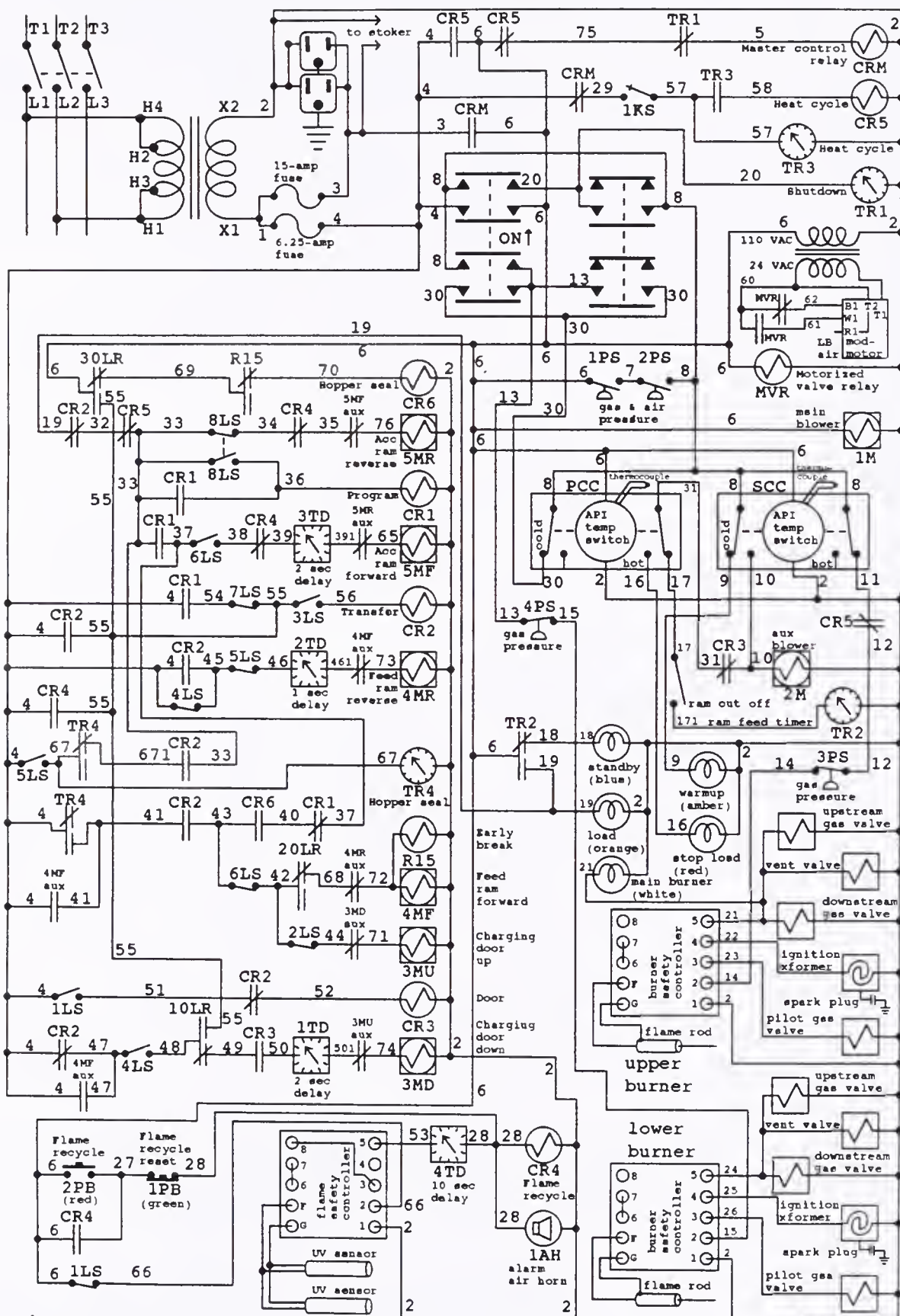


Figure A-1. Original incinerator control system circuitry.

When powered on, a burner controller opens a valve for the corresponding pilot gas and energizes an ignition circuit that fires a spark plug. The spark plug, located where the pilot gas/air line meets the burner, ignites the pilot gas. A flame rod positioned in the pilot flame sends a microamp current signal back to an amplifier in the burner controller. When the current is strong ( $> 1.5$  micro-amp) and steady ( $< \pm 0.5$  micro-amp) enough, the burner controller opens the main valves on the corresponding gas line, and closes a vent valve between the main valves. After a few seconds, the ignition circuit is turned off. The burner controller continually reads the flame rod current to make sure the burner flame remains lit. If the flame rod current falls too low, the controller assumes the flame must have gone out and the controller goes into a lockout mode. The controller must then be reset manually by pressing a switch on its outer cover.

A flame safety controller is activated when a flame is sensed on the hopper side of the feed door. Circuitry in upper right control panel provides for the necessary feed ram cycling action needed to push the flaming material into the incinerator, thereby averting a fire in the hopper. An air horn mounted on top of the upper right control panel is sounded when this occurs.

The upper right control panel contains a power transformer, two fuses, eight relays, four timers, a ram cut-off switch, and two Analytical Products Inc. Compack I

temperature controllers (APIs) each with upper and lower temperature limit switches. Ceramic insulated thermocouples, mounted through the top of the PCC and the SCC, are wired to the corresponding APIs. Two switches and five status lamps (warm up, stand by, load, stop, and main burner) are mounted on the panel's left door. One of the door-mounted switches and two of the four timers were for an alternate (pathological waste firing) start up and shutdown mode that is not being used currently. The other door-mounted switch is used to turn the incinerator on and off. This switch is wired directly to the main blower. The third timer is for the ram feed cycle, and the fourth is for a delay in the ram feed operation.

When the temperature in the PCC rises above the lower set point on the PCC's API, the PCC burner controller is turned off. If the temperature in the PCC rises above the upper set point, the ram-feed timer is cut off and the stop status lamp is lit. When the temperature in the SCC rises above the lower set point on the SCC's API, the auxiliary blower is turned on. If the temperature in the SCC rises above the upper set point, the SCC's burner controller is turned off. During normal operation, the SCC temperature is between its two API temperature limits (1500 °F and 2500 °F) and the PCC temperature cycles between being below and between its two limits (1800 °F and 2500 °F).

When the ram feed (or program) timer [94] completes its cycle, the accumulator ram (see Figure 2-1 in Chapter 2)

pulls back allowing waste in the chute to fall in front of the accumulator ram on top of the feed ram. When the accumulator ram triggers limit switch 8LS (see Figure A-1), it waits two seconds and then reverses and compacts the waste against the bulkhead, while the belt in the hopper, which is chained to the accumulator ram, deposits more waste in the chute. After limit switch 7LS is triggered, the accumulator ram stops and the feed ram pulls back until it triggers limit switch 5LS. The feed ram then stops, the delay timer is started, and the accumulator ram pulls back allowing waste to fall in front of the feed ram. When the delay timer completes its cycle (about 0.5 seconds), both rams move forward and the feed door raises. The feed ram pushes the waste into the incinerator. The accumulator ram, feed ram, and feed door stop when limit switches 6LS, 3LS, and 2LS are triggered, respectively. The accumulator ram in this most forward position seals the hopper from exposure to the flames from the PCC. The triggering of limit switch 1LS when the door starts raising resets the ram feed timer by de-energizing it. Two seconds after limit switch 3LS is triggered, the feed ram pulls back until it triggers limit switch 4LS. After a 1-second delay the feed door then lowers until limit switch 1LS is triggered, which re-energizes the ram feed timer. The movement of the ram system takes about 1.25 minutes. This time must be added to the setting of the ram feed timer to get the actual total cycle time for ram feeds.

A butterfly valve controls the amount of air from the main blower that is directed to the underfire air ports. It has been closed since the addition of the big blower in 1988. A Honeywell Modutrol motor operates a butterfly valve that controls the amount of air from the main blower that is directed to the lower burner. It cycles the valve between full-open and half-closed so that there is a higher air flow rate when the burner is lit.

The bio blower is controlled by a breaker box switch. A schematic of the biomass feeder control subsystem is shown in Figure A-2. The biomass feeder can be operated in two modes. In the first mode, a toggle switch is used to energize and de-energize the 3-phase relay that sends power to the biomass feeder motor. In the second mode (with line 67 connected to the SPDT relay), with the toggle switch on, the biomass feeder motor runs until the ram feeder starts its cycle. When the accumulator ram reaches limit switch 5LS, a timer, mounted in the same box as the toggle switch and biomass feeder motor relay, is turned on. While the timer is running, the biomass feeder is off. After the timer has finished its cycle, the biomass feeder comes back on, and the timer is reset. The timer's interval is usually set to one-half of the ram-feed cycle time.

The control circuitry (see Figure A-3) for the stoker is located on a small panel inside the upper right control panel. When a signal is sent to the stoker controller to start its timer, the pre-timer latch relay (LR1) is tripped

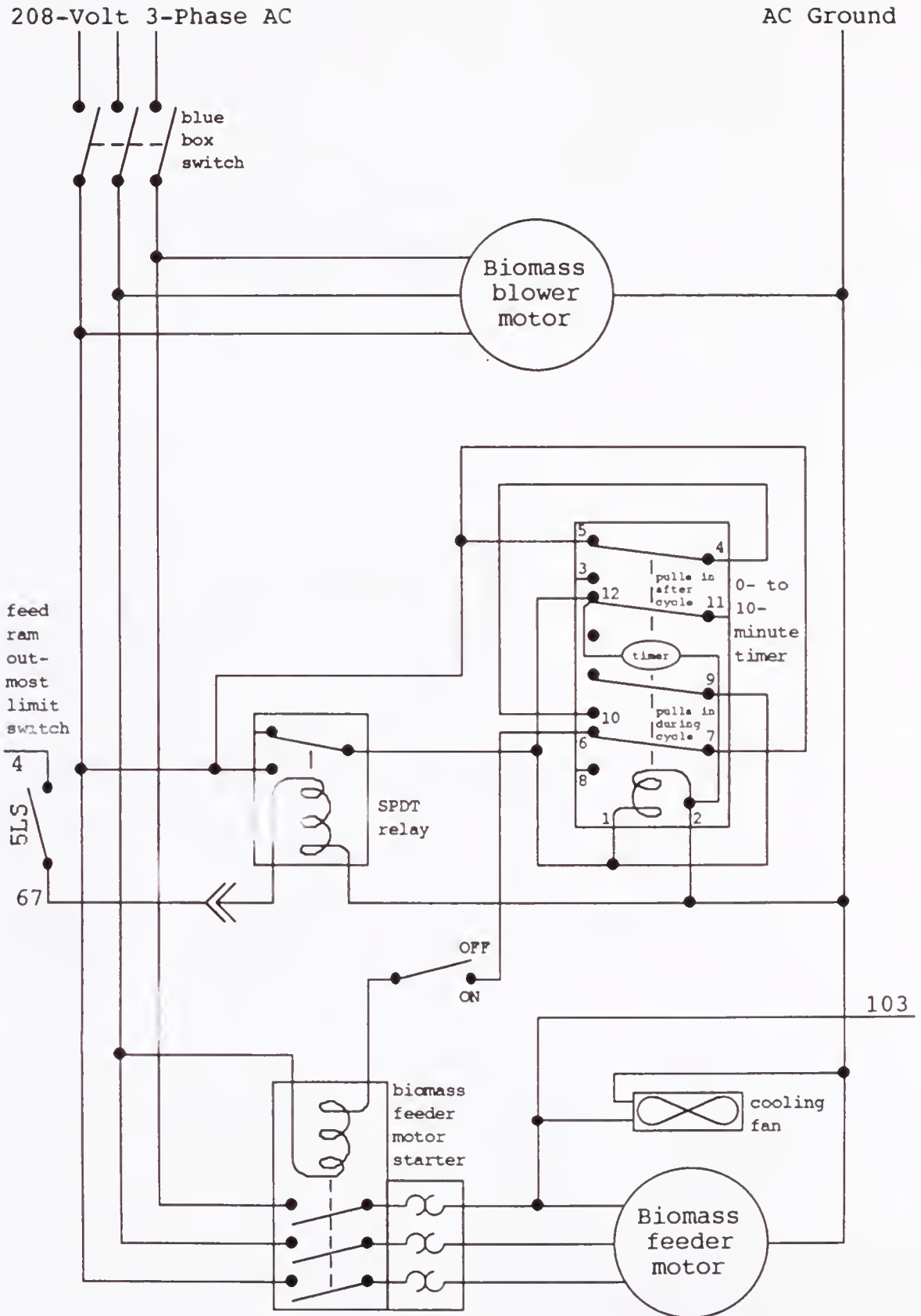


Figure A-2. Original biomass control subsystem.

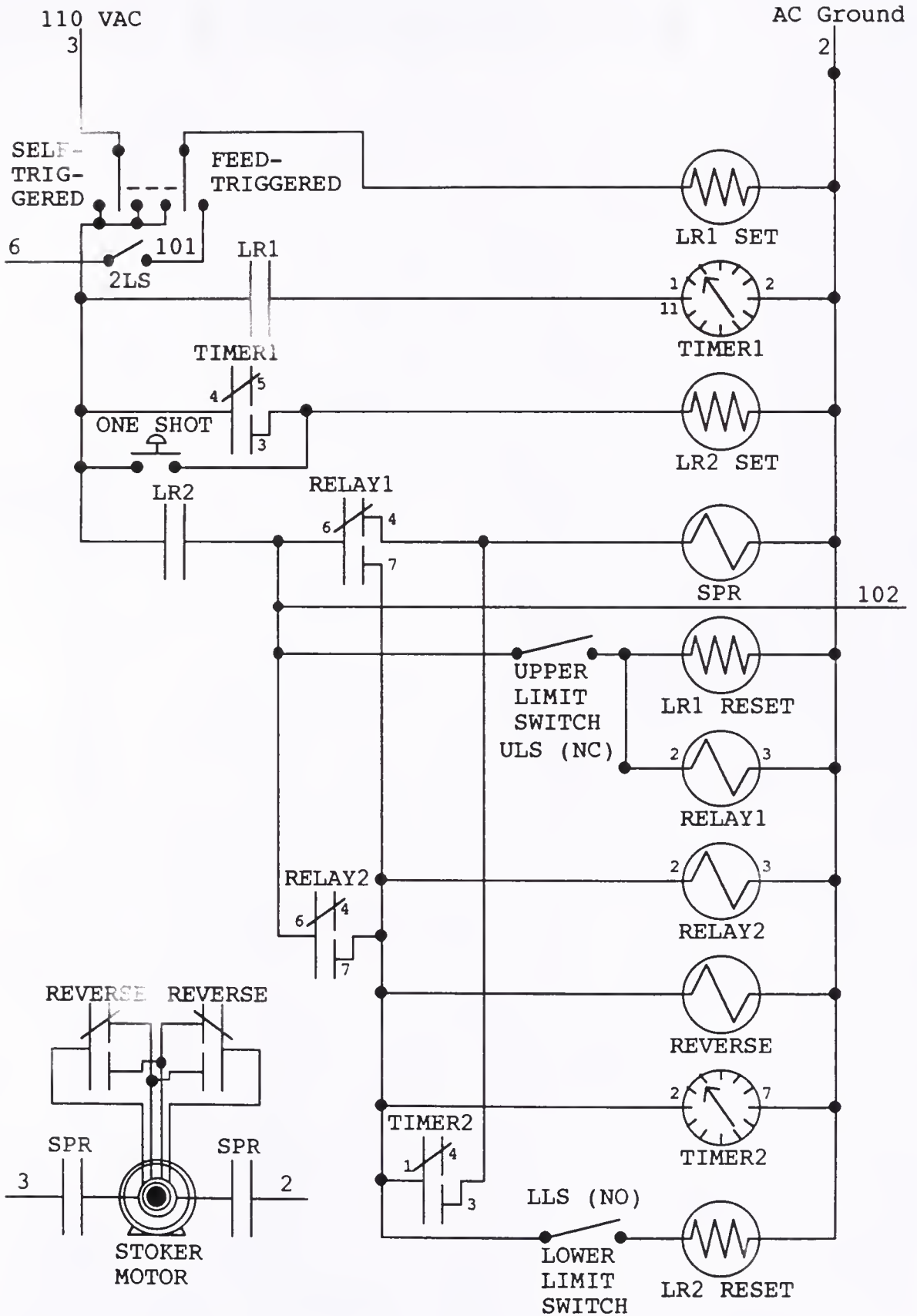


Figure A-3. Original stoker control circuitry.

and holds this signal and runs the stoker cycle timer (TIMER1). At the end of the timer's cycle the post-timer latch relay (LR2) is tripped and a relay (SPR) is energized to power the stoker. The stoker motor turns clockwise to run the stoker upwards toward the PCC burner. At the top of stoker's run, a limit switch (ULS) is triggered with latches a relay pair turning on a 2-second delay timer (TIMER2). At this point TIMER1 is reset by untripping LR1. While TIMER2 runs, the stoker motor is shut off. After TIMER2 completes its cycle, the relay pair (RELAY1 and RELAY2) powers a reversing relay (REVERSE) for the stoker motor, and the stoker motor starts, running the stoker downward. At the bottom of the stoker's run another limit switch (LLS) is triggered which sends a signal to untrip LR2. This shuts off power to the stoker motor, the stoker motor reverse relay, and the relay pair.

The stoker controller has two modes of operation, feed-triggered and self-triggered. In the feed-triggered mode the stoker controller is triggered by the ram-feed door opening. The cycle time in this mode is usually set to one-half to two-thirds of the ram feed time so that the ash pile is stoked midway between the ram feeds. In the self-triggered mode the LR1 is always tripped so that the stoker runs independently of the ram feeder. This is necessary when firing biomass instead of waste and during burndown after all waste has been fed. The cycle timer TIMER1 is set to 5 to 7 minutes in this mode. This is the time between when the

stoker is at the top of its run in one cycle and when it starts the next cycle. Since it takes about 4 minutes for the complete stoker run, the total cycle time is 2 minutes greater than what is set on TIMER1. In either mode, when TIMER1 is on but has not completed its cycle, instead of waiting for TIMER1 to count down, the one-shot button (ONE SHOT) on the stoker control panel can be pressed to trip LR2 and immediately start the stoker run.

APPENDIX B  
DETAILS ON THE INSTRUMENTATION

An external 4-way valve allows the use of a 14.3% CO<sub>2</sub> in N<sub>2</sub> span gas for calibrating the CO<sub>2</sub> monitor and the use of the CO monitor's span gas, which has no CO<sub>2</sub>, for zeroing the CO<sub>2</sub> monitor. The CO<sub>2</sub> monitor's accuracy is 0.1% CO<sub>2</sub>. The CO monitor's zero/span accessory allows the monitor to use a 87.9 ppm CO in N<sub>2</sub> span gas and a zero gas derived by passing sample gas through a catalytic converter. The accuracy of the CO monitor's is 1 ppm CO. A 7:1 dilution system is installed before the NO<sub>x</sub> analyzer. A diaphragm pump supplies the dilution air from ambient air inside the trailer. With the span and sample gas lines shut off, the dilution air is used to zero the NO<sub>x</sub> analyzer. With the span line open, gas from a 156 ppm NO in N<sub>2</sub> span tank, diluted to 22.5 ppm, is used to calibrate the NO<sub>x</sub> analyzer. The accuracy of the NO<sub>x</sub> meter at its highest range (0-25 ppm) is ±1 ppm NO<sub>x</sub>. The span gas tanks are installed inside the trailer. The O<sub>2</sub> analyzer uses ambient air drawn from outside the trailer as a 20.9% O<sub>2</sub> span gas. The analyzer has an accuracy of ±0.1% O<sub>2</sub>.

The HCl meter's pump draws 267 cc/min of dilution air through the inner tube of the drying tube and a rotameter and draws 133 cc/min of stack gas into the dilution chamber, The mixture is then drawn through the sensor cell, a second

rotameter, and the outer tube of the drying tube, where it picks up the moisture through the drying tube membrane.

The CO<sub>2</sub> monitor has a 0- to 5-volt analog output that is proportional to its 0-100% full scale reading, which corresponds to a 0-20% CO<sub>2</sub> concentration. The full scale reading is a cubic polynomial function of the CO<sub>2</sub> concentration. The analog output is connected to the 0- to 5-volt analog input of the QuaTech A/D module through a 2.2:1 voltage amplifier. The amplifier is necessary since a direct connection would overload the monitor's output. The 2.2:1 amplification is used since the maximum expected CO<sub>2</sub> concentration is 5% due to the dilution at the "T" in the stack. A 5.38% CO<sub>2</sub> reading produces a full 5-volt analog signal at the input to the A/D board. The CO monitor has a 0- to 6-volt analog output that linearly corresponds to a 0 to 100 ppm CO concentration. This output connected to the A/D module through a 6:5 voltage divider. The O<sub>2</sub> analyzer has a 0- to 3-volt analog output that linearly corresponds to a 0 to 24% O<sub>2</sub> concentration. This output is connected via a cable and through a 3:2 voltage divider to the FEM, which has a higher resolution than the QuaTech A/D module. A line exists for connecting the O<sub>2</sub> analyzer directly to the A/D module, but it needs to be amplified to keep the A/D module from shorting it out. The HCl sensor has a 4- to 20-ma current output corresponding to 0 to 100 ppm of HCl in the diluted sample gas. The current passes through a 100-ohm load resistor producing a 0.4- to 2.0-volt output signal. This signal is wired directly to the FEM.

APPENDIX C  
DATA CALCULATIONS

Continuous Emission Monitor Calculations

$$\text{CEMMR} = \text{QDRDG} * \text{C1} + \text{C2}$$

CEMMR = displayed CEM reading  
QDRDG = CEM reading from QuaTech A/D or Doric  
C1, C2 = calibration constants

$$\text{CZDC} = \text{CEMMR} - \text{CZI} - (\text{CZF} - \text{CZI}) * (\text{T} - \text{TZI}) / (\text{TZF} - \text{TZI})$$
$$\text{C} = \text{CZDC} * \text{CS} / ((\text{CSI} - \text{CZI}) + ((\text{CSF} - \text{CZF}) - (\text{CSI} - \text{CZI})) * (\text{T} - \text{TSI}) / (\text{TSF} - \text{TSI}))$$

CZDC = CEM reading corrected for zero drift  
CZI = CEM reading on zero gas at beginning  
CZF = CEM reading on zero gas at end  
T = time of reading  
TZI = time for initial CEM zero gas reading  
TZF = time for final CEM zero gas reading  
C = CEM reading corrected for zero and span drift  
CS = span tank concentration  
CSI = CEM reading on span gas at beginning  
CSF = CEM reading on span gas at end  
TSI = time for initial CEM span gas reading  
TSF = time for final CEM span gas reading

$$\text{CO2} = 0.0000079 * \text{CCO2}^3 + 0.00034 * \text{CCO2}^2 + 0.087 * \text{CCO2}$$

CO2 = CO2 concentration (%dry)  
CCO2 = CO2 CEM reading corrected for zero and span drift

$$\text{C7} = \text{C} * 13.9 / (20.9 - \text{O2})$$

C7 = CEM reading corrected to 7% O2  
O2 = O2 concentration (%dry)

Temperature, Feed Rate, and Power Calculations

$$\text{Vavg} = (\sum \text{Vi}) / \text{NP}$$

Vavg = average reading during sampling  
Vi = reading during sampling  
NP = number of readings during sampling

$$\text{NHWFR} = \text{TWG} / \text{TNF} * \text{NFD} / (\text{TFE} - \text{TFS})$$

NHWFR = garbage feed rate during sampling (lb/hr)  
 TGW = total weight of garbage fed (lb)  
 TNF = total number of non-empty feeds  
 NFD = number of non-empty feeds during sampling & feed  
 before sampling  
 TFE = time of first feed after sampling (hr)  
 TFS = time of first feed before sampling (hr)

$$\text{BIOFR} = \text{BCFR} * \text{FOCF}$$

BIOFR = biomass feed rate (lb/hr)  
 BCFR = biomass continuous feed rate (lb/hr)  
 FOCF = fraction of time biomass feeder

$$\text{RATE} = (\text{R2} - \text{R1}) / (\text{T2} - \text{T1}) * 400 / 3$$

RATE = natural gas flow rate (cuft/hr)  
 R2 = gas reading after sampling (100 cuft)  
 R1 = gas reading before sampling (100 cuft)  
 T2 = time of gas reading after sampling (hr)  
 T1 = time of gas reading before sampling (hr)

$$\text{BHV} = \text{BDHV} * (1 - \text{BPMC} / 100)$$

BHV = biomass heating value (BTU/lb)  
 BDHV = biomass dry heating value (BTU/lb)  
 BPMC = biomass moisture content (%)

$$\text{GIP} = \text{RATE} * \text{GHV}$$

$$\text{WIP} = \text{NHWFR} * \text{WHV}$$

$$\text{BIP} = \text{BIOFR} * \text{BHV}$$

$$\text{TIP} = \text{GIP} + \text{WIP} + \text{BIP}$$

GIP = gas input power (BTU/hr)  
 GHV = gas heating value (BTU/cuft)  
 WIP = garbage input power (BTU/hr)  
 WHV = garbage heating value (BTU/cuft)  
 BIP = biomass input power (BTU/hr)  
 TIP = total input power (BTU/hr)

$$\text{TOP} = \text{OMFR} * \text{CP} * (\text{THSTK} - \text{TAMB})$$

TOP = total output power (BTU/hr)  
 OMFR = output mass flow rate (lb/hr)  
 CP = specific heat (BTU/lb °F)  
 THSTK = hot stack gas temperature (°F)  
 TAMB = ambient temperature (°F)  
 ETA = thermal efficiency (%)

$$\text{OVFR} = \text{OVFRD} / (1 - \text{SGMC} / 100)$$

$$\text{TTEE} = \text{TSMPT} + 77$$

$$\text{TOPC} = \text{OVFR} * \text{CPC} * (\text{TTEE} - \text{TAMB})$$

$$\text{ETAC} = 100 * \text{TOPC} / \text{TIP}$$

OVFRD = dry output volumetric flow rate (dscf/hr)  
 SGMC = stack gas moisture content (%)  
 TTEE = temperature at tee (°F)  
 TSMPT = temperature at sampling port (°F)  
 CPC = specific heat (BTU/cuft °F)  
 TOPC = total output power (BTU/hr)  
 ETAC = thermal efficiency (%)

### Methods 2 and 5 Calculations

$$Vm(std) = 17.64 Y Vm (Pb + dH/13.6) / Tm$$

$Vm(std)$  = volume of dry gas sampled (dscf)  
 $Y$  = meter box calibration constant  
 $Vm$  = volume of dry gas as read by meter (dcf)  
 $Pb$  = barometric pressure (in Hg)  
 $dH$  = average pressure drop of gas across orifice in meter box (in H<sub>2</sub>O)  
 $Tm$  = average temperature of gas in meter box (R)

$$Vw(std) = 0.0471 (Vwc(std) + Vwsg(std))$$

$$Bws = Vw(std) / (Vw(std) + Vm(std))$$

$Vw(std)$  = volume of water sampled (scf)  
 $Vwc(std)$  = volume of water gained in first three impingers (ml)  
 $Vwsg(std)$  = vol. of water gained in silica gel (g (ml))  
 $Bws$  = water volume fraction in stack gas

$$Md = 0.44 (\%CO_2) + 0.32 (\%O_2) + 0.28 (\%CO + \%N_2)$$

$$Ms = Md (1 - Bws) + 18 Bws$$

$Md$  = molecular weight of dry stack gas (lb/lbmol)  
 $\%CO_2$  = dry volume percentage of CO<sub>2</sub> in stack gas (%)  
 $\%O_2$  = dry volume percentage of O<sub>2</sub> in stack gas (%)  
 $\%CO$  = dry volume percentage of CO in stack gas (%)  
 $\%N_2$  = dry volume percentage of N<sub>2</sub> in stack gas (%)  
 $Ms$  = molecular weight of stack gas (lb/lbmol)

$$Vs = 85.49 C_p ASDP \sqrt{(Ts / Ps Ms)}$$

$$Qs = 63530 Vs (1 - Bws) A_s Ps / Ts$$

$Vs$  = average stack gas velocity (ft/s)  
 $C_p$  = pitot tube constant  
 $ASDP$  = average square root of pitot tube pressure difference (in<sup>1/2</sup>)  
 $Ts$  = average stack temperature (R)  
 $Ps$  = stack pressure (in Hg)  
 $Qs$  = average dry stack gas volumetric flow rate (dscf/hr)  
 $A_s$  = stack cross-sectional area (ft<sup>2</sup>)

$$\%I = 100 Vm(std) As / \theta Qs An$$

$\%I$  = percentage of isokinetic (%)  
 $\theta$  = total sampling time (hr)  
 $An$  = nozzle cross-sectional area (in<sup>2</sup>)

$$PL = 0.2205 As mn / An \theta \%I Pin$$

$$Cs = 15.43 mn / Vm(std)$$

$$Cs7 = 13.9 Cs / (20.9 - \%O2)$$

$PL$  = particulate loading based on input power (lb/MMBTU)  
 $mn$  = mass of particulate collected (g)  
 $Pin$  = average input power (MMBTU/hr)  
 $Cs$  = particulate loading based on volume flow (gr/dscf)  
 $Cs7$  = part. loading based on volume flow, corrected to 7% O<sub>2</sub> (gr/dscf)

### HCl Emission Rate Calculations

$$Vm(std) = 17.64 Y Vm Pbar / (Tm + 459.7)$$

$Vm(std)$  = standard volume of dry gas sampled (dscf)  
 $Y$  = meter calibration constant  
 $Vm$  = volume of dry gas as read by meter (dcf)  
 $Pbar$  = barometric pressure (in Hg)  
 $Tm$  = temperature of gas through meter (°F)

$$m = 1.0284 (S Vs - B Vb)$$

$m$  = mass of HCl sampled ( $\mu$ g)  
 $Vs$  = volume of diluted sample (ml)  
 $Vb$  = volume of diluted blank (ml)  
 $S$  = concentration of Cl<sup>-</sup> in sample ( $\mu$ g Cl<sup>-</sup>/ml)  
 $B$  = concentration of Cl<sup>-</sup> in blank ( $\mu$ g Cl<sup>-</sup>/ml)

$$C = m / Vm(std)$$

$$E = C Q / 453592000$$

$C$  = concentration of HCl in stack gas ( $\mu$ g/dscf)  
 $E$  = emission rate of HCl (lb/hr)  
 $Q$  = stack volumetric flow rate (dscf/hr)

$$QHCl = 10.57 E$$

$$Cv = 1000000 QHCl / Q$$

$$Evc = 13.9 Cv / (20.9 - \%O2)$$

$QHCl$  = volumetric flow rate of HCl (dscf/hr)  
 $Cv$  = concentration of HCl in stack gas (ppmvd)  
 $Evc$  =  $Cv$  corrected to 7% O<sub>2</sub> (ppmvd)  
 $\%O2$  = stack gas O<sub>2</sub> concentration (%)

VOST Results Calculations

$$VS = 499.5 * Y * Vm * Pb / (Tm + 459.67)$$

VS = volume of stack gas collected (dry std liters)

Y = meter box calibration factor

Vm = meter box volume change (ft<sup>3</sup>)

Pb = barometric pressure (in Hg)

Tm = average meter box temperature (°F)

$$CNC = BFB * 25 * RF$$

CNC = amount of pollutant collected on trap (ng)

RF = pollutant's response factor (25ng/%BFB)

BFB = 100 \* response for poll./response for BFB (%BFB)

$$CNT = CNCS1 + CNCS2$$

$$CNTB = CNCB1 + CNCB2$$

$$BCCNT = CNT - CNTB$$

CNT = amount of pollutant collected on sample traps (ng)

CNCS1 = amount of poll. coll. on Tenax sample trap (ng)

CNCS2 = amount of pollutant collected on Tenax/Charcoal sample trap (ng)

CNTB = amount of pollutant collected on blank traps (ng)

CNCS1 = amount of poll. coll. on Tenax blank trap (ng)

CNCS2 = amount of pollutant collected on Tenax/Charcoal blank trap (ng)

BCCNT = blank corrected CNT (ng)

$$CNM = 1000 * CNT / VS$$

$$BCCNM = 1000 * BCCNT / VS$$

CNM = concentration of pollutant in stack gas ( $\mu\text{g}/\text{Nm}^3$ )

BCCNM = blank corrected CNM

$$EUH = CNM * Q / 16018463$$

$$BCEUH = BCCNM * Q / 16018463$$

EUH = emission rate of pollutant ( $\mu\text{lb}/\text{hr}$ )

Q = stack gas volumetric flow rate (dscf/hr)

BCEUH = blank corrected EUH

$$EUK = 1000 * EUH / TFR$$

$$BCEUK = 1000 * BCEUH / TFR$$

EUK = normalized emission rate of pollutant ( $\mu\text{g}/\text{kg}$ )

TFR = garbage feed rate (lb/hr)

BCEUK = blank corrected EUK

## APPENDIX D VOST EMISSIONS

Date Sampled	06-16-90	08-04-90	08-10-90	08-10-90	08-24-90	11-10-90	12-01-90	12-15-90	01-26-91	01-26-91	03-21-91	04-24-91
Run Number	A3A	A6A	A7A	A7B	A8A	A13A	A14A	A15A	A16A	A16B	A17A	A18A
Volume collected (dnl)	28.31	16.42	18.44	18.47	15.77	15.95	15.33	20.11	19.03	18.38	21.29	20.31
Vol. flow rate (dacf/hr)	210000	210000	210000	210000	210000	191534	195000	194615	194993	194993	200649	174268
Total feed rate (lb/hr)	406.56	357.90	471.72	474.29	241.87	377.47	373.11	393.73	404.07	441.07	500.61	447.56

	Concentration (ng/m3)											
Benzene	9794	1600	1879	4590	2133	9055	9205	4420	7248	37719	691	2257
Toluene	2222	13400	1525	2180	2083	3510	2237	1956	2156	17256	3801	1842
Ethylbenzene	544	187	1033	1290	447	493	587	1116	187	1766	386	200
o-Xylene	187	221	X	120	117	70	114	108	40	1503	2	44
m,p-Xylene	703	558	144	296	475	377	325	361	425	3389	40	146
n-Propylbenzene	X	X	X	X	X	X	X	68	X	X	X	X
iso-Propylbenzene	X	48	X	X	X	X	X	129	X	X	107	X
2-Ethyltoluene	X	65	X	X	22	0	21	0	X	2211	1648	5
3,4-Ethyltoluene	X	258	X	X	X	167	X	635	X	351	128	X
1,2,3-Trimethylbenzene	X	X	X	X	X	X	X	X	X	2479	X	12
1,2,4-Trimethylbenzene	X	0	X	29	X	1862	977	0	1377	2681	X	963
1,3,5-Trimethylbenzene	X	124	374	902	X	0	174	47	192	2197	X	0
Styrene	X	X	0	5091	X	X	3296	3011	2414	9797	2144	1415
Phenyl acetylene	X	X	X	X	X	X	3860	1182	1779	31307	733	X
Bromobenzene	X	X	X	X	X	X	X	X	X	X	X	X
Chlorobenzene	1148	675	1417	2886	973	1746	2173	3838	4644	4042	18522	1981
1,2-Dichlorobenzene	72	258	447	1117	301	589	627	2024	1610	1562	X	1265
1,3-Dichlorobenzene	X	238	294	789	229	375	390	1178	1060	1270	1154	1266
1,4-Dichlorobenzene	20	X	72	122	67	61	50	265	240	134	227	65
Stomofom	X	X	X	X	X	X	X	X	X	X	X	X
Dibromochloromethane	X	X	X	X	X	X	X	X	X	X	X	X
Stromodichloromethane	X	X	X	X	X	X	X	X	75	1069	X	X
Methylene chloride	29376	1411	264	456	2570	355	153	13445	1152	28395	46288	1263
Chloroform	1154	522	104	1225	285	326	235	301	256	849	X	278
Carbon tetrachloride	336	609	75	1104	323	166	490	1421	983	6938	2385	523
1,1-Dichloroethane	721	X	X	X	62	X	X	X	X	X	18553	146
1,2-Dichloroethane	X	X	X	X	X	X	X	X	X	X	12484	X
1,1,1-Trichloroethane	1307	81	0	641	124	1276	103	461	390	1433	X	1906
1,1,2-Trichloroethane	X	X	X	X	X	X	X	X	X	X	X	X
1,1,2,2-Tetrachloroethane	X	X	X	X	X	X	X	X	X	X	X	X
1,1-Dichloroethene	216	X	X	X	X	X	X	X	X	X	59928	X
cis-1,2-Dichloroethene	X	X	X	X	X	X	X	X	X	X	48953	X
trans-1,2-Dichloroethene	X	X	X	X	X	X	X	X	X	X	X	86
Trichloroethene	102	X	333	85	X	64	X	893	397	14572	36080	615
Tetrachloroethene	81	X	126	179	121	X	X	178	X	X	6419	93
1,1-Dichloropropane	X	X	X	X	X	X	X	X	X	X	X	X
1,2-Dichloropropane	X	X	X	X	X	X	X	X	X	X	X	X
1,3-Dichloropropane	X	X	X	X	X	X	X	X	X	X	X	1235
1,2,3-Trichloropropane	X	X	X	X	X	X	X	X	X	X	X	X
1,1,1,2-Tetrachloropropane	X	X	X	X	X	X	X	X	X	X	X	X
cis-1,3-Dichloropropene	X	X	X	X	X	X	X	X	X	X	X	X
trans-1,3-Dichloropropene	X	X	X	X	X	X	X	X	X	X	135	X
2-Chloroethylvinyl ether	X	X	X	X	X	X	X	X	X	X	X	X

	Concentration (ng/m3), Blank Corrected											
Benzene	7789	1633	1561	4273	1627	-8017	3324	3791	6987	37437	381	1952
Toluene	1375	13305	1334	1989	1903	1545	1812	1406	1985	17071	3635	1771
Ethylbenzene	502	184	1033	1290	447	493	502	990	86	1657	294	200
o-Xylene	122	208	X	120	95	29	114	46	19	1480	2	44
m,p-Xylene	394	506	122	274	413	-186	-11	127	367	3327	40	146
n-Propylbenzene	X	X	X	X	X	X	X	X	X	X	X	X
iso-Propylbenzene	X	48	X	X	X	X	X	129	X	X	107	X
2-Ethyltoluene	X	85	X	X	-14	-176	21	-93	X	2211	1648	0
3,4-Ethyltoluene	X	242	X	X	X	167	X	590	X	351	128	X
1,2,3-Trimethylbenzene	X	X	X	X	X	X	X	X	X	2479	X	12
1,2,4-Trimethylbenzene	X	-17	X	29	X	1751	977	-50	1307	2605	X	894
1,3,5-Trimethylbenzene	X	124	374	902	X	-24	174	47	185	2190	X	-9
Styrene	X	X	-10	5082	X	X	3296	2851	2254	9625	2006	1401
Phenyl acetylene	X	X	X	X	X	X	3860	792	1573	31085	457	X
Bromobenzene	X	X	X	X	X	X	X	X	X	X	X	X
Chlorobenzene	1121	675	1417	2886	948	1746	2173	2868	1855	1032	4919	1975
1,2-Dichlorobenzene	72	258	447	1117	301	589	627	2024	1286	1212	X	1265
1,3-Dichlorobenzene	X	238	294	789	229	375	390	1178	1060	1270	1020	1266
1,4-Dichlorobenzene	-80	X	72	122	67	61	50	265	240	134	227	65
Stomofom	X	X	X	X	X	X	X	X	X	X	X	X
Dibromochloromethane	X	X	X	X	X	X	X	X	X	X	X	X
Stromodichloromethane	X	X	X	X	X	X	X	X	75	1069	X	X
Methylene chloride	4698	802	-14	178	-5851	-48758	-108	-50565	266	27439	-15070	932
Chloroform	1084	522	104	1225	285	326	235	-84	-89	476	X	0
Carbon tetrachloride	336	609	75	1104	323	166	490	-32406	-26430	-22637	1832	523
1,1-Dichloroethane	495	X	X	X	62	X	X	X	X	X	3561	146
1,2-Dichloroethane	X	X	X	X	X	X	X	X	X	X	3812	X
1,1,1-Trichloroethane	1307	81	-27	614	124	-513	103	278	-6872	-6402	X	1906
1,1,2-Trichloroethane	X	X	X	X	X	X	X	X	X	X	X	X
1,1,2,2-Tetrachloroethane	X	X	X	X	X	X	X	X	X	X	X	X
1,1-Dichloroethene	216	X	X	X	X	X	X	X	X	X	-35543	X
cis-1,2-Dichloroethene	X	X	X	X	X	X	X	X	X	X	X	414
trans-1,2-Dichloroethene	X	X	X	X	X	X	X	X	X	X	X	86
Trichloroethene	36	X	333	85	X	64	X	-12749	-14950	-1985	8644	615
Tetrachloroethene	-17	X	126	179	-11	X	X	178	X	X	1657	93
1,1-Dichloropropane	X	X	X	X	X	X	X	X	X	X	X	X
1,2-Dichloropropane	X	X	X	X	X	X	X	X	X	X	X	X
1,3-Dichloropropane	X	X	X	X	X	X	X	X	X	X	X	1235
1,2,3-Trichloropropane	X	X	X	X	X	X	X	X	X	X	X	X
1,1,1,2-Tetrachloropropane	X	X	X	X	X	X	X	X	X	X	X	X
cis-1,3-Dichloropropene	X	X	X	X	X	X	X	X	X	X	X	X
trans-1,3-Dichloropropene	X	X	X	X	X	X	X	X	X	X	X	X
2-Chloroethylvinyl ether	X	X	X	X	X	X	X	X	X	X	135	X





```

nt=0
ntt=0
ispwtn=0
tbase=0.0
open(l1,file='k4.inp',status='old')
10 read(l1,'(A)') line
if (line(1:9).eq.'REACTIONS') then
    write(*,*) 'processing reactions...'
    goto 10
endif
if (line(1:14).eq.'AMOUNTS') goto 200
if (line(1:1).eq.'X') goto 10
if (line(1:1).eq.'x') goto 10
if (line(1:1).eq.'-') goto 10
therxn=line(1:39)
arrdat=line(40:72)
nr=nr+1
read(arrdat,*) a(nr),p(nr),u(nr),h(nr)
cc write(*,*) therxn
cc write(*,'(d9.3,f9.1,f9.1,f9.1)') a(nr),p(nr),u(nr),h(nr)

lr=-1
tmprxn=therxn
80 call getspe(therxn,ks,lr)
if (ks.eq.0) goto 10
cc write(*,*) s(ks),ks,lr
if (lr.eq.1) goto 140
nrct(nr)=nrct(nr)+1
lrct(nr,nrct(nr))=ks
nrds(ks)=nrds(ks)+1
lrds(ks,nrds(ks))=nr
goto 80
140 nrps(ks)=nrps(ks)+1
lrps(ks,nrps(ks))=nr
goto 80

200 if (ispwtn.eq.1) goto 212
write(*,*) nr, ' reactions'
cc do 190 i=1,nr
cc 190 write(*,'(i3,d12.3,f9.1,f9.1,f9.1,2x,5a12)')
cc & i,a(i),p(i),u(i),h(i),(s(lrct(i,j))),j=1,nrct(i))
212 write(*,*) 'processing amounts...'
20 read(l1,'(A)') line
if (line(1:10).eq.'TIME STEPS') goto 210
if (line(1:1).eq.'-') goto 20
tmprxn=line(1:10)
amount=line(10:72)
call getspe(tmprxn,ks,lr)
read(amount,*) mw,amt
b(ks)=b(ks)+amt*0.45359237/mw
cc write(*,*) s(ks),b(ks)
goto 20

210 if (ispwtn.eq.1) goto 222
write(*,*) ns, ' species'
cc open(l4,file='species.out',status='new')
open(l4,file='k4.out',status='new')
write(l4,*) ' ',ns, ' species'
do 220 i=1,ns
cc write(*,'(i3,2x,a10,d10.4)') i,s(i),b(i)
write(l4,'(lx,a10)') s(i)
cc write(*,'(lh+,l5i5)') (lrps(i,j),j=1,nrps(i))
cc write(*,'(lh-,l5i5)') (lrds(i,j),j=1,nrds(i))
220 continue
222 write(*,*) 'processing time steps...'
160 read(l1,'(A)') line
if (line(1:27).eq.'TIME-TEMPERATURE PARAMETERS') goto 170
if (line(1:1).eq.'-') goto 160
nt=nt+1
read(line,*) ts(nt)
cc write(*,*) ts(nt)
goto 160

```

```

170 write (*,*) nt, ' time steps'
ck4   write (14,*) ' ',nt,' time steps'
cc   write (*,'(9f8.4)') (ts(i),i=1,nt)

      write (*,*) 'processing time-temperature parameters...'

172 read(11,'(A)') line
      if (line(1:1).eq.'-') goto 172
      read(line,*) tto,ttl,tt2,gamma
cc   write (*,'(f8.1,f8.4,f8.4,f8.4)') tto,ttl,tt2,gamma
c-----
      write (*,*) 'integrating...'

      itol = 2
      rtol = 1.d-4
      do 350 j=1,ns
350  atol(j) = 1.d-10
      itask = 1
      istate = 1
      iopt = 0
      lrw = nrwork
      liw = niwork
      mf = 22
c-----
c      call ieee
c      call abrupt_underflow()

      ti=0.0
      if (gamma.gt.0.0) then
          tf=tto*dexp(ti/ttl)*dexp(-ti/tt2)/(gamma+dexp(ti/ttl))
      else
          tf=tto+ttl*ti
      endif
      t=(tf+459.67d0)/1.8d0
      write(14,'(1x,f7.4,f8.1)') tbase,t
178  write(14,'(6d11.3)') (b(j),j=1,ns)
cv   write(*,*) tbase,t
cv   write(*,*) (b(j),j=1,ns)

c      start loop

      do 180 i=1,nt
      if (i.eq.1) then
          tin=0.0
      else
          tin=ts(i-1)
      endif
      tinn=tin
      tout=ts(i)
      ti=tout

c      write(6,*) i,'th call to integrator'
c      write(6,*) 'tin = ',tin,' tout = ',tout

      call lsode(cdot,ns,b,tin,tout,itol,rtol,atol,itask,istate,
1      iopt,rwork,lrw,iwork,liw,jac,mf)

c check if step excuted successssfully:
c      write(6,*)'iteration: ',i,' istate: ',istate
c      write(*,'(1x,i3,f9.4,f9.4,f9.1,i4)')
c      &      ntt+i,tbase+tinn,tbase+tout,tf,istate
c  istate = 2  if lsode was successful, negative otherwise.
c      -1 means excess work done on this call (perhaps wrong mf).
c      -2 means excess accuracy requested (tolerances too small).
c      -3 means illegal input detected (see printed message).
c      -4 means repeated error test failures (check all inputs).
c      -5 means repeated convergence failures (perhaps bad jacobian
c      supplied or wrong choice of mf or tolerances).
c      -6 means error weight became zero during problem. (solution
c      component i vanished, and atol or atol(i) = 0.)

```

```

C-----
C write time,temp,conc to a separate file
C
  if (gamma.gt.0.0) then
    tf=tto*dexp(ti/tt1)*dexp(-ti/tt2)/(gamma+dexp(ti/tt1))
  else
    tf=tto+tt1*ti
  endif
  t=(tf+459.67d0)/1.8d0
  write(14,'(1x,f7.4,f8.1)') tbase+tout,t
  write(14,'(6d11.3)') (b(j),j=1,ns)
  if (istate.ne.2) istate=1
180 continue

  ispwtn=1
  ntt=ntt+nt
  nt=0
  write(*,'(3(2x,a10,d11.3,3h |))') (s(j),b(j),j=1,ns)
  tbase=tbase+tout

184 read(11,'(A)',end=182) line
  if (line(1:1).eq.'=') goto 184
  if (line(1:14).eq.'AMOUNTS') goto 200
  if (line(1:10).eq.'TIME STEPS') goto 210
  if (line(1:27).eq.'TIME-TEMPERATURE PARAMETERS') goto 170

182 write(14,'(1x,f8.1,f8.1)') -99.0,-99.0
  write (14,'(1x)')
  close(11)
  stop
  end
C-----
  subroutine getspe(rxn,is,lr)
  parameter(nrx=300,nrr=50,nls=5)
  parameter(nsp=101,nts=200,nrwork=22+9*nsp+nsp**2,niwork=20+nsp)
  character rxn*39,tmp*41
  character s(nsp)*10,sp*10
  common /spe/s,ns,icd,iis

  if (icd.eq.0) goto 330
  is=iis
  icd=icd-1
  goto 70

330 tmp=rxn
  tmp(40:41)=' @'
  50 if (tmp(1:1).eq.'@') then
    is=0
    goto 70
  endif
  if (tmp(1:1).eq.'+') goto 60
  if (tmp(1:1).eq.'-') goto 60
  if (tmp(1:1).eq.'>') goto 120
  if (tmp(1:1).ge.'0'.and.tmp(1:1).le.'9') goto 340
  if (tmp(1:1).ne.' ') goto 40
  60 tmp=tmp(2:)
  goto 50

340 read (tmp,*) icd
  icd=icd-1
  n=index(tmp,' ')
  tmp=tmp(n:)
  goto 50

120 lr=1
  goto 60

  40 n=index(tmp,' ')
  sp=tmp(:n-1)
  if (sp.ne.'M') goto 150
  is=nsp
  goto 110

```

```

150 do 90 i=1,ns
      if (sp.eq.s(i)) goto 100
  90   continue
      ns=ns+1
      s(ns)=sp
      is=ns
      goto 110
100  is=i
110  rxn=tmp(n:)
      goto 70

  70  iis=is
      return
      end
c-----
c      subroutine jac(mn,ti,c,ml,mu,pd,nrpd)
c      provides jacobian matrix if mf = 21 or 24
      implicit real*8 (a-h,o-z)
      dimension pd(nrpd,mn)
      return
      end
c-----
      subroutine cdot(ns,ti,b,e)
      implicit double precision (a-h,o-z)
      parameter(nrx=300,nrr=50,nls=5)
      parameter(nsp=101,nts=200,nrwork=22+9*nsp+nsp**2,niwork=20+nsp)
      double precision a(nrx),p(nrx),u(nrx),h(nrx),ra(nrx)
      double precision c(nsp),b(nsp),d(nsp),e(nsp)
      integer nrct(nrx),lrct(nrx,nls)
      integer nrds(nsp),lrds(nsp,nrr),nrps(nsp),lrps(nsp,nrr)
      common /rct/a,p,u,h,nrct,lrct,nrds,lrds,nrps,lrps,nr
      common /ttp/tto,ttl,tt2,gamma

cc      write (*,*) ns
cc      write(*,'(f8.1,f8.4,f8.4,f8.4)') tto,ttl,tt2,gamma
      if (gamma.gt.0.0) then
          tf=tto*dexp(ti/ttl)*dexp(-ti/tt2)/(gamma+dexp(ti/ttl))
          else
          tf=tto+ttl*ti
          endif
      t=(tf+459.67d0)/1.8d0
      b(nsp)=0.0
      do 290 i=1,ns
290    b(nsp)=b(nsp)+b(i)
      v=b(nsp)*0.082058*t/1.0
      do 295 i=1,ns
295    c(i)=b(i)/v
      c(nsp)=b(nsp)/v
      do 390 i=1,nr
390    ra(i)=a(i)*t**p(i)*dexp(-u(i)/t)
      do 240 i=1,ns
          d(i)=0.0
          do 250 j=1,nrps(i)
              it=lrps(i,j)
              pc=1.0
              do 260 k=1,nrct(it)
260                pc=pc*c(lrct(it,k))
250            d(i)=d(i)+ra(it)*pc
          do 270 j=1,nrds(i)
              it=lrds(i,j)
              pc=1.0
              do 280 k=1,nrct(it)
280                pc=pc*c(lrct(it,k))
270            d(i)=d(i)-ra(it)*pc
240    continue
      do 245 i=1,ns
245    e(i)=d(i)*v
cc      write (*,'(d14.4,1x,d14.4,1x,d14.4,1x,d14.4,1x,d14.4)')
cc      & (d(i),i=1,ns)
      return
      end

```

APPENDIX F  
KINETICS CODE INPUT FILE

REACTIONS	A	P=n	U=E /R	$\Delta H$
			<u>a</u> <u>u</u>	<u>s</u>
CH4 + OH --> CH3 + H2O	3.02D10	0.0	2520.0	-16370.0
CH4 + H --> CH3 + H2	2.00D11	0.0	5990.0	-3510.0
CH4 + O --> CH3 + OH	2.00D10	0.0	3470.0	1560.0
CH4 + M --> CH3 + H + M	2.00D14	0.0	44500.0	104190.0
CH3 + O --> CH2O + H	7.08D10	0.0	500.0	-69910.0
CH3 + O2 --> CH2O + OH	3.02D10	0.0	8810.0	-54030.0
CH3 + O2 --> CHO + H2O	2.00D07	0.0	0.0	-97330.0
CH3 + OH --> CH2 + H2O	6.31D07	0.7	1010.0	-7920.0
CH3 + OH --> CH2O + H2	3.98D09	0.0	0.0	-71850.0
CH3 + O --> CHO + H2	1.00D11	0.0	0.0	-98232.0
CH3 + H --> CH2 + H2	1.58D11	-0.3	6260.0	7050.0
CH2O + M --> CO + H2 + M	2.00D13	0.0	17620.0	2800.0
CH2O + M --> CHO + H + M	3.98D09	0.0	18500.0	79370.0
CH2O + OH --> CHO + H2O	2.51D10	0.0	500.0	-43300.0
CH2O + O --> CHO + OH	3.02D10	0.0	0.0	-26380.0
CH2O + H --> CHO + H2	1.70D10	0.0	1510.0	-28330.0
CHO + M --> CO + H + M	2.00D09	0.5	14500.0	31130.0
CHO + O2 --> CO + HO2	3.02D10	0.0	0.0	-18760.0
CHO + O2 --> CO2 + OH	7.41D08	0.5	0.0	-80720.0
CHO + O --> CO + OH	5.37D08	0.5	0.0	-74620.0
CHO + O --> CO2 + H	5.37D08	0.5	0.0	-96590.0
CHO + OH --> CO + H2O	1.00D11	0.0	0.0	-91540.0
CHO + H --> CO + H2	1.58D09	0.5	0.0	-76570.0
CO + OH --> CO2 + H	5.50D08	0.0	540.0	-21970.0
CO + O + M --> CO2 + M	3.63D12	-1.0	1260.0	-127720.0
CO + O2 --> CO2 + O	1.58D10	0.0	20630.0	-6098.0
H + O2 --> OH + O	2.19D11	0.0	8460.0	15870.0
H + O2 + M --> HO2 + M	1.41D13	0.0	-500.0	-49890.0
H + OH + H2O --> H2O + H2O	1.41D17	-2.0	0.0	-122670.0
H + OH + M --> H2O + M	7.08D13	-1.0	0.0	-122670.0
H + O + M --> OH + M	3.98D12	-1.0	0.0	-105750.0
H + H + M --> H2 + M	2.00D13	-1.0	0.0	-107700.0
H + HO2 --> OH + OH	2.00D11	0.0	1010.0	-39990.0
H2 + O2 --> H + HO2	1.26D10	0.2	29440.0	57810.0
H2 + O2 --> OH + OH	1.70D10	0.0	24230.0	17820.0
H2 + O --> H + OH	1.70D10	0.0	4760.0	-1052.0
H2 + OH --> H2O + H	2.19D10	0.0	2620.0	-14970.0
HO2 + O --> O2 + OH	2.51D10	0.0	0.0	-58860.0
HO2 + OH --> O2 + H2O	2.51D10	0.0	0.0	-72780.0
OH + OH --> H2O + O	6.03D09	0.0	340.0	-16918.0
O + O + M --> O2 + M	3.98D12	-1.0	0.0	-127624.0
CH2 + OH --> CH + H2O	5.00D08	0.5	3000.0	-0.0
CH2 + O --> CH + OH	2.00D08	0.7	13000.0	-0.0
CH2 + O --> CHO + H	5.00D08	0.5	2000.0	-0.0
CH2 + O2 --> CH2O + O	5.00D08	0.5	3500.0	-0.0
CH2 + H --> CH + H2	3.20D08	0.7	2500.0	-0.0
CH + O2 --> CHO + O	5.00D08	0.5	3000.0	-0.0
CH + OH --> CHO + H	5.00D08	0.5	5000.0	-0.0
CH + O --> CO + H	6.30D08	0.5	0.0	-0.0
CH + HO2 --> CH2 + O2	1.00D07	0.5	7550.0	-0.0
CH + HO2 --> CHO + OH	5.00D08	0.5	3000.0	-0.0
CH + CHO --> CH2 + CO	3.20D07	0.7	500.0	-0.0
C2 + O --> C + CO	6.30D08	0.5	0.0	-0.0
C + CO --> C2 + O	1.00D09	0.5	58025.0	-0.0
C2 + H --> C + CH	1.60D10	0.5	30450.0	-0.0

C + CH --> C2 + H	6.30D08	0.5	0.0	-0.0
CO + H --> C + OH	2.00D10	0.5	77755.0	-0.0
C + OH --> CO + H	6.30D08	0.5	0.0	-0.0
C + O2 --> CO + O	6.30D08	0.5	0.0	-0.0
C2 + O2 --> 2 CO	5.44D04	0.0	8057.0	-0.0
-----				
garb -> tar + 5 CO2 + 11 H2O	4.57D-22	7.0	0.0	-0.0
tar -> char + 10 CH2	4.57D-22	7.0	0.0	-0.0
char -> 3 C2	4.57D-22	7.0	0.0	-0.0
-----				
H2O(LIQ) -> H2O	1.00D02	0.0	0.0	-0.0
-----				
C2H2 + H --> C2H + H2	2.00D14	0.0	9760.0	-0.0
C2H2 + OH --> C2H + H2O	6.03D12	0.0	3520.0	-0.0
C2H2 + M --> C2H + H + M	6.03D14	0.0	40260.0	-0.0
C2H2 + O2 --> 2 CO + 2 H	1.00D14	0.0	19120.0	-0.0
C2H2 + O --> CO + CH2	5.01D12	0.0	1260.0	-0.0
C2H2 + O --> C2H + OH	3.24D15	-0.6	8560.0	-0.0
C2H + OH --> CO + CH2	6.03D12	0.0	0.0	-0.0
C2H + O2 --> CO + CHO	1.00D13	0.0	3520.0	-0.0
C2H + O --> CH + CO	5.01D13	0.0	0.0	-0.0
CH2 + OH --> CHO + H2	7.08D13	0.0	0.0	-0.0
-----				
PVC --> HCl + C2H2	1.72D02	0.0	2320.0	-0.0
POLYSTYRN --> STYRENE	2.19D02	0.0	1985.0	-0.0
STYRENE --> C6H6 + C2H2	1.00D11	0.0	5000.0	-0.0
C6H6 + OH --> PHENOL + H	2.00D08	0.0	5335.0	-0.0
-----				
C6H6 --> 3 C2H2	7.95D06	0.0	19124.0	-0.0
PHENOL --> 3 C2H2 + O	2.20D11	0.0	33216.0	-0.0
-----				
PHENOL+PHENOL-->FURAN+H2O+H2	1.42d04	0.0	5000.0	-0.0
PHENOL+PHENOL-->DIOXIN+2 H2	5.26d03	0.0	5000.0	-0.0
-----				
2 HCl + O -> Cl2 + H2O	4.00d10	0.0	0.0	-0.0
C6H6 + Cl2 -> C6H5Cl + HCl	1.52d03	0.0	5000.0	-0.0
PHENOL + Cl2 -> ClPh + HCl	2.60D05	0.0	5000.0	-0.0
FURAN + Cl2 -> ClFR + HCl	6.60D06	0.0	5000.0	-0.0
DIOXIN + Cl2 -> ClDX + HCl	6.60D06	0.0	5000.0	-0.0

## AMOUNTS

N2	28.0	2038.2
O2	32.0	615.6
H2O	18.0	25.2
garb	630.0	250.0
H2O(LIQ)	18.0	100.0
POLYSTYRN	104.0	20.0
PVC	62.5	2.0
CH4	16.0	30.0

## TIME STEPS

0.001  
0.002  
0.004  
0.006  
0.008  
0.010  
0.015  
0.020  
0.030  
0.040  
0.050  
0.060  
0.070  
0.080  
0.090  
0.100  
0.120  
0.150  
0.200  
0.300  
0.400

0.500  
 0.600  
 0.700  
 0.800  
 1.000  
 1.300  
 1.600  
 2.000  
 2.400  
 2.800

-----  
 TIME-TEMPERATURE PARAMETERS  
 1850.0 0.1329 30.52 0.8575  
 =====

AMOUNTS

N2	28.0	2038.2
O2	32.0	615.6
H2O	18.0	25.2
CH4	16.0	37.0

-----  
 TIME STEPS

0.010  
 0.020  
 0.040  
 0.060  
 0.080  
 0.100  
 0.150  
 0.200  
 0.300  
 0.400  
 0.500  
 0.600  
 0.700  
 0.800  
 0.900  
 1.000  
 1.100  
 1.200  
 1.300  
 1.400

-----  
 TIME-TEMPERATURE PARAMETERS  
 2054.0 0.07441 7.497 0.1853  
 =====

AMOUNTS

N2	28.0	7540.3
O2	32.0	2277.5
H2O	18.0	93.2

-----  
 TIME STEPS

0.010  
 0.020  
 0.040  
 0.060  
 0.080  
 0.100  
 0.150  
 0.200  
 0.300  
 0.400  
 0.500  
 0.600  
 0.700  
 0.800  
 0.900

-----  
 TIME-TEMPERATURE PARAMETERS  
 777.0 -85.56 0.0 -1.0

APPENDIX G  
TEMPERATURE-TIME PROFILE CALCULATIONS

Residence Time Calculations

The time-temperature profile of the combustion gases as they flow through the incinerator's primary and secondary chambers, the flue, and the chimney is modelled on temperature and flow rate measurements at the CCTL incinerator.

EPA Method 2 [137] stack gas volumetric flow rate measurements have recently shown an average 200000 dscf/hr flow rate down the horizontal flue at the Method 5 port, assuming a 6% by volume wet moisture content, or 212766 scf/hr with the moisture included. A standard cubic foot (scf) of gas is here defined as being at 68 °F and 29.92 in Hg (1 atm). The stack gas velocity averages 23 ft/sec. The temperature at the sampling port is usually about 700 °F. The static pressure in the stack is essentially the same as the ambient barometric pressure.

Since the flue is 34.6 ft long, the residence time of the stack gas in the flue is  $34.6/23$  or 1.5 seconds. Early simultaneous temperature measurements at the M5 port (260" downstream of the dilution "T") and the CEM port (100" downstream of the "T") showed that the temperature of the gas would be approximately 77 °F hotter at the "T" than at the M5 sampling port and about 50 °F cooler at the chimney

interface than at the M5 sampling port. Residence time from the "T" to the M5 sampling port is 0.9 seconds.

From oxygen concentration measurements of the undiluted stack gas while burning just natural gas and stoichiometry, an estimated 5428 lb/hr of combustion gas exited the SCC while burning just natural gas. Adding a typical 372 lb/hr of ash-free waste brings the total combustion gas rate to 5800 lb/hr. Residence time in the 75-ft<sup>3</sup> SCC at 337000 ft<sup>3</sup>/hr and 1850 °F and in the 50-ft<sup>3</sup> stack section before the "T" at at 308000 ft<sup>3</sup>/hr and 1650 °F is about 1.4 seconds. With about half the 5800 lb/hr flowing from the 125-ft<sup>3</sup> PCC (or 167000 ft<sup>3</sup>/hr at an average 1750 °F), residence time in the PCC and 5-ft<sup>3</sup> connecting passage is about 2.8 seconds.

#### Temperature Versus Time Equations for the Three Sections

The earlier work investigating pyrolysis and combustion of coal [116] used a time-temperature equation of the form

$$T = \frac{T_0 \exp(t/t_1) \exp(-t/t_2)}{g + \exp(t/t_1)} \quad (G-1)$$

This equation is a simplification of one used to provide good analytic fits to laboratory flame temperature data. For the CCTL incinerator, the system up to the dilution "T" could be modeled by the same equation, but in two parts, with one set of parameters ( $T_0$ ,  $t_1$ ,  $t_2$ ,  $g$ ) for the PCC and another set for the SCC including the flue up to the "T".

For the PCC a preliminary time-temperature history after initial heating was developed, starting at 1000 °F, rising

quickly to 1800 °F after 0.55 seconds, and slowly falling to 1690 °F after 2.8 seconds (see Figure 5-2 in Chapter 5). After filling in appropriate temperatures between these times, a non-linear least squares program fit Equation G-1 to the temperature versus time data, with results of  $T_0=1850$  °F,  $t_1=0.1329$  seconds,  $t_2=30.52$  seconds, and  $g=0.8575$ .

For the SCC and flue up to the "T", the estimated time-temperature history starts where the primary chamber ended at 1690 °F, rising quickly to 1975 °F after 0.2 seconds, slowly falling to 1850 °F at 0.8 seconds at the outlet of the SCC, and down to 1670 °F at "T" after a total of 1.2 seconds. After filling in appropriate temperatures between these times the non-linear least squares fit results were  $T_0=2054$  °F,  $t_1=0.07441$  seconds,  $t_2=7.497$  seconds, and  $g=0.1853$ .

For the flue pipe from the "T" to the chimney, due to its lower temperature and insulation, a simple linear time-temperature relation was developed:

$$T = T_0 - t_1 t \quad (G-2)$$

A linear profile was used because a constant heat loss in the stack was assumed. Starting at 777 °F at the "T" for a typical 700 °F sampling port temperature 0.9 seconds downstream the "T" leads to results of  $T_0=777$  °F and  $t_1=85.56$  seconds. The temperature falls to 649 °F at the chimney after 1.5 seconds with this formula. The temperature-time profile in the chimney also has been modelled as a linear drop of temperature with time, but it is not used in the study here.

APPENDIX H  
BASE CASE KINETICS CODE OUTPUT

	time (s)	temp (K)	CH4	OH	CH3	H2O	H2
	0.000	808.7	8.50E-01	1.00E-25	1.00E-25	6.35E-01	1.00E-25
	0.001	810.6	8.50E-01	1.22E-10	1.12E-09	8.75E-01	2.59E-09
	0.002	812.5	8.50E-01	2.31E-10	2.21E-09	1.09E+00	2.89E-08
	0.004	816.3	8.50E-01	4.17E-10	4.21E-09	1.47E+00	4.01E-07
	0.006	820.1	8.50E-01	5.88E-10	6.12E-09	1.77E+00	1.94E-06
	0.008	823.9	8.50E-01	7.66E-10	8.06E-09	2.02E+00	5.90E-06
	0.010	827.7	8.50E-01	9.66E-10	1.01E-08	2.23E+00	1.38E-05
	0.015	837.1	8.50E-01	1.68E-09	1.66E-08	2.60E+00	5.92E-05
	0.020	846.4	8.50E-01	2.85E-09	2.65E-08	2.82E+00	1.49E-04
	0.030	865.0	8.50E-01	7.00E-09	6.15E-08	3.04E+00	4.22E-04
	0.040	883.3	8.50E-01	1.22E-08	1.08E-07	3.12E+00	7.07E-04
	0.050	901.3	8.50E-01	1.49E-08	1.38E-07	3.15E+00	9.35E-04
	0.060	918.9	8.50E-01	1.47E-08	1.43E-07	3.17E+00	1.10E-03
	0.070	936.1	8.50E-01	1.43E-08	1.49E-07	3.18E+00	1.24E-03
	0.080	952.9	8.50E-01	1.53E-08	1.67E-07	3.19E+00	1.38E-03
	0.090	969.2	8.50E-01	1.73E-08	1.99E-07	3.19E+00	1.54E-03
PCC	0.100	985.0	8.50E-01	2.06E-08	2.45E-07	3.20E+00	1.74E-03
	0.120	1015.0	8.50E-01	3.11E-08	3.90E-07	3.22E+00	2.28E-03
	0.150	1056.0	8.49E-01	6.06E-08	7.86E-07	3.26E+00	3.80E-03
	0.200	1113.1	8.44E-01	1.66E-07	2.13E-06	3.35E+00	9.95E-03
	0.300	1189.3	8.11E-01	7.69E-07	8.98E-06	3.65E+00	5.36E-02
	0.400	1228.6	6.88E-01	2.80E-06	2.73E-05	4.16E+00	1.76E-01
	0.500	1246.7	4.37E-01	5.21E-06	3.58E-05	4.89E+00	3.52E-01
	0.600	1253.8	2.26E-01	5.96E-06	2.47E-05	5.60E+00	4.56E-01
	0.700	1255.4	1.04E-01	6.31E-06	1.39E-05	6.17E+00	4.75E-01
	0.800	1254.5	4.34E-02	6.53E-06	6.89E-06	6.64E+00	4.46E-01
	1.000	1249.6	6.34E-03	6.73E-06	1.27E-06	7.31E+00	3.48E-01
	1.300	1240.2	2.98E-04	6.43E-06	7.34E-08	7.95E+00	2.32E-01
	1.600	1230.7	1.65E-05	5.65E-06	4.21E-09	8.32E+00	1.66E-01
	2.000	1218.0	5.84E-07	4.52E-06	1.45E-10	8.61E+00	1.14E-01
	2.400	1205.4	3.77E-08	3.59E-06	8.95E-12	8.76E+00	8.22E-02
	2.800	1193.1	3.77E-09	2.88E-06	2.32E-12	8.85E+00	6.03E-02
	2.800	1218.1	1.05E+00	2.88E-06	2.32E-12	9.48E+00	6.03E-02
	2.810	1236.1	1.01E+00	8.52E-06	7.96E-05	9.54E+00	8.26E-02
	2.820	1252.3	9.61E-01	9.19E-06	8.11E-05	9.60E+00	1.06E-01
	2.840	1279.5	8.64E-01	1.12E-05	8.72E-05	9.75E+00	1.58E-01
	2.860	1300.9	7.55E-01	1.35E-05	9.12E-05	9.91E+00	2.13E-01
	2.880	1317.2	6.41E-01	1.55E-05	9.02E-05	1.01E+01	2.65E-01
	2.900	1329.5	5.29E-01	1.72E-05	8.41E-05	1.03E+01	3.09E-01
	2.950	1346.9	2.98E-01	1.96E-05	5.84E-05	1.07E+01	3.56E-01
	3.000	1352.6	1.51E-01	2.08E-05	3.44E-05	1.10E+01	3.28E-01
	3.100	1348.1	3.03E-02	2.32E-05	9.12E-06	1.14E+01	1.91E-01
SCC	3.200	1336.3	3.65E-03	2.86E-05	1.60E-06	1.16E+01	7.67E-02
	3.300	1322.6	1.49E-04	3.77E-05	1.09E-07	1.17E+01	1.94E-02
	3.400	1308.7	7.73E-07	4.03E-05	8.94E-10	1.17E+01	3.30E-03
	3.500	1294.7	4.55E-10	3.40E-05	2.66E-12	1.17E+01	1.06E-03
	3.600	1281.0	1.00E-25	2.87E-05	1.00E-25	1.17E+01	7.82E-04
	3.700	1267.4	2.10E-13	2.44E-05	1.00E-25	1.17E+01	7.02E-04
	3.800	1254.0	1.00E-25	2.08E-05	1.00E-25	1.17E+01	6.55E-04
	3.900	1240.8	3.06E-13	1.76E-05	1.66E-16	1.17E+01	6.20E-04
	4.000	1227.7	1.00E-25	1.49E-05	3.16E-16	1.17E+01	5.93E-04
	4.100	1214.8	1.72E-13	1.25E-05	1.00E-25	1.17E+01	5.73E-04
	4.200	1202.1	9.23E-14	1.05E-05	2.44E-16	1.17E+01	5.58E-04
	4.200	687.0	9.23E-14	1.05E-05	2.44E-16	1.41E+01	5.58E-04
	4.210	686.6	9.16E-14	2.19E-06	4.20E-19	1.41E+01	5.57E-04
	4.220	686.1	9.15E-14	3.55E-07	6.83E-20	1.41E+01	5.57E-04
	4.240	685.1	9.15E-14	4.93E-08	9.98E-21	1.41E+01	5.57E-04
	4.260	684.2	9.15E-14	4.28E-08	1.18E-20	1.41E+01	5.57E-04
	4.280	683.2	9.14E-14	4.26E-08	6.41E-20	1.41E+01	5.57E-04
	4.300	682.3	9.14E-14	4.27E-08	8.36E-21	1.41E+01	5.57E-04
Stack	4.350	679.9	9.14E-14	4.25E-08	7.86E-21	1.41E+01	5.58E-04
	4.400	677.5	9.14E-14	4.21E-08	7.48E-21	1.41E+01	5.59E-04
	4.500	672.8	9.13E-14	4.10E-08	6.79E-21	1.41E+01	5.61E-04
	4.600	668.0	9.13E-14	3.96E-08	6.16E-21	1.41E+01	5.63E-04
	4.700	663.3	9.13E-14	3.82E-08	5.59E-21	1.41E+01	5.65E-04
	4.800	658.5	9.12E-14	3.66E-08	5.07E-21	1.41E+01	5.67E-04
	4.900	653.8	9.12E-14	3.51E-08	4.60E-21	1.41E+01	5.68E-04
	5.000	649.0	9.12E-14	3.36E-08	4.18E-21	1.41E+01	5.70E-04
	5.100	644.3	9.12E-14	3.20E-08	3.79E-21	1.41E+01	5.72E-04

PCC: 0.0 ≤ time ≤ 2.8  
 SCC: 2.8 ≤ time ≤ 4.2  
 Stack: 4.2 ≤ time ≤ 5.1

All values in kmol/hr  
 Values < 1.00E-25 are set to 1.00E-25

O	CH2O	O2	CHO	CH2	CO	HO2	CO2
1.00E-25	1.00E-25	8.73E+00	1.00E-25	1.00E-25	1.00E-25	1.00E-25	1.00E-25
2.54E-10	5.99E-08	8.73E+00	4.77E-13	3.21E-10	2.83E-05	2.82E-05	9.38E-05
5.12E-10	4.28E-07	8.73E+00	1.01E-12	1.20E-09	1.16E-04	1.16E-04	1.89E-04
1.01E-09	3.01E-06	8.73E+00	2.17E-12	4.41E-09	4.91E-04	4.87E-04	3.85E-04
1.47E-09	8.95E-06	8.72E+00	3.50E-12	9.04E-09	1.16E-03	1.15E-03	5.87E-04
1.87E-09	1.84E-05	8.72E+00	5.04E-12	1.44E-08	2.17E-03	2.14E-03	7.96E-04
2.19E-09	3.06E-05	8.72E+00	6.87E-12	2.00E-08	3.55E-03	3.50E-03	1.01E-03
2.70E-09	6.36E-05	8.71E+00	1.35E-11	3.16E-08	8.87E-03	8.69E-03	1.58E-03
4.14E-09	8.40E-05	8.70E+00	2.44E-11	3.79E-08	1.72E-02	1.68E-02	2.20E-03
3.13E-09	7.38E-05	8.66E+00	6.09E-11	3.88E-08	4.27E-02	4.17E-02	3.61E-03
3.46E-09	4.30E-05	8.61E+00	9.30E-11	3.12E-08	7.63E-02	7.46E-02	5.25E-03
4.14E-09	2.21E-05	8.56E+00	9.12E-11	2.22E-08	1.09E-01	1.07E-01	7.15E-03
5.31E-09	1.18E-05	8.53E+00	7.41E-11	1.62E-08	1.34E-01	1.31E-01	9.32E-03
7.06E-09	7.69E-06	8.50E+00	6.63E-11	1.41E-08	1.51E-01	1.48E-01	1.18E-02
9.48E-09	6.09E-06	8.48E+00	6.91E-11	1.44E-08	1.64E-01	1.59E-01	1.45E-02
1.27E-08	5.39E-06	8.47E+00	7.89E-11	1.61E-08	1.73E-01	1.68E-01	1.77E-02
1.68E-08	5.08E-06	8.46E+00	9.48E-11	1.89E-08	1.80E-01	1.75E-01	2.12E-02
2.87E-08	4.98E-06	8.44E+00	1.47E-10	2.72E-08	1.91E-01	1.84E-01	2.95E-02
5.88E-08	5.35E-06	8.43E+00	2.91E-10	4.69E-08	2.02E-01	1.90E-01	4.55E-02
1.58E-07	6.56E-06	8.41E+00	7.81E-10	1.02E-07	2.17E-01	1.89E-01	8.31E-02
6.95E-07	1.04E-05	8.35E+00	3.26E-09	2.91E-07	2.85E-01	1.53E-01	2.04E-01
2.59E-06	1.70E-05	8.14E+00	9.98E-09	5.26E-07	4.59E-01	7.69E-02	3.94E-01
6.34E-06	1.87E-05	7.62E+00	1.35E-08	7.44E-07	7.35E-01	4.64E-02	6.71E-01
9.65E-06	1.52E-05	7.05E+00	9.83E-09	9.11E-07	9.55E-01	4.09E-02	9.87E-01
1.28E-05	1.23E-05	6.56E+00	6.27E-09	1.01E-06	1.09E+00	3.46E-02	1.30E+00
1.56E-05	1.04E-05	6.14E+00	3.94E-09	1.04E-06	1.16E+00	2.86E-02	1.60E+00
1.93E-05	8.06E-06	5.45E+00	2.08E-09	9.99E-07	1.21E+00	2.02E-02	2.12E+00
2.11E-05	5.90E-06	4.66E+00	1.49E-09	8.16E-07	1.20E+00	1.34E-02	2.76E+00
2.03E-05	4.25E-06	4.10E+00	1.11E-09	6.16E-07	1.16E+00	9.81E-03	3.25E+00
1.79E-05	2.69E-06	3.59E+00	6.56E-10	3.99E-07	1.07E+00	6.99E-03	3.71E+00
1.55E-05	1.72E-06	3.27E+00	3.60E-10	2.49E-07	9.66E-01	5.19E-03	4.04E+00
1.35E-05	1.11E-06	3.05E+00	1.91E-10	1.54E-07	8.70E-01	3.95E-03	4.26E+00
1.35E-05	1.11E-06	1.18E+01	1.91E-10	1.54E-07	8.70E-01	3.95E-03	4.26E+00
6.27E-06	1.96E-05	1.17E+01	2.85E-08	8.68E-08	8.94E-01	1.56E-02	4.29E+00
6.95E-06	1.81E-05	1.16E+01	2.89E-08	9.11E-08	9.18E-01	2.39E-02	4.31E+00
8.97E-06	1.65E-05	1.15E+01	3.10E-08	9.79E-08	9.65E-01	3.39E-02	4.36E+00
1.16E-05	1.51E-05	1.13E+01	3.24E-08	1.02E-07	1.01E+00	3.87E-02	4.43E+00
1.47E-05	1.35E-05	1.11E+01	3.20E-08	1.05E-07	1.05E+00	4.06E-02	4.52E+00
1.79E-05	1.16E-05	1.09E+01	2.99E-08	1.05E-07	1.08E+00	4.09E-02	4.61E+00
2.60E-05	7.18E-06	1.04E+01	2.09E-08	1.00E-07	1.08E+00	3.72E-02	4.87E+00
3.38E-05	4.08E-06	1.01E+01	1.24E-08	9.04E-08	1.00E+00	2.97E-02	5.12E+00
5.18E-05	1.20E-06	9.60E+00	3.47E-09	6.70E-08	7.58E-01	1.47E-02	5.52E+00
8.52E-05	3.47E-07	9.36E+00	7.68E-10	4.72E-08	5.43E-01	5.78E-03	5.78E+00
1.67E-04	1.40E-07	9.23E+00	2.10E-10	3.27E-08	3.83E-01	1.81E-03	5.97E+00
3.35E-04	1.01E-07	9.15E+00	1.33E-10	2.36E-08	2.68E-01	5.23E-04	6.09E+00
4.26E-04	8.56E-08	9.10E+00	8.67E-11	1.80E-08	1.94E-01	2.35E-04	6.18E+00
3.74E-04	7.34E-08	9.07E+00	5.69E-11	1.39E-08	1.47E-01	1.71E-04	6.23E+00
3.06E-04	6.39E-08	9.05E+00	3.80E-11	1.08E-08	1.16E-01	1.41E-04	6.27E+00
2.49E-04	5.65E-08	9.03E+00	2.57E-11	8.53E-09	9.60E-02	1.21E-04	6.29E+00
2.04E-04	5.07E-08	9.02E+00	1.75E-11	6.82E-09	8.17E-02	1.07E-04	6.31E+00
1.68E-04	4.60E-08	9.02E+00	1.21E-11	5.52E-09	7.15E-02	9.57E-05	6.32E+00
1.39E-04	4.23E-08	9.01E+00	8.38E-12	4.52E-09	6.39E-02	8.71E-05	6.33E+00
1.15E-04	3.94E-08	9.01E+00	5.88E-12	3.74E-09	5.83E-02	8.04E-05	6.34E+00
1.15E-04	3.94E-08	4.13E+01	5.88E-12	3.74E-09	5.83E-02	8.04E-05	6.34E+00
1.66E-05	4.75E-07	4.13E+01	1.45E-13	2.99E-10	5.82E-02	7.26E-05	6.34E+00
2.72E-06	1.06E-06	4.13E+01	4.82E-14	3.10E-10	5.82E-02	7.22E-05	6.34E+00
4.19E-07	2.36E-06	4.13E+01	1.58E-14	3.10E-10	5.82E-02	7.20E-05	6.34E+00
3.63E-07	3.60E-06	4.13E+01	1.72E-14	3.12E-10	5.82E-02	7.19E-05	6.34E+00
3.53E-07	4.76E-06	4.13E+01	1.00E-25	3.52E-10	5.82E-02	7.18E-05	6.34E+00
3.45E-07	5.85E-06	4.13E+01	3.18E-14	3.07E-10	5.82E-02	7.17E-05	6.34E+00
3.27E-07	8.30E-06	4.13E+01	4.26E-14	3.04E-10	5.82E-02	7.17E-05	6.34E+00
3.10E-07	1.04E-05	4.13E+01	5.08E-14	3.01E-10	5.82E-02	7.18E-05	6.34E+00
2.81E-07	1.40E-05	4.13E+01	6.20E-14	2.95E-10	5.82E-02	7.24E-05	6.34E+00
2.55E-07	1.70E-05	4.13E+01	6.87E-14	2.90E-10	5.82E-02	7.32E-05	6.34E+00
2.33E-07	1.97E-05	4.13E+01	7.26E-14	2.85E-10	5.82E-02	7.41E-05	6.34E+00
2.13E-07	2.21E-05	4.13E+01	7.48E-14	2.79E-10	5.82E-02	7.52E-05	6.34E+00
1.95E-07	2.43E-05	4.13E+01	7.57E-14	2.75E-10	5.82E-02	7.63E-05	6.34E+00
1.79E-07	2.64E-05	4.13E+01	7.58E-14	2.70E-10	5.82E-02	7.75E-05	6.34E+00
1.64E-07	2.85E-05	4.13E+01	7.52E-14	2.65E-10	5.82E-02	7.87E-05	6.34E+00

CH	C2	C	garb	tar	char	H2O(LIQ)	C2H2
1.00E-25	1.00E-25	1.00E-25	1.80E-01	1.00E-25	1.00E-25	2.52E+00	1.00E-25
7.66E-20	1.02E-13	2.97E-24	1.80E-01	1.88E-05	9.77E-10	2.28E+00	1.76E-03
5.77E-19	8.36E-13	4.90E-23	1.80E-01	3.78E-05	3.97E-09	2.06E+00	3.47E-03
4.03E-18	7.02E-12	8.17E-22	1.80E-01	7.69E-05	1.64E-08	1.69E+00	6.71E-03
1.20E-17	2.49E-11	4.20E-21	1.80E-01	1.17E-04	3.82E-08	1.38E+00	9.73E-03
2.53E-17	6.20E-11	1.32E-20	1.80E-01	1.59E-04	7.02E-08	1.13E+00	1.25E-02
4.45E-17	1.27E-10	3.19E-20	1.80E-01	2.02E-04	1.13E-07	9.27E-01	1.50E-02
1.20E-16	4.86E-10	1.49E-19	1.80E-01	3.15E-04	2.77E-07	5.62E-01	1.99E-02
2.38E-16	1.30E-09	4.43E-19	1.80E-01	4.38E-04	5.34E-07	3.41E-01	2.28E-02
5.38E-16	5.64E-09	2.04E-18	1.79E-01	7.13E-04	1.42E-06	1.25E-01	2.26E-02
6.83E-16	1.71E-08	6.88E-18	1.79E-01	1.03E-03	2.97E-06	4.62E-02	1.66E-02
5.23E-16	4.28E-08	2.07E-17	1.79E-01	1.40E-03	5.46E-06	1.70E-02	9.42E-03
3.02E-16	9.44E-08	5.87E-17	1.78E-01	1.81E-03	9.24E-06	6.24E-03	4.52E-03
1.87E-16	1.91E-07	1.58E-16	1.78E-01	2.29E-03	1.48E-05	2.30E-03	2.19E-03
1.42E-16	3.61E-07	4.03E-16	1.77E-01	2.83E-03	2.25E-05	8.46E-04	1.16E-03
1.32E-16	6.48E-07	9.71E-16	1.77E-01	3.43E-03	3.33E-05	3.11E-04	6.48E-04
1.29E-16	1.12E-06	2.22E-15	1.76E-01	4.10E-03	4.77E-05	1.14E-04	3.76E-04
1.71E-16	3.00E-06	1.02E-14	1.74E-01	5.66E-03	9.19E-05	1.55E-05	1.38E-04
4.04E-16	1.08E-05	7.54E-14	1.71E-01	8.57E-03	2.15E-04	7.69E-07	3.94E-05
2.12E-15	6.21E-05	1.17E-12	1.64E-01	1.49E-02	6.79E-04	5.06E-09	1.35E-05
2.83E-14	7.14E-04	5.94E-11	1.45E-01	3.15E-02	3.42E-03	1.81E-13	1.05E-05
2.03E-13	2.72E-03	8.67E-10	1.22E-01	4.77E-02	9.36E-03	7.37E-18	9.80E-06
6.19E-13	3.80E-03	3.16E-09	9.91E-02	5.92E-02	1.77E-02	1.27E-21	8.83E-06
9.74E-13	4.06E-03	5.56E-09	7.96E-02	6.49E-02	2.65E-02	2.65E-25	7.81E-06
1.27E-12	4.10E-03	7.99E-09	6.36E-02	6.62E-02	3.44E-02	1.00E-25	6.73E-06
1.49E-12	3.99E-03	1.01E-08	5.08E-02	6.43E-02	4.06E-02	1.00E-25	5.73E-06
1.71E-12	3.68E-03	1.31E-08	3.27E-02	5.58E-02	4.76E-02	1.00E-25	4.13E-06
1.58E-12	3.21E-03	1.45E-08	1.73E-02	4.05E-02	4.75E-02	1.00E-25	2.64E-06
1.20E-12	2.73E-03	1.35E-08	9.48E-03	2.79E-02	4.11E-02	1.00E-25	1.78E-06
7.17E-13	2.14E-03	1.06E-08	4.46E-03	1.65E-02	3.05E-02	1.00E-25	1.13E-06
4.00E-13	1.61E-03	7.62E-09	2.21E-03	9.74E-03	2.14E-02	1.00E-25	7.60E-07
2.19E-13	1.18E-03	5.19E-09	1.15E-03	5.82E-03	1.47E-02	1.00E-25	5.34E-07
2.19E-13	1.18E-03	5.19E-09	1.15E-03	5.82E-03	1.47E-02	1.00E-25	5.34E-07
6.68E-14	1.80E-03	9.65E-10	1.13E-03	5.73E-03	1.45E-02	1.00E-25	4.36E-07
7.63E-14	2.39E-03	1.43E-09	1.11E-03	5.64E-03	1.44E-02	1.00E-25	4.40E-07
1.02E-13	3.35E-03	2.62E-09	1.06E-03	5.43E-03	1.39E-02	1.00E-25	4.39E-07
1.32E-13	3.88E-03	3.99E-09	1.00E-03	5.19E-03	1.35E-02	1.00E-25	4.28E-07
1.60E-13	3.92E-03	5.19E-09	9.41E-04	4.94E-03	1.30E-02	1.00E-25	4.10E-07
1.84E-13	3.62E-03	5.96E-09	8.82E-04	4.69E-03	1.25E-02	1.00E-25	3.86E-07
2.17E-13	2.47E-03	6.16E-09	7.39E-04	4.06E-03	1.12E-02	1.00E-25	3.15E-07
2.20E-13	1.66E-03	5.56E-09	6.13E-04	3.48E-03	9.89E-03	1.00E-25	2.43E-07
1.99E-13	7.91E-04	4.27E-09	4.21E-04	2.55E-03	7.72E-03	1.00E-25	1.36E-07
1.91E-13	3.46E-04	3.15E-09	2.94E-04	1.88E-03	6.05E-03	1.00E-25	7.29E-08
2.07E-13	1.26E-04	2.29E-09	2.10E-04	1.42E-03	4.79E-03	1.00E-25	3.59E-08
2.01E-13	4.59E-05	1.68E-09	1.54E-04	1.09E-03	3.84E-03	1.00E-25	1.58E-08
1.42E-13	2.68E-05	1.25E-09	1.15E-04	8.46E-04	3.11E-03	1.00E-25	8.74E-09
8.67E-14	2.31E-05	9.51E-10	8.80E-05	6.71E-04	2.56E-03	1.00E-25	6.48E-09
5.29E-14	2.16E-05	7.31E-10	6.86E-05	5.40E-04	2.12E-03	1.00E-25	5.23E-09
3.32E-14	2.06E-05	5.69E-10	5.44E-05	4.41E-04	1.79E-03	1.00E-25	4.39E-09
2.13E-14	1.98E-05	4.47E-10	4.39E-05	3.65E-04	1.52E-03	1.00E-25	3.76E-09
1.40E-14	1.90E-05	3.55E-10	3.60E-05	3.06E-04	1.30E-03	1.00E-25	3.27E-09
9.32E-15	1.85E-05	2.85E-10	2.99E-05	2.60E-04	1.13E-03	1.00E-25	3.01E-09
6.29E-15	1.80E-05	2.30E-10	2.52E-05	2.23E-04	9.91E-04	1.00E-25	2.60E-09
6.29E-15	1.80E-05	2.30E-10	2.52E-05	2.23E-04	9.91E-04	1.00E-25	2.60E-09
1.59E-17	1.08E-05	4.33E-12	2.51E-05	2.23E-04	9.91E-04	1.00E-25	4.63E-13
5.15E-19	1.08E-05	7.21E-13	2.51E-05	2.23E-04	9.90E-04	1.00E-25	2.30E-12
7.38E-19	1.25E-05	1.27E-13	2.51E-05	2.23E-04	9.90E-04	1.00E-25	8.36E-12
1.00E-25	1.43E-05	1.73E-13	2.51E-05	2.23E-04	9.89E-04	1.00E-25	1.42E-11
1.00E-25	1.61E-05	9.31E-13	2.51E-05	2.23E-04	9.89E-04	1.00E-25	1.79E-11
1.00E-25	1.78E-05	1.49E-13	2.51E-05	2.23E-04	9.88E-04	1.00E-25	2.02E-11
3.12E-19	2.20E-05	1.74E-13	2.50E-05	2.22E-04	9.87E-04	1.00E-25	2.27E-11
3.06E-19	2.61E-05	1.96E-13	2.50E-05	2.22E-04	9.86E-04	1.00E-25	2.30E-11
2.97E-19	3.37E-05	2.29E-13	2.49E-05	2.21E-04	9.84E-04	1.00E-25	2.16E-11
2.77E-19	4.07E-05	2.51E-13	2.49E-05	2.21E-04	9.82E-04	1.00E-25	2.01E-11
2.62E-19	4.72E-05	2.66E-13	2.48E-05	2.20E-04	9.80E-04	1.00E-25	1.82E-11
2.49E-19	5.32E-05	2.74E-13	2.47E-05	2.20E-04	9.78E-04	1.00E-25	1.64E-11
2.32E-19	5.89E-05	2.78E-13	2.47E-05	2.19E-04	9.76E-04	1.00E-25	1.48E-11
2.19E-19	6.41E-05	2.78E-13	2.46E-05	2.19E-04	9.74E-04	1.00E-25	1.34E-11
2.06E-19	6.91E-05	2.74E-13	2.46E-05	2.19E-04	9.73E-04	1.00E-25	1.20E-11

C2H	PVC	HC1	POLYSTYRN	STYRENE	C6H6	PHENOL	FURAN
1.00E-25	1.46E-02	1.00E-25	8.72E-02	1.00E-25	1.00E-25	1.00E-25	1.00E-25
1.55E-14	1.45E-02	1.43E-04	8.56E-02	7.73E-09	1.63E-03	6.00E-15	1.00E-25
5.80E-14	1.43E-02	2.85E-04	8.40E-02	7.52E-09	3.24E-03	4.67E-14	1.00E-25
2.05E-13	1.41E-02	5.68E-04	8.08E-02	7.11E-09	6.39E-03	3.49E-13	1.00E-25
4.20E-13	1.38E-02	8.49E-04	7.78E-02	6.73E-09	9.46E-03	1.12E-12	1.00E-25
7.01E-13	1.35E-02	1.13E-03	7.48E-02	6.36E-09	1.24E-02	2.58E-12	1.00E-25
1.06E-12	1.32E-02	1.40E-03	7.19E-02	6.01E-09	1.54E-02	5.00E-12	1.00E-25
2.42E-12	1.25E-02	2.09E-03	6.50E-02	5.22E-09	2.22E-02	1.80E-11	1.00E-25
4.68E-12	1.19E-02	2.75E-03	5.86E-02	4.52E-09	2.86E-02	4.99E-11	1.00E-25
1.13E-11	1.06E-02	4.04E-03	4.72E-02	3.38E-09	4.00E-02	2.55E-10	2.75E-24
1.45E-11	9.39E-03	5.25E-03	3.77E-02	2.51E-09	4.95E-02	8.51E-10	4.46E-23
1.00E-11	8.26E-03	6.37E-03	2.97E-02	1.85E-09	5.75E-02	1.97E-09	3.56E-22
4.78E-12	7.22E-03	7.41E-03	2.32E-02	1.35E-09	6.40E-02	3.47E-09	1.63E-21
2.28E-12	6.27E-03	8.36E-03	1.79E-02	9.85E-10	6.93E-02	5.21E-09	5.14E-21
1.29E-12	5.41E-03	9.22E-03	1.37E-02	7.12E-10	7.35E-02	7.28E-09	1.29E-20
8.29E-13	4.64E-03	9.99E-03	1.04E-02	5.11E-10	7.68E-02	9.89E-09	2.87E-20
5.76E-13	3.95E-03	1.07E-02	7.81E-03	3.65E-10	7.94E-02	1.33E-08	5.95E-20
3.23E-13	2.82E-03	1.18E-02	4.28E-03	1.83E-10	8.28E-02	2.38E-08	2.30E-19
1.83E-13	1.63E-03	1.30E-02	1.63E-03	6.19E-11	8.53E-02	5.72E-08	1.60E-18
1.73E-13	5.90E-04	1.40E-02	2.80E-04	9.20E-12	8.58E-02	2.22E-07	3.28E-17
6.43E-13	5.87E-05	1.46E-02	5.52E-06	1.52E-13	8.16E-02	1.78E-06	3.74E-15
2.27E-12	4.66E-06	1.46E-02	7.87E-08	2.00E-15	7.30E-02	8.09E-06	1.12E-14
4.22E-12	3.31E-07	1.46E-02	9.68E-10	2.38E-17	6.24E-02	2.31E-05	1.12E-14
4.84E-12	2.26E-08	1.46E-02	1.16E-11	2.82E-19	5.19E-02	3.92E-05	6.6E-15
4.97E-12	1.67E-09	1.46E-02	3.31E-13	8.02E-21	4.29E-02	5.25E-05	1.7E-15
4.85E-12	1.56E-10	1.46E-02	8.81E-15	1.60E-22	3.54E-02	6.25E-05	3.54E-11
4.25E-12	7.59E-13	1.46E-02	5.20E-18	1.00E-25	2.44E-02	7.51E-05	8.53E-11
3.13E-12	1.00E-25	1.46E-02	1.38E-20	7.10E-25	1.47E-02	8.21E-05	1.80E-10
2.15E-12	1.00E-25	1.46E-02	3.32E-25	1.00E-25	9.32E-03	8.19E-05	2.5E-10
1.27E-12	1.00E-25	1.46E-02	1.00E-25	1.00E-25	5.52E-03	7.78E-05	4.1E-10
7.57E-13	1.00E-25	1.46E-02	1.00E-25	1.00E-25	3.53E-03	7.30E-05	5.1E-10
4.63E-13	1.00E-25	1.46E-02	1.00E-25	1.00E-25	2.42E-03	6.90E-05	5.1E-10
4.63E-13	1.00E-25	1.46E-02	1.00E-25	1.00E-25	2.42E-03	6.90E-05	5.1E-10
2.09E-13	1.00E-25	1.46E-02	1.00E-25	1.00E-25	2.39E-03	6.87E-05	5.1E-10
2.31E-13	1.00E-25	1.46E-02	1.00E-25	1.00E-25	2.35E-03	6.84E-05	5.1E-10
2.88E-13	1.00E-25	1.46E-02	1.00E-25	1.00E-25	2.25E-03	6.73E-05	6.00E-10
3.48E-13	1.00E-25	1.46E-02	1.00E-25	1.00E-25	2.12E-03	6.55E-05	6.03E-10
3.97E-13	1.00E-25	1.46E-02	1.00E-25	1.00E-25	1.97E-03	6.30E-05	6.05E-10
4.30E-13	1.00E-25	1.46E-02	1.00E-25	1.00E-25	1.81E-03	5.98E-05	6.08E-10
4.38E-13	1.00E-25	1.46E-02	1.00E-25	1.00E-25	1.41E-03	5.01E-05	6.13E-10
3.88E-13	1.00E-25	1.46E-02	1.00E-25	1.00E-25	1.06E-03	4.02E-05	6.16E-10
2.72E-13	1.00E-25	1.46E-02	1.00E-25	1.00E-25	6.01E-04	2.57E-05	6.20E-10
2.00E-13	1.00E-25	1.46E-02	1.00E-25	1.00E-25	3.58E-04	1.77E-05	6.21E-10
1.51E-13	1.00E-25	1.46E-02	1.00E-25	1.00E-25	2.28E-04	1.32E-05	6.22E-10
9.56E-14	1.00E-25	1.46E-02	1.00E-25	1.00E-25	1.54E-04	1.06E-05	6.23E-10
5.62E-14	1.00E-25	1.46E-02	1.00E-25	1.00E-25	1.11E-04	9.02E-06	6.23E-10
3.54E-14	1.00E-25	1.46E-02	1.00E-25	1.00E-25	8.34E-05	7.94E-06	6.23E-10
2.32E-14	1.00E-25	1.46E-02	1.00E-25	1.00E-25	6.54E-05	7.20E-06	6.23E-10
1.58E-14	1.00E-25	1.46E-02	1.00E-25	1.00E-25	5.32E-05	6.69E-06	6.23E-10
1.10E-14	1.00E-25	1.46E-02	1.00E-25	1.00E-25	4.47E-05	6.33E-06	6.23E-10
7.89E-15	1.00E-25	1.46E-02	1.00E-25	1.00E-25	3.85E-05	6.07E-06	6.23E-10
5.69E-15	1.00E-25	1.46E-02	1.00E-25	1.00E-25	3.39E-05	5.88E-06	6.24E-10
4.30E-15	1.00E-25	1.46E-02	1.00E-25	1.00E-25	3.05E-05	5.74E-06	6.24E-10
4.30E-15	1.00E-25	1.46E-02	1.00E-25	1.00E-25	3.05E-05	5.74E-06	6.24E-10
7.18E-20	1.00E-25	1.46E-02	1.00E-25	1.00E-25	3.05E-05	5.74E-06	6.24E-10
1.00E-25	1.00E-25	1.46E-02	1.00E-25	1.00E-25	3.05E-05	5.74E-06	6.24E-10
1.00E-25	1.00E-25	1.46E-02	1.00E-25	1.00E-25	3.05E-05	5.74E-06	6.24E-10
1.20E-17	1.00E-25	1.46E-02	1.00E-25	1.00E-25	3.05E-05	5.74E-06	6.24E-10
2.01E-16	1.00E-25	1.46E-02	1.00E-25	1.00E-25	3.05E-05	5.74E-06	6.24E-10
4.04E-20	1.00E-25	1.46E-02	1.00E-25	1.00E-25	3.05E-05	5.74E-06	6.24E-10
1.48E-20	1.00E-25	1.46E-02	1.00E-25	1.00E-25	3.05E-05	5.74E-06	6.24E-10
1.48E-20	1.00E-25	1.46E-02	1.00E-25	1.00E-25	3.05E-05	5.74E-06	6.24E-10
1.34E-20	1.00E-25	1.46E-02	1.00E-25	1.00E-25	3.05E-05	5.74E-06	6.24E-10
1.21E-20	1.00E-25	1.46E-02	1.00E-25	1.00E-25	3.05E-05	5.74E-06	6.24E-10
1.05E-20	1.00E-25	1.46E-02	1.00E-25	1.00E-25	3.05E-05	5.74E-06	6.24E-10
9.02E-21	1.00E-25	1.46E-02	1.00E-25	1.00E-25	3.05E-05	5.74E-06	6.24E-10
7.85E-21	1.00E-25	1.46E-02	1.00E-25	1.00E-25	3.05E-05	5.74E-06	6.24E-10
6.71E-21	1.00E-25	1.46E-02	1.00E-25	1.00E-25	3.05E-05	5.74E-06	6.24E-10
5.73E-21	1.00E-25	1.46E-02	1.00E-25	1.00E-25	3.05E-05	5.74E-06	6.24E-10

DIOXIN	C12	C6H5Cl	C1PH	C1FR	C1DX	N2	H
1.00E-25	1.00E-25	1.00E-25	1.00E-25	1.00E-25	1.00E-25	3.30E+01	1.00E-25
1.00E-25	5.63E-18	1.00E-25	1.00E-25	1.00E-25	1.00E-25	3.30E+01	5.10E-11
1.00E-25	8.91E-17	1.06E-25	1.00E-25	1.00E-25	1.00E-25	3.30E+01	1.07E-10
1.00E-25	1.40E-15	6.57E-24	1.00E-25	1.00E-25	1.00E-25	3.30E+01	2.32E-10
1.00E-25	6.83E-15	7.25E-23	1.00E-25	1.00E-25	1.00E-25	3.30E+01	3.78E-10
1.00E-25	2.06E-14	3.96E-22	1.00E-25	1.00E-25	1.00E-25	3.30E+01	5.44E-10
1.00E-25	4.77E-14	1.46E-21	1.00E-25	1.00E-25	1.00E-25	3.30E+01	7.30E-10
1.00E-25	2.04E-13	1.48E-20	1.00E-25	1.00E-25	1.00E-25	3.30E+01	1.28E-09
1.00E-25	5.34E-13	7.27E-20	1.00E-25	1.00E-25	1.00E-25	3.30E+01	1.92E-09
1.02E-24	1.89E-12	6.26E-19	4.20E-25	1.00E-25	1.00E-25	3.30E+01	3.21E-09
1.65E-23	4.50E-12	2.76E-18	4.88E-24	1.00E-25	1.00E-25	3.30E+01	3.86E-09
1.32E-22	8.99E-12	8.67E-18	3.18E-23	1.00E-25	1.00E-25	3.30E+01	3.46E-09
6.05E-22	1.65E-11	2.26E-17	1.40E-22	1.00E-25	1.00E-25	3.30E+01	2.57E-09
1.90E-21	2.90E-11	5.21E-17	4.73E-22	1.00E-25	1.00E-25	3.30E+01	1.87E-09
4.79E-21	4.89E-11	1.11E-16	1.36E-21	1.00E-25	1.00E-25	3.30E+01	1.46E-09
1.06E-20	7.98E-11	2.21E-16	3.51E-21	1.00E-25	1.00E-25	3.30E+01	1.17E-09
2.20E-20	1.26E-10	4.16E-16	8.49E-21	1.00E-25	1.00E-25	3.30E+01	9.59E-10
8.53E-20	2.84E-10	1.29E-15	4.30E-20	1.00E-25	1.00E-25	3.30E+01	6.54E-10
5.93E-19	7.97E-10	5.31E-15	3.80E-19	1.00E-25	1.00E-25	3.30E+01	4.13E-10
1.21E-17	3.02E-09	3.31E-14	8.32E-18	1.00E-25	1.00E-25	3.30E+01	3.91E-10
1.38E-15	1.88E-08	3.91E-13	7.68E-16	2.57E-23	9.53E-24	3.30E+01	1.09E-09
4.14E-14	7.46E-08	2.05E-12	1.95E-14	4.35E-21	1.61E-21	3.30E+01	2.72E-09
5.15E-13	2.37E-07	7.42E-12	2.47E-13	2.38E-19	8.82E-20	3.30E+01	6.40E-09
2.47E-12	5.15E-07	1.91E-11	1.39E-12	3.78E-18	1.40E-18	3.30E+01	9.48E-09
6.64E-12	8.97E-07	3.75E-11	4.53E-12	2.48E-17	9.17E-18	3.30E+01	1.12E-08
1.31E-11	1.37E-06	6.19E-11	1.08E-11	9.81E-17	3.63E-17	3.30E+01	1.19E-08
3.16E-11	2.54E-06	1.24E-10	3.64E-11	6.66E-16	2.47E-16	3.30E+01	1.14E-08
6.68E-11	4.58E-06	2.30E-10	1.14E-10	4.04E-15	1.50E-15	3.30E+01	9.31E-09
1.04E-10	6.65E-06	3.32E-10	2.38E-10	1.30E-14	4.81E-15	3.30E+01	7.24E-09
1.49E-10	9.23E-06	4.47E-10	4.59E-10	3.72E-14	1.38E-14	3.30E+01	5.03E-09
1.87E-10	1.15E-05	5.37E-10	7.22E-10	7.77E-14	2.88E-14	3.30E+01	3.45E-09
2.20E-10	1.35E-05	6.06E-10	1.01E-09	1.35E-13	5.00E-14	3.30E+01	2.38E-09
2.20E-10	1.35E-05	6.06E-10	1.01E-09	1.35E-13	5.00E-14	6.60E+01	2.38E-09
2.21E-10	1.35E-05	6.07E-10	1.02E-09	1.36E-13	5.04E-14	6.60E+01	2.03E-09
2.21E-10	1.35E-05	6.08E-10	1.02E-09	1.37E-13	5.07E-14	6.60E+01	2.60E-09
2.22E-10	1.36E-05	6.10E-10	1.03E-09	1.39E-13	5.15E-14	6.60E+01	4.32E-09
2.23E-10	1.36E-05	6.12E-10	1.04E-09	1.41E-13	5.23E-14	6.60E+01	6.77E-09
2.24E-10	1.36E-05	6.14E-10	1.05E-09	1.44E-13	5.32E-14	6.60E+01	9.72E-09
2.25E-10	1.36E-05	6.15E-10	1.06E-09	1.46E-13	5.41E-14	6.60E+01	1.27E-08
2.27E-10	1.37E-05	6.19E-10	1.08E-09	1.53E-13	5.65E-14	6.60E+01	1.80E-08
2.28E-10	1.38E-05	6.22E-10	1.10E-09	1.59E-13	5.90E-14	6.60E+01	1.90E-08
2.30E-10	1.42E-05	6.26E-10	1.13E-09	1.73E-13	6.40E-14	6.60E+01	1.43E-08
2.30E-10	1.47E-05	6.29E-10	1.15E-09	1.87E-13	6.91E-14	6.60E+01	8.95E-09
2.30E-10	1.57E-05	6.30E-10	1.16E-09	2.01E-13	7.44E-14	6.60E+01	5.15E-09
2.31E-10	1.78E-05	6.31E-10	1.17E-09	2.16E-13	8.00E-14	6.60E+01	2.74E-09
2.31E-10	2.12E-05	6.32E-10	1.18E-09	2.33E-13	8.63E-14	6.60E+01	1.51E-09
2.31E-10	2.47E-05	6.33E-10	1.19E-09	2.53E-13	9.36E-14	6.60E+01	9.49E-10
2.31E-10	2.78E-05	6.34E-10	1.20E-09	2.75E-13	1.02E-13	6.60E+01	6.35E-10
2.31E-10	3.03E-05	6.34E-10	1.22E-09	2.98E-13	1.10E-13	6.60E+01	4.40E-10
2.31E-10	3.24E-05	6.34E-10	1.23E-09	3.23E-13	1.20E-13	6.60E+01	3.14E-10
2.31E-10	3.42E-05	6.35E-10	1.24E-09	3.48E-13	1.29E-13	6.60E+01	2.29E-10
2.31E-10	3.56E-05	6.35E-10	1.24E-09	3.74E-13	1.38E-13	6.60E+01	1.70E-10
2.31E-10	3.69E-05	6.36E-10	1.25E-09	3.99E-13	1.48E-13	6.60E+01	1.29E-10
2.31E-10	3.69E-05	6.36E-10	1.25E-09	3.99E-13	1.48E-13	1.88E+02	1.29E-10
2.31E-10	3.69E-05	6.36E-10	1.25E-09	4.00E-13	1.48E-13	1.88E+02	1.52E-12
2.31E-10	3.69E-05	6.36E-10	1.25E-09	4.00E-13	1.48E-13	1.88E+02	2.47E-13
2.31E-10	3.69E-05	6.36E-10	1.25E-09	4.00E-13	1.48E-13	1.88E+02	3.42E-14
2.31E-10	3.69E-05	6.36E-10	1.25E-09	4.00E-13	1.48E-13	1.88E+02	2.99E-14
2.31E-10	3.69E-05	6.36E-10	1.25E-09	4.00E-13	1.48E-13	1.88E+02	3.46E-14
2.31E-10	3.69E-05	6.36E-10	1.25E-09	4.00E-13	1.48E-13	1.88E+02	2.93E-14
2.31E-10	3.69E-05	6.36E-10	1.25E-09	4.01E-13	1.48E-13	1.88E+02	2.89E-14
2.31E-10	3.69E-05	6.36E-10	1.25E-09	4.01E-13	1.48E-13	1.88E+02	2.83E-14
2.31E-10	3.69E-05	6.36E-10	1.25E-09	4.02E-13	1.49E-13	1.88E+02	2.71E-14
2.31E-10	3.69E-05	6.36E-10	1.26E-09	4.02E-13	1.49E-13	1.88E+02	2.57E-14
2.31E-10	3.69E-05	6.36E-10	1.26E-09	4.03E-13	1.49E-13	1.88E+02	2.43E-14
2.31E-10	3.69E-05	6.36E-10	1.26E-09	4.03E-13	1.49E-13	1.88E+02	2.29E-14
2.31E-10	3.69E-05	6.36E-10	1.26E-09	4.04E-13	1.50E-13	1.88E+02	2.15E-14
2.31E-10	3.69E-05	6.36E-10	1.26E-09	4.04E-13	1.50E-13	1.88E+02	2.01E-14
2.31E-10	3.69E-05	6.36E-10	1.26E-09	4.05E-13	1.50E-13	1.88E+02	1.89E-14

APPENDIX I  
ADDITIONAL DETAILS ON THE CONTROL SYSTEM

On/Off Control Circuits

The computer's parallel printer port provides eight 0- to 3.3-volt data and four 0- to 5-volt control digital (on/off) output signals, as well as five 0- to 5-volt status digital input signals. The parallel port is used instead of the digital signals from the QuaTech I/O board so as not to disturb the previously existing circuitry used to read the status of the burners, feeders, and stoker. Since that status of the parallel port lines is unknown when the computer is powered up, the 12-volt supply line is disconnected via the double-pole, double-throw (DPDT) switch until the control computer program is running. Relays with 5- and 12-volt DC coils and contacts rated at 125 VAC, 1-10 amps are used to turn on and off the 110-VAC power lines (see Figure 7-1 in Chapter 7). Switching (2N2222-type) NPN transistors provide the necessary current to drive each relay. The 2200-, 3160-, and 3300-ohm resistors between the parallel port on the transistors limit the current drawn from the parallel port. When a signal from the parallel port line is off of low (0 volts), its transistor does not allow current to flow through its relay. When the signal is on or high (3.3 volts), the transistor allows current to flow through the

relay, which causes the relays normally open contacts to close. The computer's own power supply is tapped to provide the 5 and 12 volts DC needed for the relays and support circuitry. A connector installed on the tapped computer power supply line and a standard parallel port connector allow the computer to be removed from the instrument trailer for office use with out disturbing the control circuitry.

#### Ram Timer Circuit

The ram feed subsystem requires its 110-VAC signal to be held on for about 30 seconds before the signal is latched allowing the ram feeder to finish its cycle without further signals. The control computer program can accomplish this by using the above described circuitry to turn on the 110-VAC ram feed signal, wait 30 seconds, and then turn it off. This method, however, would tie up the computer for too long. A software timer could be set up when the computer program turns on the ram feed signal. The program would then continue its control operations until it is interrupted by timer when it elapses, at which point the program would turn off the signal. The interruption, though brief, may interfere with control operations. To take this burden off the software, a timer circuit was built to create the necessary 30-second signal. One-half of a 556 dual timer integrated circuit (IC) chip was regulated by a 470 kilo-ohm (R) resistor and a 47 microfarad (C) capacitor. The on-time for this circuit is given by  $1.26 RC$ , or 29.6 seconds in this

case. The computer's power supply again supplied the necessary 12 volts DC needed. The 556 chip provides up to 200 ma of current so no current amplifying transistor is needed to drive the relay. The 0- to 5-volt strobe line from the computer's parallel port provided the trigger for the timer chip. The strobe line is normally at 5 volts when off or low. When the strobe line is dropped briefly to 0 volts (when on or high), the timer is triggered. The 0- to 5-volt parallel port strobe line is used here instead of a 0- to 3.3-volt line since the timer starts when the voltage on its trigger pin falls below one-third of its supply voltage, which in this case produces a 4-volt trigger level.

In test operation, this circuit was being falsely triggered when one or two other relays were being turned off after being turned on. A 2200-ohm resistor and NPN switching type transistor was installed between the strobe line and trigger pin of the timer chip to isolate the timer from the rest of the circuitry on the board. The transistors collector was tied to 12 volts, the base was connected to the resistor opposite the strobe line, and the emitter was connected to the 556's trigger pin. This modification cured the false triggering during test operation.

When the board was actually installed in the instrument trailer and connected to the AC lines being controlled, the false triggering problem recurred. Since the problem may lay inside the parallel port itself, the timer circuit was replaced by the same type of transistor and relay circuit

used for the simple on/off control lines. This circuit requires the normal off condition of the parallel port line to be 0 volts. Since the strobe line when off is 5 volts, the connection to the parallel port was switched to the data bit 7 line. When a ram feed is now needed by the control system, the program will turn on the ram feed trigger line, leave it on for three 15-second cycles, and turn it off. The computer does not have to actually wait the 45 seconds. A cycle counter in the control program keeps track of when to turn off the ram feed timer. This counter is also used for other control purposes. Remnants of the timer circuit--the 470-kilo-ohm resistor, the 47 microfarad capacitor, and the 14-pin socket--are shown in Figure 7-1 in Chapter 7.

#### Alarm Timer

When the alarm circuit is energized, the 47 microfarad capacitor is slowly charged (see Figure 7-1 in Chapter 7). When the voltage across the capacitor reaches 7.1 volts after 30 seconds the 4050 non-inverting buffer/driver triggers a Darlington TIP120 NPN transistor that causes the 12-volt alarm relay to be energized. A positive 3.3-volt pulse from the parallel port will trigger another transistor that allows the capacitor to discharge through a 2200-ohm resistor in less than 0.25 seconds. The discharging of the capacitor resets the timer circuit. Under normal operations the control program will send out a pulse to reset the timer once every data gathering cycle, i.e., about every 15 seconds. If

the control program or the computer itself stops running, this timer will not be reset and after 30 seconds the timer will energize the alarm relay. The alarm relay then powers visible (a light) and audible (a bell) warnings to alert the operator(s), and turns off the override relay(s), allowing the incinerator to run under more or less original conditions of temperature-controlled, approximately half-open gas valves. The operator(s) can then determine the problem and restart the computer system. The 12-volt power supply for this timer comes from a separate power supply (see Figure I-1) located in the upper right incinerator control panel, instead of from the computer. The 12-volt line for the computer would be off if the computer shuts down. The light used for the alarm is on the incinerator upper right control panel's door. It was originally used to indicate when the lower burner was lit, but had been cut out of that circuit some time ago. Also there already exist lights in the lower right control panel to indicate when the burners on are. The alarm bell is an old telephone ringer. It is mounted inside the control panel on the same door that the alarm light is on. It is still audible even with the noise of all the blowers and burners. The very loud air horn on top of the same control panel could have been used, but it is tied in with the flame safety control that detects when there is a fire inside the ram feed system. Activating the air horn also starts the ram feeder, which would push the burning mass into the incinerator.

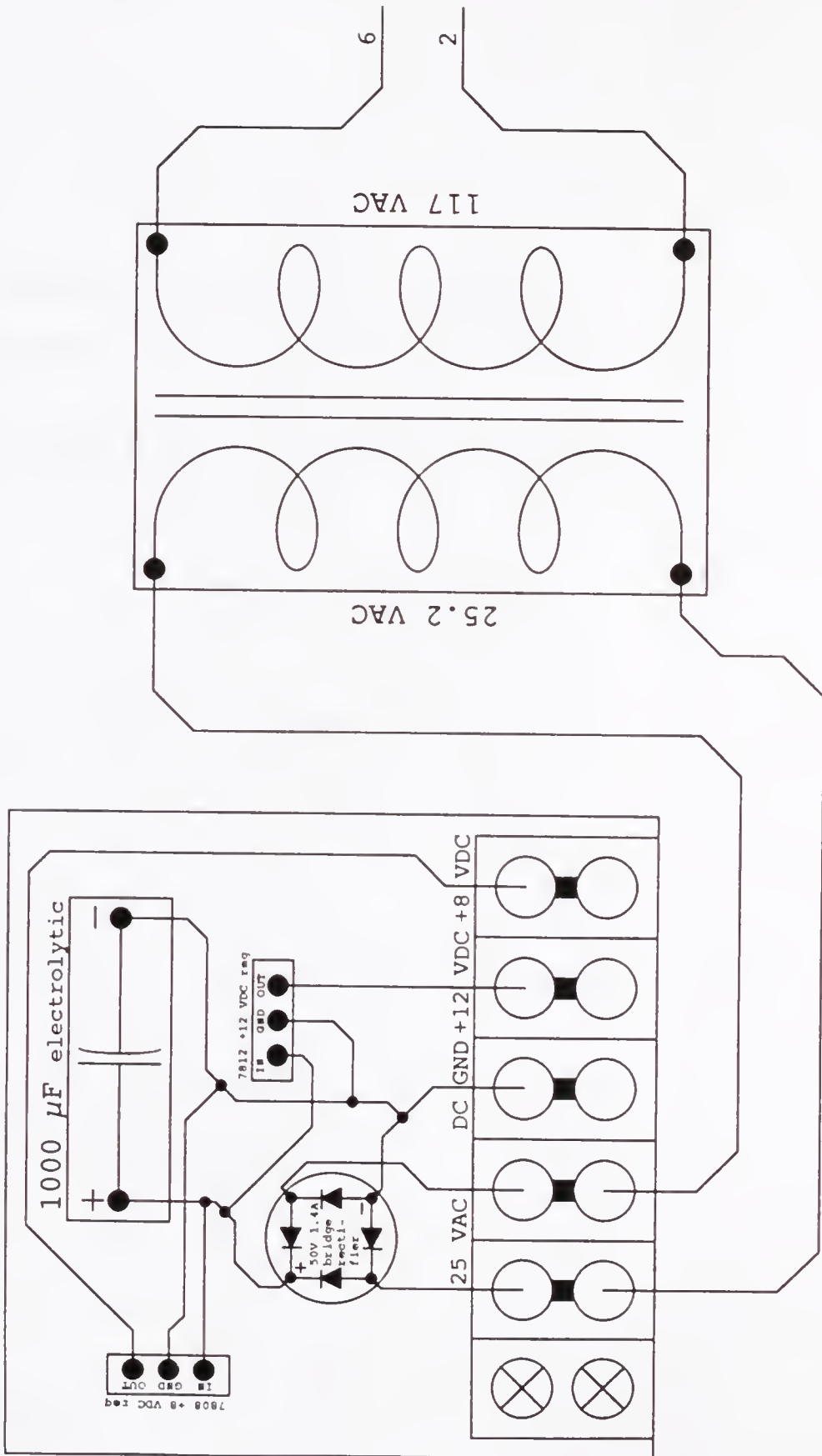


Figure I-1. Power supply board with transformer.

### Modmotor Modifications

The shaft position of a normal modmotor (see Figure I-2) is set by connecting a 200-ohm, 10-watt potentiometer (pot) (the set pot) across three terminals (W, R, and B) in the top of the modmotor. The shaft drives the wiper of another pot (the position pot) inside the modmotor. A balancing circuit inside the modmotor causes the modmotor to rotate in the direction that makes the shaft voltage and equal to the set pot voltage. A dual two-coil relay in series with the two pots pulls a contact in the center of the relay toward the side with the higher voltage drop, causing the one of the motor's two windings to be energized, which turns the motor's shaft in the direction to equilibrate the draw from the two coils. When the coils draw equally, the contact stays in the center of the relay, so neither motor winding is energized and the shaft does not rotate. Limit switches on the shaft shut off current to the motor in case the shaft is turned far clockwise or counterclockwise.

To control the modmotor without modifying it requires that the computer be able to adjust a pot. The computer could drive a stepper motor whose shaft is coupled to the shaft of the set pot. However, the exact position of the shaft would not be known unless the AC voltage across the pot could be read by the computer. The QuaTech A/D board reads a signal too quickly to be able to accurately sense the voltage of even a rectified AC signal. Also the computer program would be involved in this feedback circuit.

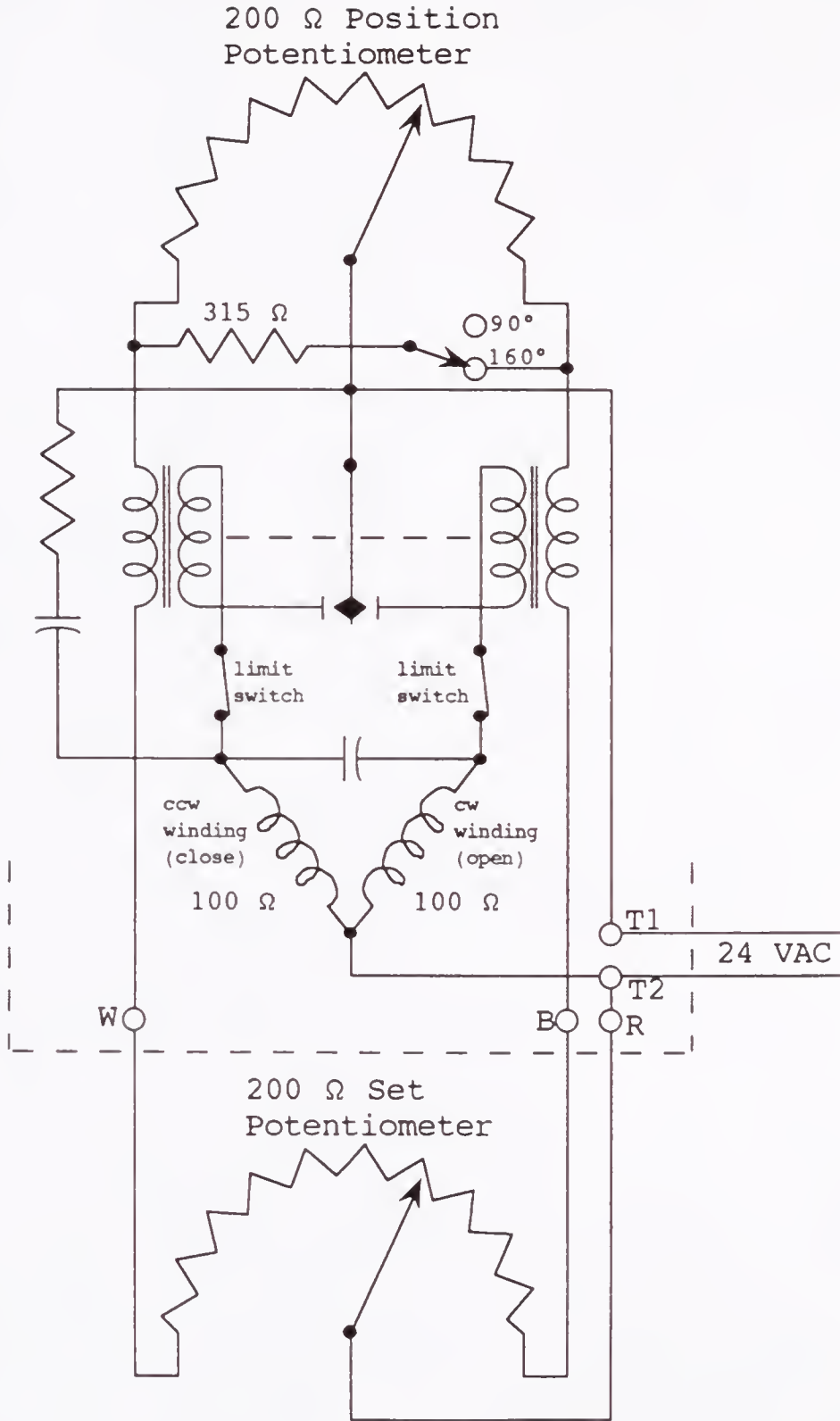


Figure I-2. Original modmotor circuitry.

To take the burden of sensing the set pot's position away from the computer, the computer should just send out a 0- to 5-volt signal proportional to the desired modmotor shaft position, and circuitry at the modmotor would take care of running the modmotor motor so that it turns the shaft to the desired position. The 0- to 5-volt analog signals are generated by the QuaTech D/A board inside the computer.

The modification to the modmotor is shown in Figure I-3. The 12-volt power supply (see Figure I-1) is the same one used to power the alarm timer. The set pot is replaced by a pair of 100-ohm 10-watt resistors, with the common lead between the resistors connected to terminal that the wiper of the set pot would have been connected to. The position pot is removed from the circuit, but not from the modmotor, and is replaced by a pair of 50-ohm 10-watt resistors. Again the common lead between the resistors replaces the wiper of the position pot. Each side of the dual two-coil relay has the same voltage across it and draws equally at the center contact. The center contact is physically removed just in case the relay is not balanced. The relay also acts as a transformer for the motor, so it is not removed from the modmotor. The switching job of the dual two-relay is taken over by a pair of 12-volt, 10-amp contact relays. The limit switches have been retained. Five volts DC are placed across the position pot. The voltage from the position pot's wiper to its ground leg indicates the shafts position. This position voltage is compared to the set voltage from the computer. If



the position voltage is higher than the set voltage, the 324 op-amp powers the 12-volt relay that energizes the counter-clockwise winding of the motor, closing the valve until the position voltage is equal to or less than the set voltage. If the position voltage is lower than 98% of the set voltage, the 324 op-amp powers the 12-volt relay that energizes the clockwise winding of the motor, opening the valve until the position voltage is equal to or greater than 98% of the set voltage. The 98% voltage level is produced by a 21.6-kilo-ohm/1-mega-ohm voltage divider. The 98% voltage level on the opening side allows for motor overrun in both directions. With the same voltage being compared on both the opening and closing sides the circuit would cause the motor to flip-flop across the set point. Even a 99% voltage level on the opening side causes some flip-flop. The 98% voltage level does cause some hysteresis, but it is less than 1%, which is about the accuracy of the set and position voltages.

#### Upper Burner Extra Gas Line Valve

The solenoid valve for the upper burner extra gas line is triggered from the D/A board through an op-amp circuit, not from the parallel port. When the voltage from line 6 of the D/A board is greater than 2.5 volts, the op-amp circuit opens the solenoid valve.

#### Gas Line Orifice Meter

The 8-volt power supply (see Figure I-1) for the gas line and air flow orifice meter's transducers (see Figure 7-3

in Chapter 7 and Figure 3-1 in Chapter 3) is on the same board used to power the alarm timer and modmotor controller. The transducers are wired to the Doric FEM through 3:5 voltage dividers. A tee in the upstream pressure line allows the upstream pressure to be sent to both transducers. Ports are tapped into the pipe at the vena contracta positions (1 pipe diameter (2-1/16 inches) upstream and 0.759 pipe diameters (1-9/16 inches) downstream of the orifice plate). The ports do not extend beyond the inside pipe wall so as not to disturb the flow. A sleeve was made to fit inside the upstream half of the union to cover the inside of the union and make a smooth path for the natural gas up to the orifice plate. The downstream pipe screwed up to the smooth part of the its half of the union, so no sleeve was needed there.

#### Patching Into the Incinerator's Existing Control Circuitry

When the master override signal is sent from the on/off control board, the following four relays are energized: the API override relay, the gas line override relay, the biomass override relay, and the stoker override relay (see Figures I-4 and I-5). The API override relay is a triple-pole, double-throw (TPDT) relay. It is installed in the upper right incinerator control panel on the APIs' mounting bracket. This relay (1) bypasses the PCC's API lower temperature set point so that the PCC burner controller is constantly powered (under normal operation), (2) bypasses the SCC's API lower temperature set point so that the auxiliary blower is brought

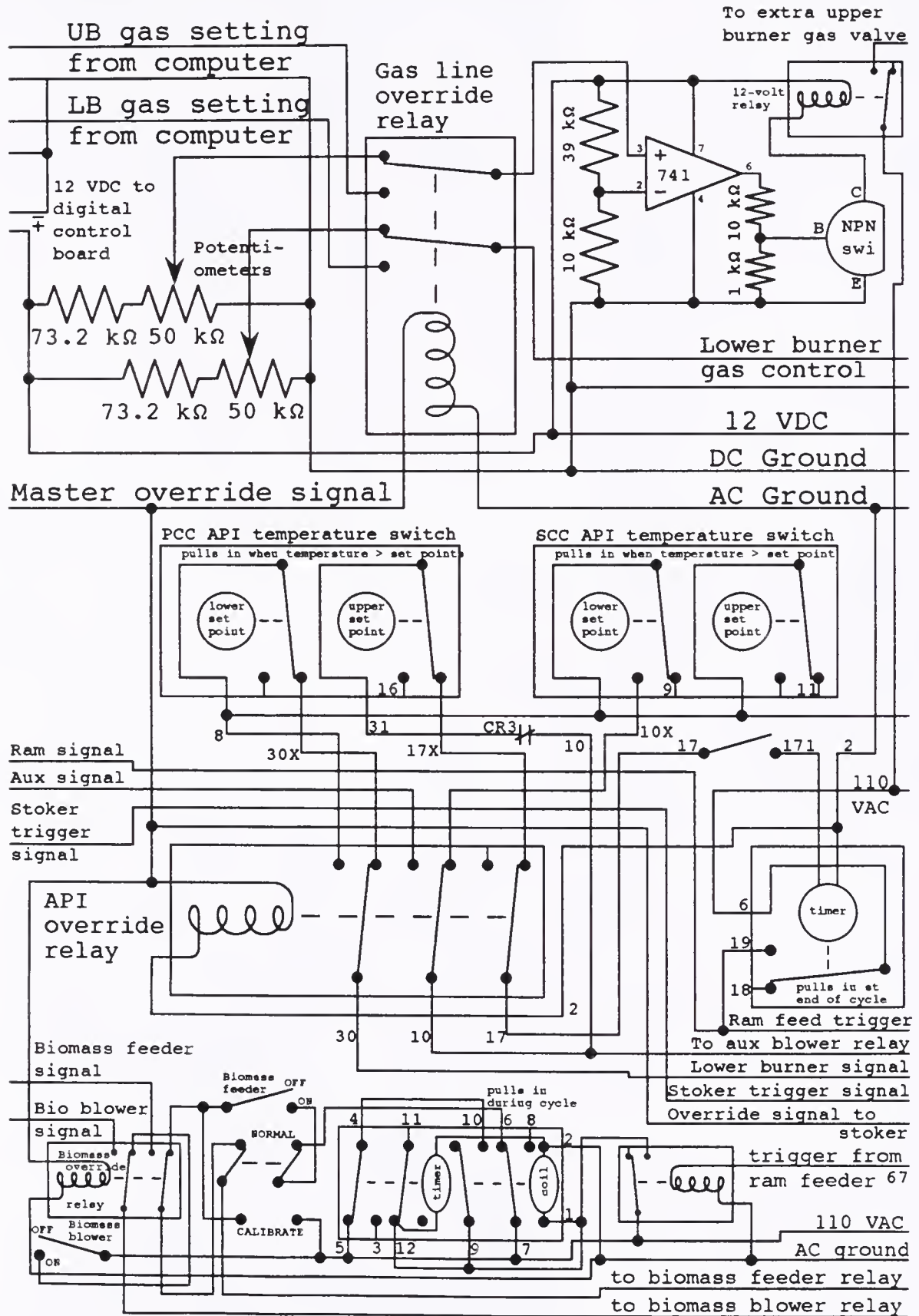


Figure I-4. Override relays configuration.

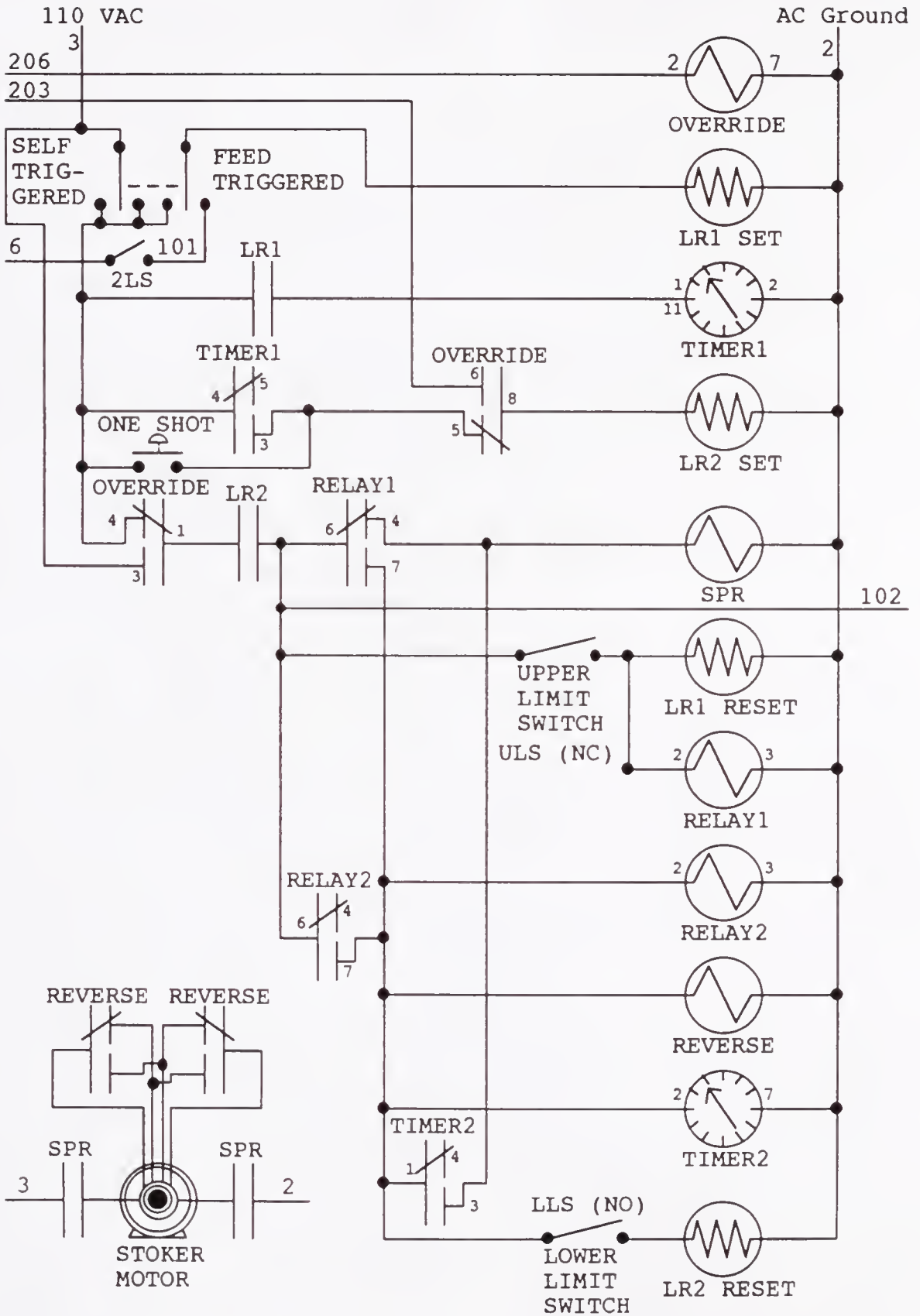


Figure I-5. Stoker control circuitry with override relay.

under computer control, and (3) shuts off any signal from the APIs to the ram feed timer so that the ram feed system is only triggered by the computer. The upper burner can still be shut off by the API if the SCC temperature exceeds the upper API upper set point. This safety shut-off feature is not normally expected since the upper temperature set point is 2500 °F, which is about 300 °F above any expected transient operating temperature.

The gas line override relay is a double-pole, double-throw (DPDT) relay. Installed the same control panel as the API override relay. When it is off, the gas line override relay, sends a 2.5-volt signal (50% open) to the PCC modmotor controller, and a 1.5-volt (closed) signal to the upper burner extra gas line solenoid valve (UBXG) control op-amp. The voltage signals are adjustable with the potentiometers shown in Figure I-4. When the voltage to the UBXG control op-amp exceeds 2.5 volts, the op-amp energizes a 12-volt relay, which then sends 110 VAC power to the solenoid valve, thus opening the UBXG. When the gas line override relay is energized, the computer's signals are sent to the modmotor controller and the UBXG control op-amp.

A 2-hp 3-phase motor starter had to be spliced into the power line to the biomass blower so that the 110-VAC signal from the control board could activate the blower. An on/off switch was installed with the motor starter to allow manual operation of the blower when the control system is off. The DPDT biomass override relay is installed in biomass feeder

delay timer control panel (see Figure I-4). When this relay is energized it bypasses the biomass feeder's delay timer and on/off switch and the biomass blower's on/off switch, bringing the biomass feeder and blower under direct computer control. A DPDT switch was later added to the biomass feeder control circuitry. When switched to calibrate mode, this switch allows direct manual on/off control of the biomass feeder for calibration purposes without interference from the control system when it is on or from the feed ram-triggered delay timer when the control system is off.

The fourth override relay (see Figure I-5) bypasses the stoker's input power line and ram feed- or self-triggered delay timer so that the stoking frequency is brought under computer control.

APPENDIX J  
ADDITIONAL DETAILS ON THE CONTROL COMPUTER PROGRAM

The start logging data function commands the computer to record to disk for each data acquisition cycle all the temperature, CEM, orifice meter, incinerator system status, and control system status readings. The start controlling incinerator function allows the program to control the operation of the incinerator. This controlling function is described later. The CEM calibration function has not yet been implemented. When the function is selected the computer screen is redrawn, which was useful in debugging the program. The shell to operating system (or DOS, the Disk Operating System) function allows the computer user to execute system commands such as formatting diskettes or copying files. The Doric terminal function allows the user direct access to the Doric Dataport 236 data logger, which can be used to view the actual voltages from the CEMS and orifice meters instead of the computed readings.

The view recently recorded data function allows the user to scroll through all the data that has been recorded during the day. During the CEM calibration, shell to operating system, Doric terminal, manual data entry and control, and view recently recorded functions data acquisition, display, and logging and control operation is suspended.

When logging data the computer program writes to two different data files. The first data file is in a plain ASCII format that, without any modification, can be directly printed or imported into a word processor for viewing. The second data file is in a more compact binary format that allows faster and more direct loading into a specialized data processing program used for analyzing the data. The two files are written onto different diskettes while the program is running. In effect, since the files contain the same data, one file can act as a backup for the other file should that file be corrupted, unreadable, or lost.

Originally, the bio and big blowers were turned on during the warm-up phase. When the PCC temperature reached its peak and levels off, the bio blower was turned on, and if necessary the upper burner extra gas line valve was reopened. When the PCC temperature levelled off again, the operator was instructed to turn on big blower, and if necessary the program reopened the upper burner extra gas line valve. When all three blowers were on the program switched to the post-warm up mode of control. After test firing, the bio and big blowers were turned on during the post-warm up phase, which occurs at the end of the preset warm up time and now lasts only long enough to turn the blowers on.

## REFERENCES

1. Roy Neulicht, Results of the Combustion and Emissions Research Project at the Vicon Incinerator Facility in Pittsfield, Massachusetts, Final Report, Volume I, prepared by Midwest Research Institute for New York State Energy Research and Development Authority, Report 87-16, June, 1987.
2. Richard S. Magee, Plastics in Municipal Solid Waste Incineration: A Literature Study, prepared by the New Jersey Institute of Technology Hazardous Substance Management Center for the Society of Plastics Industry, Inc., January, 1989.
3. Alex Green, John Wagner, Joseph Blake, and Xie-Qi Ma, "Strategies For Toxic Minimization when Cofiring with Biomass", Presented at the 1991 Southern Biomass Conference, Technical Session IVB, Paper IV.B.2, Baton Rouge, LA, Jan 7-10, 1991.
4. Alex Green, John Wagner, Craig Saltiel, and Max Jackson, "Pollution Prevention and Institutional Incineration", Proceedings of the ASME Solid Waste Processing Conference, Detroit, MI, May 17-20, 1992.
5. Alex Green, John Wagner, Craig Saltiel, Joseph Blake, and Xie-Qi Ma, "Medical Waste Incineration with a Toxic Prevention Protocol", Proceedings of the 84th Annual Meeting of the Air & Waste Management Association, Paper 91-33.5, Vancouver, BC, June 16-21, 1991.
6. A. Green, C. Batich, J. Wagner, J. Blake, D. Powell, C. Schmidt, M. Jackson, and B. Andrews, "Advances in Uses of Modular Waste to Energy Systems", Published in ASME booklet Advances in Solid Fuels Technologies, FACT-Vol. 9, Vol. G00522, A.E.S. Green and W.E. Lear (eds.), and Presented at the ASME/IEEE/ASCE/VGB 1990 International Joint Power Generation Conference & Exposition, Boston, MA, October 21-25, 1990.
7. A.E.S. Green, J.C. Wagner, and S. Mahadevan, "Chlorinated Toxics from Incineration", to be presented at the ASME Joint Power Generation Conference and published in a booklet, Atlanta, GA, October 18-22, 1992.

8. Alex E.S. Green, John C. Wagner, and Ken J. Lin, "Phenomenological Models of Chlorinated Hydrocarbons", Chemosphere, Vol. 22, Nos. 1-2, pp. 121-135, 1991.
9. D.P.Y. Chang, N.W. Sorbo, and Cynthia Castronovo, Workshop and Panel Discussion on Surrogates for Solid Waste Incineration, submitted for California Air Resources Board Contract A6-221-45, Dept. of Civil Engr., Univ. of Calif., Davis, CA, pp. 6-7 & C20, November, 1988.
10. William C. Pfefferle, "Catalytically Stabilized Thermal Incineration", Innovative Hazardous Waste Treatment Series: Thermal Processes, Vol 1., Harry M. Freeman (ed.), Technomic Publishing Co., p. 228, 1990.
11. S.B. Karra and S.M. Senkan, "Chemical Structures of sooting  $\text{CH}_3\text{Cl}/\text{CH}_4/\text{O}_2/\text{Ar}$  and  $\text{CH}_4/\text{O}_2/\text{Ar}$  Flames", Comb. Sci. & Tech., Vol 54, pp. 333-347, 1987.
12. S. Hung and L. Pfefferle, "Methyl Chloride and Methylene Chloride Incineration in a Catalytically Stabilized Thermal Combustor", Environmental Science and Technology, Vol. 53, p. 1083, 1989.
13. Wing Tsang, "Mechanisms for the Formation and Destruction of Chlorinated Organic Products of Incomplete Combustion", Combustion Science and Technology, Vol. 74, p. 108, 1990.
14. B.K. Gullett, K.R. Bruce, L.O. Beach, "Formation of Chlorinated Organics During Solid Waste Combustion", Waste Management and Research, Vol. 8, pp. 203-214, 1990.
15. B.K. Gullett, K.R. Bruce, L.O. Beach, "The Effect of Metal Catalysts on the Formation of Polychlorinated Dibenzop-dioxins and Polychlorinated Dibenzofurans Precursors", Chemosphere, Vol. 19, pp. 1945-1952, 1989.
16. Prakash Acharya, Steven G. DeCicco, and Rudy G. Novak, "Factors that Can Influence and Control the Emissions of Dioxins and Furans from Hazardous Waste Incinerators", Proceedings of the 84th Annual Meeting of the Air & Waste Management Association, Paper 91-103.28, Vancouver, BC, June 16-21, 1991.
17. L. Cassito, "Destruction of the Organo-Chlorinated Micropollutants in the Combustion Process", 7th Miami Intl. Conf. on Alternate Energy Sources, 1985.
18. U.S. EPA, Municipal Waste Combustion Study, Report to Congress, EPA/530-SW-87-028, p. xiii, June 1987.

19. Yu-Min Chang, Yu-Fu Lo, and Chin-Chen Ho, "Application of Fluidized Bed Combustion to Industrial Waste Treatment", Environmental Pollution, Vol. 71, pp. 31-42, 1991.
20. Calvin R. Brunner and Courtney H. Brown, "Hospital Waste Disposal by Incineration: Waste Streams, Technology, and State Regulations", JAPCA, Vol. 38, No. 10, p. 1297-1309, October, 1988.
21. Simonds, Leading the Way in Waste Incineration and Heat Recovery Systems, catalog from Simonds Manufacturing Corporation, Auburndale, FL, 1983.
22. Barbara C. Klenke, Consertherm® Waste-to-Energy System, Proposal No. C-1643-86 for Florida Hospital, Industronics, Inc., South Widsor, CT April 11, 1986.
23. Modular Incinerator Systems with Energy Recovery and Materials Handling Equipment, brochure from Stock Equipment Company, Lynn HAVen ,FL, 1987.
24. Fixed Hearth Incineration Systems, catalog from Cleaver Brookes, Milwaukee, WI, April, 1987.
25. Brochure from Hi Temp Tech Corporation, March, 1986.
26. Institutional, Industrial, Municipal Incineration and Energy Recovery System, catalog from Ecolaire Combustion Products, Inc., Charlotte, NC, 1985.
27. Systems and Equipment for Energy-Related Process Management, catalog from Ecolaire Incorporated, Malvern, PA (no date)
28. Controlled Air Incineration, catalog from Ecolaire Combustion Products, Inc., Charlotte, NC (no date).
29. Dorata Z. Przewalska, Mobile Incineration Systems for Processing Hazardous Waste, M&S Engineering & Manufacturing Company, Inc, Broad Brook, CT (no date).
30. The Modern Basic Incinerator Success Story, catalog, Basic Environmental Engineering Inc., Glen Ellyn, IL, pp. 6-7, 1985.
31. 1991 Annual Report, Ogden Projects, Inc., Fairfield, NJ, p. 12, 1991.
32. American Ref-Fuel Waste-to-Energy Services, brochure from American Ref-Fuel Company, Houston, TX, Mar. 1991.
33. ABB Resource Recovery Systems, pamphlet from Asea Brown Boveri.

34. D.E. Burnham, D.R., Gibbs, J.S. Gittinger, and H.E. Johnson, "The Evolution of RDF Boiler Designs Through the State-of-the-Art System at Palm Beach", Babcock & Wilcox technical paper BR-1393, presented to the 1989 Conference on Municipal Solid Waste as a Utility Fuel, Springfield, MA, Oct. 10-12, 1989.
35. E. Timothy Oppelt, "Incineration of Hazardous Waste: a Critical Review", JAPCA, Vol. 37, No. 5, pp. 558-586, May 1987.
36. Min-Da Ho, Joyce M. Perdeck, James P. Stumbar, and Robert H. Sawyer, "Field Demonstration of the Linde Oxygen Combustion System on the EPA Mobile Incinerator", JAWMA, Vol. 42, No. 4, pp. 493-499, April 1992.
37. Florida Administrative Code, 17-2, Aug. 29-30, 1989.
38. Florida Administrative Code, 17-712, Aug. 29-30, 1989.
39. C.C. Lee, George L. Huffman, and Richard P. Nalesnik, "Medical waste Management: the State of the Art", Env. Sci. Tech., Vol. 25, No. 3, pp. 360-363, 1991.
40. R.G. Barton, G.R. Hassel, W.S. Lanier, and W.R. Seeker, State-of-the-Art Assessment of Medical Waste Thermal Treatment, Report for the Risk Reduction Engineering Laboratory, US EPA Contract #68-03-3365 and California Air Resources Board Contract #A832-155, Energy and Environmental Research Corporation, Irvine, CA, 1989.
41. L.G. Doucet, State-Of-The-Art Hospital and Institutional Waste Incineration: Selection, Procurement, and Operations, Tech. Document Series, Peekskill, NY, 1991.
42. Jack D. Lauber and Donald A. Drum, "Best Controlled Technologies for Regional Biomedical Waste Incineration", Presented at the 83rd Annual Meeting & Exhibition of the Air & Waste Management Association, Paper No. 90-27.2, Pittsburgh, PA, June 24-29, 1990.
43. C.C. Lee, G.L. Huffman, and R.P. Nalesnik, Medical Waste Management: The State of the Art, Office of Research and Development, EPA, Cincinnati, OH, 1991.
44. James D. Kilgore, W. Steve Lanier, and T. Rob von Alten, "Development of Good Combustion Practice for Municipal Waste Combustors", Proceedings of 1992 National Waste Processing Conference, Fifteenth Biennial Conference, SWP Div., ASME, Detroit MI, pp. 145-156, May 17-20, 1992.
45. M.M. Bulley, "Incineration of Medical Wastes: Treating the Cause Rather than the Symptom", Clean Air, pp. 51-53, May 1991.

46. M.M. Bulley, "Medical Waste Incineration in Australasia", Presented at the 83rd Annual Meeting & Exhibition of the Air & Waste Management Association, Paper No. 90-27.5, Pittsburgh, PA, June 24-29, 1990.
47. M.M. Bulley, "The Impact of Design, Procurement, and Disposal Options on Medical Waste Incineration in Australasia", Presented at the 84th Annual Meeting & Exhibition of the Air & Waste Management Association, Paper No. 91-33.3, Vancouver, BC, June 16-21, 1991.
48. Profylakse Institute A/S, product brochure for System PI A/S incinerator system, Copenhagen, Denmark.
49. John C. Wagner, Joseph A. Blake, Xie-Qi Ma, and Alex E.S. Green, "Control Strategy for Incineration Emissions Minimization", Engineering Science Preprints - 28, Paper ESP28.91041, 28th Annual Technical Meeting of the Society of Engineering Science, Gainesville, FL, Nov. 6-8, 1991.
50. Floyd Hasselriis, "How Environmental Risk from Leaching of Heavy Metals in Ash Residues from Combustion of Municipal Solid Waste Can Be Minimized By Control of Combustion, Emissions and Ash Residues Management" (draft), for presentation at the Conference on Solid Waste Disposal, Amherst, MA, April 12, 1988.
51. Floyd Hasselriis, "Optimization of Combustion Conditions to Minimize Dioxin Emissions", Waste Management & Research, Vol. 5, pp. 311-326, 1987.
52. Floyd Hasselriis, "Relationship Between Waste Composition and Environmental Impact", Presented at the 83rd Annual Meeting & Exhibition of the Air & Waste Management Association, Paper No. 90-38.2, Pittsburgh, PA, June 24-29, 1990.
53. Floyd Hasselriis, "Effect of Waste Composition and Charging Frequency on Combustion Efficiency of Medical and Other Solid Waste Combustors", to be presented at the 15th National Waste Processing Conference, Detroit, MI, May 17-20, 1992.
54. Shyan-Lung Chung and Sheung-Man Tsang, "Soot Control During the Combustion of Polystyrene", J. Air Waste Manage. Assoc., Vol. 41, No. 6, pp. 821-826, June 1991.
55. Rachel Nihart, John C. Kramlich, Gary S. Samuelsen, and W. Randall Seeker, Continuous Performance Monitoring Techniques for Hazardous Waste Incinerators, EPA/600/S2-89/021, August 1989.
56. Laurel J. Stately, Marta K. Richards, George L. Huffman, and Daniel P.Y. Chang, Incinerator Operating

Parameters Which Correlate with Performance,  
EPA/600/S2-86/091, February 1987.

57. Jill Weldon and David S. Beacher, "Comparison of Surrogate Measurements Used to Indicate Dioxin Emissions from Municipal Waste Combustor", presented at the 1992 National Waste Processing Conference, Fifteenth Biennial Conference, SWP Div., ASME, Detroit MI, May 17-20, 1992.
58. J.D. Lauber "Best Available Control Technologies for Regional Hospital and Hazardous Waste Coincineration", Israel Ecological Society, 4th Int'l Conf., Jerusalem, Israel, June 4, 1989.
59. U.S. EPA, Hospital Waste Combustion Study, Data Gathering Phase, Final Draft Report, October, 1987.
60. F.W. Hasselriis, Technical Guidance Relative to Municipal Waste Incineration, prepared for the NYC Dept. of Env. Conserv. Task Force on MSW Incineration, August 28, 1985.
61. B. Dellinger, W. Rubey, D.L. Hall, and J.L. Graham, "Incinerability of Hazardous Waste", Hazardous Waste and Hazardous Materials, Vol. 3, No. 2, 1986.
62. M.J. Clarke, "Discussion Paper on BACT for Resource Recovery from a Municipality's Perspective", Fourth Annual Resource Recovery Conference, Washington, DC, March 27, 1985.
63. Kun-chieh Lee, Research Areas for Improved Incineration Performance, JAPCA, Vol. 38, No. 12, pp. 1542-1550, Dec. 1988.
64. Clean Air Act Amendments of 1990, House Report 101-058, 1990.
65. Federal Register, Vol. 54, No. 243, pp. 52251-52304, December 20, 1989.
66. Solar Energy Research Institute, RD&D Priorities for Energy Production and Resource Conservation from Municipal Solid Waste: Draft Final Report, Prepared by ICF Incorporated, p. 206, Oct. 31, 1991.
67. A. Green (Ed.), Coal Burning Issues, University Presses of Florida, Gainesville, FL, 1980.
68. A. Green (Ed.), An Alternative to Oil, Burning Coal with Gas, University Presses of Florida, Gainesville, FL, pp. 1-140, 1981.

69. A. Green and B. Green, Development of Gas-Coal Combustor, (unpublished) 1981.
70. A. Green and B. Green, "Method of Retrofitting An Oil-Fired Boiler to use Coal and Gas Combustion", U.S. Patent No. 4,561,364, December 1985.
71. A. Green and B. Green, Notes on Simultaneous Gas-Coal Combustion, (unpublished) 1981.
72. A. Green, "Clean Combustion Technology", Proc. of Conf. There is No Away. University of Florida Law School, Gainesville, FL. Available through EPA-NTIS, 1986.
73. A. Green, J. Wagner, W. Gattle, J. Schwartz, B. Green, P. West, S. Gaffney, and E. Mize, "Minimal Cost Oil-Boiler Conversions", Proceedings of the Eighth International Symposium on Coal Slurry Fuels Preparation and Utilization, Paper 58, Orlando, FL, May 27-30, 1986.
74. A.E.S. Green, E.J. Mize, D.S. De, B.A. Green, P. West, M. Sandifer, and C. Niven, "Natural Gas Use to Facilitate Coal and Waste Combustion", Proc. of the Conf. on Select Use of Natural Gas for Environmental Purposes, American Gas Association, Arlington, VA, 1985.
75. Alex Green, Bruce Green, John Wagner, Donald Clauson, Jerome Schwartz, David Williams, Stephen Gaffney, "Emission Control by Coburning with Gas", Proc. of 1987 FAPCA Meeting, Melbourne, FL, Sept. 27-29, 1987.
76. Alex Green, Bruce Green, John Wagner, Jerry Schwartz, William Gattle, P. West, and E.L. Mize, "Coal Water Gas Combustion In A Water Tube Boiler", Proceedings of Conference on Coal-Liquid Mixtures: The Pathway to Commercialization, Tampa, FL, Feb. 3-4, 1986.
77. Alex Green, John Wagner, Bruce Green, and Jerry Schwartz, "Synergisms in Coburning Gas and Coal", ASME Paper 87-JPGC-FACT-10, Presented at the Joint ASME/IEEE Power Generation Conf., Miami Beach, FL, Oct. 4-8, 1987.
78. Alex Green, John Wagner, William Gattle, Bruce Green, Jerry Schwartz, P. West, and E.L. Mize, "Coal-Water-Gas, An All American Fuel For Oil Boilers", Proceedings of the Eleventh International Conference on Slurry Technology, pp. 251-262, Hilton Head, SC, March 16-18, 1986.
79. Alex Green, John Wagner, William Gattle, Bruce Green, Jerry Schwartz, Ady Mann, David Williams, Shun-Tie Chai, David Stein, Donald Clauson, Michael Kawejsza, Patrick Ummel, Alex Feinberg, Stephen Gaffney, Pat West, Skipper Mize, "Radiation Enhancement by Coal

- Slurries", Proceedings of the Twelfth International Conference on Slurry Technology, New Orleans, LA, March 31-April 3, 1987.
80. John C. Wagner, Radiation Enhancement of Natural Gas Flames, Master's Thesis, Dept. of Mech. Engr., University of Florida, (unpublished) August, 1987.
  81. Alex E.S. Green, Bruce A.S. Green, and John C. Wagner, "Radiation Enhancement in Oil/Coal Boilers Converted to Natural Gas", U.S. Patent No. 4,978,367, Dec. 18, 1990.
  82. Alex E.S. Green, Bruce A.S. Green, and John C. Wagner, "Radiation Enhancement in Oil/Coal Boilers Converted to Natural Gas", U.S. Patent No. 5,048,433, Sep. 17, 1991.
  83. A. Green, C. Batich, D. Powell, J. Street, D. Williams, J. Wagner, J. Blake, D. Clauson, B. Green, H. van Ravenswaay, C. Schmidt, K. Awuma, S. Mu, M. Jackson, and B. Andrews, "Toxic Products from Co-Combustion of Institutional Waste", Proceedings of the 83rd Annual Meeting of the Air & Waste Management Association, Paper 90-38.4, Pittsburgh, PA, June 24-29, 1990.
  84. A. Green, "Community Waste to Energy System Technologies (CWEST)", Florida Scientist, Vol. 52, No. 2, pp. 104-118, 1989.
  85. A. Green, G. Prine, D. Rockwood, P. Mislevy, C. Batich, J. Winefordner, D. Williams, B. Green, J. Wagner, J. Schwartz, H. van Ravenswaay, T. Yurchison, D. Clauson, S. Mills, A. Feinberg, R. Storer, F. Jenkins, S. Gaffney, K. McNally, D. English, R. Nefzger, and E. Powell, "Co-Combustion in Community Waste to Energy Systems", Published in ASME booklet Co-Combustion, FACT-Vol. 4, Alex E.S. Green (ed.), pp. 13-28, and Presented at the 1988 Joint Power Generation Conference, Philadelphia, PA, Sept. 25-29, 1988.
  86. A. Green, H. van Ravenswaay, J. Wagner, B. Green, T. Cherry, and D. Clauson, "Co-feeding and Co-firing Biomass with Non-Hazardous Waste and Natural Gas", Bioresource Technology, Vol. 36, pp. 215-221, 1991.
  87. A. Green, J. Wagner, B. Green, H. van Ravenswaay, D. Clauson, J. Schwartz, T. Yurchison, D. Rockwood, G. Prine, P. Mislevy, F. Jenkins, and S. Gaffney, "Co-Combustion of Waste, Biomass, and Natural Gas", Biomass, Vol. 20, pp. 249-262, 1989.
  88. Alex Green, David Powell, Jimmy Street, Christopher Batich, John Wagner, Henk van Ravenswaay, Don Clauson, Bruce Green, Thomas Cherry, and Barry Andrews "Toxic Products from Cofiring Institutional Waste, Biomass,

- and Natural Gas", Presented at the Florida Section APCA Annual Meeting, Hollywood, FL, September 24-26, 1989.
89. Alex Green, Gordon Prine, Richard Yost, Bruce Green, David Williams, Jerry Schwartz, John Wagner, Donald Clauson, Bruce Proctor, Alex Feinberg, Steve Mills, and Stephen Gaffney, "Co-Burning in Institutional Incinerators", Proceedings of APCA International Specialty Conference on Thermal Treatment of Municipal, Industrial, and Hospital Wastes, pp. 61-81, Pittsburgh, PA, Nov. 3-6, 1987
  90. John C. Wagner, Alex E.S. Green, "Cofiring in Modular Systems", Presented at the AIChE 1990 Spring National Meeting, Paper 54G, March 18-22, 1990.
  91. A. Green, C. Batich, J. Wagner, J. Blake, Xie-Qi Ma, C. Saltiel, and M. Goodman, "A "Florida Approach" to Institutional Waste Management", Presented at the 1991 Meeting of the Florida Air & Waste Management Association, Clearwater, FL, Sept. 15-17, 1991.
  92. J. Blake, X. Ma, J. Wagner, and A. Green, "Use of a Bench Scale Combustor for Incineration Research", Engineering Science Preprints - 28, Paper ESP28.91042, 28th Annual Technical Meeting of the Society of Engineering Science, Gainesville, FL, Nov. 6-8, 1991.
  93. Joseph A. Blake, Laboratory Combustion of Solid Wastes to Simulate Their Combustion and Emission Characteristics In Incineration Systems, Master's Thesis, Dept. of Mech. Engr., University of Florida, (unpublished) May, 1992.
  94. Environmental Control Products, Operating, Maintenance, and Parts Manual, Manual no. PO 3852 for ECP model T-500 incinerator, Charlotte, NC, November 1971.
  95. Code of Federal Regulations, Title 40, Part 60, Appendix A, Method 5, 1990.
  96. "Method 26--Determination of Hydrogen Chloride Emissions From Stationary Sources", Federal Register, Vol. 54, No. 243, pp. 52201-52207, December 20, 1989.
  97. Test Methods for Evaluating Solid Waste, SW-846, 3rd Ed., Method 0010, U.S. EPA, Washington, DC, 1987.
  98. Code of Federal Regulations, Title 40, Part 136, 1990.
  99. Hansen, E.M., Protocol for the Collection and Analysis of Volatile POHC's Using VOST, EPA-600/8-84-007, P384-170042, March 1984.

100. Test Methods for Evaluating Solid Waste, SW-846, 3rd Ed., Method 0030, U.S. EPA, Washington, DC, 1987.
101. Test Methods for Evaluating Solid Waste, SW-846, 3rd Ed., Method 5040, U.S. EPA, Washington, DC, 1987.
102. Xie-Qi Ma, Joseph Blake, John Wagner, and Alex Green, The Application of Gas Chromatography/Electron Capture Detector to Analysis of Chlorinated Hydrocarbons from Stack Gas, (unpublished) 1991.
103. Xie-Qi Ma, Joseph Blake, John C. Wagner, and Alex E.S. Green, "Extension of Sorbent Trapping/Thermal Desorption Techniques for Chlorinated Hydrocarbons", Presented at the 1991 Meeting of the Florida Air & Waste Management Association, Clearwater, FL, Sept. 15-17, 1991.
104. Test Methods for Evaluating Solid Waste, SW-846, 3rd Ed., Method 7000, U.S. EPA, Washington, DC, 1987.
105. Test Methods for Evaluating Solid Waste, SW-846, 3rd Ed., Method 9040, U.S. EPA, Washington, DC, 1987.
106. Code of Federal Regulations, Title 40, Part 261.21, 1990.
107. Test Methods for Evaluating Solid Waste, SW-846, 3rd Ed., Method 1310, U.S. EPA, Washington, DC, 1987.
108. Characterization of Municipal Waste Combustor Ash, Ash Extracts, and Leachates, EPA 530-SW-90-029A, 1990.
109. Alex E.S. Green and John C. Wagner, Quality Assurance Plan, for Florida Department of Environmental Regulation Contract "Measurement and Minimization of Toxic Incineration Products", Revision 1, (unpublished) May 15, 1990.
110. C.A. Kodres, "Theoretical Thermal Evaluation of Energy Recovery Incinerators--Part I: Modelling", Journal of Energy Resources Technology, Vol. 109, pp. 79-83., June 1987.
111. C.A. Kodres, "Theoretical Thermal Evaluation of Energy Recovery Incinerators--Part II: Parametric Examination", Journal of Energy Resources Technology, Vol. 109, pp. 84-89., June 1987.
112. C.A. Kodres, Theoretical Thermal Evaluation of Energy Recovery Incinerators, NCEL Tech. Rep. No. R-916, Naval Civil Engineering Lab., Port Hueneme, CA, Dec. 1985.
113. C.A. Kodres, Computer Program to Simulate the Thermal Characteristics of Heat Recovery Incinerators, NCEL

Technical Report No. N-1745, Naval Civil Engineering Laboratory, Port Hueneme, CA, February 1986.

114. K. Wark, Thermodynamics, 4th Ed., McGraw-Hill Book Company, New York, NY, p. 823, 1983.[SFE] Richard L. Scheaffer and James T. McClave, Statistics for Engineers, Duxbury Press, Boston, 1982.
115. A.E.S. Green, R.R. Meyreddy, and K.M. Pamidimukkala, "A Molecular Model of Coal Pyrolysis", Int. J. of Quantum Chem.: Quantum Chem. Symp. 18, pp. 589-599, 1984.
116. Alex E.S. Green and Krishna M. Pamidimukkala, Synergistic Combustion of Coal with Natural Gas, Energy, Vol. 9, No. 6, pp. 477-484, 1984.
117. Alan C. Hindmarsh, "Odepack, a Systematized Collection of ODE Solvers", Scientific Computing, R.S. Stepleman, et al. (eds.), North-Holland, Amsterdam, pp. 55-64, 1983.
118. L. Douglas Smoot and David T. Pratt, Pulverized-Coal Combustion and Gasification, pp. 169-182, 1979.
119. Francis Westley, Table of Recommended Rate Constants for Chemical Reactions Occurring in Combustion, Report No. NSRDS-NBS 67, Nat. Bureau of Standards, April 1980.
120. J.T. McKinnon and J.B Howard, "Application of Soot Formation Model: Effects of Chlorine", Comb. Sci. Tech., Vol 74, pp. 175-197, 1990.
121. George S. Darivakis, Jack B. Howard, and William A. Peters, "Release Rates of Condensables and Total Volatiles from Rapid Devolatilization of Polyethylene and Polystyrene", Comb. Sci. Tech., Vol. 74, p. 272, 1990.
122. Joseph L. Tessitore, Edward DeCresie, and John G. Pinion, Thermal Destruction of Air Toxics, Cross/Tessitore & Associates, P.A., Orlando FL, 1990.
123. Richard D. Smith and Allen L. Johnson, "Mass Spectrometric Study of the High Temperature Chemistry of Benzene", Comb. & Flame, Vol. 51, p. 6, 1983.
124. C.H. Bamford and C.F.H. Tipper (Eds.), Comprehensive Chemical Kinetics, Vol. 14, Elsevier Publishing Co., Amsterdam, NY, pp. 79 & 123, 1983.
125. John Wagner, Alex Green, Craig Saltiel, "Kinetic Simulations of the Formation of Chlorinated Organics in a Medical Waste Incinerator", Presented at the Fourth International Conference on Combustion, Sponsored by Society for Industrial and Applied Mathematics (SIAM), St. Petersburg Beach, FL Dec. 2-4, 1991.

126. John S. Morse, Jamil A. Khan, and Debabrata Pal, "Modelling an Industrial Rotary Kiln Incinerator-- Adiabatic Vs. Constant Heat Flux Walls", presented at the 1992 National Waste Processing Conference, Fifteenth Biennial Conference, SWP Div., ASME, Detroit MI, May 17-20, 1992.
127. K. Kobayashi, J. Howard, and A. Sarofim, "Coal Devolatization at High Temperatures", Sixteenth Symposium (Intl.) on Combustion, pp. 411, 1976.
128. Richard L. Scheaffer and James T. McClave, Statistics for Engineers, Duxbury Press, Boston, 1982.
129. Rudolf J. Freund and Paul D. Minton, Regression Analysis, a Tool for Data Analysis, Marcel Dekker, Inc., New York, p. 65, 1979.
130. William D. Berry and Stanley Feldman, Multiple Regression in Practice, Sage Publications, Beverly Hills, 1985.
131. C.F. Cusick (Ed.), Flow Meter Engineering Handbook, 4th Ed., Honeywell Automation, Industrial Division, Fort Washington, PA, 1968.
132. John G. Bollinger and Neil A. Duffie, Computer Control of Machines and Processes, Addison-Wesley Publishing Company, Reading, MA, p. 453, 1988.
133. R.L. Youngblood, "Fuzzy Logic: What is it? Has it got 'legs'?", Power, pp. 63-64, March 1992.
134. Louis Theodore, Air Pollution Control and Waste Incineration for Hospitals and other Medical Facilities, Van Nostrand Reinhold, New York, NY, p.299, 1990.
135. R.J. Allen, G.R. Brennum, and C. Darling, "Air pollution from the Incineration of Hospital Waste", JAPCA, Vol. 36, No. 7, p. 830, July 1986.
136. Kenneth Wagener, Christopher Batich, and Alex Green, "Polymer Substitutes For Medical Grade Polyvinylchloride (PVC)", Chapter 8 in Medical Waste Incineration and Pollution Prevention, Alex Green (ed.), Van Nostrand Reinhold, New York, NY, 1992.
137. Code of Federal Regulations, Title 40, Part 60, Appendix A, Method 2, 1990.

## BIOGRAPHICAL SKETCH

John Charles Wagner was born on October 8, 1963, in the state of Illinois. After living in the suburbs of Chicago for fifteen and one-half years, he moved with his family to central Florida. He graduated with honors from Central Florida Community College in Ocala in 1983 and graduated with high honors from University of Florida in 1985 with a Bachelor of Science in Mechanical Engineering degree. While earning his Master of Science and Doctor of Philosophy degrees at University of Florida he coauthored and presented several papers on the coburning of natural gas and coal slurries and on waste incineration. His research for his Master of Science degree led to two patents, entitled "Radiation Enhancement in Oil/Coal Boilers Converted to Natural Gas." He plans to seek a career in industry in combustion research, design, and/or development.

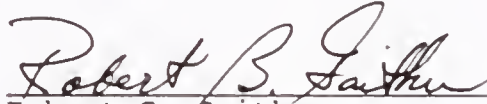
I certify that I have read this study and that in my opinion it conforms to acceptable standards of scholarly presentation and is fully adequate, in scope and quality, as a dissertation for the degree of Doctor of Philosophy.



---

Alex E. S. Green, Chairman  
Graduate Research Professor of  
Mechanical Engineering

I certify that I have read this study and that in my opinion it conforms to acceptable standards of scholarly presentation and is fully adequate, in scope and quality, as a dissertation for the degree of Doctor of Philosophy.



---

Robert G. Gaither  
Professor of Mechanical  
Engineering

I certify that I have read this study and that in my opinion it conforms to acceptable standards of scholarly presentation and is fully adequate, in scope and quality, as a dissertation for the degree of Doctor of Philosophy.



---

Vernon P. Roan, Jr.  
Professor of Mechanical  
Engineering

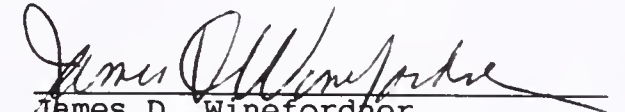
I certify that I have read this study and that in my opinion it conforms to acceptable standards of scholarly presentation and is fully adequate, in scope and quality, as a dissertation for the degree of Doctor of Philosophy.



---

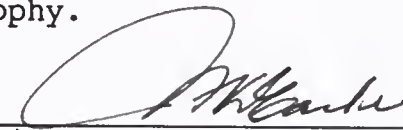
Craig J. Saltiel  
Assistant Professor of  
Mechanical Engineering

I certify that I have read this study and that in my opinion it conforms to acceptable standards of scholarly presentation and is fully adequate, in scope and quality, as a dissertation for the degree of Doctor of Philosophy.

  
James D. Winefordner  
Graduate Research Professor of  
Chemistry

This dissertation was submitted to the Graduate Faculty of the College of Engineering and to the Graduate School and was accepted as partial fulfillment of the requirements for the degree of Doctor of Philosophy.

August 1992

  
for Winfred M. Phillips  
Dean, College of Engineering

\_\_\_\_\_  
Madelyn M. Lockhart  
Dean, Graduate School

